

## Synthetic chemistry with nitrous oxide and triazenes

Présentée le 28 janvier 2022

Faculté des sciences de base  
Laboratoire de chimie supramoléculaire  
Programme doctoral en chimie et génie chimique

pour l'obtention du grade de Docteur ès Sciences

par

**Iris Roswitha LANDMAN**

Acceptée sur proposition du jury

Prof. S. Gerber, présidente du jury  
Prof. K. Severin, directeur de thèse  
Prof. E. Hevia, rapporteuse  
Prof. M. Westerhausen, rapporteur  
Prof. X. Hu, rapporteur



# Acknowledgements

Throughout the PhD and writing this thesis, I have received a great deal of support and assistance. First and foremost, I would like to thank my supervisor, Prof. Kay Severin, for giving me the opportunity to conduct my doctoral studies in his lab. I am deeply grateful for his invaluable advice and continuous support throughout the PhD. Your supervision has contributed greatly to my development as a chemist, and I thank you for your trust in me and my research. I hope our paths will continue to cross in the future.

Prof. Sandrine Gerber, Prof. Matthias Westerhausen, Prof. Eva Hevia, and Prof. Xile Hu are thanked for taking time to evaluate my PhD thesis and be part of my thesis defense. Thank you for the insightful comments and suggestions.

The Swiss National Science Foundation, and the Ecole Polytechnique Fédérale de Lausanne (EPFL) are acknowledged for the financial support of the research in this thesis.

The work in this thesis could not be done without the great technical support from the NMR (Dr. Aurélien Bornet, Emilie Baudet, Anto Barisic), MS (Dr. Daniel Oritz, Dr. Laure Menin, Francisco Sepulveda), X-ray (Dr. Euro Solari, Dr. Farzaneh Fadaei-Tirani, Dr. Rosario Scopelliti) teams and the biological assay screening center. Thanks for answering questions and for the guidance in the experiments when needed. Furthermore, thanks to the administrative staff, I am particularly grateful to Christina Zamanos-Epremian, Anne Lene Odegaard, and Séverine Roque. Also, many thanks to the BCH magasin team and the IT-support team.

Thanks to Prof. Giulia Tagliabue for giving me valuable advice in the final year of my PhD.

I would like to express my gratitude to the current and past LCS members for their support, scientific discussions, lunches (at the banane), coffee breaks (on the balcony), and apéros (especially the ones at the lake). Thank you for the wonderful collaborations and the pleasant time. Lab 3419 was a great place with good atmosphere to carry out this research. Special thanks to Carl, Wolfram, Sylvain, Cristian, Cesare, Dong, and Rujin for proof reading and scientific discussions in the lab (or at satellite with a beer). Erica, José, and Ophélie, thank you for all your efforts for the lab and the nice tea breaks.

Then, I would like to thank the students that I supervised, Emilio and Carolina. Emilio I am very grateful for your work and our fruitful collaboration. Carolina, it was a pleasure working with you.

During my time in Switzerland, I had the chance to meet a lot of great people. Thank you all for the stimulating discussions as well as happy distractions to rest my mind outside of my research. Many of you are now located worldwide, and I wish to stay in touch and meet up in the future.

Special thanks to Aryan and Dorsa, for your optimistic spirits and our travels together. Emmi and Lana, for the enjoyable moments together. My fellow Dutchies in Switzerland, Dieuwertje, Matthijs and Bastiaan, thanks for the fun snow and hiking trips, and dinners. Tim, Mark, Carl, Marylin, and Suzanne, thanks for the nice discussions and we had great fondues and beer o' clocks. Suzanne, thanks for your support, and for our awesome and unforgettable (motorcycle) adventures. Thanks to my motorcycle friends for the amazing rides in Europe.

Thanks to my friends in the Netherlands for staying in touch. Tessa, Natascha, and Aniek, our trips in Switzerland and Europe were very enjoyable and we had great laughs.

I would like to thank my family in the Netherlands and Israel for their support. Milko and Tamar, thank you for encouraging me throughout my career. Last but not least, I would like to thank my parents, Esther and Gerald, and my brother, Gijs. I am grateful for the wise council (around the campfire), the endless patience, and the sympathetic ear. Thank you so much for your unconditional support and believing in me so I can pursue my dreams.

Lausanne, November 1<sup>st</sup> 2021

# Abstract

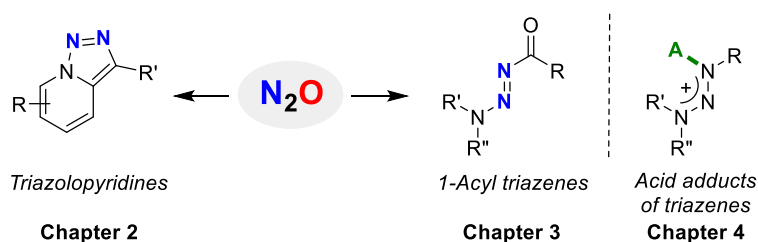
Nitrous oxide ( $\text{N}_2\text{O}$ ) has gained much interest because of its physiological effects (“laughing gas”) and its negative environmental impact (“greenhouse gas”, “ozone-depleting substance”): It has a lifetime of more than 100 years in the atmosphere. Its persistent character shows how challenging it is to convert  $\text{N}_2\text{O}$  into more valuable products. From a synthetic point of view,  $\text{N}_2\text{O}$  has potential as diazo ( $\text{N}_2$ ) transfer reagent, but applications in synthetic organic chemistry are scarce. The main challenges are to capture  $\text{N}_2\text{O}$ , avoid the loss of  $\text{N}_2$ , and to overcome poor-selectivity and -yields.

Herein, we describe two examples of the incorporation of two nitrogen atoms into the final product. Firstly, we use  $\text{N}_2\text{O}$  as diazo transfer reagent in the preparation of triazolopyridines, which are valuable starting materials for heterocyclic compounds. The reactions can be performed under mild conditions and give synthetically interesting triazoles in moderate to good yields. Secondly, general methods to N1 acylated triazenes were missing previously. We developed routes to 1-acyl triazenes via acid-catalyzed hydration, or by gold- or iodine-catalyzed oxidation of 1-alkynyl triazenes. The latter compounds are prepared from  $\text{N}_2\text{O}$ . The properties of the N1 acylated triazenes are distinct compared to other triazenes, displaying different physical and chemical properties. Under strong acidic conditions, 1-acyl triazenes act as acylation reagents. Finally, despite that triazene chemistry is known for more than 160 years, the preferred coordination site of acids still remained a matter of debate (N1, N2, or N3). In search of experimental evidence, we have analyzed triflic acid,  $\text{B}(\text{C}_6\text{F}_5)_3$ , and  $\text{PdCl}_2$  adducts of triazenes by IR, NMR spectroscopy and single crystal X-ray crystallography. For all cases, we found the acid coordinating to the N1 atom of the triazene. This preference should be taken into account for future acid- and transition metal-catalyzed reactions with triazenes.

Altogether, this thesis contributes to triazene chemistry and synthetic chemistry with  $\text{N}_2\text{O}$ . In this way, we provide further evidence that  $\text{N}_2\text{O}$  can be used as a diazo donor to get to synthetically interesting N-containing products.

## Keywords

Nitrous oxide, diazo transfer, triazolopyridines, triazenes, synthetic organic chemistry



# Résumé

Le protoxyde d'azote ( $N_2O$ ) a suscité beaucoup d'intérêt pour ses effets physiologiques ("gaz hilarant") et son impact environnemental négatif ("gaz à effet de serre", "substance appauvrissant la couche d'ozone") : il a une durée de vie de plus de 100 ans dans l'atmosphère. Son caractère persistant montre à quel point il peut être difficile de convertir le  $N_2O$  en produits plus précieux. D'un point de vue synthétique, le  $N_2O$  a un potentiel en tant que réactif de transfert diazo ( $N_2$ ), mais les applications en chimie organique synthétique sont rares. Les principaux défis sont de capturer le  $N_2O$ , d'éviter la perte de  $N_2$  et de surmonter la mauvaise sélectivité et les rendements.

Ici, nous décrivons deux exemples de l'incorporation de deux atomes d'azote dans le produit final. Premièrement, nous utilisons  $N_2O$  comme réactif de transfert diazo dans la préparation de triazolopyridines, qui sont des matières premières précieuses pour les composés hétérocycliques. Les réactions peuvent être effectuées dans des conditions douces et donnent des triazoles synthétiquement intéressants avec des rendements modérés à bons. Deuxièmement, car les méthodes générales pour les triazènes acylés N1 manquaient auparavant, nous avons développé des voies vers les 1-acyl triazènes via une hydratation catalysée par un acide, ou par oxydation catalysée par l'or ou l'iode de 1-alcynyl triazènes. Ces derniers composés sont préparés à partir de  $N_2O$ . Les propriétés des triazènes acylés N1 sont distinctes par rapport aux autres triazènes, affichant des propriétés physiques et chimiques différentes. Dans des conditions fortement acides, les 1-acyl triazènes agissent comme des réactifs d'acylation. Enfin, bien que la chimie des triazènes soit connue depuis plus de 160 ans, le site de coordination préféré des acides restait encore un sujet de débat (N1, N2 ou N3). À la recherche de preuves expérimentales, nous avons analysé les adduits d'acide triflique,  $B(C_6F_5)_3$  et  $PdCl_2$  des triazènes par spectroscopie IR, RMN et cristallographie aux rayons X sur un seul cristal. Pour tous les cas, nous avons trouvé l'acide se coordonnant à l'atome N1 du triazène. Cette préférence doit être prise en compte pour les futures réactions catalysées par des acides et des métaux de transition avec des triazènes.

Au total, cette thèse contribue à la chimie des triazènes et à la chimie de synthèse avec  $N_2O$ . De cette façon, nous fournissons une preuve supplémentaire que le  $N_2O$  peut être utilisé comme donneur diazoïque pour obtenir des produits contenant de l'azote synthétiquement intéressants.

## Mot clés

Protoxyde d'azote, transfert diazo, triazolopyridines, triazènes, chimie organique de synthèse

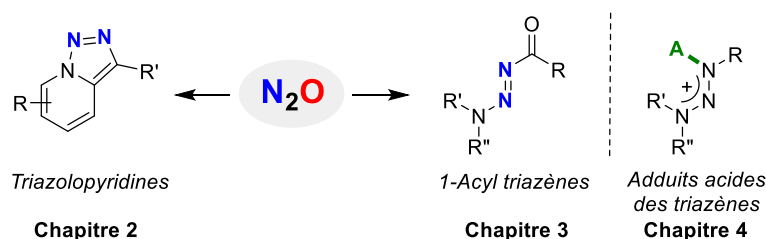


# Table of contents

Acknowledgements.....	i
Abstract.....	iii
Résumé.....	iv
Table of contents.....	v
List of abbreviations and symbols .....	ix
1 Introduction.....	1
1.1 General introduction to N <sub>2</sub> O .....	2
1.2 N <sub>2</sub> O as oxygen atom donor .....	3
1.3 N <sub>2</sub> O as nitrogen atom donor.....	10
1.4 Synthesis and chemistry of 1-alkynyl triazenes .....	14
1.5 Objectives of the thesis .....	18
2 Nitrous oxide as diazo transfer reagent: the synthesis of triazolopyridines .....	19
2.1 Introduction.....	20
2.2 Synthesis of the triazoles <b>2.1–2.10</b> .....	20
2.3 Synthesis of the triazoles <b>2.11–2.15</b> .....	23
2.4 Synthesis of the triazole <b>2.17</b> .....	26
2.5 Mechanistic considerations .....	29
2.6 Conclusion .....	32
3 Synthesis and properties of 1-acyl triazenes .....	33
3.1 Introduction.....	34
3.2 Synthesis of the alkyl 1-acyl triazenes <b>3.1–3.9</b> .....	35
3.3 Synthesis of the olefinic 1-acyl triazenes <b>3.10–3.16</b> .....	37
3.4 Synthesis of the 1,2-diketo triazenes <b>3.17–3.22</b> .....	39
3.5 Synthesis of the $\alpha$ -halogenated 1-acyl triazenes <b>3.23–3.28</b> .....	41
3.6 X-ray crystallographic data.....	41
3.7 NMR Coalescence studies .....	43
3.8 Temperature stability .....	46
3.9 Hydrolytic stability .....	48
3.10 Acid sensitivity .....	49
3.11 Reactivity studies .....	51
3.12 Biological assays.....	52

3.13	Conclusion .....	54
4	Brønsted and Lewis acid adducts of triazenes .....	55
4.1	Introduction.....	56
4.2	Brønsted acid adducts of 1-acyl triazenes <b>4.1–4.3</b> .....	57
4.3	Brønsted acid adduct of 1-aryl-3,3-dialkyl triazene <b>4.4</b> .....	61
4.4	Lewis acid adducts of triazenes <b>4.5–4.7</b> .....	61
4.5	Bond length comparison .....	63
4.6	Conclusion .....	64
5	Conclusion and outlook .....	65
	Experimental section (ES) .....	67
	ES.1 Materials and methods .....	68
	ES.1.1 Notes for Chapter 2: .....	68
	ES.1.2 Notes for Chapter 3: .....	68
	ES.1.3 Notes for Chapter 4: .....	69
	ES.2 Experimental section: triazolopyridines .....	69
	ES.2.1 Synthesis of the triazoles <b>2.1–2.10</b> .....	69
	ES.2.2 Synthesis of the triazoles <b>2.11–2.15</b> .....	74
	ES.2.3 Synthesis of the triazole <b>2.17</b> .....	78
	ES.2.4 X-ray crystallographic data .....	79
	ES.2.5 Biological assays .....	81
	ES.2.6 Selected NMR Spectra .....	82
	ES.3 Experimental section: 1-acyl triazenes.....	88
	ES.3.1 Synthesis of the triazenes <b>3.a–3.b</b> .....	88
	ES.3.2 Synthesis of the alkyl 1-acyl triazenes <b>3.1–3.9</b> .....	89
	ES.3.3 Synthesis of the olefinic 1-acyl triazenes <b>3.10–3.16</b> .....	94
	ES.3.4 Synthesis of the 1,2-diketo triazenes <b>3.17–3.22</b> .....	98
	ES.3.5 Synthesis of the $\alpha$ -halogenated 1-acyl triazenes <b>3.23–3.28</b> .....	101
	ES.3.6 Synthesis of the unpublished triazenes <b>3.31–3.33</b> .....	104
	ES.3.7 NMR Coalescence studies.....	105
	ES.3.8 Temperature stability.....	106
	ES.3.9 Hydrolytic stability.....	106
	ES.3.10 Acid sensitivity.....	106
	ES.3.11 Reactivity studies .....	107

ES.3.12 X-ray crystallographic data .....	111
ES.3.13 Biological assays .....	114
ES.3.14 Selected NMR Spectra .....	117
ES.4 Experimental section: triazene adducts .....	122
ES.4.1 Synthesis of the protonated 1-acyl triazenes <b>4.1–4.3</b> .....	122
ES.4.2 Synthesis of the B(C <sub>6</sub> F <sub>5</sub> ) <sub>3</sub> adducts <b>4.5</b> and <b>4.6</b> .....	123
ES.4.3 Synthesis of the Pd complex <b>4.7</b> .....	125
ES.4.4 IR Spectroscopic data.....	126
ES.4.5 X-ray crystallographic data .....	128
ES.4.6 NMR Spectra.....	132
References.....	139
Curriculum Vitae .....	149



# List of abbreviations and symbols

°	degree	equiv	equivalent
Å	Angstrom	ESI-MS	electrospray ionization mass spectrometry
ACN	acetonitrile		
AcOH	acetic acid	Et	ethyl
Anal. Calcd.	combustion elemental analysis	<i>et al.</i>	<i>et alias</i> , and others
	calculated	Et <sub>2</sub> O	diethyl ether
APCI	atmospheric pressure chemical ionization	EtOAc	ethyl acetate
APPI	atmospheric pressure photoionization	g	gram
aq.	aqueous	GC-MS	gas chromatography mass spectrometry
BCF	tris(pentafluorophenyl) borane	h	hour
Br <sub>2</sub>	bromine	hept	heptet
Bn	benzyl	HMPA	hexamethylphosphoramide
°C	degree Celsius	HRMS	high-resolution mass spectrometry
<i>ca.</i>	circa	Hz	Hertz (s <sup>-1</sup> )
calc.	calculated	I <sub>2</sub>	iodine
CDCl <sub>3</sub>	deuterated chloroform	IC <sub>50</sub>	half maximal inhibitory concentration
CD <sub>2</sub> Cl <sub>2</sub>	deuterated dichloromethane		
CD <sub>3</sub> CN	deuterated acetonitrile	<i>i</i> Pr	iso-propyl
CD <sub>3</sub> OD	deuterated methanol	IR	infrared
cm <sup>-1</sup>	1/centimeter	<i>J</i>	coupling constant
Cy	cyclohexyl	K	Kelvin
δ	chemical shift	L	Liter
d	doublet	LDA	lithiumdiisopropylamide
DCE	dichloroethane	LTQ	linear trap quadrupole
DCM	dichloromethane	μ	micro
dd	doublet of doublets	m	multiplet (NMR) or medium (IR)
ddd	doublet of doublets of doublets	<i>m</i>	<i>meta</i>
dddd	doublet of doublet of doublet of doublets	M	molar (mol/L)
	doublets	<i>m/z</i>	mass number over charge number
ddt	doublet of doublet of triplets	Me	methyl
Dipp	2,6-diisopropylphenyl	Mes	mesityl
DMF	dimethylformamide	mg	milligram
DMSO	dimethylsulfoxide	MHz	megahertz
DNA	deoxyribonucleic acid	min	minute
dq	doublet of quintets	ml	milliliter
dt	doublet of triplets	mM	millimolar (mmol/L)
<i>ee</i>	enantiomeric excess	mmol	millimole
<i>e.g.</i>	exempla gratia	mol	mole
EI	electron impact ionization	mol%	mol percent

MS	mass spectrometry
MW	molecular weight
NBS	<i>N</i> -Bromosuccinimide
NCS	<i>N</i> -Chlorosuccinimide
NIS	<i>N</i> -Iodosuccinimide
nm	nanometer
NMR	nuclear magnetic resonance
N <sub>2</sub> O	nitrous oxide
<i>n</i> -Bu	<i>n</i> -butyl
NMR	nuclear magnetic resonance
NTf <sub>2</sub>	triflimide, bis(trifluoromethane)sulfonimide
<i>o</i>	ortho
OTf	triflate, trifluoromethanesulfonate
<i>p</i>	para
Ph	phenyl
ppm	parts per million
q	quartet
QTOF	quadrupole time of flight
Ref.	Reference
RP-HPLC	Reversed phase high performance liquid chromatography
RT or rt	room temperature
s	singlet
sat.	saturated
<i>s</i> -Bu	<i>sec</i> -butyl
<i>t</i>	<i>tert</i>
t	time or triplet
T	temperature
<i>t</i> -Bu	<i>tert</i> -butyl
td	triplet of doublets
TFA	trifluoroacetic acid
TGA	thermogravimetric analysis
THF	tetrahydrofuran
Tipp	C <sub>6</sub> H <sub>2</sub> -2,4,6- <i>i</i> Pr <sub>3</sub>
TLC	thin-layer chromatography
TMEDA	tetramethylethylenediamine
TMP	2,2,6,6-tetramethylpiperidine
TON	turn over number
tt	triplet of triplets
ν <sub>max</sub>	maximum wavenumber
<i>vac</i>	vacuum
XRD	X-ray diffraction

Note: other abbreviations for specific compounds are defined within the thesis

# 1 Introduction



## 1.1 General introduction to N<sub>2</sub>O

Nitrous oxide (N<sub>2</sub>O), commonly known as “laughing gas”, has had a remarkable journey throughout history.<sup>1</sup> It was discovered by Joseph Priestly in 1772, and not long after that, the euphoric effects upon inhalation were discovered. That was picked up by dentistry and surgery, and nowadays N<sub>2</sub>O is used as an anaesthetic and it is listed as one of essential medicines by the World Health Organization (WHO).<sup>2</sup> Besides that, N<sub>2</sub>O has been applied as a food additive (E942, aerosol spray propellant) in whipped cream and cooking sprays. Other than that, it is added to rocket fuel to increase the power of the engine (Figure 1.1).

Despite of its many applications, there is a dark side of N<sub>2</sub>O: its negative environmental impact.<sup>3–7</sup> With a global warming potential (GWP) of 265-298, N<sub>2</sub>O is the third most emitted greenhouse gas and is acknowledged as an ozone-depleting substance. The atmospheric lifetime of N<sub>2</sub>O is more than 100 years,<sup>8</sup> which indicates how difficult it can be to break it down, and, thus, it is often regarded as an inert molecule. In nature, N<sub>2</sub>O is produced and converted to N<sub>2</sub> via an enzymatic pathway in microbial processes.<sup>9,10</sup> Despite of this natural decrease process, emissions of N<sub>2</sub>O are increasing.

Close to two thirds of N<sub>2</sub>O in the atmosphere is produced in oceans and soils. The other third is due to human-based emissions via agriculture and industrial processes.<sup>3,11–13</sup> Since 1980, human-induced emissions have increased by 30%, which is faster than scientists had assumed previously.<sup>5</sup> The largest industrial sources of N<sub>2</sub>O as by-product are the manufacturing of nitric acid (the Ostwald process) as raw material for fertilizer, and the synthesis of adipic acid and caprolactam for Nylon production. Consequently, attention has increased in climate control discussions to set regulations to limit emissions, to capture, and abate N<sub>2</sub>O.<sup>4</sup>

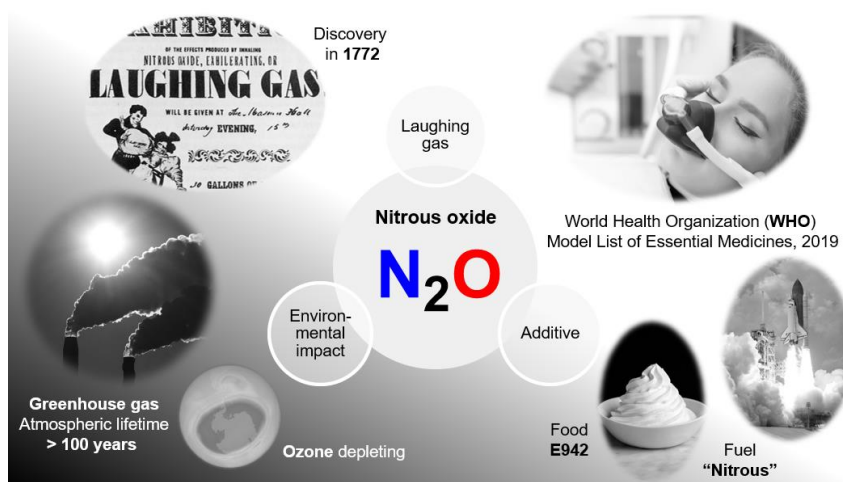


**Figure 1.1** Discovery, applications, and environmental impact of N<sub>2</sub>O.

From a synthetic point of view,  $\text{N}_2\text{O}$  is a promising reagent in organic synthesis.<sup>14</sup> In 2018,  $\text{N}_2\text{O}$  was incorporated in the Encyclopedia of Reagents for Organic Synthesis (Figure 1.2).<sup>15</sup> Despite of its inert character, scientists have discovered ways to successfully activate  $\text{N}_2\text{O}$  and use it as a building block in synthetic chemistry. To obtain an acceptable conversion, high pressures ( $> 25$  bar) and high temperatures ( $> 200$  °C) are often required, but recent studies employ milder, and more general conditions. Furthermore, several methods have shown that using  $\text{N}_2\text{O}$  over comparable reagents is advantageous for the reaction outcomes. Moreover, new products can be made of which  $\text{N}_2\text{O}$  is an essential building block. More applications towards fine chemical synthesis are emerging to get new synthetically interesting products, *e.g.* starting materials for pharmaceuticals or other functional materials.

In this chapter, we highlight and discuss developments of  $\text{N}_2\text{O}$  in synthetic organic chemistry, particularly aiming at generalized methods, mild conditions, and scope explorations of synthetically interesting products. Note that heterogeneous/homogeneous catalytic reactions, and metal-free, main group chemistry (frustrated Lewis Pairs)<sup>16</sup> and bio(in)organic chemistry (*e.g.* Nitrous Oxide Reductase) of  $\text{N}_2\text{O}$  are discussed extensively in the literature.<sup>9,17–20</sup>

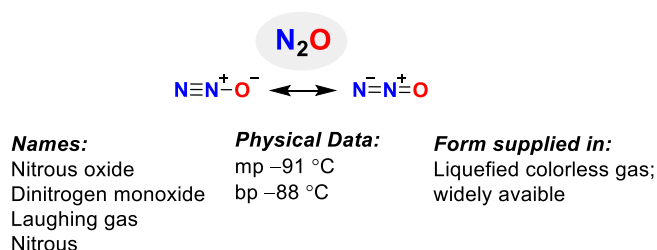


**Figure 1.2** General properties of  $\text{N}_2\text{O}$ . Adapted from J. H. Conway, *Encycl. Reagents Org. Synth.* 2018.<sup>15</sup>

## 1.2 $\text{N}_2\text{O}$ as oxygen atom donor

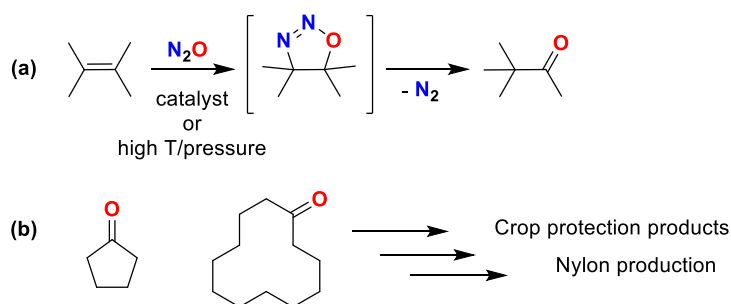
### 1.2.1 High temperature, pressure, and/or heterogeneous catalysts

The selective oxidation of olefins to ketones or aldehydes is a challenging reaction. In the Wacker process, the oxidation of alkenes is performed with oxygen and homogeneous  $\text{PdCl}_2/\text{CuCl}_2$  catalyst in the presence of  $\text{HCl}$ . However, high selectivity remains challenging, chlorinated waste products are formed, and it can be difficult to recover the catalyst. To optimize the selective oxidation,  $\text{N}_2\text{O}$  has been explored as alternative oxidant.  $\text{N}_2\text{O}$  is a thermodynamically strong oxidant, producing in principle only  $\text{N}_2$  as a side product. Compared to  $\text{O}_2$ , the release of the oxygen atom is energetically more favorable ( $\Delta_r G^0_{298} = 30.5$  kcal/mol for  $\text{N}_2\text{O}$  vs.  $\Delta_r G^0_{298} = 55.3$  kcal/mol for  $\text{O}_2$ ). However,  $\text{N}_2\text{O}$  is

kinetically inert and thus requires overcoming a higher activation barrier (50-60 kcal/mol).<sup>21</sup> Therefore, high temperatures, high pressures or catalysts are required to successfully perform oxidations with N<sub>2</sub>O (Scheme 1.1 a).

In non-catalytic approaches, high temperatures (> 180 °C) and pressures (> 10 bar) lead to the oxidation of C=C bonds in the gas-phase, liquid-phase and polymers,<sup>22,23</sup> or the oxidization of C=O bonds such as for benzaldehyde.<sup>24</sup> Via ball milling of sodium oxides and alkali metal and halide salts, compounds *cis*-Na<sub>2</sub>N<sub>2</sub>O<sub>2</sub> and NaNO<sub>3</sub> are produced in the presence of N<sub>2</sub>O.<sup>25</sup>

In these cases, harsh conditions are applied to obtain acceptable yields and the scopes are sometimes rather limited. Alternatively, heterogeneous catalysts have been employed in selective oxidations, such as Fe-containing ZSM-5 zeolites for the oxidation of benzene and other aromatic compounds to alcohols,<sup>26</sup> and the oxidation of methane and ethane to alcohols and aldehydes.<sup>27</sup> In particular, the oxidation of benzene to phenol with ~100% selectivity has been remarkable, as efforts with oxygen have not been successful. Apparently, N<sub>2</sub>O has the unique property to selectively oxidize double bonds, due to the non-radical reaction mechanism and its inertness to other types of bonds. Moreover, it is a rather cheap reagent, readily accessible and convenient to handle. Demonstrating the practical applicability of N<sub>2</sub>O, BASF developed and commissioned in 2019 two new industrial processes for the oxidation of olefins to ketones by N<sub>2</sub>O (Scheme 1.1 b).<sup>22</sup> In these industrial processes, two valuable products, cyclopentanone (for crop protection products) and cyclodecanone (for raw materials in Nylon production), are synthesized by using N<sub>2</sub>O that has been recovered from the waste gas of the adipic acid production.



**Scheme 1.1** General oxidation reaction of alkenes by N<sub>2</sub>O (a). Ketones synthesized on industrial scale via N<sub>2</sub>O (b).

## 1.2.2 Transition metal activation and catalysis

1.2.2.1 Activation and characterization of the  $N_2O$  complex

Another strategy to activate  $N_2O$  is by using transition metal complexes. It is known that  $N_2O$  is a poor ligand,<sup>28</sup> and thus it is challenging to activate it and fully characterize the resulting complex. Nonetheless, more examples of well-characterized  $N_2O$  complexes are emerging with metal centers, such as with Ru, V, Ni, Cu, Rh, and Co atoms (Figure 1.3).<sup>29–36</sup> These structures provide valuable knowledge on the coordination modes of  $N_2O$  and demonstrate that  $N_2O$  can act as a ligand. The right balance of  $\pi$ -basicity is obtained by tuning the metal center and corresponding ligands, while preventing the oxidation of the metal center. Nowadays, well-characterized  $N_2O$  complexes by NMR, IR, and XRD, with various transition metal centers have been reported.

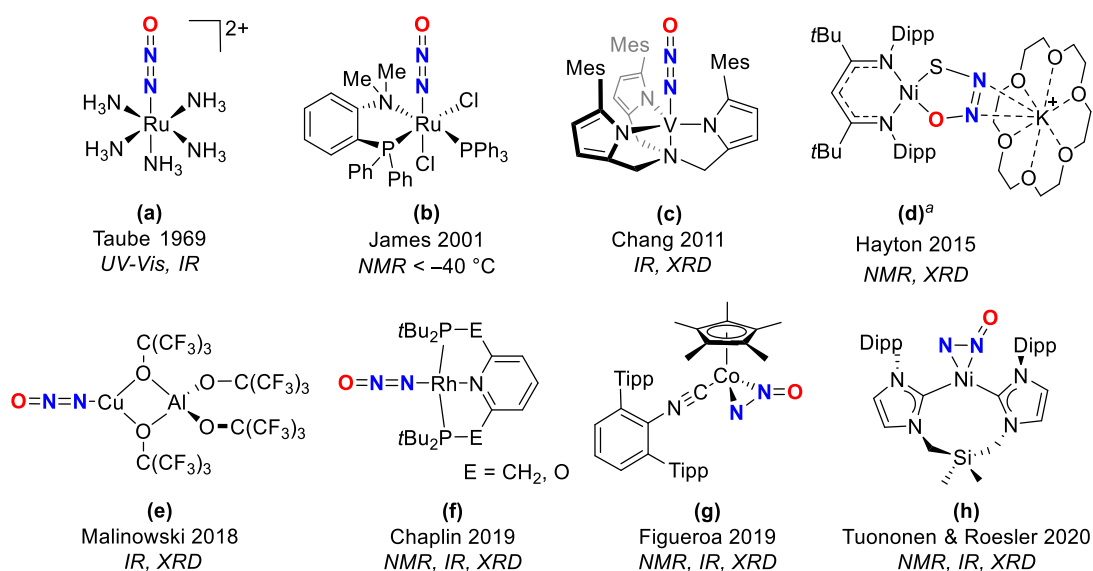


**Figure 1.3** Synthesis of structurally characterized  $N_2O$  transition metal complexes. <sup>a</sup>  $N_2O$  activated transition-metal complex.

### 1.2.2.2 Oxygen transfer to the complex

Compared to molecular intact  $\text{N}_2\text{O}$ -complexes, more studies on oxygen transfer reactions with transition metal complexes have been reported. Known oxidations of the ligand and/or metal center are with Ti, Cr, V, Ni, Ru, Ir, Sm, and U transition metal complexes.<sup>14</sup> Recent examples (Figure 1.4) show the oxidation of Ir pincer complexes,<sup>37,38</sup> a dinuclear cobalt pincer complex,<sup>39</sup> a nickel thioperoxide complex,<sup>40</sup> and a di-iron imidophosphorane complex.<sup>41</sup>

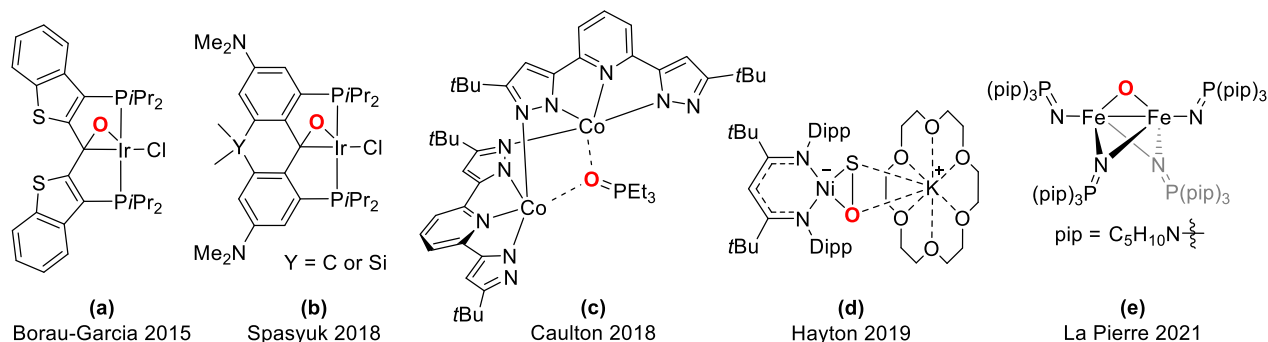


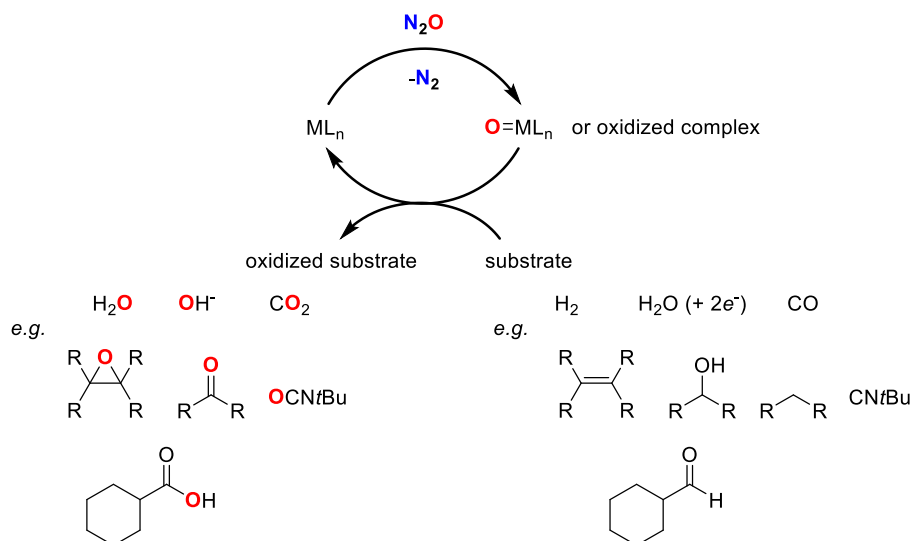
**Figure 1.4** Oxygen transfer reaction to transition metal complexes recent examples.

### 1.2.2.3 Oxygen transfer to substrate

Important progress has also been made in the utilization of  $\text{N}_2\text{O}$  as an oxidant in homogeneous, transition metal-catalyzed reactions (Scheme 1.2).

First reports on the hydrogenation of  $\text{N}_2\text{O}$  to water have been reported, but were limited to stoichiometric activation.<sup>37,42,43</sup> Then, a catalytic hydrogenation was achieved using a Ru PNP pincer complex (TON 417).<sup>44</sup> This reaction proceeds under relatively mild reaction conditions (65 °C) in comparison to the heterogeneous catalyzed hydrogenation of  $\text{N}_2\text{O}$  (250-500 °C).<sup>45-47</sup> In 2021, a bimetallic Rh-Pt catalyst was developed that exceeds the previous efficiency (TON 587).<sup>48</sup> A recent reported silylene-iron complex was able to deoxygenate  $\text{N}_2\text{O}$ , with a TON of up to 1400.<sup>49</sup> The deoxygenation of  $\text{N}_2\text{O}$  can also be achieved in the presence of Re complexes photocatalytically to form water,<sup>50</sup> or electrochemically to form hydroxide ions.<sup>51</sup>

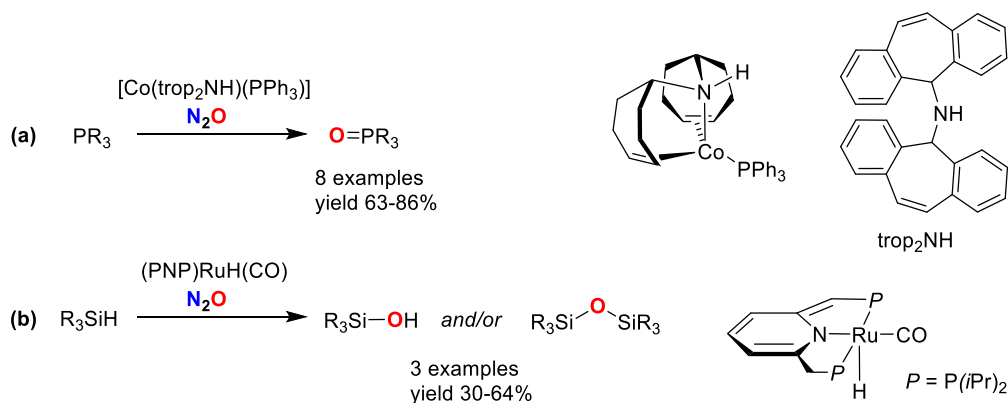
Other transition metal-catalyzed reactions include the oxidation of CO to  $\text{CO}_2$  by pincer complexes,<sup>52</sup> different organic substrates with Ru-porphyrin<sup>53,54</sup> or polyoxometalate catalysts,<sup>55-57</sup> and isocyanide in the presence of an organometallic Mo catalyst.<sup>58</sup> The oxidative coupling of Grignard reagents can be realized via metal catalysis.<sup>59</sup>



**Scheme 1.2** Catalytic cycle of  $\text{N}_2\text{O}$  oxidation and examples of substrates and products.

Recently, new applications of oxygen transfer from  $\text{N}_2\text{O}$  under relatively mild conditions with broader scopes have emerged. For example, the transfer of oxygen to phosphines to form the corresponding phosphine oxides is possible with a cobalt catalyst under mild conditions (25–70 °C, 7–22 h, 2 bar  $\text{N}_2\text{O}$ ) (Scheme 1.3 a).<sup>60</sup> Some of the employed phosphanes are highly  $\text{O}_2/\text{H}_2\text{O}$  sensitive, and benefit from the selective oxidation by  $\text{N}_2\text{O}$ , resulting in higher efficiency compared to other standard oxidation methods.

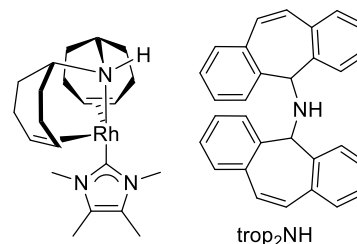
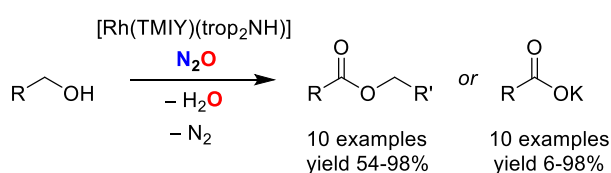
In another transition metal-catalyzed oxygen atom transfer, the hydrosilylation of  $\text{N}_2\text{O}$  was achieved using a Ru-pincer complex (Scheme 1.3 b).<sup>44</sup> Initially, the reaction was optimized for the hydrogenation of  $\text{N}_2\text{O}$  to form  $\text{H}_2\text{O}$ . With the optimal catalyst, oxygen transfer is applicable to three different silanes, resulting in moderate yields under mild conditions (65 °C, 36–72 h, ~3.5 bar  $\text{N}_2\text{O}$ ).



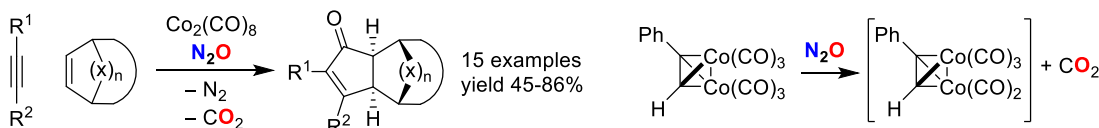
**Scheme 1.3** Oxygen transfer from  $\text{N}_2\text{O}$  to substrate transition-metal catalyzed.

Other recent studies have used  $\text{N}_2\text{O}$  to activate the catalyst by selective oxidation in synthetic transformations (Scheme 1.4). With a Rh-catalyst, nitrous oxide acts as hydrogen acceptor for the dehydrogenative coupling of alcohols (Scheme 1.4 a).<sup>61</sup> The reaction proceeds under mild conditions and low catalyst loadings (50 °C, 7–22 h, 1 bar  $\text{N}_2\text{O}$ ). By varying the amount of  $\text{KO}t\text{Bu}$ , either the carboxylate or the ester was obtained in yields ranging from 6–98%. In another example, Pauson–Khand cycloadditions are promoted by  $\text{N}_2\text{O}$  (Scheme 1.4 b).<sup>62</sup> The role of  $\text{N}_2\text{O}$  is to oxidize the CO ligand, rather than the Co atom. With this method, no pre-synthesis of an acetylene complex is required and only gaseous byproducts are formed. This reaction has been applied in the total synthesis of (+)-Waihoensene (Scheme 1.4 c).<sup>63</sup> To perform the cycloaddition, several conditions were initially screened, such as combinations of  $\text{Co}_2(\text{CO})_8$  and other oxygen atom transfer reagents (*e.g.* trimethylamine *N*-oxide, methyl morpholine *N*-oxide, and tetramethyl thiourea), as well as other catalysts, such as Pd- or Rh-based ones. However, only low yields (< 38%) were obtained. The use of  $\text{N}_2\text{O}$ , however, was advantageous and yielded 59% with 93% *ee*.

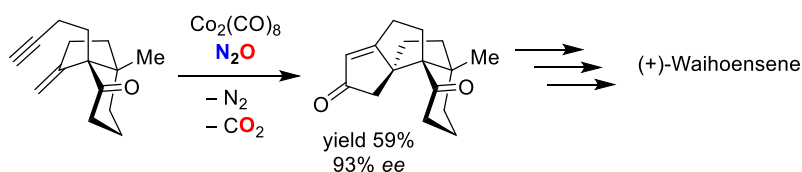
**(a) Dehydrogenative coupling of alcohols**



**(b) Pauson-Khand**



**(c) Pauson-Khand applied in total synthesis**



**Scheme 1.4** Nitrous oxide as hydrogen acceptor (a). Oxygen transfer from  $\text{N}_2\text{O}$  to activate the catalyst in a Pauson-Khand reaction (b). Application of an  $\text{N}_2\text{O}$ -promoted Pauson-Khand reaction in total synthesis (c).

## 1.2.3 Main group compounds

The selective oxidation of low valent main group compounds by  $\text{N}_2\text{O}$  is also possible. Examples include low valent silicon, germanium, basic phosphines, phosphorane, sodium sulphite, and boranes.<sup>14</sup> Recent examples (Figure 1.5) are the silanones,<sup>64,65</sup> monoalumoxane anion,<sup>66</sup> P-B system in the frustrated Lewis pair,<sup>67</sup> dialumenes,<sup>68</sup> two-coordinate acyclic iminosiloxysilylene,<sup>69</sup> and a boraalkene stabilized internally by a N-heterocyclic carbene.<sup>70</sup> For the monoalumoxane anion and the acyclic iminosiloxysilylene, the compound with intact  $\text{N}_2\text{O}$  were also isolated and fully characterized.

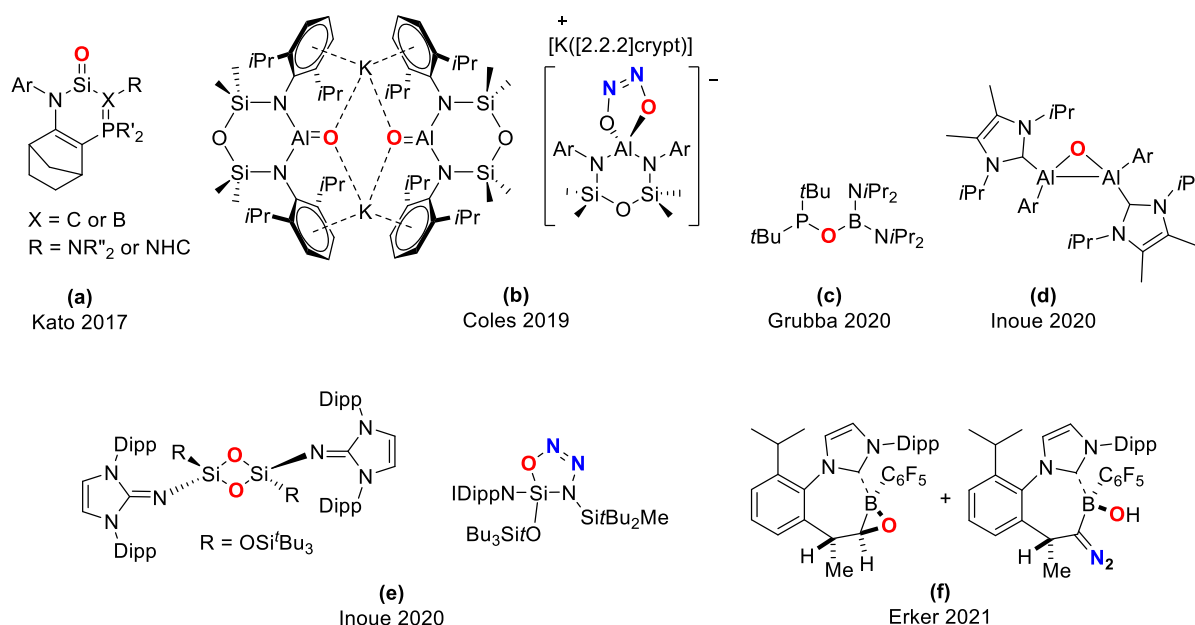
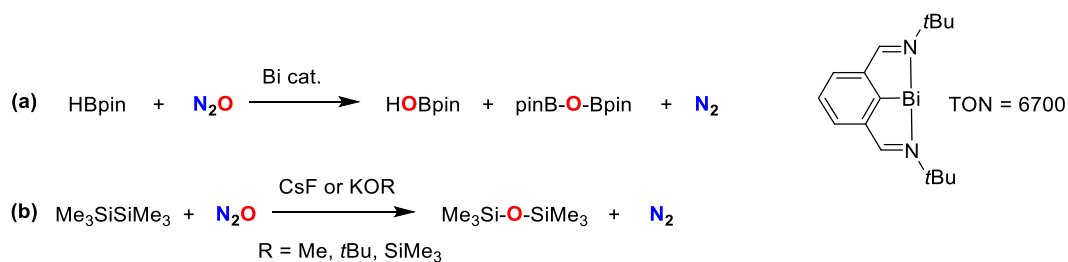


**Figure 1.5** Recent examples of oxidation of low valent main group compounds by  $\text{N}_2\text{O}$ .

Interestingly, catalytic activation can be achieved with a low-valent bismuth redox platform in the deoxygenation of  $\text{N}_2\text{O}$  (Scheme 1.5 a). A TON of up to 6700 was achieved.<sup>71</sup> Another metal-free catalytic reaction is the deoxygenation of  $\text{N}_2\text{O}$  with disilanes (Scheme 1.5 b). A catalytic amount of fluoride anions or alkoxides allowed for mild reduction at ambient pressure and temperature.<sup>72</sup>



**Scheme 1.5** Catalytic examples of the reduction of  $\text{N}_2\text{O}$  by main group compounds.

### 1.3 N<sub>2</sub>O as nitrogen atom donor

Using N<sub>2</sub>O as an oxygen atom donor has been studied extensively, as is described in the previous section. In contrast, applying N<sub>2</sub>O as a diazo transfer reagent has been limited so far. The main challenges are: 1) finding reactants that can activate N<sub>2</sub>O, 2) avoiding reactions which lead to loss of N<sub>2</sub>, and 3) ensuring the selective formation of a desired product.

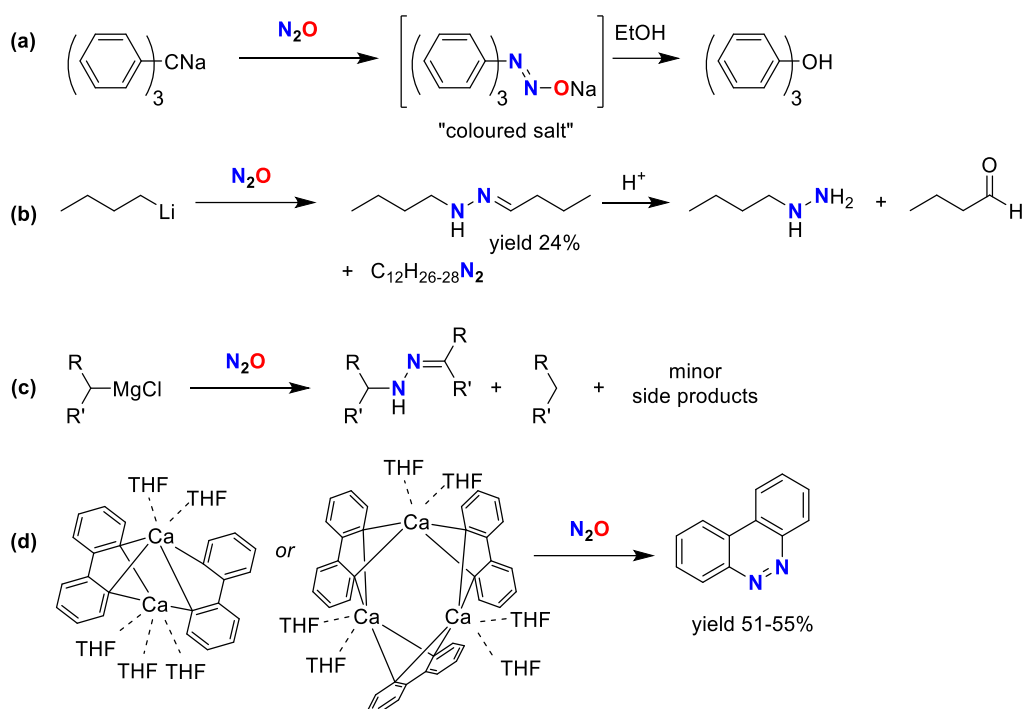
One notable example of N<sub>2</sub>O-diazo transfer dates back to 1892, when Wislicenus discovered the synthesis of sodium azide (NaN<sub>3</sub>) from NaNH<sub>2</sub> and N<sub>2</sub>O.<sup>73</sup> To date, this is an industrial method for preparing NaN<sub>3</sub> on large scale, which is a useful compound for biomedical applications, agricultural uses, and in synthetic chemistry for the preparation of other chemical compounds.<sup>74</sup> Moving onward from NaNH<sub>2</sub>, multiple metalated organic compounds were investigated for their ability of N<sub>2</sub>O activation and transfer of the nitrogen atoms. As a result, nitrogen containing compounds were observed with lithium-,<sup>75–84</sup> sodium-,<sup>85</sup> magnesium-,<sup>86</sup> and calcium-organic compounds,<sup>87–89</sup> but the transformations were often found to be non-selective, poor-yielding, and/or of limited scope.

In 1928, N<sub>2</sub>O activation was achieved by triphenyl sodium (Scheme 1.6 a),<sup>85</sup> forming a “coloured salt”, which can be attributed to the diazotate. Upon the addition of an alcoholic solvent, the final product triphenyl methanol was obtained. The diazotate intermediate is often depicted as the intermediate in organometallic N<sub>2</sub>O activation. Diazotates are highly reactive and are potentially explosives.<sup>90</sup> Due to the high reactivity of these compounds, it can be challenging to isolate it and control the reactivity. Further reactions with nucleophiles are sometimes unavoidable, such as in the presence of organometallic compounds. Other proposed reaction pathways are the formation of the reactive diazo species with the loss of metal hydroxide, or a bimolecular reaction with the removal of metal oxides.

In the case of *n*-butyl lithium (*n*-BuLi), the main product, the hydrazone, is formed in 24% yield (Scheme 1.6 b), indicating that at least two moles of *n*-BuLi had reacted.<sup>84</sup> Other than that, multiple side products are reported, including other N-containing products. For other organolithium reactions with N<sub>2</sub>O, various substituents have been screened, such as primary, secondary, and tertiary alkyl substituents, amines, and aromatic substituents.<sup>75–84</sup> A mixture of products and poor selectivity was also found with these substituents.

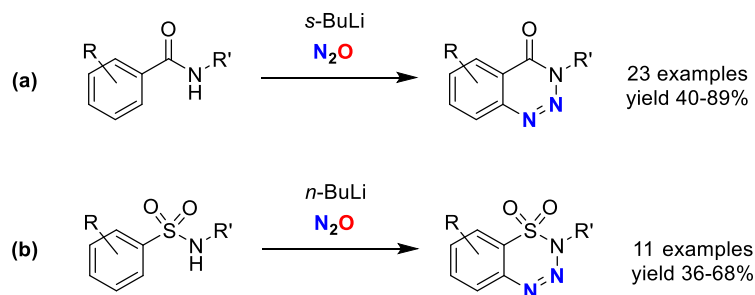
For organomagnesium compounds, it was generally assumed that they do not react with N<sub>2</sub>O. Early attempts in 1913 by Zerner showed no conversion of MeMgI with N<sub>2</sub>O, which was later confirmed by Beringer in 1953.<sup>84,91</sup> Despite of the general assumption that Grignard reagents do not react with N<sub>2</sub>O, Severin and co-workers showed that reactions of *i*PrMgCl and BnMgCl with N<sub>2</sub>O do give hydrazones (Scheme 1.6 c), and their corresponding hydrazinium salts were isolated in 44-63% yield.<sup>86</sup>

Finally, some organocalcium complexes activating  $\text{N}_2\text{O}$  have been reported. For example, the biphenyl calcium complexes for the biphenyl heterocycle in moderate yields (Scheme 1.6 d).<sup>87</sup> A substrate scope was not explored in this case.



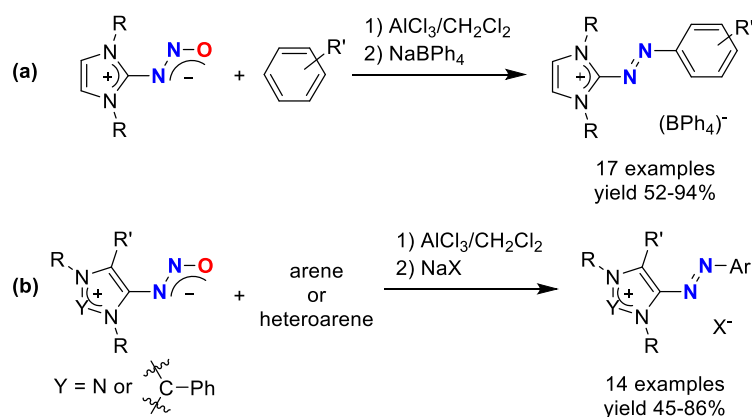
**Scheme 1.6** Examples of alkali-metal reagents with  $\text{N}_2\text{O}$  forming nitrogen containing products.

Only recently, synthetically interesting diazo transfer reactions with  $\text{N}_2\text{O}$  have emerged. For example, the synthesis of different benzotriazinones results from the treatment of amides and sulfonamides with BuLi reagents and  $\text{N}_2\text{O}$  (Scheme 1.7).<sup>92</sup> It is known that these types of heterocycles can be biologically active and they are used as building blocks in organic synthesis.



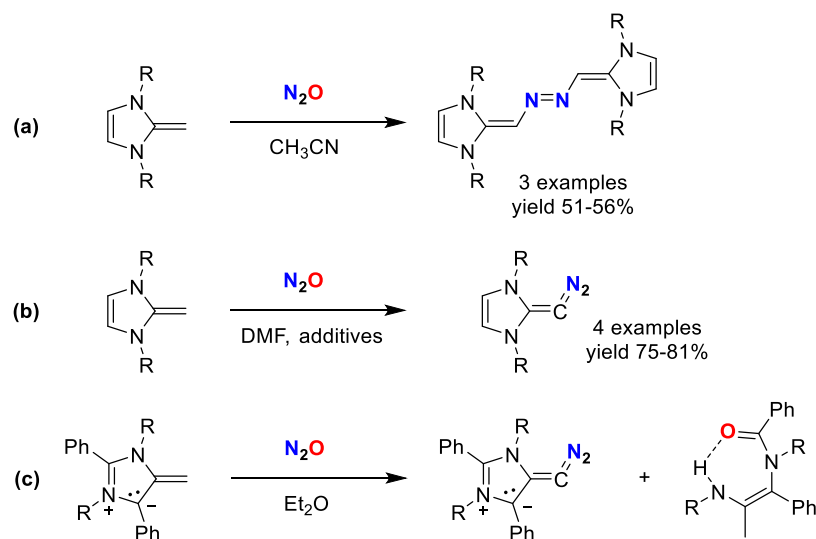
**Scheme 1.7**  $\text{N}_2\text{O}$  in the synthesis of benzotriazinones from amides (a), and sulfonamides (b).

The discovery of  $\text{N}_2\text{O}$  activation by N-heterocyclic carbenes, has led to the development of the synthesis of azoimidazolium salts.<sup>93</sup> The salts can be prepared from N-heterocyclic carbenes, arenes, and  $\text{N}_2\text{O}$  (Scheme 1.8).<sup>94,95</sup> These azo compounds are strongly colored, making them suitable for applications as dyes. Furthermore, they can be reduced to give stable aminyl radicals,<sup>96,97</sup> and they can serve as precursors for mesoionic carbene ligands.<sup>98</sup>



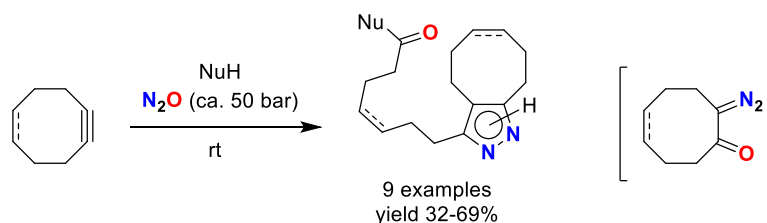
**Scheme 1.8**  $\text{N}_2\text{O}$  activation by N-heterocyclic carbenes and the coupling to form azo dyes.

Most recently,  $\text{N}_2\text{O}$  was used to prepare novel organic reducing agents based on N-heterocyclic olefins (Scheme 1.9 a).<sup>99</sup> These dimers can be converted into stable radical cations or a dicationic imidazolium salts. Their oxidation potentials allow for the reduction of aryl iodides, which demonstrates their utility as reducing agents in synthetic chemistry. When the solvent was switched to DMF and additives were added, diazoolefins were isolated in high yields (Scheme 1.9 b).<sup>100</sup> Isolation and characterization of these elusive intermediates for the first time allows for exploring new types of reactivities. For a mesoionic N-heterocyclic olefin, a similar product was obtained (Scheme 1.9 c).<sup>101</sup>



**Scheme 1.9**  $\text{N}_2\text{O}$  activation by N-heterocyclic olefins to form azo dimers (a), and diazoolefins (b, c).

The most atom economical reaction is to incorporate all the atoms into the final product. Plefka and Banert have achieved this goal by applying strained alkynes and a high pressure of  $\text{N}_2\text{O}$  to synthesize pyrazole derivatives (Scheme 1.10).<sup>102</sup> The reaction is proposed to proceed via a cycloaddition as 1,3-dipole of the diazonium betaine type, based on Huisgen's classification. The intermediate undergoes normally a rapid Wolff rearrangement. However, in the presence of a nucleophile, the pyrazole ring is formed and acylation takes place. The cycloaddition with  $\text{N}_2\text{O}$  is presumed to be the rate determining step.



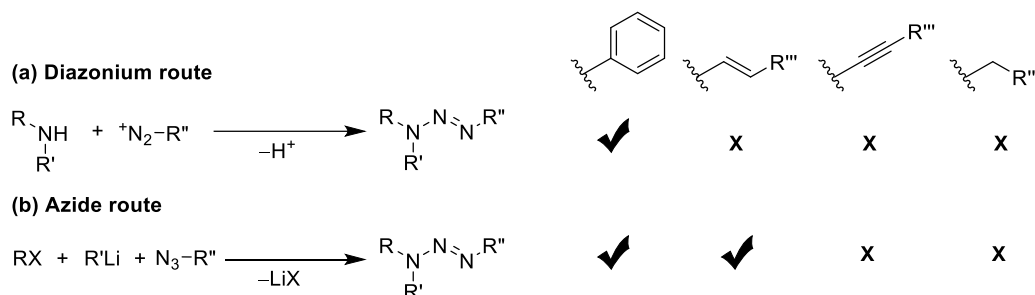
**Scheme 1.10** Full atom transfer of  $\text{N}_2\text{O}$ .

Finally, nitrous oxide can also be used to build triazenes, which is described in more detail below (section 1.4).

## 1.4 Synthesis and chemistry of 1-alkynyl triazenes

Triazenes are explored for more than 160 years and to date their scope and synthetic utility are ever expanding.<sup>103–105</sup> Because of their intrinsic reactivity, triazenes are, for example, applied as anti-cancer agents in medicinal chemistry,<sup>106,107</sup> as protecting groups in total synthesis,<sup>108</sup> as traceless solid-phase linkers in synthetic chemistry,<sup>109,110</sup> and as building tools in polymer technology.<sup>111</sup>

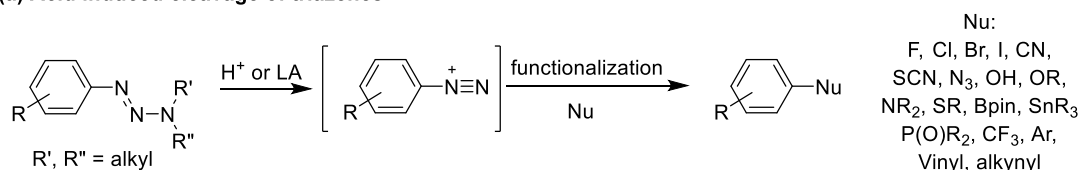
To date, there are a couple of general synthetic routes to prepare triazenes (Scheme 1.11). One of the first and most explored route is the coupling of aryl diazonium salts with secondary amines to obtain 1-aryl-3,3-dialkyl triazenes (Scheme 1.11 a).<sup>112</sup> Although this method is applicable to various amines, the diazonium salts are limited to aryl substituents, because alkyl, vinyl, or alkynyl substituents for diazonium salts are unstable. With the azide route it is also possible to access vinyl triazenes (Scheme 1.11 b).<sup>113,114</sup>



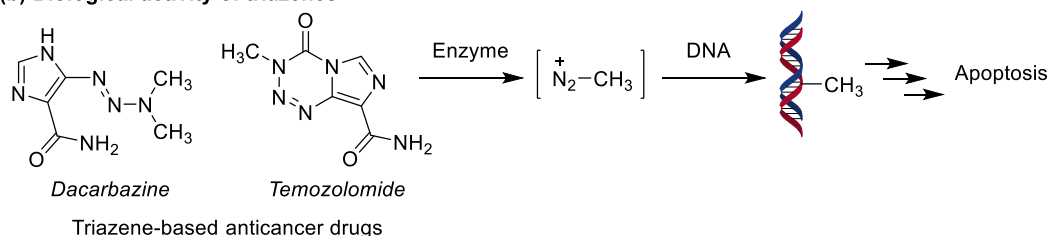
**Scheme 1.11** General synthetic routes to triazenes.

The key synthetic utility is the cleavage of triazenes and to install a range of nucleophiles (Scheme 1.12 a). Therefore, triazenes can be regarded as masked diazonium salts. The acid-induced cleavage of triazenes has been studied extensively with kinetic<sup>115–124</sup> and theoretical studies,<sup>125–129</sup> which is of interest for the synthetic utility of triazenes and their potential biological activity.<sup>130,131</sup> Two triazene-based drugs have been developed as anticancer agents: dacarbazine and temozolamide (Scheme 1.12 b). In the presence of an enzyme, the compound releases a DNA-alkylating agent, which eventually leads to cell apoptosis and cell death. When R'' = H and in the presence of a base, the triazenide is formed, which act as a ligand for transition and main group metals (Scheme 1.12 c).<sup>132–138</sup>

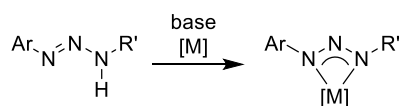
## (a) Acid induced cleavage of triazenes



## (b) Biological activity of triazenes

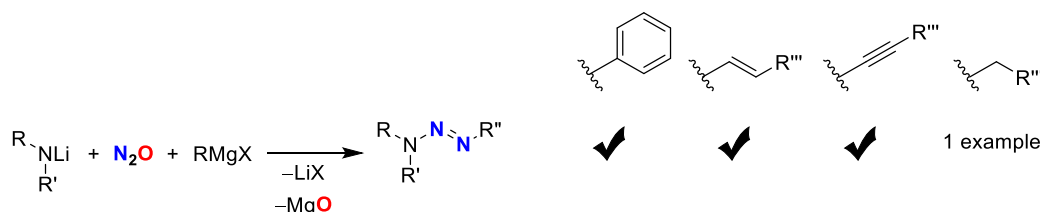


## (c) Metal complexation



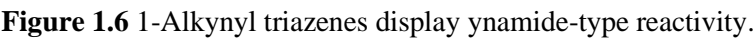
**Scheme 1.12** Brønsted or Lewis acid-induced conversion of 1-aryl-3,3-dialkyltriazenes into diazonium compounds (a). Bioactivity of triazenes and two clinically used triazenes (b). Metal complexation of triazenes (c).

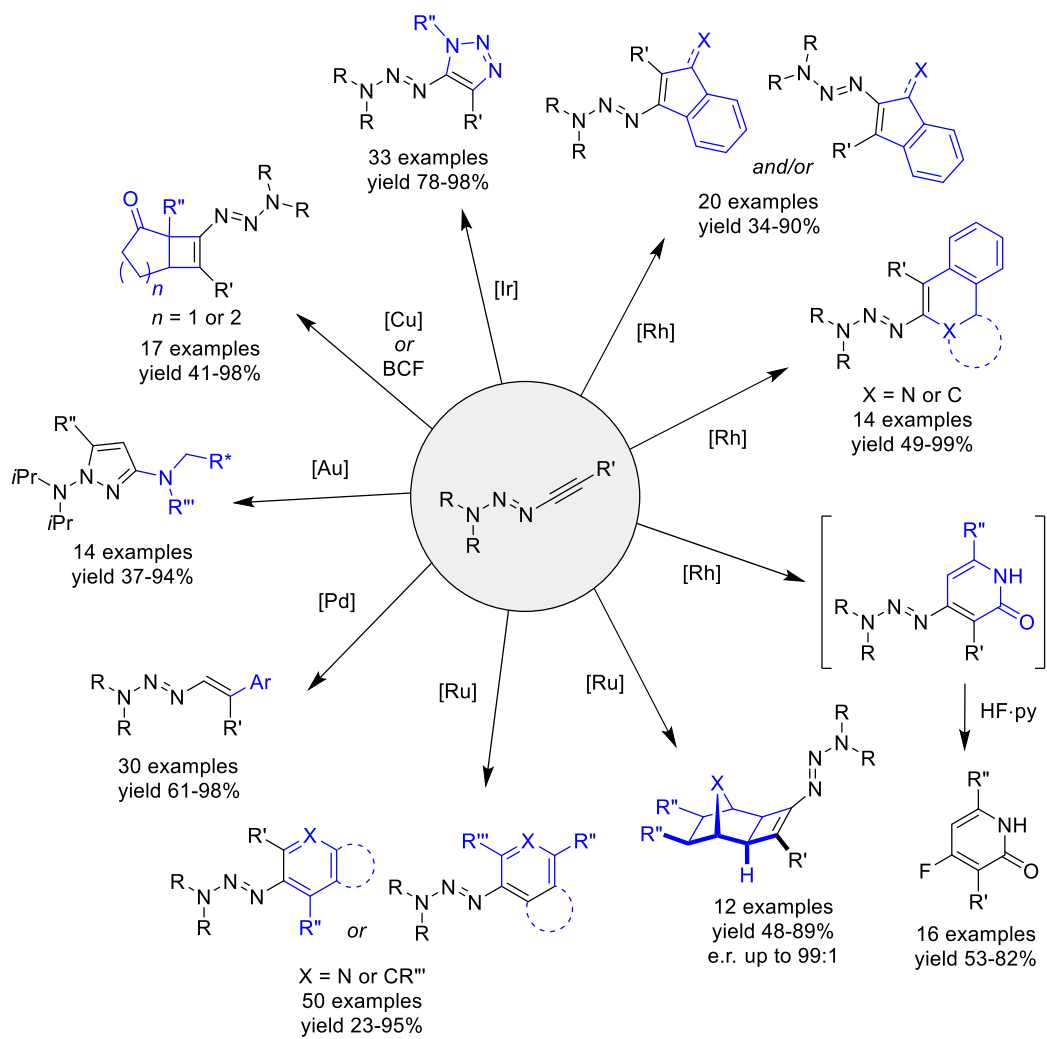
Finally, nitrous oxide can also be used to build triazenes.<sup>139</sup> Notably, it is possible to access 1-alkynyl triazenes (Scheme 1.13), which had not been prepared before. Lithiated amines form diazotates upon subjection to N<sub>2</sub>O atmosphere, and the addition of a Grignard reagent results in triazenes.<sup>139</sup> Besides alkynyl substituents, also aryl, vinyl, and one example with alkyl triazene have been reported.



**Scheme 1.13** General synthetic routes to prepare triazenes via N<sub>2</sub>O.

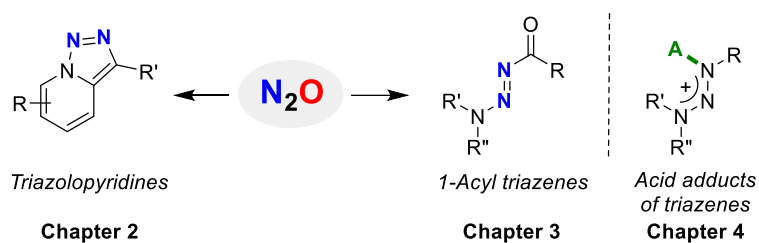
Due to the electron-donating nature of the triazene functionality, 1-alkynyl triazenes show an ynamide-type reactivity with an activated triple bond (Figure 1.6), and thus open-up a range of possible further reactions.<sup>105</sup> Examples include organic transformations (Scheme 1.14) by regioselective addition of acid,<sup>140</sup> isomerization to allenyl triazenes,<sup>141</sup> Lewis acid-catalyzed diastereoselective four-component reaction,<sup>142</sup> and reactions with ketenes,<sup>140</sup> donor-acceptor-substituted cyclopropanes,<sup>140</sup> or with tetracyanoethylene.<sup>140</sup>



**Scheme 1.15** Metal-catalyzed transformations of 1-alkynyl triazenes.

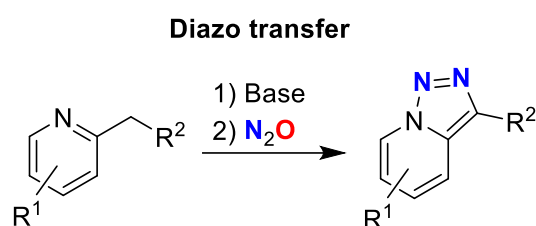
## 1.5 Objectives of the thesis

The overall objectives of the work described in the present thesis were: to use nitrous oxide as diazo transfer reagent to form triazolopyridines- and quinolines (Chapter 2), develop general routes towards 1-acyl triazenes and study their chemical, physical, and biological properties (Chapter 3), and investigate triazene intermediates formed upon the addition of acids (Chapter 4). These studies contribute to the fields of synthetic chemistry with nitrous oxide and triazenes, and they provide fundamental knowledge on the activation of nitrous oxide and synthesizing valuable organic precursors, which will have potential in further organic transformations.



**Scheme 1.16** Overview objectives of thesis.

## 2 Nitrous oxide as diazo transfer reagent: the synthesis of triazolopyridines



This chapter has been published in:

**I. R. Landman**, F. Fadaei-Tirani and K. Severin, *Chem. Commun.*, 2021, 57, 11537–11540

DOI: 10.1039/d1cc04907k

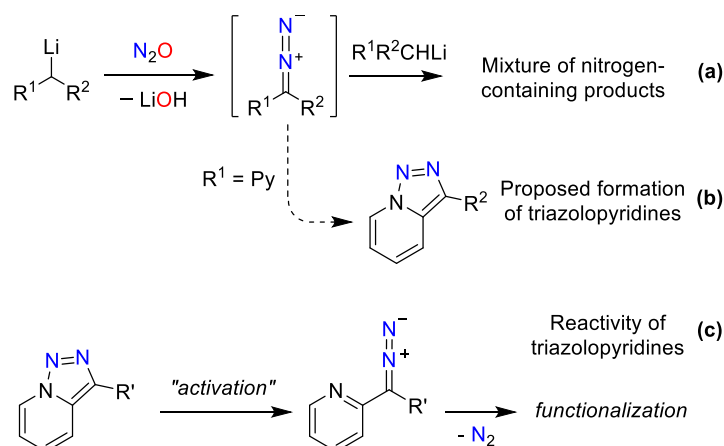
Reprinted in an adapted version with permission from RSC Publishing and all authors.

For the corresponding GIF, scan:



## 2.1 Introduction

A first report about the activation of  $\text{N}_2\text{O}$  by organolithium compounds was published in 1953 by Beringer, Farr and Sands.<sup>84</sup> Reactions of alkyllithium compounds were found to give different nitrogen-containing products (*e.g.* hydrazones or azines). It was proposed that these transformations involve diazo compounds as intermediates, which can react further with the alkyllithium reagent (Scheme 2.1 a).<sup>79–84</sup> Diazo compounds, which are directly linked to 2-pyridyl groups, rapidly cyclize to give triazolopyridines.<sup>152–157</sup> Therefore, we assumed that the reaction of metallated 2-alkylpyridines with  $\text{N}_2\text{O}$  might give triazolopyridines as main reaction products (Scheme 2.1 b).<sup>158</sup> Triazolopyridines represent highly valuable starting materials for heterocycle synthesis.<sup>152–157</sup> These fused 1,2,3-triazoles are unique heterocycles with fluorescent and coordination properties,<sup>159,160</sup> and they are applied in materials science and organic chemistry,<sup>154,156,157,161–165</sup> and show preliminary results for pharmaceutical applications.<sup>166,167</sup> The triazole ring can be activated by being subjected to high temperatures or transition-metal complexes (Scheme 2.1 c).

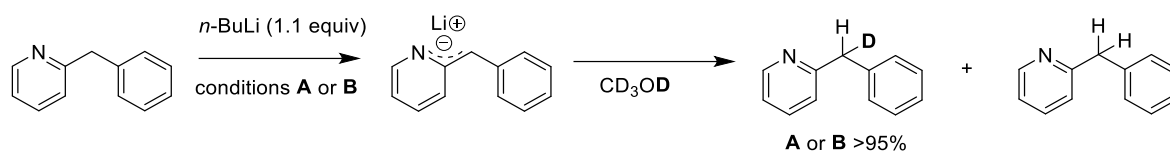


**Scheme 2.1** The reaction of alkyllithium compounds with  $\text{N}_2\text{O}$  gives nitrogen-containing products, and diazo compounds were discussed as putative intermediates (refs <sup>79–84</sup>) (a). Proposed formation of triazolopyridines (b). Reactivity of triazolopyridines (c).

## 2.2 Synthesis of the triazoles 2.1–2.10

To test our hypothesis, we lithiated 2-benzylpyridine and subjected it to an atmosphere of  $\text{N}_2\text{O}$ . Analysis of the mixture after a reaction time of 1 h at room temperature showed that triazole **2.1** had indeed formed. Subsequently, the conditions were optimized.

First, the lithiation efficiency was examined by performing the lithiation in Et<sub>2</sub>O or THF and then dissolving a small amount of the lithiated salt in dry CD<sub>3</sub>OD (Scheme 2.2). For both, Et<sub>2</sub>O and THF, the lithiation was nearly complete under the given conditions.



**Scheme 2.2** Investigation of the lithiation efficiency. **A**: Et<sub>2</sub>O (0.1 M), 0 °C to rt, 1 h, **B**: THF (0.1 M), –78 °C to rt, 2 h. Yield calculated based on CH<sub>2</sub> vs CHD <sup>1</sup>H NMR signal after quenching with CD<sub>3</sub>OD.

Starting from the lithiated 2-benzylpyridine, an initial optimization was performed to find conditions for the N<sub>2</sub>O conversion (Table 2.1). The reaction conditions were varied and the crude reaction mixtures were analyzed by <sup>1</sup>H NMR (CD<sub>2</sub>Cl<sub>2</sub>) by comparing the α-H signal of the pyridyl group of product **A** (8.76 ppm), side-product **B** (8.55 ppm), and starting material **C** (8.50 ppm). The initial screening indicated that at rt and 0 °C (entry 1 and 2), the reaction does not go to full completion. Increasing the temperature to 50 °C (entry 4) was beneficial for the conversion. For reactions at higher concentration (0.1 M, entry 6 and 7), a new side-product was detected, which was not identified. We have chosen the conditions given under entry 5 (50 °C for 2 h) for further studies.

**Table 2.1** Screening of reaction conditions.

Entry	T (°C)	Conc. (M)	Time (h)	Conversion (%)		
				A	B	C
1	rt	0.048	1	52	48	0
2	0	0.048	1	23	67	10
3	40	0.024	1	>95	2	<5
4	50	0.024	1	>95	0	<5
5 <sup>a</sup>	50	0.048	2	>95	0	<5
6 <sup>b,c</sup>	50	0.1	1	93 <sup>a</sup>	3	4
7 <sup>b,c</sup>	50	0.1	2	>95 <sup>a</sup>	0	<5

<sup>a</sup> 350 mg instead of 50 mg. <sup>b</sup> 200 mg instead of 50 mg. <sup>c</sup> New set of signals appeared.

Subsequently, the reaction was followed and optimized over two steps in one pot. For the reaction screening (Table 2.2), an aliquot of the organic phase was evaporated and the ratio of product and side-products was determined by  $^1\text{H}$  NMR ( $\text{CD}_2\text{Cl}_2$ ). Starting with THF as solvent (entry 1–3), the increase in equivalents of *n*-BuLi did not lead to a higher conversion into the desired product. In the case of 4 equiv (entry 3), there was a mixture of signals, suggesting some side-reactions had taken place. Switching to  $\text{Et}_2\text{O}$  and 1.1 equiv (entry 4) gave the desired clean conversion, which was selected as the optimal reaction conditions. Heating overnight also produced side-products (entry 5).

**Table 2.2** Screening of reaction conditions, two-step reaction, one-pot.

1) *n*-BuLi  
Solvent (0.1 M)  
–78 or 0 °C to rt, 2 h

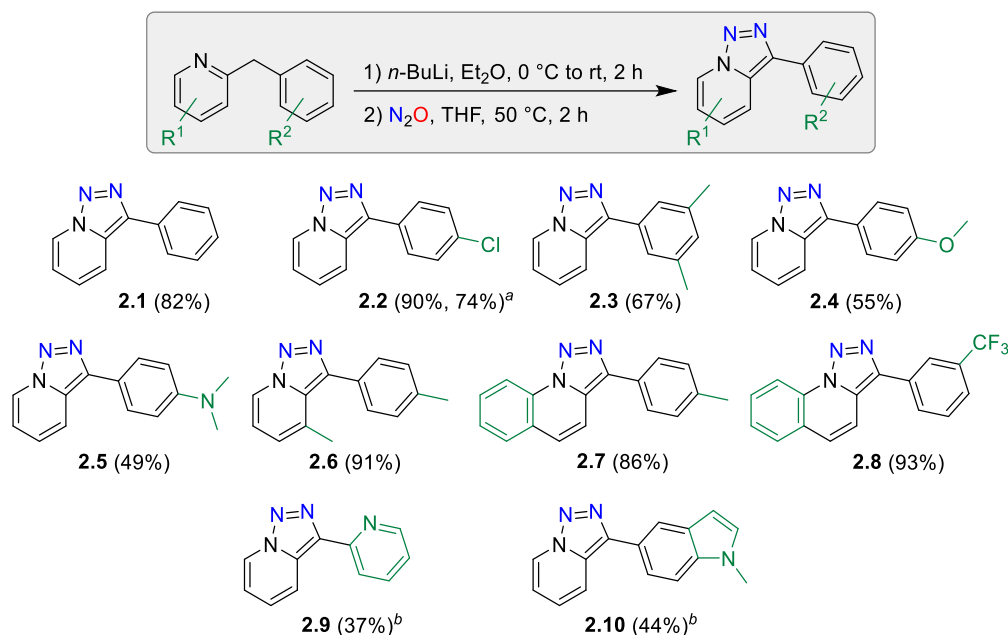
2)  $\text{N}_2\text{O}$ , THF (0.05 M),  
50 °C, 2 h

**A** + **B** + **C**

Entry	<i>n</i> -BuLi (equiv)	Solvent	<i>T</i> (°C)	Conversion (%)		
				A	B	C
1	1.5	THF	–78	88	5	7
2	2	THF	–78	55	40	5
3	4	THF	–78	<i>Mixture of signals</i>		
4	1.1	$\text{Et}_2\text{O}$	0	>95	<5	<5
5 <sup>a</sup>	1.1	$\text{Et}_2\text{O}$	0	<i>Mixture of signals</i>		

<sup>a</sup>  $\text{N}_2\text{O}$  reaction overnight instead of 2 h.

From the reaction optimization, it appeared that mild heating at 50 °C for 2 h in THF (0.05 M) was advantageous for the diazo transfer reaction. A cleaner reaction was observed when the lithiation step was performed in diethyl ether, followed by a solvent switch to THF for the reaction with  $\text{N}_2\text{O}$ . Under these conditions, triazole **2.1** could be isolated in 82% yield (Scheme 2.3).



**Scheme 2.3** Synthesis of triazolopyridines and triazoloquinolines with  $\text{N}_2\text{O}$ . The values in brackets refer to isolated yields. <sup>a</sup> Reaction performed on a 5 mmol scale/ gram scale. <sup>b</sup> Extended reaction times for the reaction with  $\text{N}_2\text{O}$ , **2.9**: 19 h, and **2.10**: 4 h.

The scope of the diazo transfer reaction was examined next (Scheme 2.3). Chloro (**2.2**) and methyl substituents (**2.3**) on the phenyl ring were well-tolerated, whereas the more electron donating groups OMe (**2.4**) and  $\text{N}(\text{Me})_2$  substituents (**2.5**) gave lower yields. Apparently, side-reactions take place when the phenyl ring is too strongly activated. Changing the pyridine moiety to lutidine (**2.6**) and quinoline (**2.7** and **2.8**) resulted in good yields. Finally, replacing the phenyl group with 2-pyridyl or 5-indolyl provided the desired products **2.9** and **2.10** in moderate yields. It is worth noting that the anion in lithiated bis(2-pyridyl)methane (the precursor of **2.9**) is highly delocalized, with  $\text{Li}^+$  coordinating to both pyridyl groups.<sup>168</sup> The delocalization is expected to lower the nucleophilicity of the organolithium compound, hampering the reaction with  $\text{N}_2\text{O}$ . We have also examined reactions of pyridines with simple alkyl instead of benzyl substituents. A complex mixture of products was observed, and further analyses were not performed.

## 2.3 Synthesis of the triazoles **2.11**–**2.15**

Stentzel and Klumpp reported that reactions of *trans*-1,2-di(2-pyridyl)ethylene with organolithium reagents give stable 2-alkylpyridine anions, which can be trapped with electrophiles.<sup>169,170</sup> These results prompted us to explore if we can combine a C–C coupling reaction with the nitrous oxide-induced triazole formation.

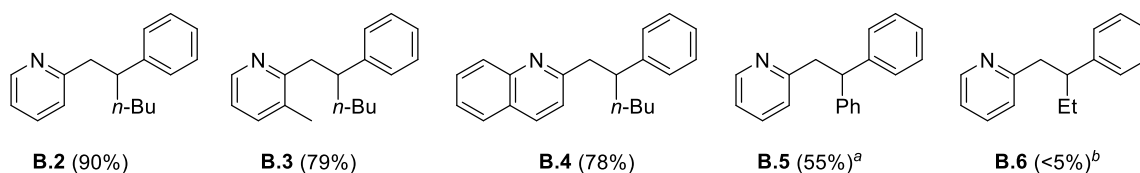
First, the lithiation efficiency was examined according to the procedures by Stentzel and Klumpp.<sup>169</sup> The yields were calculated by integration of selected <sup>1</sup>H NMR signals (Table 2.3). A large excess of *n*-BuLi resulted in a mixture of signals (entry 2). Both, the presence of TMEDA (entry 3) and without (entry 1), showed a good conversion. In the case of HMPA (entry 4), a higher conversion was not obtained.

**Table 2.3** Screening of lithiation conditions.

Entry	Additive	<i>n</i> -BuLi (equiv)	Conversion (%)	
			A.1	B.1
1	-	1.5	<5	83
2 <sup>a</sup>	-	7	<5	<5
3	TMEDA (1 equiv)	1.5	<5	86
4	HMPA (1 equiv)	1.5	5	72

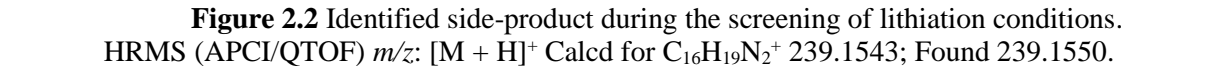
<sup>a</sup> Mixture of signals.

It has been reported that olefinic N-heterocycles react poorly with organolithium and Grignard reagents.<sup>169</sup> Under the conditions of entry 1 (Table 2.3), we briefly examined other organolithium and EtMgBr for a couple of olefinic N-heterocycles. In the case of *n*-BuLi, we observed good to high yields (**B.2-4**), while for PhLi a lower yield was obtained (**B.5**). For EtMgBr, only traces of the product were observed (**B.6**).

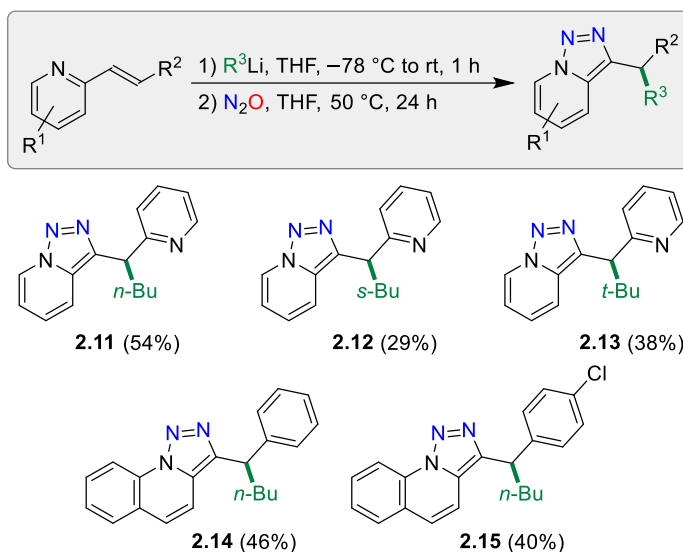


**Figure 2.1** Screening addition reaction of organolithium and magnesium compounds to various olefinic N-heterocycles. <sup>1</sup>H NMR yields. <sup>a</sup> With PhLi, 1.5 equiv. <sup>b</sup> With EtMgBr, 1.5 equiv.

Next, the reaction was optimized over two steps in one pot (Table 2.4). The yield was calculated by integration of selected <sup>1</sup>H NMR signals. First, the reaction under N<sub>2</sub>O was followed over time (entry 1a–d) indicating that prolonged reaction times were beneficial for the yield. Then, changing the size of the flask (entry 2 and 3) or adding TMEDA (entry 4) did not lead to higher yields. A side-product was identified by HRMS as is shown in Figure 2.2, which can be assigned to the dehydration of **B**.

<sup>a</sup> NMR yield calculated based on the ratio of the three products instead of an internal standard.

25



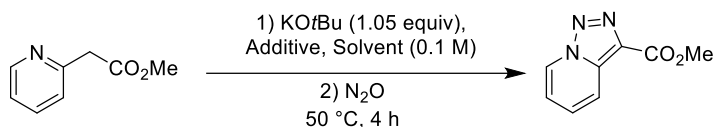
**Scheme 2.4** Synthesis of triazoles by sequential reaction of alkenyl pyridines or quinolines with first organolithium reagents and then  $\text{N}_2\text{O}$ . The values in brackets refer to isolated yields.

Overall, the isolated yields for these sequential C–C, C–N coupling reactions were only modest (29–54%). However, it should be noted that structurally complex triazolopyridines are formed in a simple one-pot procedure.

## 2.4 Synthesis of the triazole **2.17**

Triazolopyridines with ester substituents are frequently used as substrates for synthetic transformations.<sup>152–157</sup> In order to examine if compounds of this kind can be obtained with nitrous oxide, we have investigated the reaction of metalated methyl 2-(pyridine-2-yl)acetate with  $\text{N}_2\text{O}$ .

A quick optimization was performed (Table 2.5). In DMSO and in THF, oligomers were formed, which hampered the conversion (entry 1 and 4). Addition of 18-crown-6 did prevent the formation of oligomers (entry 2 and 5), whereas TMEDA was not suited (entry 3). The conversion was followed by  $^1\text{H}$  NMR in  $d_6$ -DMSO (entry 2) and  $d_8$ -THF (entry 5). In  $d_8$ -THF, a mixture of products was observed. In  $d_6$ -DMSO, the conversion was clean and a more detailed  $^1\text{H}$  NMR study was performed.

**Table 2.5** Screening of reaction conditions.

Entry	Solvent	Additive	T	Result
1	DMSO	-	rt	Oligomers
2	DMSO	18-crown-6	rt	Dissolved → followed by NMR
3	DMSO	TMEDA	rt	Oligomers
4	THF	-	rt	Oligomers
5	THF	18-crown-6	rt, 50 °C for 1 h	Dissolved → followed by NMR: Mixture of products

In a J-Young's NMR tube, methyl 2-pyridylacetate (3  $\mu$ l) was dissolved in *d*<sub>6</sub>-DMSO/DMSO (1:1, 0.5 ml) and KOtBu (1.05 eq) and 18-crown-6 (1.0 eq) were added. A blank measurement was taken after which the sample was subjected to an N<sub>2</sub>O atmosphere (3x N<sub>2</sub>O/*vac* cycles) and heated at 50 °C. The conversion was followed by <sup>1</sup>H NMR over time (Figure 2.3).

According to the <sup>1</sup>H NMR measurements, the deprotonation by KOtBu was quantitative. After 2.5 h, the reaction was nearly complete. Under basic conditions, H/D exchange of acidic protons can occur in *d*<sub>6</sub>-DMSO.<sup>171,172</sup> The proton next to the N-atom in the ring of the triazolopyridine is known to be acidic, and partial H/D exchange was observed. Moreover, cleavage of the ester of the product was observed as the signal of methanol has appeared. The by-product KOH had induced simultaneous hydrolysis of the ester function.<sup>162</sup>

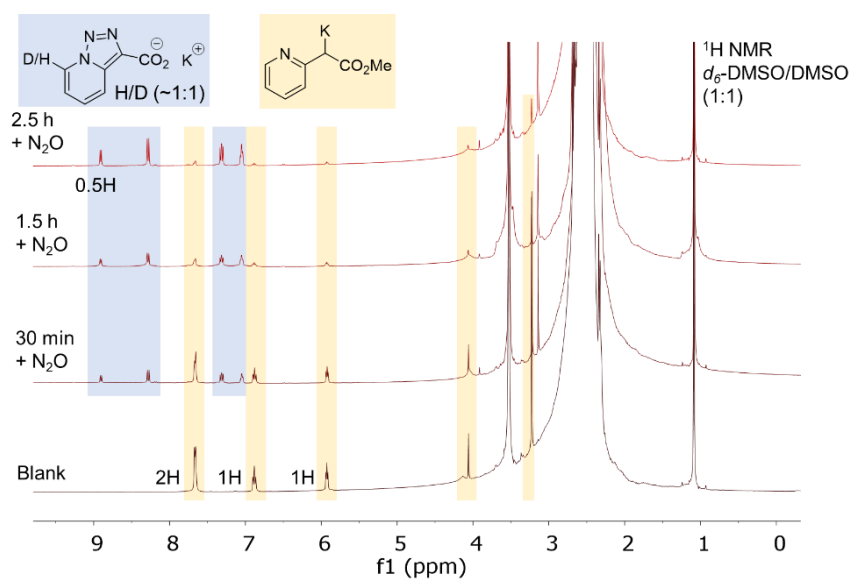


**Figure 2.3** <sup>1</sup>H NMR spectra for the conversion of metalated methyl 2-pyridylacetate into **2.16** using the conditions given in entry 2, Table 2.5.

The formation of salt **2.16** was corroborated by X-ray diffraction (Figure 2.4). Single crystals of **2.16** were obtained within two weeks after layering the DMSO sample with ethyl acetate. The product crystallized as a cluster with the molecular formula  $C_{42}H_{26}K_2N_{18}Na_4O_{13}$ .

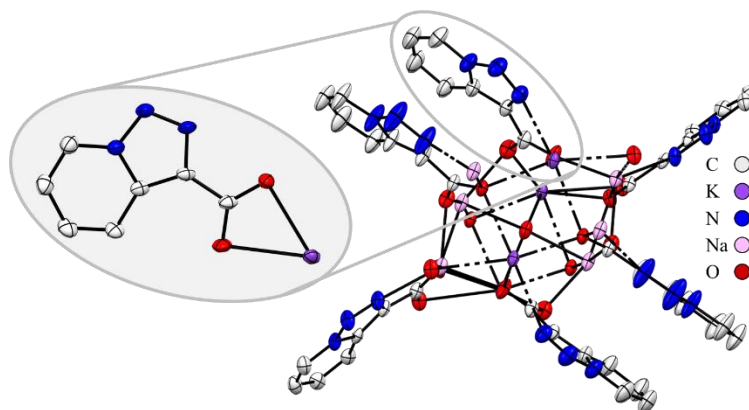
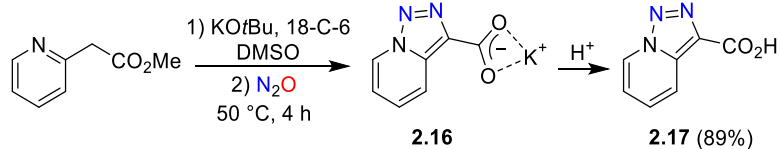


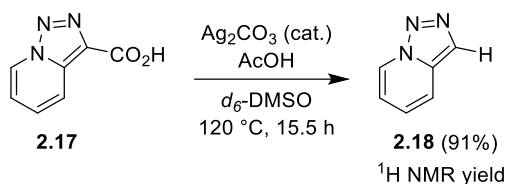
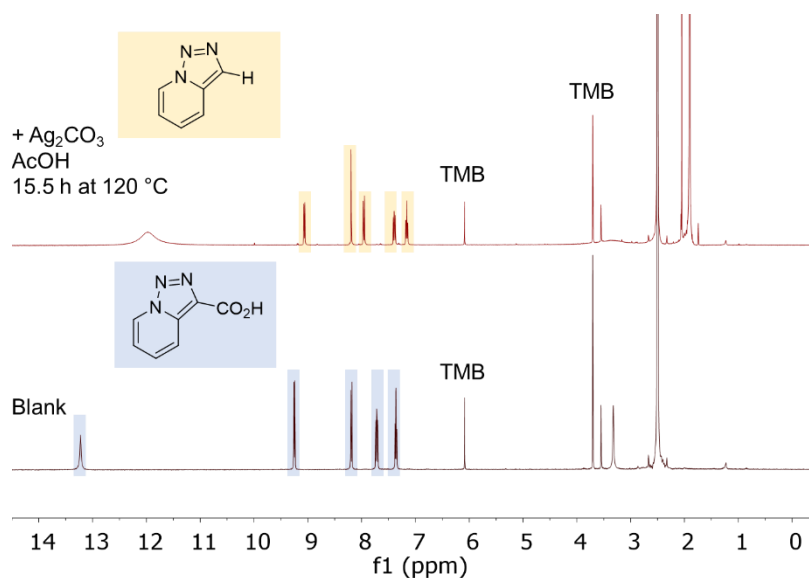
**Figure 2.4** Molecular structure of **2.16** in the crystal. Thermal ellipsoids are drawn at 50% and hydrogen atoms are not shown for clarity.

The optimization studies showed that deprotonation of the ester was achieved by KO $t$ Bu in DMSO.<sup>173,174</sup> 18-Crown-6 (18-C-6) was used as additive to facilitate solubilization of the metallated pyridine. Subsequent addition of N<sub>2</sub>O along with gentle heating at 50 °C resulted in the clean formation of potassium salt **2.16** (Scheme 2.5). Acidic work-up gave carboxylic acid **2.17**, which was isolated in 89% yield.



**Scheme 2.5** Synthesis of triazolopyridine **2.17**.

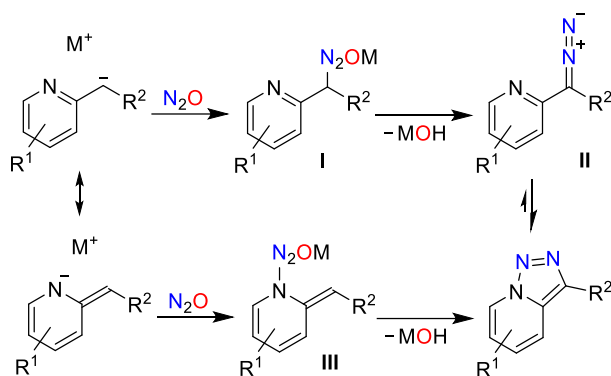
Next, we have investigated the removal of the CO<sub>2</sub>H group via Ag(I)-catalysis to give the plain triazole **2.18** (Scheme 2.6).<sup>175</sup> A nearly clean conversion was observed and the <sup>1</sup>H NMR yield of [1,2,3]triazolo[1,5-*a*]pyridine **2.18** was 91% (Figure 2.5). Note that triazolopyridines will decompose at higher temperatures and release N<sub>2</sub>.<sup>176</sup>

Scheme 2.6 Decarboxylation of **2.17**.

**Figure 2.5** <sup>1</sup>H NMR spectra for the protodecarboxylation of **2.17** to **2.18** in *d*<sub>6</sub>-DMSO. TMB = trimethoxybenzene.

## 2.5 Mechanistic considerations

With regard to the mechanism of the reactions discussed herein, one can propose an initial nucleophilic attack of the carbanion to N<sub>2</sub>O to give a diazotate of type **I** (Scheme 2.7). Elimination of MOH would provide diazo compounds of type **II**, which are prone to cyclize to give the final products. However, it is also conceivable that the nucleophilic attack occurs via the pyridyl N-atom, since metalated 2-alkylpyridines display significant charge density at the N-atom.<sup>168,173</sup> In this case, the reaction with N<sub>2</sub>O would give aminodiazotates of type **III**. It is worth noting that aminodiazotates have previously been observed in reactions of lithiated amines with N<sub>2</sub>O.<sup>139</sup> Elimination of MOH from **III** would give triazolopyridines without involvement of diazo compounds.



**Scheme 2.7** Proposed mechanism for the synthesis of triazolopyridines from  $\text{N}_2\text{O}$ .

Attempts to identify intermediates by *in situ*  $^1\text{H}$  NMR spectroscopy were not successful. For example, we followed the reaction by  $^1\text{H}$  NMR spectroscopy (Figure 2.6). In a J-Young's NMR tube, lithiated 2-benzylpyridine (~2 mg) was dissolved in  $d_8$ -THF (0.5 ml) and an initial blank spectrum was recorded. Subsequently,  $\text{N}_2\text{O}$  was added and the sample was heated for 1 h at 50 °C. A clean conversion was observed with a trace of the starting material remaining. The reaction was complete within ~5 min. The difference in reaction time compared to the up-scale reaction we attribute to the difference in mass transfer and concentration.

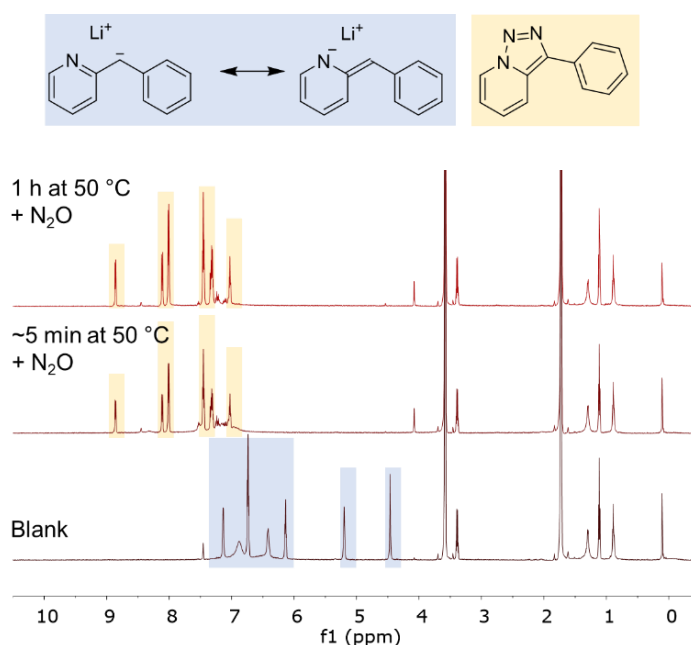


**Figure 2.6**  $^1\text{H}$  NMR spectra for the conversion of lithiated 2-benzylpyridine into **2.1** at 50 °C in  $d_8$ -THF.

We then further investigated the reaction at lower temperatures: In a J-Young's NMR tube, lithiated 2-benzylpyridine (~4 mg) was dissolved in  $d_8$ -THF (0.5 ml) and first the sample was analyzed

at  $-20\text{ }^{\circ}\text{C}$  (Figure 2.7). Then the sample was frozen in liquid nitrogen and  $\text{N}_2\text{O}$  was added. While cold, the sample was inserted into the NMR spectrometer and the spectra were recorded at different temperatures (Figure 2.7). Going from  $-20$  and to  $25\text{ }^{\circ}\text{C}$ , the reaction proceeds. A clean conversion from lithiated 2-benzylpyridine to triazolopyridine **2.1** was observed with no signs of an intermediate. Noteworthy is that the chemical shift of **2.1** is temperature dependent.

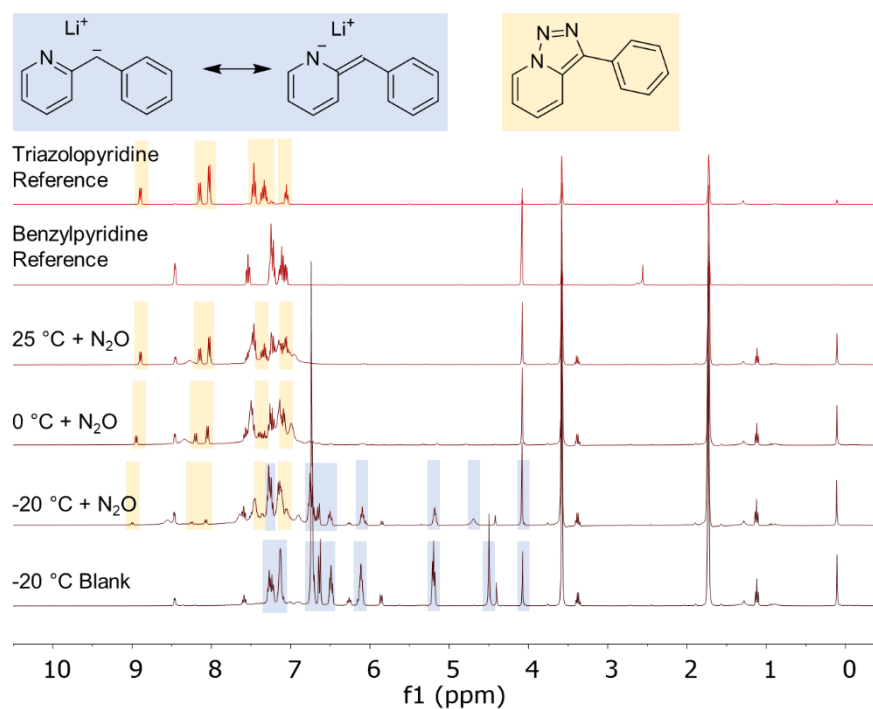
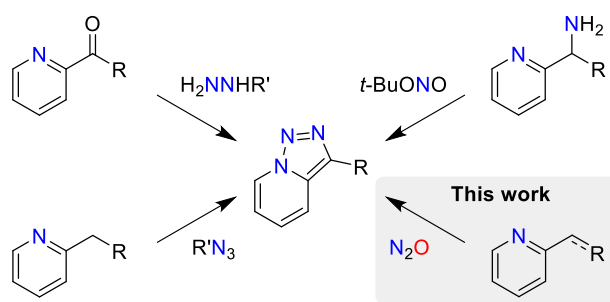


**Figure 2.7** Following the reaction by VT NMR spectroscopy.

In these preliminary studies, intermediates could not be identified by *in situ*  $^1\text{H}$  NMR. Further studies on the mechanism would be needed to determine the precise reaction pathways of the diazo transfer reactions.

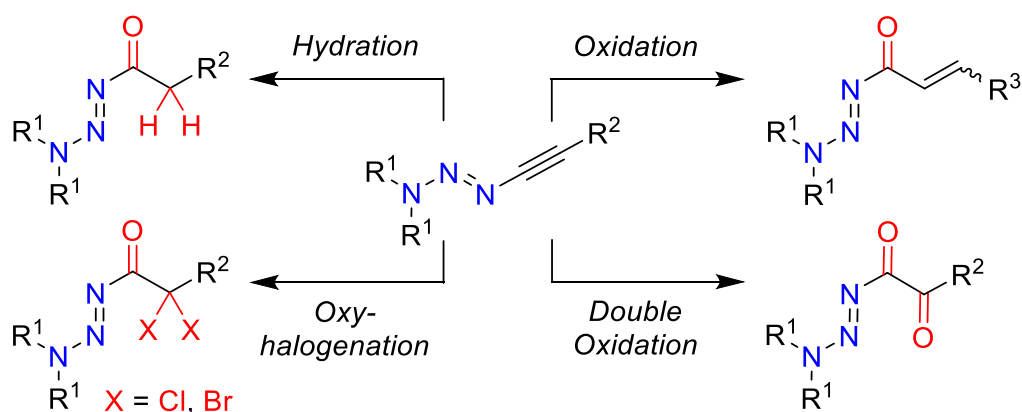
## 2.6 Conclusion

In conclusion, we have shown that nitrous oxide can be used as a diazo transfer reagent for the synthesis of triazolopyridines and triazoloquinolines. The  $N_2O$ -based methodology allows accessing synthetically interesting triazoles in moderate to good yields. Traditionally, triazoles with aryl substituents in 3-position (*e.g.* **2.1**) are prepared from 2-acylpyridines by condensation with hydrazine ( $H_2NNHR'$ ) followed by oxidation (Scheme 2.8).<sup>177</sup> Alternatively, 2-pyridyl amines can be oxidized with tert-butyl nitrite ( $t\text{-BuONO}$ ).<sup>178</sup> Our procedure is distinct since it employs 2-alkyl or 2-alkenyl pyridines as starting materials.<sup>179</sup> Furthermore, the compounds are obtained using operationally facile one-pot reactions. More generally, our results are further evidence for the utility of  $N_2O$  in synthetic organic chemistry.



**Scheme 2.8** General synthetic routes to triazolopyridines.

### 3 Synthesis and properties of 1-acyl triazenes



Part of this chapter has been published in:

**I. R. Landman**, E. Acuña-Bolomey, R. Scopelliti, F. Fadaei-Tirani and K. Severin,

*Org. Lett.*, 2019, 21, 6408–6412.

DOI: [10.1021/acs.orglett.9b02248](https://doi.org/10.1021/acs.orglett.9b02248)

Reprinted in an adapted version with permission from ACS Publications and all authors.

Subchapter 3.12 contains unpublished data.

For the corresponding GIF, scan:



### 3.1 Introduction

Triazenes with acyl groups attached to the N3 atom (Figure 3.1) have been studied extensively over the past decades in medicinal and synthetic chemistry.<sup>180–182</sup> These compounds are typically prepared by acylation of 1,3-disubstituted triazenes.<sup>103,180–184</sup> Alternative synthetic pathways include the reaction of deprotonated amides with diazonium salts,<sup>185–187</sup> the condensation of hydrazides with aromatic nitroso compounds,<sup>188</sup> or the reaction of benzoyl azide with a Grignard reagent.<sup>189</sup> 3-Acyl triazenes have found considerable interest in medicinal chemistry, and numerous bioactive compounds have been reported in the literature.<sup>190–195</sup> In this context, the reactivity of 3-acyl triazenes has been studied in detail, from both a theoretical<sup>127</sup> and experimental<sup>190,191,200–202,192–199</sup>, point of view. 3-Acyl triazenes have also been used as precursors for aminyl radicals,<sup>203</sup> as acylating agents,<sup>204</sup> and as chemodosimeters for cyanide.<sup>205</sup>

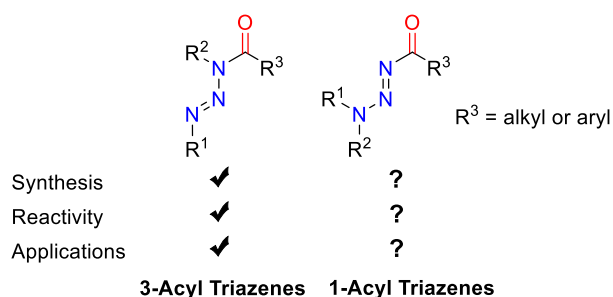


**Figure 3.1** 3-Acyl triazenes versus 1-acyl triazenes.

In contrast to the well-established chemistry of 3-acyl triazenes, there are hardly any reports about triazenes with carbonyl groups attached to the N1 atom. Triazenes with 1-carbamoyl and 1-alkoxycarbonyl groups have been prepared by oxidation of functionalized triazanes.<sup>206,207</sup> Furthermore, there are reports about benzo[1,2,3]triazine-4(3H)-one derivatives,<sup>208–210</sup> which can be regarded as cyclic (covalent connection between N1 and N3)<sup>211</sup> acyl triazenes. A general synthetic method for synthesizing acyclic 1-acyl triazenes (Figure 3.1) is not available so far. We found that 1-acyl triazenes are accessible by hydration or oxidation of 1-alkynyl triazenes, and details about these reactions are given below.<sup>212</sup>

The starting materials of choice to attempt the synthesis of 1-acyl triazenes were 1-alkynyl triazenes, which can be prepared from lithium amides, alkynyl Grignard reagents, and nitrous oxide.<sup>14,139</sup> These heteroatom-substituted alkynes display a similar reactivity as ynamides.<sup>140,141,144–146,150</sup> For example, ketenes react with 1-alkynyl triazenes to give [2+2] cycloaddition products under mild conditions.<sup>140</sup> Ynamides can be hydrated in the presence of Brønsted or Lewis acids to give *N*-acyl sulfonamides.<sup>44–48</sup> An analogous reaction with 1-alkynyl triazenes would give 1-acyl triazenes, and we

therefore examined reaction conditions for the hydration of 1-alkynyl triazenes. The triazene group is known to be acid-sensitive.<sup>103,180–182</sup> Therefore, the challenge was to find conditions which would allow the hydration of the triple bond without cleavage of the triazene function.

### 3.2 Synthesis of the alkyl 1-acyl triazenes 3.1–3.9

Initial attempts to hydrolyze 1-alkynyl triazenes in the presence of Ag(I) salts showed that the desired products can be formed. However, high catalyst loadings were needed, and problems with purification were encountered. Switching to acetic acid catalysis<sup>214</sup> was found to be advantageous. Optimizing the reaction conditions showed that decreasing the equivalents of acetic acid from 2.0 to 0.5 and lowering the temperature from 100 to 50 °C was beneficial for the yield (entry 1 and 2, Table 3.1). For the triazene with  $R^2 = n\text{Bu}$ , a lower yield of 68% was observed under the milder conditions (entry 3), but heating at 70 °C did not lead to a higher yield (entry 4). For  $R^2 = \text{Ph}$ , only low yields were observed at 50 °C (entry 5 and 6). In this case, heating with 2.0 equivalents of acetic acid at elevated temperature resulted in a higher yield (entry 7). At last, for  $R^1 = \text{Cy}$  (entry 8), only a small amount of the desired compound was observed, which could be attributed to the low solubility of the starting material in acetone/water.

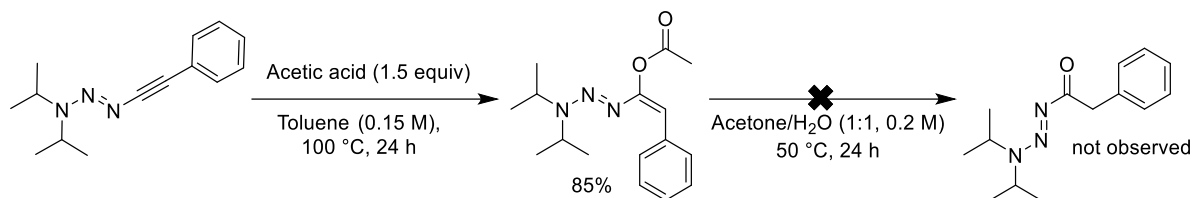
**Table 3.1** Screening of reaction conditions.

Entry	Triazene	Acetic acid (x equiv)	T (°C)	Time (h)	Yield (%) <sup>a</sup>
1	$R^1 = i\text{Pr}, R^2 = t\text{Bu}$	2.0	100	2	27
2	$R^1 = i\text{Pr}, R^2 = t\text{Bu}$	0.5	50	4.5	82
3	$R^1 = i\text{Pr}, R^2 = n\text{Bu}$	0.5	50	5	68
4	$R^1 = i\text{Pr}, R^2 = n\text{Bu}$	0.5	70	5	58
5	$R^1 = i\text{Pr}, R^2 = \text{Ph}$	0.5	50	4.5	15
6	$R^1 = i\text{Pr}, R^2 = \text{Ph}$	0.5	50	24	26
7	$R^1 = i\text{Pr}, R^2 = \text{Ph}$	2.0	100	2	36
8	$R^1 = \text{Cy}, R^2 = n\text{Bu}$	0.5	50	24	8 <sup>b</sup>

<sup>a</sup> Isolated yields. <sup>b</sup> Poor yield, presumably because the starting material is poorly soluble in acetone/water.

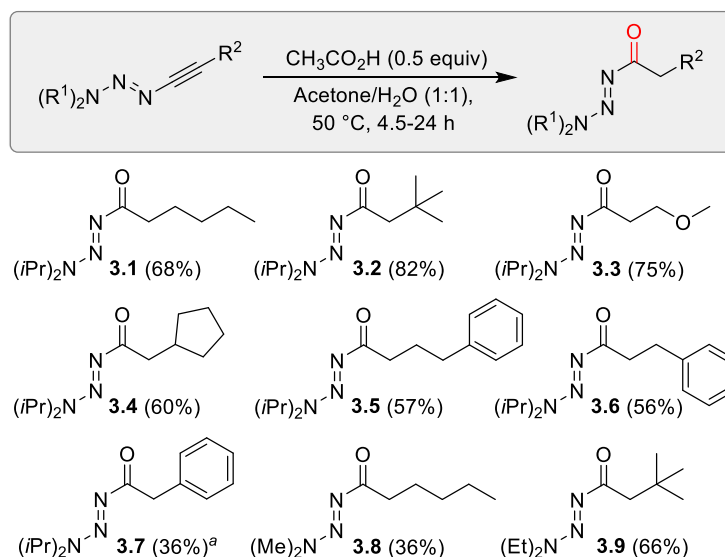
In order to examine if an acetic acid adduct is formed as an intermediate, a two-step reaction was performed (Scheme 3.1). First, the acetic acid adduct was synthesized and isolated according to a reported procedure.<sup>140</sup> The isolated product was then subjected to the reaction conditions

(water/acetone, 50 °C, 24 h). The acetic acid adduct was stable under these conditions, and no 1-acyl triazene was formed.



**Scheme 3.1** Attempted hydrolysis of an acetic acid adduct.

Our brief screening indicated that 0.5 equivalents of acetic acid and a reaction temperature of 50 °C was suited for hydrolysis reactions of most alkynyl triazenes. Moderate to good yields were obtained for alkynyl triazenes containing various alkyl substituents at the triple bond (**3.1–3.6**, Scheme 3.2). As mentioned above, the hydration of a phenylethynyl triazene ( $R^2 = \text{Ph}$ ) is more difficult and the corresponding acyl triazene **3.7** was isolated in only 36% yield. Most likely, these hydration reactions are initiated by protonation of the alkyne at the  $\beta$ -carbon atom, and this position is less nucleophilic in the case of the phenylethynyl triazene. Variation of the alkyl substituents at the N3 position is possible, as evidenced by the successful synthesis of the acyl triazenes **3.8** and **3.9**.

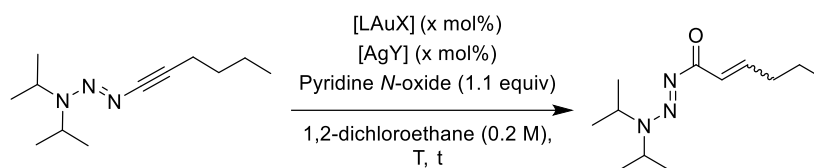


**Scheme 3.2** Acetic acid-catalyzed hydration of alkynyl triazenes. <sup>a</sup> The reaction was performed in a closed vial at 100 °C with 2 equiv  $\text{CH}_3\text{CO}_2\text{H}$ .

### 3.3 Synthesis of the olefinic 1-acyl triazenes **3.10–3.16**

Next, we explored the oxidation of 1-alkynyl triazenes with pyridine *N*-oxides in the presence of Au(I) catalysts.<sup>218,219</sup> Screening of different catalysts and reaction conditions (Table 3.2) showed that (JohnPhos)AuCl in combination with AgNTf<sub>2</sub> (both 5 mol %) and pyridine *N*-oxide can be used for the clean formation of the olefinic acyl triazene **3.10** (entry 2).

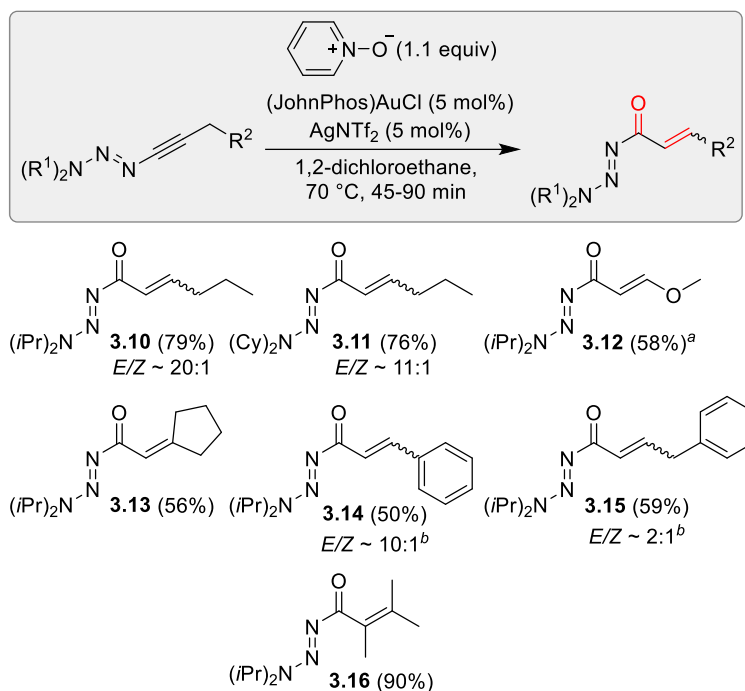
**Table 3.2** Screening of reaction conditions.



Entry	Catalyst ( <b>LAuX</b> )	(mol%)	AgY	(mol%)	T (°C)	Time (min)	Yield (%) <sup>c</sup>	<i>E/Z</i> ratio <sup>c</sup>
<b>1</b>	(CyJohnPhos)AuCl	5	AgNTf <sub>2</sub>	5	70	30	86	8.1
<b>2</b>	(JohnPhos)AuCl	5	AgNTf <sub>2</sub>	5	70	30	97	8.9
<b>3</b>	(JohnPhos)AuCl	2.5	AgNTf <sub>2</sub>	2.5	70	30	55	8.8
<b>4</b>	(dppe)Au <sub>2</sub> Cl <sub>2</sub>	2.5	AgNTf <sub>2</sub>	2.5	70	30	15	5.5
<b>5</b>	(Ipr)AuNTf <sub>2</sub>	2.5	x	2.5	70	30	31	8.0
<b>6</b>	(PPh <sub>3</sub> )AuCl	2.5	AgNTf <sub>2</sub>	2.5	70	30	15	6.0
<b>7<sup>a</sup></b>	(JohnPhos)AuCl	2.5	AgOTf	2.5	70	30	60	8.8
<b>8<sup>a</sup></b>	(JohnPhos)AuCl	5	AgOTf	5	70	30	86	9.4
<b>9</b>	(JohnPhos)AuCl	2.5	AgSbF <sub>6</sub>	2.5	70	30	45	9.0
<b>10</b>	(JohnPhos)AuCl	5	AgNTf <sub>2</sub>	5	50	30	88	8.6
<b>11</b>	(JohnPhos)AuCl	5	AgNTf <sub>2</sub>	5	25	30	45	5.0
<b>12</b>	x	x	x	x	70	75	0	0
<b>13</b>	(JohnPhos)AuCl	5	x	x	70	30	0	0
<b>14<sup>b</sup></b>	x	x	AgNTf <sub>2</sub>	5	70	30	11	4.0
<b>15<sup>b</sup></b>	x	x	AgOTf	5	70	30	32	5.0
<b>16<sup>b</sup></b>	x	x	AgOTf	20	70	30	11	3.9

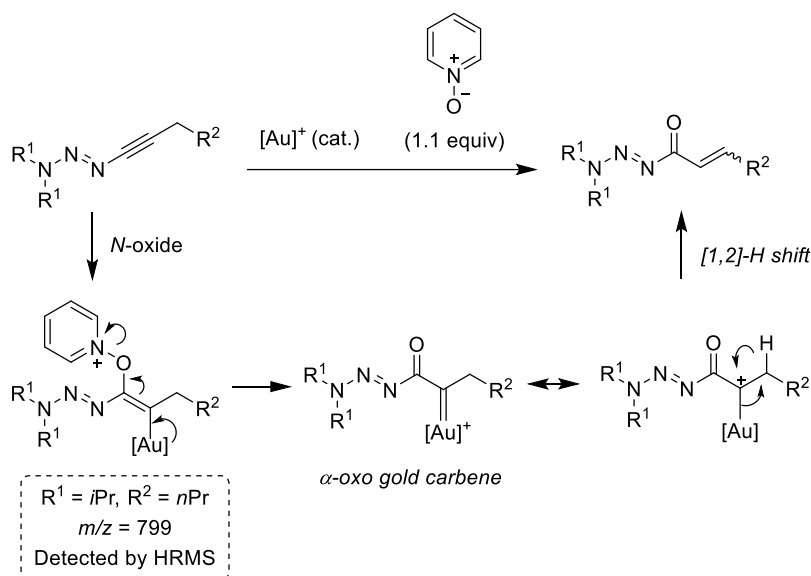
<sup>a</sup> AgOTf does not dissolve well in DCE, which could explain the rate differences. <sup>b</sup> Black particles were observed when the silver salt was used as sole catalyst. <sup>c</sup> Yields and *E/Z* ratio based on <sup>1</sup>H NMR spectra.

The optimized reaction conditions were then used to synthesize the acryloyl triazenes **3.10–3.16**, which were obtained in moderate to good yields (Scheme 3.3). The reactions gave predominantly the *E*-isomer. The oxidation of internal alkynes with pyridine *N*-oxides is prone to give mixtures of regioisomers.<sup>220</sup> In our case, oxygen atom transfer was perfectly site-specific, as it was observed for ynamides.<sup>218</sup> The high selectivity can be attributed to the polarization of the triple bond of alkynyl triazenes.<sup>140</sup>



**Scheme 3.3** Au-catalyzed oxidation of alkynyl triazenes. <sup>a</sup> Only the *E*-isomer observed.  
<sup>b</sup> The *E/Z* mixture could not be fully separated.

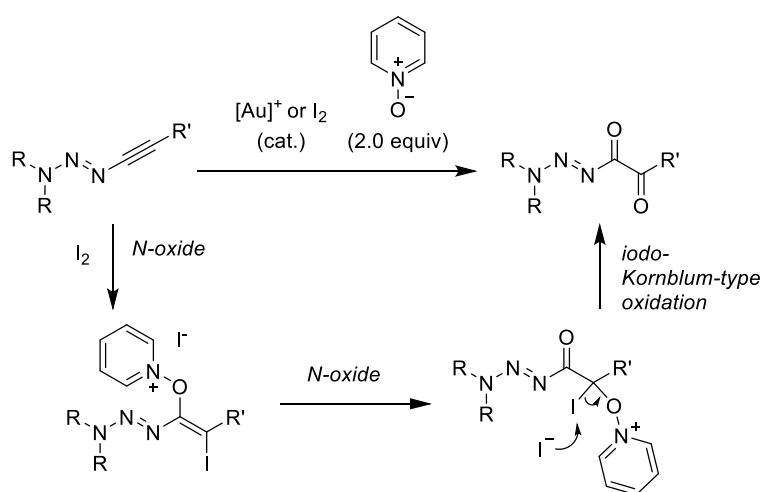
The likely mechanism of the reaction involves a nucleophilic attack of the pyridine *N*-oxide at the  $\text{C}_\alpha$  position of the Au-activated triple bond, followed by N–O bond rupture and formation of an  $\alpha$ -oxo gold carbenoid (Scheme 3.4).<sup>221</sup> Product formation then occurs via a [1,2]-H shift or [1,2]-Me shift in the case of **3.16**.



**Scheme 3.4** Proposed mechanism of the Au-catalyzed formation of olefinic 1-acyl triazenes.

### 3.4 Synthesis of the 1,2-diketo triazenes **3.17–3.22**

If [1,2] shifts are not possible, the intermediate gold carbenoid is susceptible to another attack by pyridine *N*-oxide, leading to a double oxidation of the alkyne.<sup>218</sup> Arylethynyl triazenes are not able to undergo [1,2] shifts after a first oxidation, so they appeared to be suited substrates for the synthesis of 1,2-diketones. First test reactions with phenylethynyl triazene showed that Au-catalyzed double oxidation reactions can indeed be realized when an excess of pyridine *N*-oxide is employed. However, we also examined if the reaction could be catalyzed by iodine, which is proposed to follow a similar mechanistic pathway (Scheme 3.5).<sup>222</sup>



**Scheme 3.5** Proposed mechanism of the iodine-catalyzed reaction.

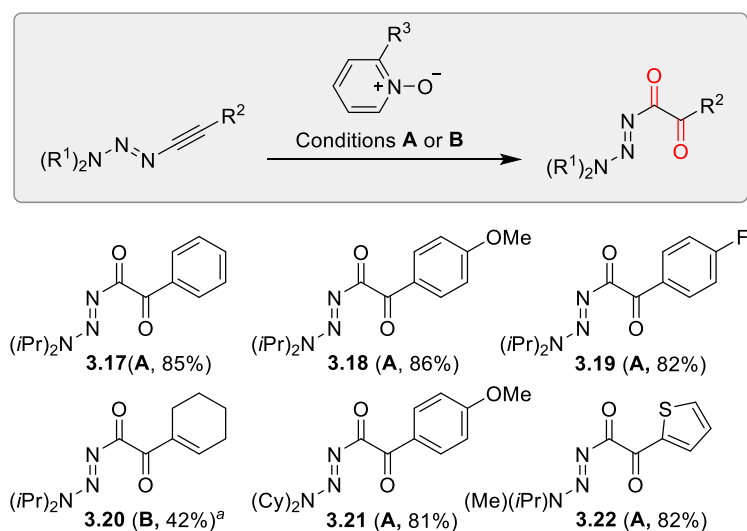
In the optimization studies, the screening of catalytic loading of  $I_2$  showed that 50 mol% led to the highest conversion (Table 3.3, entry 1-3). With pyridine-*N*-oxide, a lower yield was obtained (entry 4) and without *N*-oxide no conversion was observed (entry 5). The formation of the 1,2-diketo triazene was attempted with  $R = nBu$ , but a mixture of products was obtained instead (entry 6).

**Table 3.3** Screening of reaction conditions.

Entry	R	I <sub>2</sub> (x mol%)	Pyridine <i>N</i> -oxide (x equiv)	Time (min)	Yield (%) <sup>a</sup>
1	Ph	10	2-Cl-PNO (3 equiv)	50	36
2	Ph	20	2-Cl-PNO (3 equiv)	50	77
3	Ph	50	2-Cl-PNO (3 equiv)	50	94
4	Ph	20	PNO (3 equiv)	50	55
5	Ph	20	-	30	0
6	<i>n</i> Bu	50	2-Cl-PNO (3 equiv)	50	Mixture of products, trace of starting material

<sup>a</sup> Yields based on <sup>1</sup>H NMR spectra.

Using the optimized I<sub>2</sub>-catalyzed method, we explored the scope of the reaction (Scheme 3.6). Compared to the Au-method, the yield for the metal-free oxidation was superior (for **3.17**: 85 vs 61%). Triazenes with *p*-methoxyphenyl or *p*-fluorophenyl groups could be oxidized with similar yields (**3.18** and **3.19**). When using a triazene with a cyclohexenyl instead of an aryl group attached to the triple bond, the I<sub>2</sub> activation method was not successful. Here, the Au-catalyzed procedure turned out to be better, allowing the isolation of the diketone **3.20** in 42% yield. Varying the alkyl substituents on N3 (Cy or Me instead of *i*Pr) gave the corresponding acyl triazenes **3.21** and **3.22** in good yields using the I<sub>2</sub>-based procedure.

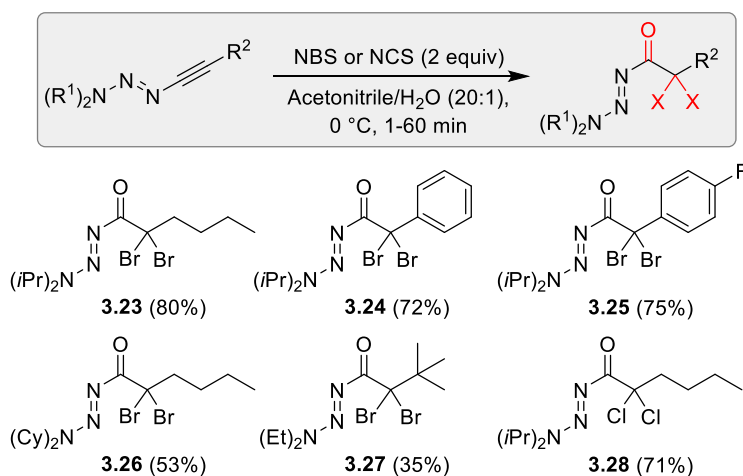


**Scheme 3.6** Double oxidation of alkynyl triazenes. Conditions **A**: 2-chloro pyridine *N*-oxide (R<sup>3</sup> = Cl, 3 equiv), I<sub>2</sub> (0.5 equiv), acetonitrile (0.1 M), rt, 50 min, conditions **B**: pyridine *N*-oxide (R<sup>3</sup> = H, 2.2 equiv), (JohnPhos)AuCl (10 mol%), AgNTf<sub>2</sub> (10 mol%), 1,2-dichloroethane (0.2 M), 70 °C, 1.5 h.

<sup>a</sup> Only conditions B gave the desired product.

### 3.5 Synthesis of the $\alpha$ -halogenated 1-acyl triazenes **3.23**–**3.28**

To expand the scope even further, we examined oxyhalogenation reactions<sup>223–226</sup> with alkynyl triazenes. Using *N*-bromosuccinimide (NBS), we were able to obtain the dibrominated 1-acyl triazenes **3.23**–**3.27** in mostly good yields (Scheme 3.7). The reactions can be performed under mild conditions (0 °C) without a catalyst, in contrast to most oxyhalogenation reactions with NBS described in the literature.<sup>223–226</sup> Changing NBS to *N*-chlorosuccinimide (NCS) led to the formation of  $\alpha$ -dichlorinated acyl triazene **3.28** in 71% yield. With *N*-iodosuccinimide (NIS), on the other hand, we were not able to prepare the corresponding diiodo compound. For the oxyhalogenation of alkynes with NXS reagents, ionic and radical mechanisms have been discussed.<sup>223–226</sup> In our case, the involvement of radicals seems likely because the reaction was found to be light sensitive. When the synthesis of **3.23** was performed in the strict absence of light, we were able to detect a significant amount of a mono-brominated acyl triazene in addition to the dibrominated product **3.23**. When the reactions were carried out under ambient light, the mono-brominated triazene was not detected. We attribute the ease of the transformation to the intrinsic reactivity of the alkynyl triazenes.



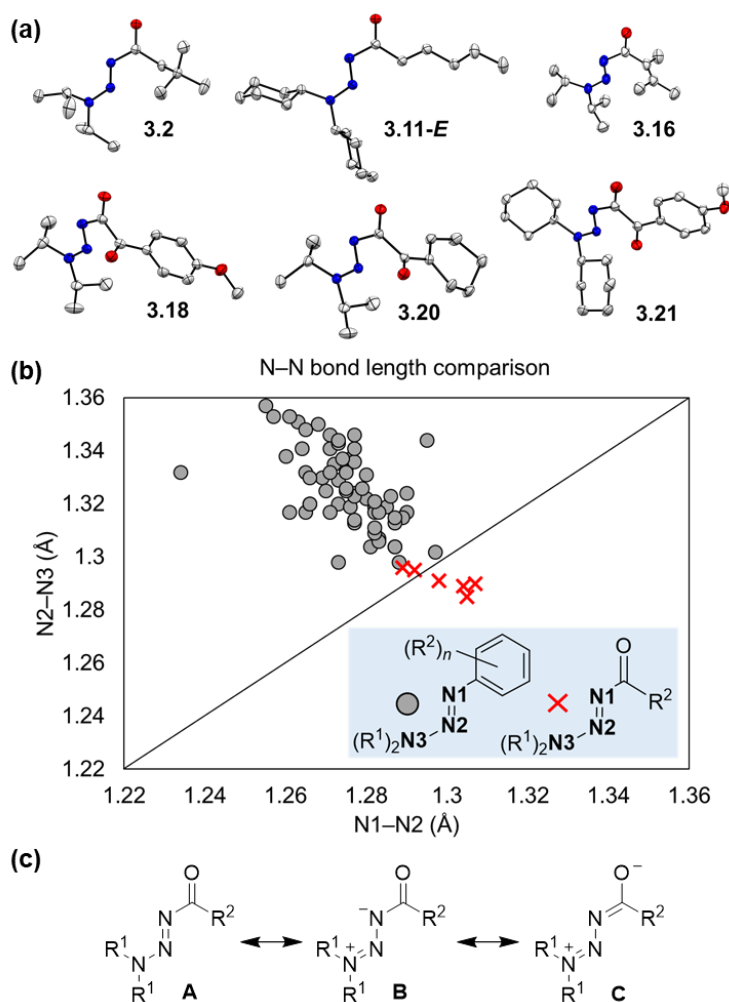
**Scheme 3.7** Oxyhalogenation of 1-acyl triazenes.

### 3.6 X-ray crystallographic data

After having established methodologies for the synthesis of four types of 1-acyl triazenes, we focused on exploring the properties of these new compounds.

The solid-state structures of **3.2**, **3.11-E**, **3.16**, **3.18**, **3.20**, and **3.21** were determined by single crystal X-ray diffraction (Figure 3.2 a). For all six compounds, the N–C=O group was found to be in plane with the triazene group, indicating electronic communication between the two.

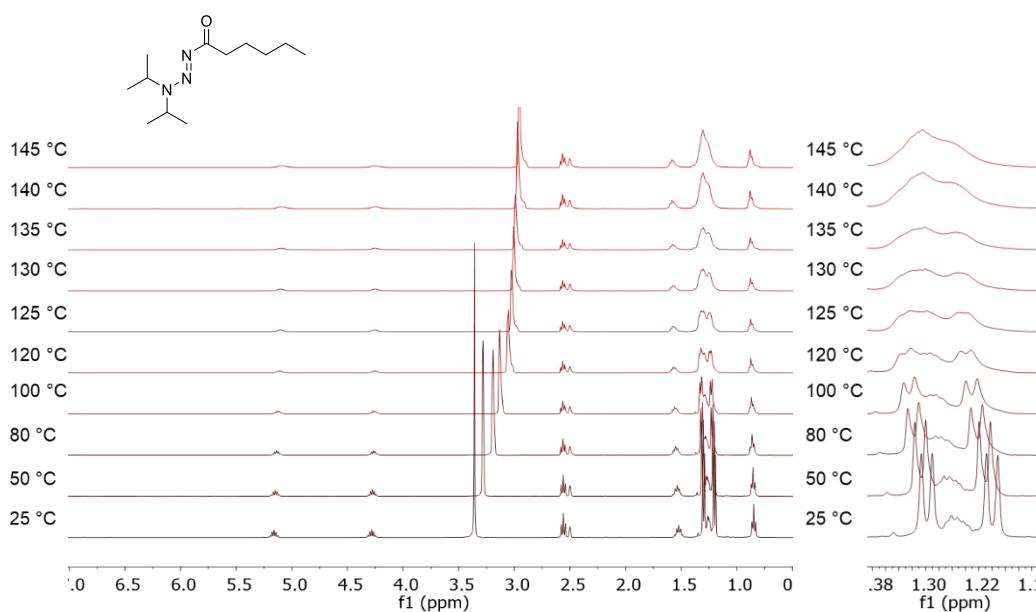
The electron-withdrawing effect of the carbonyl group has a strong effect on the structure of the triazene. Notably, the formal N–N single bond between N3 and N2 is of comparable length as the formal N=N double bond between N2 and N1. For **3.16**, **3.18**, **3.20**, and **3.21**, the N2–N3 bond is even shorter than the N1–N2 bond. The pronounced influence of the acyl group is evident when comparing the structures of 1-acyl triazenes with what is found for 3,3-dialkyl-1-aryl triazenes. An analysis of 67 compounds found in the CCDC database showed that these triazenes all display a “normal” behavior, with the formal N–N single bond being longer than the formal N=N double bond (N2–N3 av. = 1.33 Å, N1–N2 av. = 1.27 Å; Figure 3.2 b). The remarkably short N2–N3 bonds of 1-acyl triazenes imply that the resonance forms **B** and **C** contribute significantly to describing the electronic structure (Figure 3.2 c).



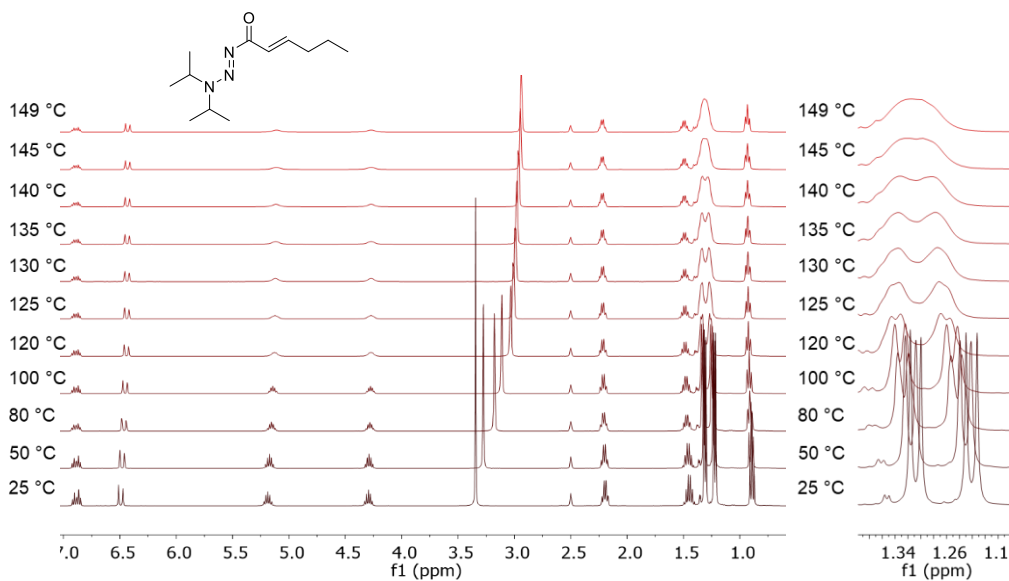
**Figure 3.2** Crystal structures of 1-acyl triazenes (a). Hydrogen atoms are omitted for clarity. N–N bond lengths of 1-aryl- and 1-acyl triazenes (b). Average bond lengths of 67 (3,3)-dialkyl-1-aryl triazenes found in the CCDC data base. Mesomeric structures of 1-acyl triazenes (c).

### 3.7 NMR Coalescence studies

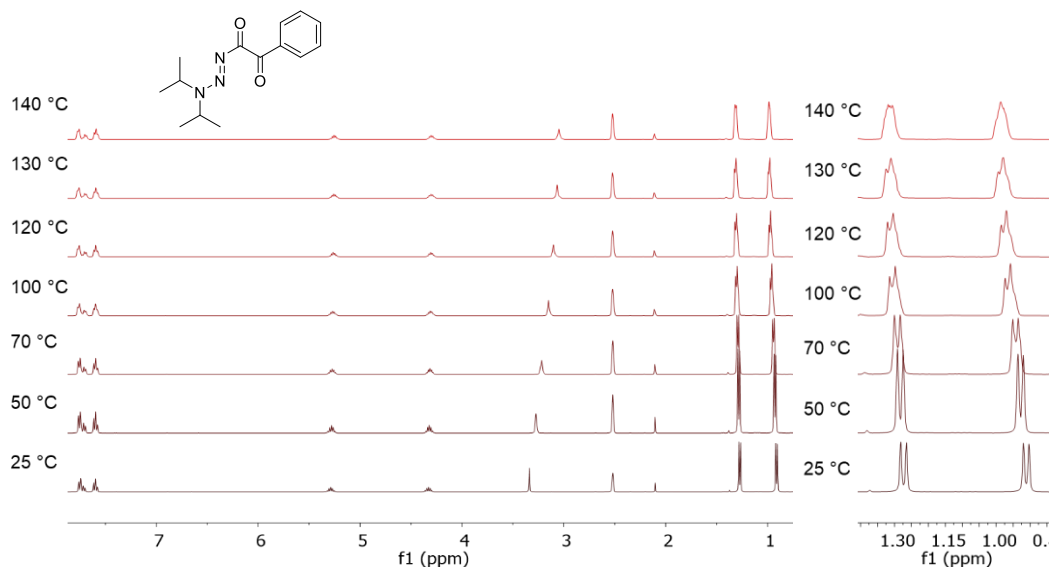
The strong double bond character of N2–N3 was also observed by NMR spectroscopy. In the case of *iso*-propyl groups at N3, there are two sets of signals observed at 25 °C, which merge into one upon raising the temperature (coalescence). To determine the rotation barrier around the N2–N3 bond, we measured  $^1\text{H}$  spectra of **3.1**, **3.10-E**, and **3.17** at variable temperatures (Figure 3.3, Figure 3.4, Figure 3.5). Based on the spectra, the corresponding rotation barriers were calculated (Table 3.4).



**Figure 3.3** Coalescence measurements with triazene **3.1**.

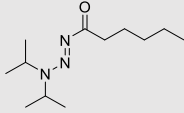
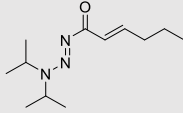
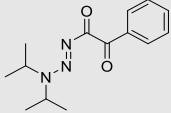


**Figure 3.4** Coalescence measurements with triazene **3.10-E**.



**Figure 3.5** Coalescence measurements with triazene **3.17**.

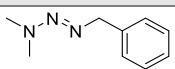
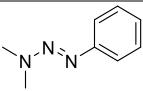
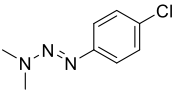
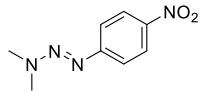
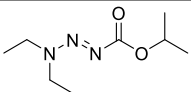
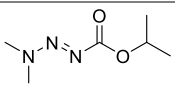
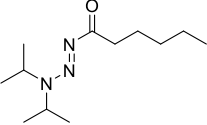
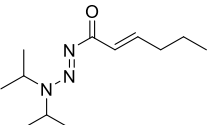
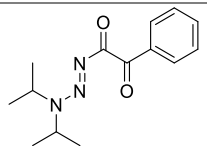
**Table 3.4** Overview of the measured and calculated values.

				
		<b>3.1</b>	<b>3.10-E</b>	<b>3.17</b>
Coalescence temperature, when two peaks merge into one	$T_c$	145 °C / 418 K	149 °C / 422 K	> 140 °C <sup>a</sup>
Separation between two signals in the absence of exchange	$\Delta\nu$	40 Hz	40 Hz	144 Hz
Rate of exchange at $T_c$	$k_c$	89 s <sup>-1</sup>	89 s <sup>-1</sup>	320 s <sup>-1</sup>
$A \xrightleftharpoons[k]{k} B$				
The free energy of activation	$\Delta G_c^\ddagger$	88 kJ mol <sup>-1</sup>	89 kJ mol <sup>-1</sup>	N.A.

<sup>a</sup> The temperature limit of the NMR spectrometer is 150 °C.

For **3.1** and **3.10-E** the measured  $T_c$  values are 145 °C and 149 °C. In the case of **3.17**, the  $T_c$  is > 140 °C, above the temperature limit of the NMR spectrometer. The rotation barriers for **3.1** and **3.10-E** were ~88-89 kJ mol<sup>-1</sup>. Compared to other triazenes (Table 3.5), it shows that the 1-acyl triazenes have high  $T_c$  and rotation barriers under the given conditions.

**Table 3.5** Comparison of  $T_c$  and rotation barriers.

Entry	Triazene	$T_c$ (°C)	$\Delta\nu$ (Hz)	$\Delta G_c^\ddagger$ (kJ/mol)	Method and solvent
<b>1<sup>a</sup></b>		-42	169	44.8 (+/- 0.8)	<sup>13</sup> C-NMR, 25.2 MHz, CDCl <sub>3</sub>
<b>2<sup>b</sup></b>		-23.5	19	57.3 (+/- 1.3)	<sup>1</sup> H-NMR, 60 MHz, CDCl <sub>3</sub>
<b>3<sup>b</sup></b>		-13	20.2	58.2 (+/- 0.8)	<sup>1</sup> H-NMR, 60 MHz, CDCl <sub>3</sub>
<b>4<sup>b</sup></b>		37	20	65.7 (+/- 0.8)	<sup>1</sup> H-NMR, 60 MHz, CDCl <sub>3</sub>
<b>5<sup>c</sup></b>		95	25.8	78.2 (+/- 1.3)	<sup>1</sup> H-NMR, 200 MHz, C <sub>6</sub> D <sub>5</sub> NO <sub>2</sub>
<b>6<sup>c</sup></b>		106	65.5	79.5 (+/- 0.8)	<sup>1</sup> H-NMR, 200 MHz, C <sub>6</sub> D <sub>5</sub> NO <sub>2</sub>
<b>7</b> <b>(3.1)</b>		145	40	88	<sup>1</sup> H-NMR, 400 MHz, <i>d</i> <sub>6</sub> -DMSO
<b>8</b> <b>(3.10-E)</b>		149	40	89	<sup>1</sup> H-NMR, 400 MHz, <i>d</i> <sub>6</sub> -DMSO
<b>9</b> <b>(3.17)</b>		>140	144	N.A.	<sup>1</sup> H-NMR, 400 MHz, <i>d</i> <sub>6</sub> -DMSO

<sup>a</sup> Sieh, D. H. *et al. J. Am. Chem. Soc.* **2005** (ref <sup>227</sup>) <sup>b</sup> Marnilo, N. P. *et al. J. Am. Chem. Soc.* **1968** (ref <sup>228</sup>). <sup>c</sup> Acta, H. C. *et al. Helv. Chim. Acta* **1983** (ref <sup>229</sup>).

### 3.8 Temperature stability

#### 3.8.1 Liquid state (NMR)

The coalescence studies showed that the 1-acyl triazenes can be heated at high temperatures for a short amount of time. To further investigate the temperature stability, we heated the samples over longer periods of time (Figure 3.6, Figure 3.7, Figure 3.8).

The *in situ* NMR experiments revealed small amounts of  $i\text{Pr}_2\text{NH}_2^+$  as a side product. It is worth noting that the products are thermally very stable. For compound **3.17**, for example, we could detect only traces of decomposition after heating a solution in  $d_6$ -DMSO for 5 days at 140 °C.

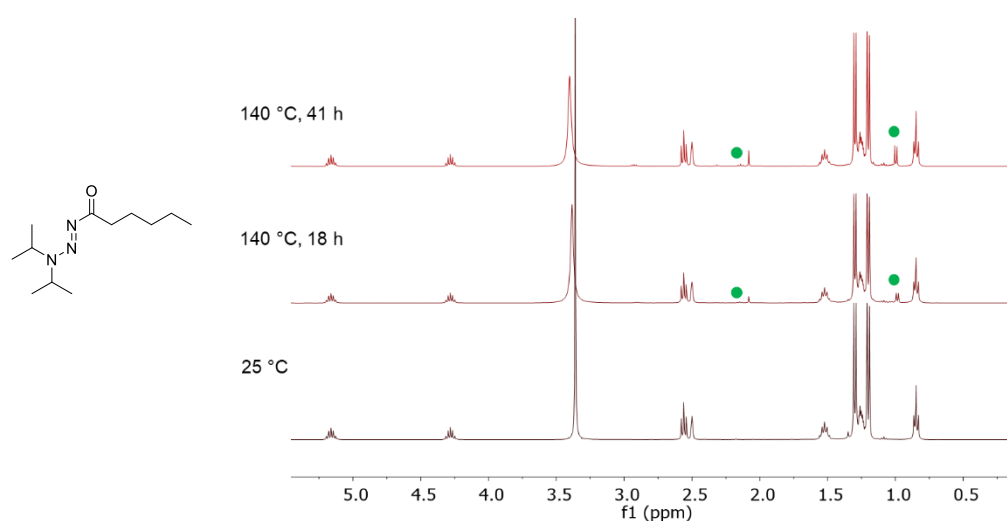


**Figure 3.6** Alkyl 1-acyl triazene **3.1** in  $d_6$ -DMSO. Formation of the free amine, indicated by the green circle.

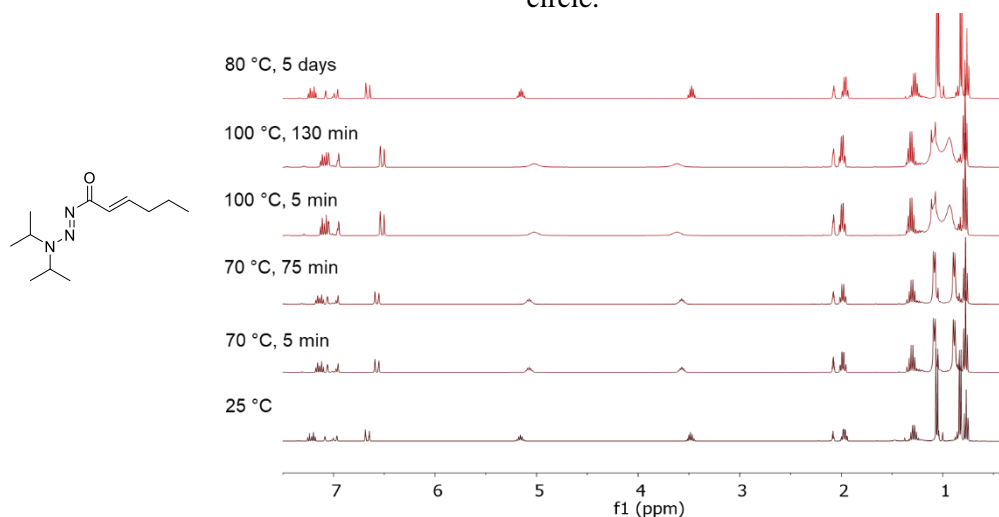


**Figure 3.7** Olefinic 1-acyl triazene **3.10-E** in  $d_8$ -toluene. The time points at 70 °C and 100 °C were measured *in situ* in the NMR spectrometer.

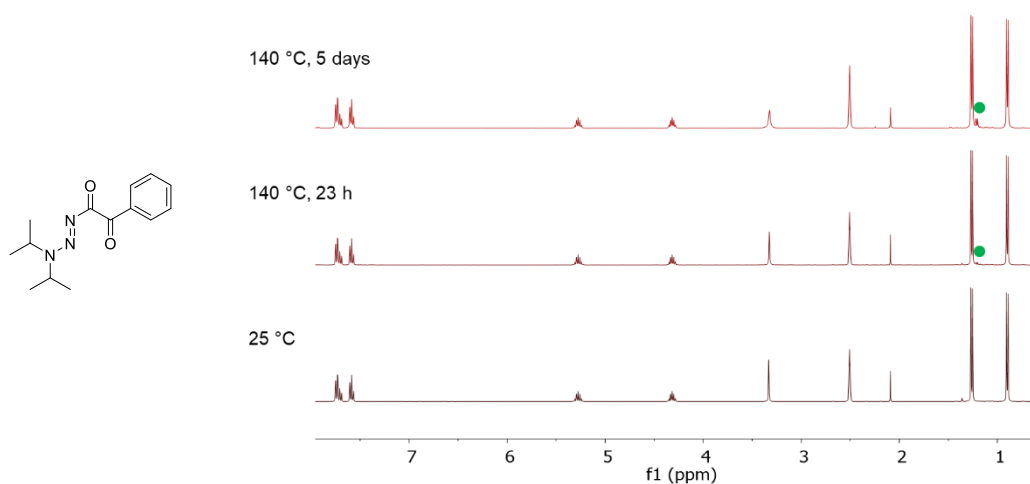


**Figure 3.8** 1,2-Diketo triazene **3.17** in in  $d_6$ -DMSO. Formation of the free amine, indicated by the green circle.

### 3.8.2 Solid state (TGA)

To determine at what temperature the triazenes decompose in the solid state, we performed thermogravimetric analyses (TGA) (Figure 3.9). Above a temperature of 100 °C, the triazenes start to decompose. A gradual decrease is observed and no sudden decrease in weight, which is the case of explosive materials. The 1,2-diketo triazene **3.17** was more stable at higher temperatures than the other measured triazenes.

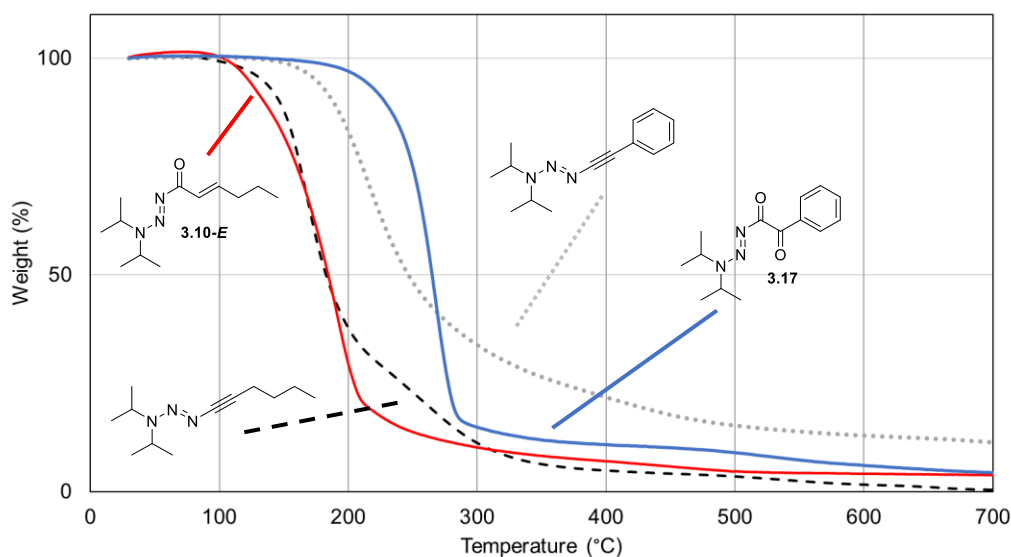
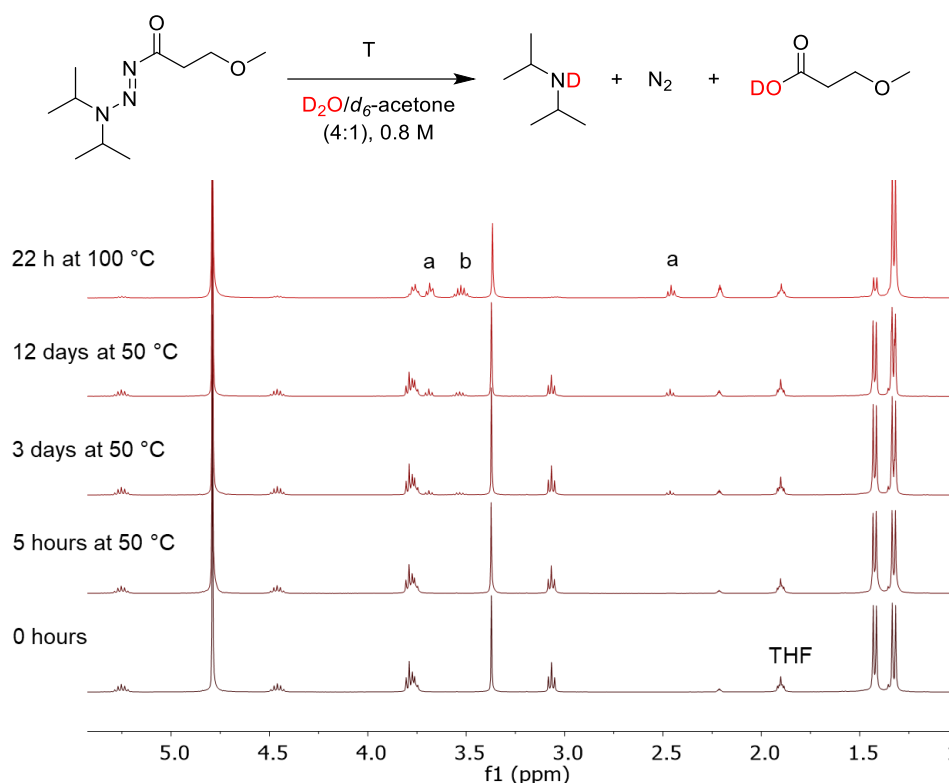


**Figure 3.9** TGA results of compounds **3.10-E** and **3.17** and 1-alkynyl triazenes.

### 3.9 Hydrolytic stability

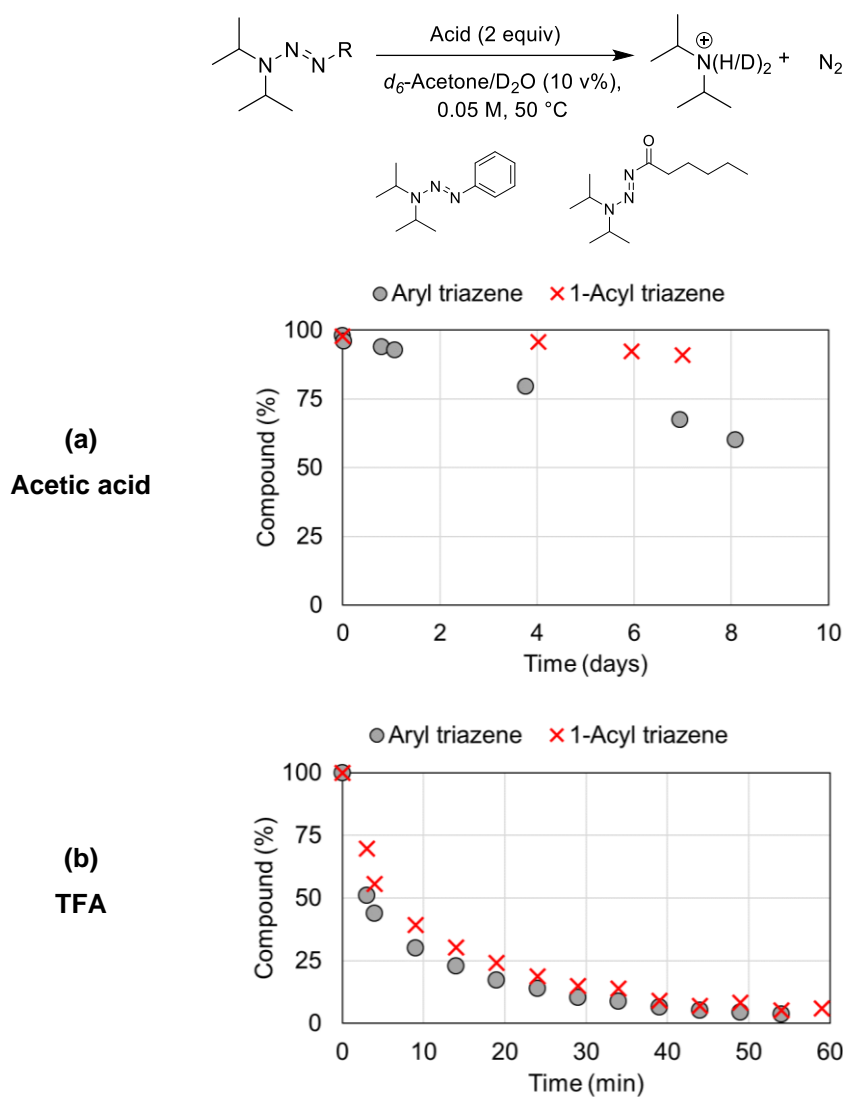
3-Acyl triazenes are known to undergo facile hydrolysis.<sup>198</sup> In order to assess the hydrolytic stability of 1-acyl triazenes, we have analyzed solutions of **3.3** in D<sub>2</sub>O/*d*<sub>6</sub>-acetone (4:1) by NMR spectroscopy (Scheme 3.8). Compound **3.3** was chosen because of its solubility in aqueous solution. After heating for 12 days at 50 °C, only partial hydrolysis was observed (28%). Heating for 22 h to reflux resulted in 61% hydrolysis. These results show that 1-acyl triazenes have a comparatively low susceptibility to hydrolysis.



**Scheme 3.8** Hydrolysis of **3.3** followed by NMR spectroscopy. Signals (a) correspond to the carboxylic acid and (b) to the diisopropylamine.

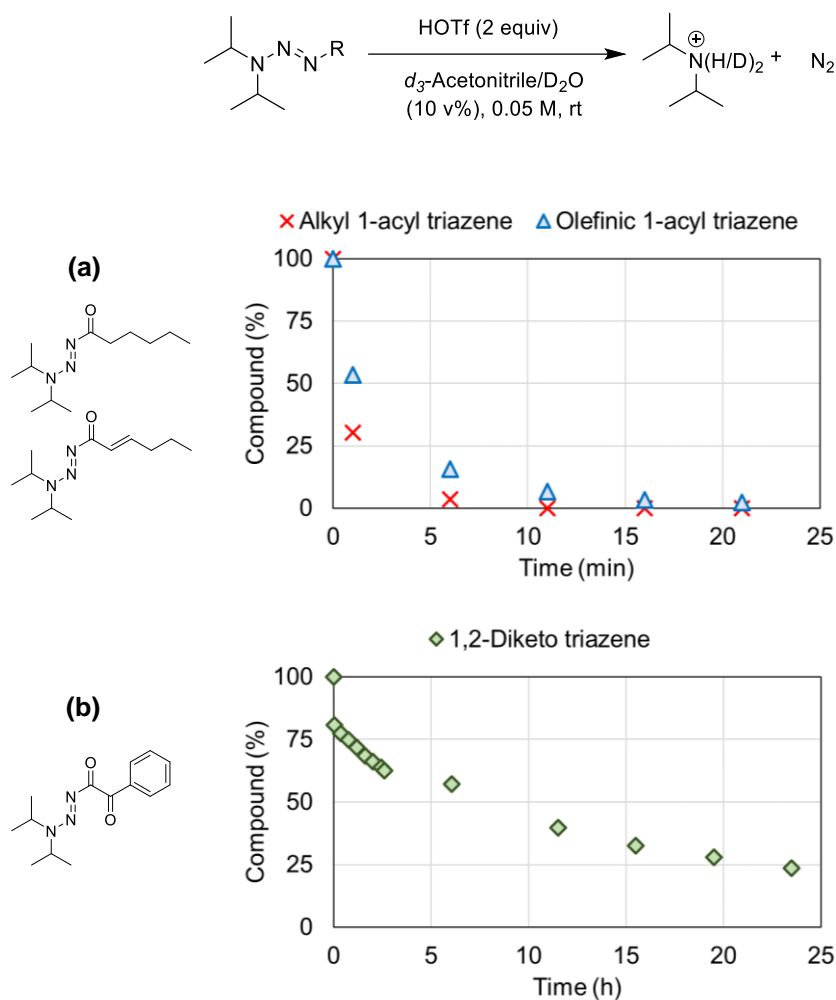
## 3.10 Acid sensitivity

The acid sensitivity of the aryl triazene  $\text{PhN}_3/\text{Pr}_2$  and the 1-acyl triazene **3.1** was evaluated using NMR spectroscopy (Scheme 3.9). The ammonium salt is formed by acid-induced cleavage of the triazene function. In the case of acetic acid, the results indicate that the 1-acyl triazene **3.1** is more stable over a couple of days than the aryl triazene under the given conditions. For TFA, the decomposition is nearly complete within 1 hour and the 1-acyl triazene **3.1** is slightly more stable than the aryl triazene.



**Scheme 3.9** Acetic acid- (a) or TFA-(b) induced decomposition of the aryl triazene and **3.1** as determined by NMR spectroscopy.

Next, the acid sensitivity of the 1-acyl triazenes **3.1**, **3.10-E** and **3.17** was evaluated with triflic acid (Scheme 3.10). Compared to TFA, the alkyl (**3.1**) and olefinic (**3.10-E**) triazenes decompose more rapidly with the stronger acid HOTf. In the case of the 1,2-diketo triazene (**3.17**), the triazene was relatively stable and it required nearly 25 hours to reach 75% decomposition.

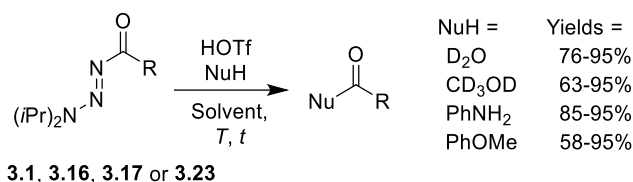


**Scheme 3.10** Triflic acid-induced decomposition of the triazenes **3.1** and **3.10-E** (a) and **3.17** (b) as determined by NMR spectroscopy.

## 3.11 Reactivity studies

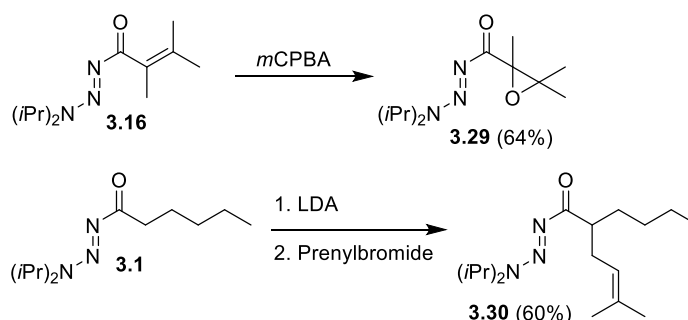
As shown above, triazenes are acid-sensitive compounds. Acid-induced N2–N3 bond cleavage of 1-acyl triazenes was expected to give highly reactive acyldiazonium compounds, which could act as acylation agents. In order to examine if such reactivity can indeed be observed, we analyzed reactions of the 1-acyl triazenes **3.1**, **3.16**, and **3.17** with HOTf in the presence of different nucleophiles (water, methanol, aniline, and anisole). In most cases, a clean acylation reaction was observed (Scheme 3.11).

Attempts to perform more challenging acylation reactions with benzene as a nucleophile were not successful. We have also examined acylation reactions with the brominated triazene **3.23**. With water and methanol, the expected products were obtained in 76% and 94% yield, respectively, but reactions with anisole and aniline gave a mixture of products, and more detailed analyses were not performed.



**Scheme 3.11** 1-Acyl triazenes as acylating agents. Yields and product ratios were determined by <sup>1</sup>H NMR spectroscopy. Conditions: HOTf (2 equiv), NuH = D<sub>2</sub>O: CD<sub>3</sub>CN/D<sub>2</sub>O, 9:1, 0.05 M, rt (for **3.23**: 70 °C), 11 – 90 min; NuH = CD<sub>3</sub>OD: neat, 0.05 M, rt, 44 – 59 min; NuH = aniline (2 equiv): CD<sub>3</sub>CN (0.05 M), 70 °C, 70 min – 18 h; NuH = anisole (2 equiv): CD<sub>3</sub>CN (0.05 M), 70 °C, 20 – 21 h.

Finally, we have briefly examined reactions under nonacidic conditions (Scheme 3.12). Oxidative conditions are compatible with the triazene function, as evidenced by the synthesis of epoxide **3.29**. Strongly basic conditions are also tolerated, and we were able to perform an alkylation reaction with prenylbromide via an enolate intermediate generated by LDA (**3.30**).



**Scheme 3.12** Reactions of the 1-acyl triazenes **3.16** and **3.1**. Conditions: **3.29**: DCM (0.2 M), *m*CPBA (1.1 equiv), rt, 2 h, isolated yield; **3.30**: LDA (1.42 equiv), prenylbromide (1.5 equiv) in THF, –78 °C, isolated yield.

### 3.12 Biological assays

An investigation of the biological activity of the new acyl triazenes appeared worthwhile. The bioactivity of previously reported triazenes is generally related to the fact that they represent masked alkylating agents.<sup>103,180–182,190–195</sup> 1-Acyl triazenes act as masked acylating, rather than alkylating, agents. Therefore, these compounds might display a biological activity which is distinct from that of other triazenes. It should be noted that triazenes can be mutagenic and/or carcinogenic and thus appropriate care and safe handling should be taken into account.

A selection of 15 compounds was submitted for cytotoxicity assays (Figure 3.10). Dose-response curves were recorded for 6 cell lines: Hela (Human cervix adenocarcinoma), A2780 (human ovarian carcinoma), MDA-MB-231 (human breast adenocarcinoma), MCF7 (human breast adenocarcinoma (metastases from pleural effusion)), MCF-10A (human epithelial breast), and HEK293T (human embryonic kidney).

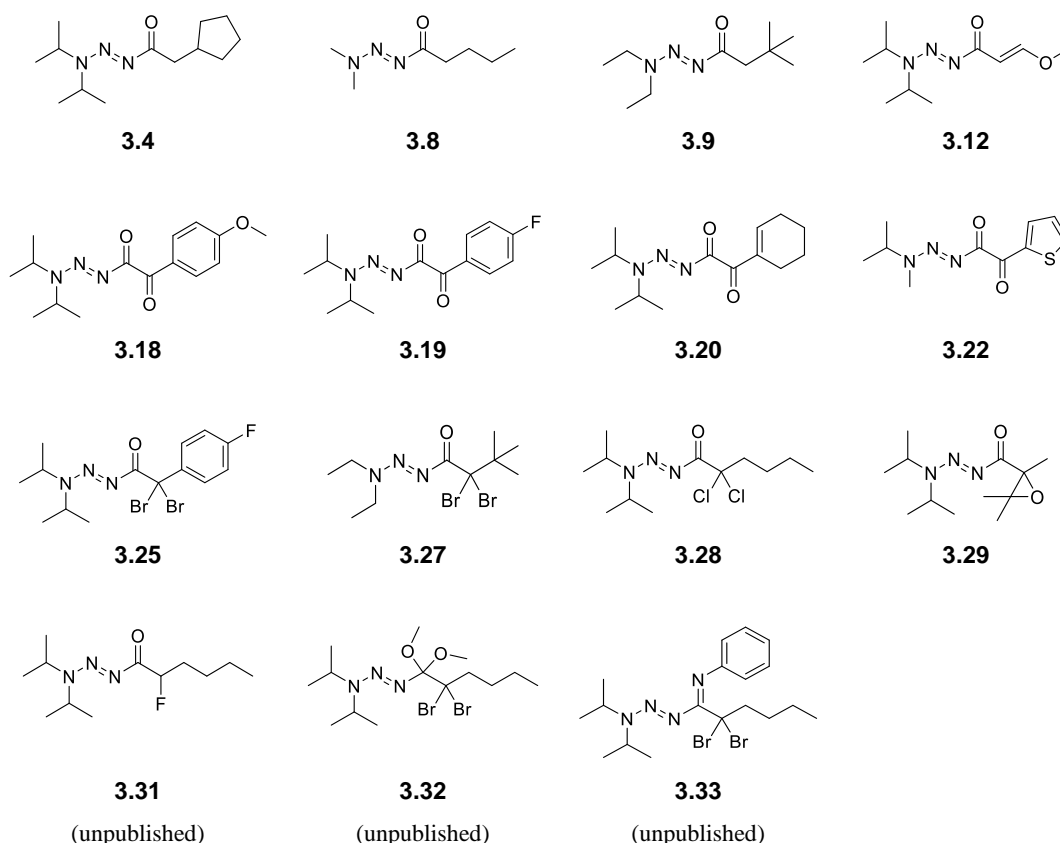


**Figure 3.10** List of compounds selected for biological assays.

Four out of the 15 triazenes showed cytotoxicity of >10% at a concentration of 10  $\mu$ M against at least one cell-line (Table 3.6). The values represent the percentage of the cell population killed by

the product, according to the fluorescence level of resazurin, which is proportional to the number of living cells. Compound **3.25** showed the highest toxicity of 70% against A2780. Compounds **3.12**, **3.27**, and **3.33** showed moderate to low cytotoxicity (<50%). The other compounds listed in Figure 3.10 were below the cytotoxicity threshold (<10%).

**Table 3.6** Cytotoxicity (%) at 10  $\mu$ M.

Compound	Hela	A2780	MDA-MB-231	MCF7	MCF-10A	HEK293T
<b>3.12</b>		33				
<b>3.25</b>	18	70	47			
<b>3.27</b>	11	47	13			
<b>3.33</b>		19				

The presence of bromine atoms was found to enhance the cytotoxicity in some cases (Figure 3.11). For example, an increased toxicity of 47% was found for **3.27** when compared to that of **3.9** (<10%). In the case of the diketo triazene **3.19**, when the acyl group is replaced by bromine atoms in **3.25**, the cytotoxicity is increased to 70% (A2780). For the 1,2-diol **3.32**, however, no significant bioactivity was observed despite of the presence of bromine atoms. In contrast, iminyltriazenes **3.33** did show some toxicity.

While a set of 1-acyl triazenes showed some cytotoxicity, their interaction with the cells and biological pathway remains unclear.

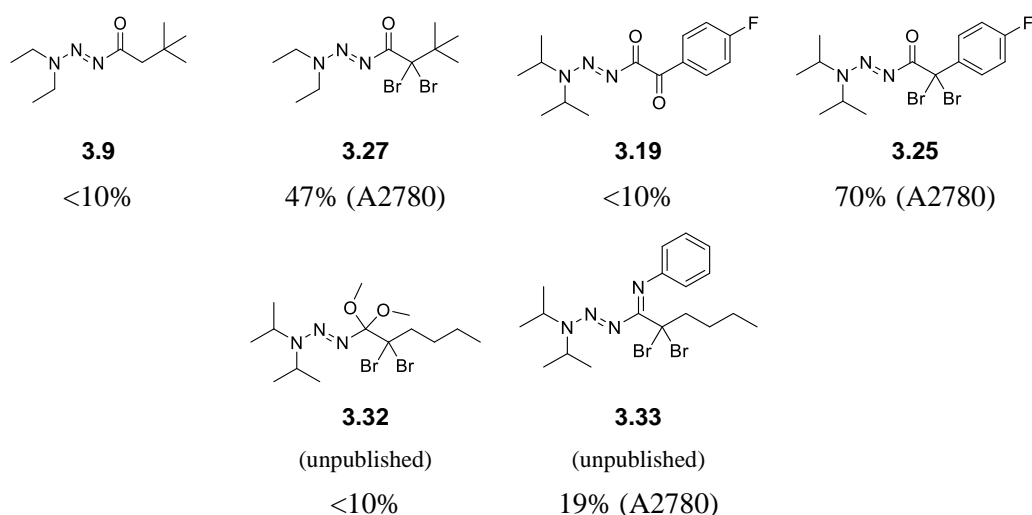


**Figure 3.11** Comparison of cytotoxicity.

For the most toxic compounds, dose-response curves were measured and the concentrations of the compound required to achieve half maximal inhibition ( $IC_{50}$ ) were calculated (Table 3.7). A flat line was observed for the dose-response curve of **3.27**, which is non-specific. It is therefore not clear what is causing the cytotoxicity. Compound **3.12** showed a promising dose-responsive curve and was active against A2780.

**Table 3.7**  $IC_{50}$  in  $\mu M$ .

Compound	Hela	A2780	MDA-MB-231	MCF7	MCF-10A	HEK293T
<b>3.12</b>		9			18	47
<b>3.25</b>	15	3	9	21	71	8
<b>3.27</b> <sup>a</sup>	>100	(2 ?)	(26 ?)			
<b>3.33</b>		14				

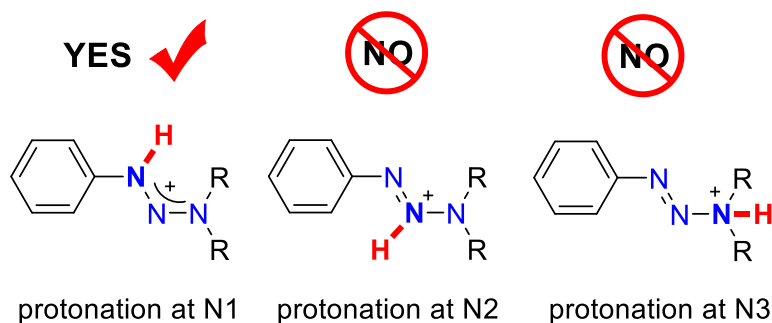
<sup>a</sup> Flat line in the dose-response curve.

To qualify as an actual “hit” in drug development, the cellular  $IC_{50}$  should be  $< 5 \mu M$ . Suitable candidates for chemotherapy or any clinical applications should have  $IC_{50}$  in the range of *ca.* 10 nM. In our case, the compounds have  $IC_{50}$  values of  $> 3 \mu M$  and therefore are considered as having low activity. Accordingly, structural variations were not further investigated. Under the assumption that 1-acyl triazenes serve as masked acylating agents, there needs to be an activating metabolism step to activate them. Further studies *in vivo* would be necessary to study the metabolic pathway in more detail.

### 3.13 Conclusion

In conclusion, we have shown that 1-acyl triazenes can be prepared by hydrolysis or oxidation of 1-alkynyl triazenes. Using these methods, we were able to synthesize for the first time a variety of 1-acyl triazenes. The acyl group at the N1 position was found to have a strong influence on the physical and chemical properties of the triazenes. Crystallographic analyses revealed extremely short N2–N3 bond lengths. Accordingly, the energy barrier for rotation around this bond is much higher than what has been reported for other triazenes. The new 1-acyl triazenes are thermally robust compounds with a low susceptibility to hydrolyze. Under acidic conditions, they act as acylating agents. Basic or oxidative conditions, on the other hand, are well tolerated by the triazene function. The investigation of the biological activity revealed that some cytotoxicity was observed, the origin of which remains unclear

## 4 Brønsted and Lewis acid adducts of triazenes



Part of this chapter has been published in:

**I. R. Landman**,\* A. A. Suleymanov,\* R. Scopelliti, F. Fadaei-Tirani, F. M. Chadwick and K. Severin, *Dalton Trans.*, 2020, 49, 2317–2322.

DOI: [10.1039/D0DT00049C](https://doi.org/10.1039/D0DT00049C)

(\* These authors contributed equally)

Reprinted in an adapted version with permission from RSC Publishing and all authors.

Author contributions: **I.R.L.** synthesized and characterized the protonated (1-acyl) triazenes by NMR and X-ray crystallography, and obtained single crystals of the Brønsted and Lewis adducts. A.A.S. contributed by obtaining NMR data of N1-protonated triazenes. F.M.C. obtained preliminary results and crystal structure of the N1-coordination of B(C<sub>6</sub>F<sub>5</sub>)<sub>3</sub>. R.S. and F.F.T. performed X-ray crystal structure analyses. K.S. supervised the research project. K.S., **I.R.L.**, and A.A.S. prepared the manuscript with contributions of all co-authors. The results obtained by A.A.S. and F.M.C. are not discussed in this chapter.



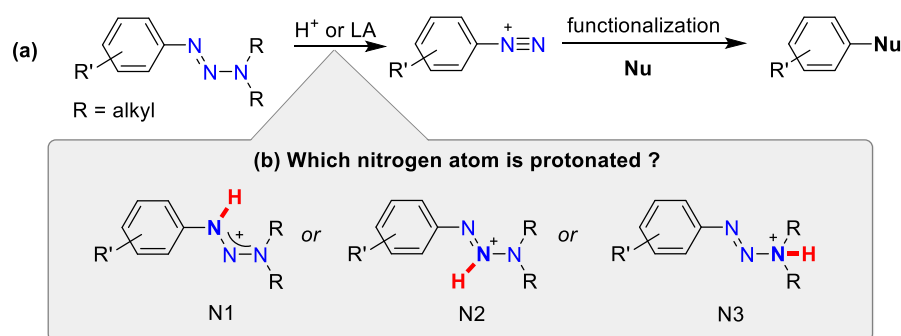
For the corresponding GIF, scan:



## 4.1 Introduction

Aryl diazonium salts are versatile reagents in synthetic organic chemistry, as was discussed in Chapter 1.<sup>230–234</sup> Handling and isolation of these sensitive compounds can be problematic, which is why they are usually generated and consumed *in situ*.<sup>235,236</sup> 1-Aryl-3,3-dialkyl triazenes represent surrogates for aryl diazonium compounds.<sup>103,104,109,237</sup> These triazenes are simple to synthesize and handle, and they are stable under neutral or basic conditions. The addition of Brønsted or Lewis acids results in the cleavage of the triazene group and liberation of an aryl diazonium compound, which can then engage in further functionalization (Scheme 4.1 a).<sup>103,104,109,237</sup>

The acid-induced cleavage of triazenes has been investigated extensively with kinetic<sup>115–124</sup> and theoretical studies,<sup>125–129</sup> which is of interest for the synthetic utility of triazenes and their potential biological activity.<sup>130,131</sup> Despite the numerous studies, it is still unclear which of the three nitrogen atoms is preferentially protonated upon addition of acid (Scheme 4.1 b). Protonation on N3 is expected to weaken the N2–N3 bond, and thus promoting the cleavage of the triazene, forming the diazonium compound. Therefore, the intermediate is suggested to be protonated on N3 for 1-aryl-3,3-dialkyl triazenes.<sup>104,238–242</sup> However, computational analyses reveal that N1 is equally or even more basic than N3 in some cases.<sup>125–129,243–247</sup> While N1 protonation can be the most energetically favorable, this is often discounted, because it does not lead to the experimentally observed reactivity of N2–N3 bond cleavage. With N1 protonation, delocalization is expected to strengthen the N2–N3 bond. N2 is considered to be the least favorable protonation site.



**Scheme 4.1** Brønsted or Lewis acid-induced conversion of 1-aryl-3,3-dialkyl triazenes into diazonium compounds (a), and the question of the relative proton affinity of the N atoms (b).

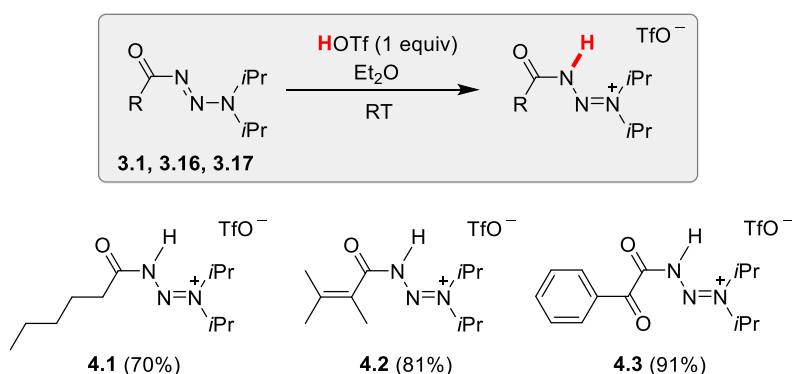
Pytela and co-workers showed indirect evidence for an N1-protonated triazene as a ‘non-reactive associate’.<sup>117</sup> Based on kinetic studies, they suggest that two molecules of trichloroacetic acid are coordinating to N1 of 3-alkyl-1,3-diaryl triazenes in hexane. A polar associate was favored over an ion pair, but the exact structure of this species was not further investigated.

In the case of 3-acyl triazenes, the protonation site and decomposition pathways become even more complex.<sup>107,126,197,198,248</sup> Firstly, there are multiple decomposition pathways depending on the pH. Secondly, the carbonyl offers an additional protonation site. Michejda and co-workers demonstrated computationally that N3-protonation is a much higher energy process than either O or N1-protonation.<sup>248</sup> Similar to aryl triazenes, N1-protonation is regarded as not important as a productive pathway for triazene cleavage.

The synthesis and properties of 1-acyl triazenes were previously discussed (Chapter 3),<sup>249</sup> which also raises the question of what their preferential protonation site is (N1, N3 or O). Since the N1-acylated triazenes were remarkably stable compared to other triazenes, we proposed to study in more detail the interaction with Brønsted and Lewis acids. As a result, we were able to obtain structural and spectroscopic experimental evidence for elusive N1-protonated intermediates.<sup>250</sup>

## 4.2 Brønsted acid adducts of 1-acyl triazenes 4.1–4.3

First, we studied the protonation of 1-acyl triazenes (**3.1**, **3.16**, and **3.17**, Scheme 4.2) with Brønsted acids. The presence of an acyl group at N1 position was expected to lower the proton affinity of this site. In addition, the oxygen atom of the acyl group represents a new potential protonation site.<sup>248</sup> Initial experiments revealed that protonated 1-acyl triazenes are stable enough to be isolated on a preparative scale (Scheme 4.2). The addition of triflic acid to a solution of the triazenes in diethyl ether at room temperature led to the immediate formation of precipitates, which were isolated in yields between 70 and 91%. All three solids were found to be stable when stored under N<sub>2</sub> atmosphere at –40 °C. The next challenge was to find experimental evidence for the protonation sites.



**Scheme 4.2** Synthesis of protonated 1-acyl triazenes.

### 4.2.1 IR spectroscopic data

Analyses of the powders by IR spectroscopy showed bands at 1765–1743  $\text{cm}^{-1}$  for the carbonyl groups. In addition, we observed new absorptions at 1579–1545  $\text{cm}^{-1}$  for all three compounds. For example, for **4.1**, the C=O stretching (\*) shifts to 1765  $\text{cm}^{-1}$  and the N-H bend (×) is visible at 1545  $\text{cm}^{-1}$  (Figure 4.1). These values corresponds to what is expected for an amide II-type band.<sup>251</sup> The IR spectra were therefore the first indirect evidence that protonation had also occurred at position N1.

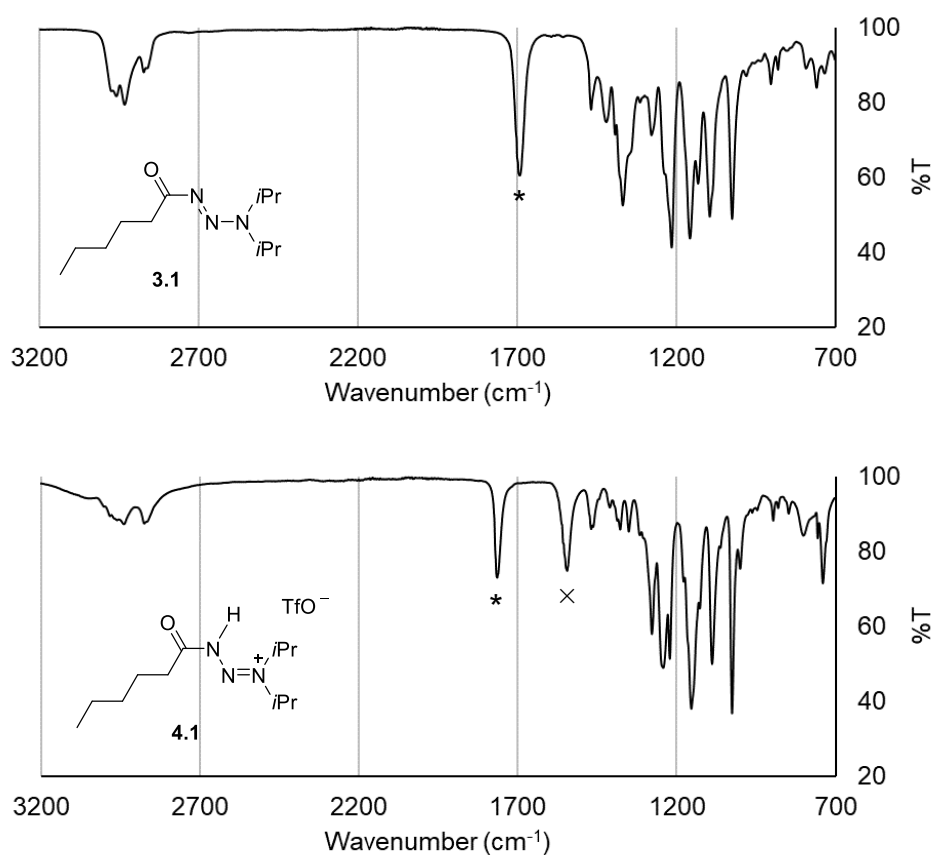
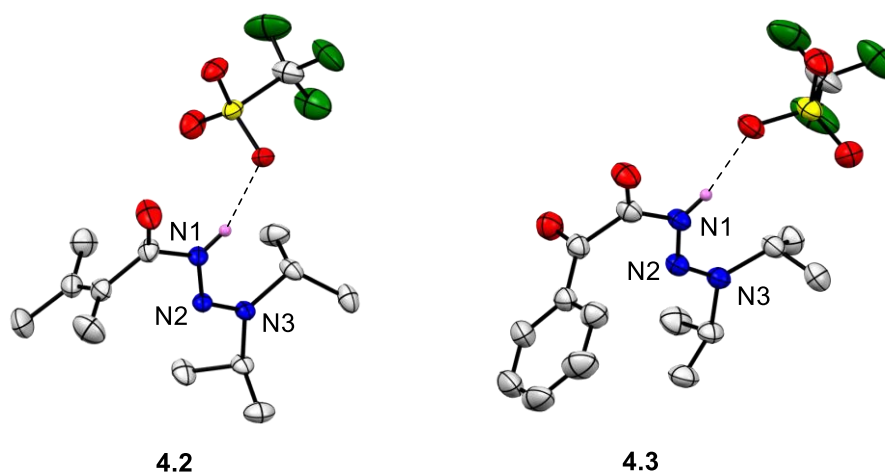


**Figure 4.1** IR spectra of **3.1** and **4.1**. For the other IR spectra, please see the Experimental Section.

### 4.2.2 X-ray crystallographic data

The salts **4.2** and **4.3** were crystallized by using layering techniques at low temperature. Crystallographic analyses revealed that in both cases, protonation had occurred at N1 position (Figure 4.2; the H atoms bound to N1 were found in a difference map and refined freely). Instead of balanced N1–N2 and N2–N3 bond distances, as is observed for the 1-acyl triazenes (see Chapter 3), we find shorter N2–N3 bonds and longer N1–N2 bonds for **4.2** and **4.3**. The bonding situation in these

compounds is therefore best described with a mesomeric form showing a double bond between N2 and N3. One can observe hydrogen bonds between the triflate anion and the N–H group of the cation. For **4.2**, the triflate anion links two adjacent cations via hydrogen bonds ( $N1\cdots O4 = 2.831(2)$  and  $2.919(2)$  Å; only one is shown in Figure 4.2), whereas for **4.3**, an individual hydrogen bond between the triflate anion (O3) and the N–H group is observed ( $N1\cdots O3 = 2.804(3)$  Å).



Compound	N1–N2 (Å)	N2–N3 (Å)	$\angle N1N2N3$ (°)
<b>4.2</b>	1.3104(19)	1.2649(19)	120.07(13)
<b>4.3</b>	1.319(2)	1.256(2)	121.18(17)

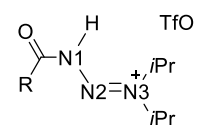


**Figure 4.2** Molecular structures of **4.2** and **4.3** in the solid state. The thermal ellipsoids are at 50% probability. With the exception of NH, hydrogen atoms are not shown for clarity.

### 4.2.3 NMR spectroscopy

In order to examine the situation in solution, we have recorded HSQC and HMBC NMR spectra of a mixture of **3.1** and HOTf to get **4.1** in  $CD_2Cl_2$  at  $-80$  °C. The direct coupling between N–H is observed in the  $^1H$ - $^{15}N$  HSQC spectrum (Figure 4.3). The other  $^{15}N$  chemical shifts were revealed in the  $^1H$ - $^{15}N$  HMBC spectrum (Figure 4.4).

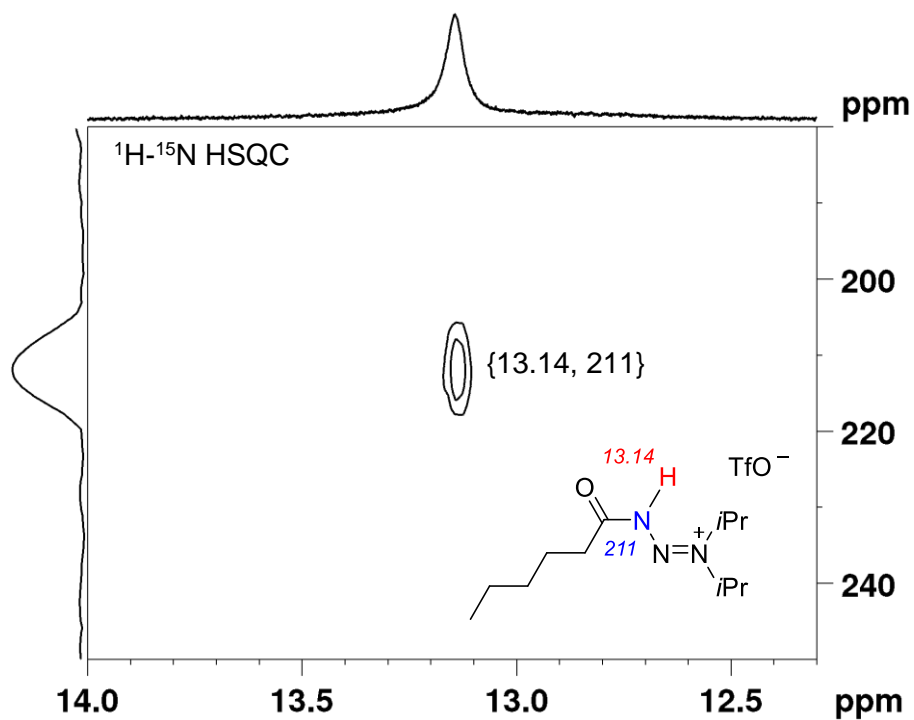


**Figure 4.3**  $^1\text{H}$ - $^{15}\text{N}$  HSQC NMR spectrum of **4.1** ( $-80^\circ\text{C}$ ,  $\text{CD}_2\text{Cl}_2$ ).

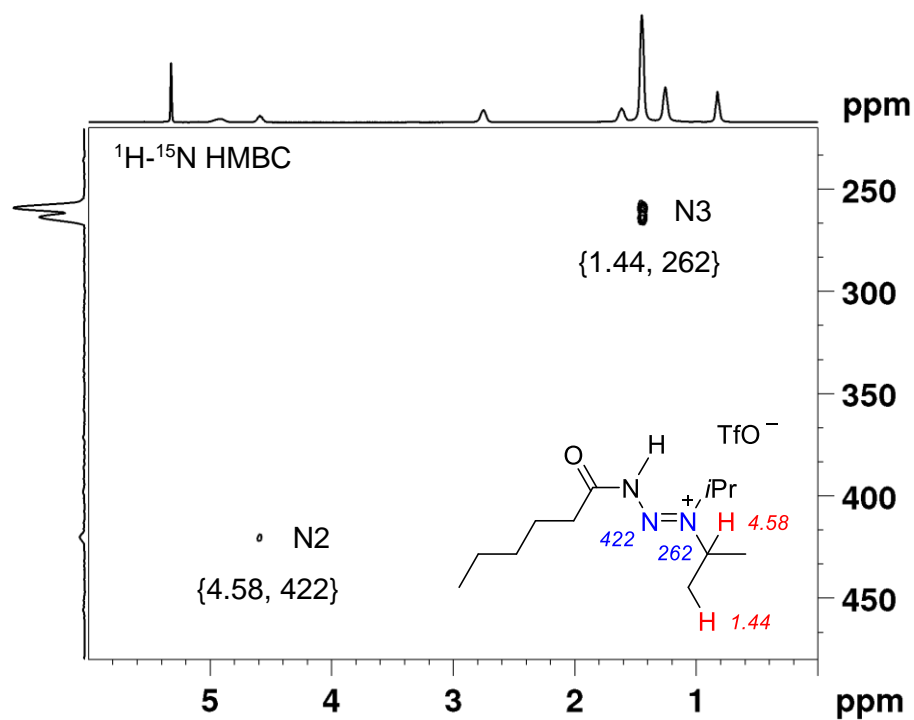
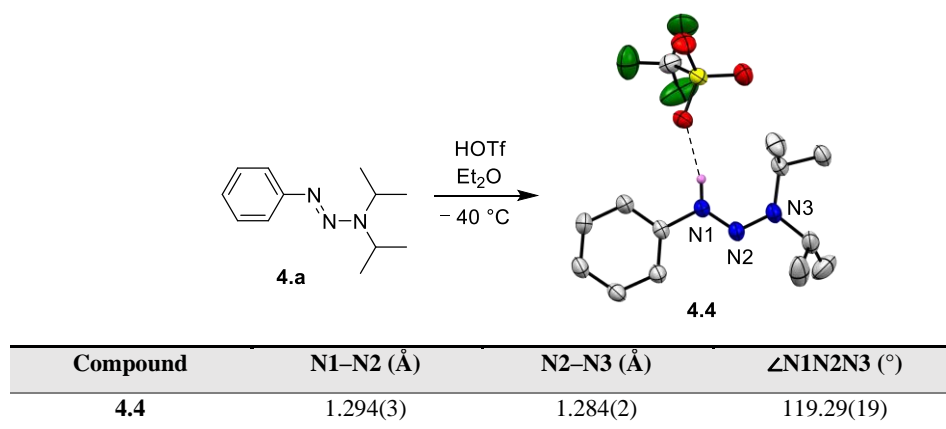


**Figure 4.4**  $^1\text{H}$ - $^{15}\text{N}$  HMBC NMR spectrum of **4.1** ( $-80^\circ\text{C}$ ,  $\text{CD}_2\text{Cl}_2$ ).

### 4.3 Brønsted acid adduct of 1-aryl-3,3-dialkyl triazene **4.4**

The combined data from IR- and NMR-spectroscopy and X-ray crystallography confirm that the nitrogen atom in position 1 is protonated.

Eager to apply our findings to the more standard 1-aryl-3,3-dialkyl triazene, we have performed low temperature crystallizations of different aryl triazene/HOTf/solvent mixtures. Suitable single crystals were finally obtained from aryl triazene **4.a**, using diethyl ether as solvent. A crystallographic analysis confirmed that the proton is located at N1 (Scheme 4.3). It is worth noting that the hydrogen atom bound to nitrogen was found in a difference map and refined freely. In line with the anticipated charge delocalization, the N2–N3 bond of **4.4** (1.284(2) Å) has a similar length as the N1–N2 bond (1.294(3) Å). The plane defined by the three nitrogen atoms of **4.4** is nearly coplanar with the plane of the phenyl ring. One oxygen atom of the triflate anion is found within hydrogen bonding distance to the N–H group ( $N1\cdots O1 = 2.859(3)$  Å).



**Scheme 4.3** Protonation of the aryl triazene **4.a** and molecular structure of **4.4** in the crystal. The thermal ellipsoids are at 50% probability. With the exception of NH, hydrogen atoms are not shown for clarity.

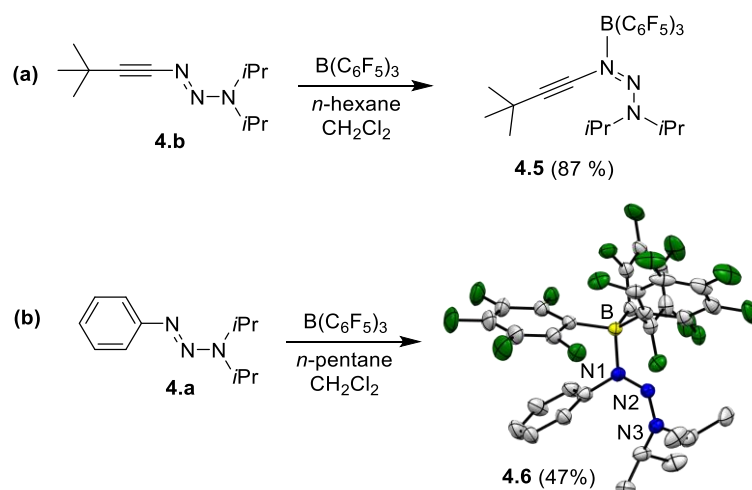
### 4.4 Lewis acid adducts of triazenes **4.5–4.7**

The results summarized in the previous section show that protonation of triazenes preferentially occurs at N1 position. The higher basicity of this site should translate to higher affinity to Lewis acids, given that steric interactions can be neglected.

For our investigations, we have used the strong Lewis acid  $B(C_6F_5)_3$ . In order to reduce the influence of steric interactions between the Lewis acid and the substituent at N1 position, we have first examined reactions with the 1-alkynyl triazene **4.b** (Scheme 4.4 a).<sup>139</sup>

A solution of **4.b** in hexane was added to a solution of  $B(C_6F_5)_3$  in dichloromethane/hexane (1:1). The mixture was then stored at  $-40\text{ }^\circ\text{C}$ , resulting in the formation of a yellow precipitate (**4.5**). Compound **4.5** was isolated in 87% yield (Scheme 4.4 a). The N1-coordination was confirmed by X-ray crystallography by Chadwick in the published paper.<sup>250</sup>

For aryl triazene **4.a**, we were also able to obtain a  $B(C_6F_5)_3$  adduct in crystalline form (**4.6**). X-ray crystallography of **4.6** confirms that the Lewis acid is coordinated to the N1 atom (Scheme 4.4 b). The dative B–N bond has a length of  $1.615(3)\text{ \AA}$ . This value is comparable to what has been reported for adducts of  $B(C_6F_5)_3$  with N-donors (average bond length B–N =  $1.626\text{ \AA}$ ). Interestingly, the bound triazene adopts an unusual *Z* configuration. Most likely, this configuration is favored because it minimizes steric interactions with the bulky Lewis acid. It is assumed that N1-coordination of the Lewis acid facilitates *E* to *Z* isomerization, because electron density is removed from the N1–N2 bond.



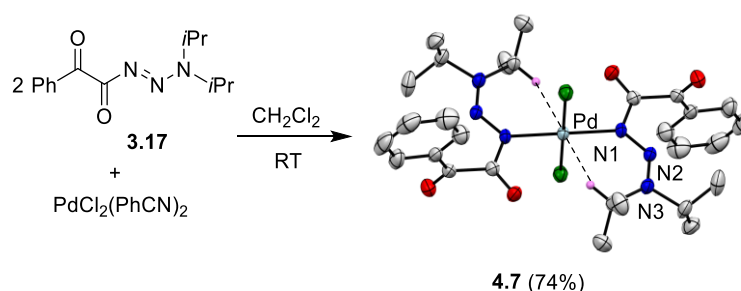
Compound	N1–N2 (Å)	N2–N3 (Å)	∠N1N2N3 (°)	N1–B (Å)
<b>4.6</b>	1.293(3)	1.288(3)	124.1(2)	1.615(3)

**Scheme 4.4** Synthesis of the  $B(C_6F_5)_3$  adducts **4.5** and **4.6**. The thermal ellipsoids are at 50% probability. Hydrogen atoms are not shown for clarity.

Since several reactions of triazenes involving Pd catalysis are reported,<sup>150,252–258</sup> we have additionally explored the coordination of triazenes with  $PdCl_2$ . Information about the binding site of neutral triazenes to transition metals has been limited,<sup>133–135,137,138,145,259–261</sup> and thus more information on the preferred coordination mode would be valuable for further mechanistic proposals.

For our study, we have used acyl triazene **3.17**. For solubility reasons,  $PdCl_2(PhCN)_2$  was employed. From mixtures of  $PdCl_2(PhCN)_2$  (1 equiv) and the respective triazene (2 equiv) in dichloromethane, we were able to obtain the Pd complex **4.7** in 74% yield (Scheme 4.5).

X-ray crystallography reveals that the 1-acyl triazene act as monodentate ligand via N1 coordination. Similar to the other triazene adducts, a strong double bond character is observed for N2–N3 as this bond is shorter than N1–N2. A noteworthy feature of complex **4.7** is the presence of close C–H···Pd contacts<sup>262</sup> involving two isopropyl groups. In the <sup>1</sup>H NMR spectrum of **4.7**, this interaction is manifested by a strongly deshielded signal for one of the CHMe<sub>2</sub> groups at 10.16 ppm (CD<sub>2</sub>Cl<sub>2</sub>).



Compound	N1–N2 (Å)	N2–N3 (Å)	∠N1N2N3 (°)	N1–Pd (Å)
<b>4.7</b>	1.304(3)	1.270(3)	123.6(2)	2.018(2)

**Scheme 4.5** The synthesis of the Pd complex **4.7**. The thermal ellipsoids are at 50% probability. Most hydrogen atoms are omitted for clarity.

## 4.5 Bond length comparison

Selected bond lengths and angles for the triazene adducts in this chapter are summarized in Table 4.1. For comparison, we have analyzed 30 structures of neutral 1-aryl-3,3-dialkyl triazenes found in the CCDC database (Figure 4.5). The average bond length observed for N1–N2 is 1.28 Å, and the average N2–N3 bond length is 1.33 Å. In the case of 1-acyl triazenes (Chapter 3), N1–N2 and N2–N3 bond lengths are more balanced. The most pronounced effect of protonation or coordination to N1 is thus a shortening of the N2–N3 distance.

**Table 4.1** Selected bond lengths (Å) and angles (°) for the triazene adducts in this chapter.

Compound	N1–N2 (Å)	N2–N3 (Å)	∠N1N2N3 (°)	N1–B/Pd (Å)
<b>4.2</b>	1.3104(19)	1.2649(19)	120.07(13)	/
<b>4.3</b>	1.319(2)	1.256(2)	121.18(17)	/
<b>4.4</b>	1.294(3)	1.284(2)	119.29(19)	/
<b>4.6</b>	1.293(3)	1.288(3)	124.1(2)	1.615(3)
<b>4.7</b>	1.304(3)	1.270(3)	123.6(2)	2.018(2)

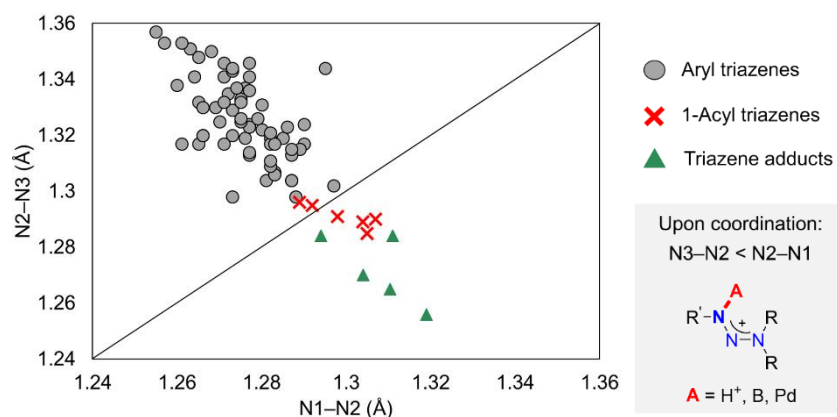


**Figure 4.5** Average bond length comparison from 30 crystal structures of neutral 1-aryl-3,3-dialkyl triazenes found in the CCDC database (●), 1-acyl triazenes from Chapter 3 (✕), and the triazene adducts shown in this chapter (▲).

## 4.6 Conclusion

We have investigated the protonation of 1-aryl and 1-acyl triazenes with triflic acid by low temperature NMR spectroscopy and single crystal X-ray analysis. The results show that the preferred protonation site is N1. Our data indicate that N1-protonation strengthens the N2–N3 bond, and thus disfavoring N2–N3 bond scission. Therefore, N1-protonated triazenes should be considered as non-productive intermediates during the acid-induced cleavage. Reversible addition should eventually lead to N3 protonation and the cleavage of the triazene.

Besides Brønsted acids, triazenes are also cleaved by strong Lewis acids.<sup>263–267</sup> Thus, we have studied triazene adducts with  $B(C_6F_5)_3$  and  $PdCl_2$ . The results show likewise that N1 is the preferred coordination site, implying that steric or chelate effects play a minor role. Similar to Brønsted acids, we assume that N1-coordinated adducts are off-pathway intermediates. These studies are of relevance since triazenes have been extensively studied in acid- and transition metal-catalyzed reactions.<sup>115,116,125–129,117–124</sup> The finding of N1-protonation preference should be taken into account for future mechanistic proposals.

## 5 Conclusion and outlook

N<sub>2</sub>O has had a remarkable journey throughout history, with applications ranging from medical purposes to additive for food or fuel. And N<sub>2</sub>O has a darker side as greenhouse gas and ozone depleting substance due to its persistent character in the atmosphere. Despite of N<sub>2</sub>O's inert character, synthetic chemists are interested in using N<sub>2</sub>O as a synthetic reagent. The oxygen atom transfer has been studied extensively (Chapter 1), in particular in selective oxidations of alkenes (also applied on industrial scale), low valent main group, and transition metal complexes. Recent studies employ milder, catalytic, and more general conditions applicable to complex reactions (*e.g.* in total synthesis). It is expected that more reactions will emerge and that selective oxidations with N<sub>2</sub>O will overcome shortcomings of other oxidation procedures.

In contrast, examples of N<sub>2</sub>O as diazo transfer reagent remained scarce (Chapter 1). The main challenges are: 1) finding reactants that can capture N<sub>2</sub>O, 2) avoiding side reactions such as the loss of N<sub>2</sub>, and 3) then forming selectively the desired product. Significant advances have been made in addressing the first challenge: activation of N<sub>2</sub>O and characterizing the corresponding product. N<sub>2</sub>O activation has been explored with transition metal complexes, frustrated Lewis pairs, N-heterocyclic carbenes and olefins, and organometallic reagents. The knowledge on how to activate N<sub>2</sub>O is increasing, however, the second goal of transferring the nitrogen atoms, remains challenging.

Synthetically interesting N-containing products from N<sub>2</sub>O have emerged only recently. Examples include, the heterocycles benzotriazinones, azoimidazolium salts as colorful dyes, and N-heterocyclic olefin based organic reducing agents. These types of compounds are potentially biologically active, have colorful properties, or serve as precursors in organic synthesis. To demonstrate the potential of N<sub>2</sub>O as diazo transfer reagent in synthetic chemistry, more examples of general procedures and new methods are required.

Herein, we demonstrated that we can apply N<sub>2</sub>O as a diazo transfer reagent for the synthesis of triazolo-pyridines and -quinolines in moderate to good yield under mild conditions (Chapter 2). Compared to other methods, our procedure employs 2-alkyl or 2-alkenyl pyridines as starting materials. With these studies we provide further evidence that N<sub>2</sub>O is a valuable reagent in synthetic chemistry. In the future, it would be interesting to use N<sub>2</sub>O in other diazo transfer reactions or even isolate the diazo compound. To get perfect atom economy, future directives should focus on incorporating the oxygen atom as well, for which only few examples have been reported to date.

That N<sub>2</sub>O was an essential N-atom donor was shown for 1-alkynyl triazenes, from which we have developed general synthetic routes to 1-acyl triazenes (Chapter 3). Previously, general routes to N1-acylated triazenes were missing. Investigating their physical and chemical properties revealed that

they are more stable than other triazenes and that they act as acylating agents under acidic conditions. In addition, they can be modified under oxidative and basic conditions, which makes them attractive to use them as new synthetic tools. Some other novel triazenes to be explored are, for example, alkyl triazenes and terminal alkynyl triazenes.

At last, while studying the triazenes in more detail, we found experimental evidence for the preferred protonation site. For both Brønsted and Lewis acid adducts of triazenes, N1 is the preferred protonation site (Chapter 4). With this experimental finding, it does raise the question how the acid goes from N1 to N3, which is proposed as the productive cleavage pathway. As more transition-metal based and new kinds of triazenes are emerging, it will be valuable to get insights into the mechanistic pathways and determine whether this finding is applicable to more triazenes in general.

To conclude, we have contributed to the synthetic chemistry of triazenes and  $\text{N}_2\text{O}$ , by 1) providing further examples of using  $\text{N}_2\text{O}$  as diazo transfer reagent to construct triazoles, 2) developing general routes of 1-acyl triazenes and analyzing their properties, and 3) investigating acid-triazene adducts.

In general, important progress has been made into the research of the synthetic utility of  $\text{N}_2\text{O}$ . For example, selective chemical transformations with  $\text{N}_2\text{O}$  can be advantageous for the reaction outcomes, such as higher yields, less side-products, simple, and general reactions. In addition, new products can be synthesized of which  $\text{N}_2\text{O}$  is the essential atom donor. Furthermore, these studies contribute to the fundamental knowledge on how to overcome the inertness of  $\text{N}_2\text{O}$ . Then perhaps in the future, it will become attractive to (continue) capture  $\text{N}_2\text{O}$  and upcycle it into more valuable products. In the meantime,  $\text{N}_2\text{O}$  will continue its bright future as a reagent in synthetic chemistry.

## Experimental section (ES)



## ES.1 Materials and methods

**Caution:** Although we have not experienced any accidents, diazo compounds and other nitrogen containing compounds are potentially explosive and toxic compounds.<sup>176</sup> In addition, alkyllithium reagents (e.g. *t*-BuLi) are pyrophoric reagents. Accordingly, their use, handling and storage should be carried out with appropriate precautions.

Unless otherwise stated, all reactions were carried out under inert atmosphere of dry N<sub>2</sub> using Schlenk or glovebox techniques. All reagents were purchased from commercial suppliers (Sigma Aldrich, Acros, TCI, VWR, Fluorochem, ABCR) and used without additional purification. Dry solvents were obtained from a solvent purification system with aluminum oxide column (Innovative Technologies). *NMR spectra* were recorded at ambient temperature (unless stated otherwise) on Bruker spectrometers: AvanceIII 400 MHz Prodigy probe 5 mm ICONNMR ATMA, Avance 400 MHz BBIZ 5mm ATMA, Avance 500 MHz CPTCIXYZ 5 mm, or Avance III HD 600 MHz CPTCIZ 5 mm. Chemical shifts in ppm were aligned with respect to the residual peak of deuterated solvent.<sup>268</sup> *Electrospray-ionisation HRMS* data were acquired on a Q-Tof Ultima mass spectrometer (Waters) or a Q-Tof 6530 Accurate mass spectrometer (Agilent) operated in the positive ionization mode and fitted with a standard Z-spray ion source equipped with the Lock-Spray interface.

### ES.1.1 Notes for Chapter 2:

Starting materials were synthesized accordingly.<sup>269–272</sup> Concentration of organolithium compounds: *n*-BuLi (2.5 M in hexanes), *s*-BuLi (1.4 M in cyclohexane) and *t*-BuLi (1.6 M in pentanes). *Column chromatography* was performed on a CombiFlash NextGen from Teledyne ISCO, using RediSep columns. *RP-HPLC*, Agilent 1260 Infinity LC, using a Kinetex 5u EVO 18 100 A column. For the rest of the NMR spectra, see: I. R. Landman, F. Fadaei-Tirani and K. Severin, *Chem. Commun.*, **2021**, 57, 11537–11540.

### ES.1.2 Notes for Chapter 3:

*Column chromatography* of triazenes and 1-acyl triazenes was carried out using pre-prepared deactivated silica by triethylamine (3 vol%) in diethyl ether, removal of the solvent under reduced pressure, and drying at room temperature under (oil pump) vacuum overnight. For the rest of the NMR spectra, see: I. R. Landman, E. Acuña-Bolomey, R. Scopelliti, F. Fadaei-Tirani and K. Severin, *Org. Lett.*, **2019**, 21, 6408–6412.

### ES.1.3 Notes for Chapter 4:

$\text{B}(\text{C}_6\text{F}_5)_3$  was purified by sublimation under vacuum prior to use. The triazenes were prepared according to published procedures.<sup>249,273</sup> IR spectra were recorded on a Perkin Elmer (UATR Two) spectrometer, using PerkinElmer Spectrum software (V 10.5.4).

## ES.2 Experimental section: triazolopyridines

### ES.2.1 Synthesis of the triazoles **2.1–2.10**

#### ES.2.1.1 Examining lithiation efficiency

In a 250 ml oven-dried Schlenk flask: 2-Benzylpyridine (1 mmol) was dissolved in THF or diethyl ether (10 ml), which was cooled to  $-78\text{ }^\circ\text{C}$  or  $0\text{ }^\circ\text{C}$ , respectively. Subsequently, *n*-BuLi was added and a red suspension formed. The mixture was stirred for 30 min at  $-78\text{ }^\circ\text{C}$  or  $0\text{ }^\circ\text{C}$ , followed by allowing to warm up to rt and stirring for additional 1.5 h. The solvent was removed under vacuum, yielding a brick-red solid. A small amount of the lithiated salt was dissolved in dry  $d_4$ -methanol. The lithiation efficiency was calculated by comparing the  $\text{CH}_2$  vs  $\text{CHD}$   $^1\text{H}$  NMR signal. For both,  $\text{Et}_2\text{O}$  and THF, the lithiation was nearly complete under the given conditions.

#### ES.2.1.2 Optimization of $\text{N}_2\text{O}$ conversion

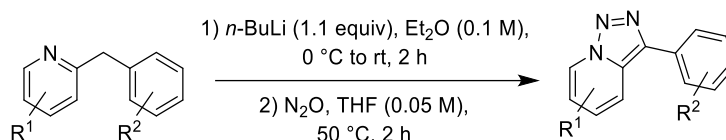
The reaction conditions were varied and the crude reaction mixtures were analyzed by  $^1\text{H}$  NMR ( $\text{CD}_2\text{Cl}_2$ ) by comparing the  $\alpha$ -H signal of the pyridyl group of product **A** (8.76 ppm), side-product **B** (8.55 ppm), and starting material **C** (8.50 ppm). In the glovebox, in an oven-dried microwave vial: Lithiated benzylpyridine (50 mg) was dissolved in THF (0.048 – 0.1 M). Next, the flask was subjected to an  $\text{N}_2\text{O}$  atmosphere (3x  $\text{N}_2\text{O}/\text{vac}$  cycles). The reaction mixture was placed in a pre-heated oil-bath. After the given time, the reaction was quenched with water, the product was extracted with ethyl acetate, and the solvent was removed under vacuum. For the scale-up reactions, a 250 ml oven-dried Schlenk was used, which was sealed with a metal clip.

#### ES.2.1.3 Reaction in two steps, one pot

In a 250 ml oven-dried Schlenk flask: 2-Benzylpyridine (0.161 ml, 1 mmol) was dissolved in THF or diethyl ether (10 ml), which was cooled to  $-78\text{ }^\circ\text{C}$  or  $0\text{ }^\circ\text{C}$ , respectively. Next, *n*-BuLi was added and a red suspension formed. The mixture was stirred for 30 min at  $-78\text{ }^\circ\text{C}$  or  $0\text{ }^\circ\text{C}$ , followed by allowing to warm up to rt and stirring for additional 1.5 h. The solvent was removed under vacuum,

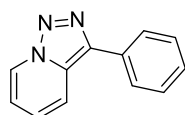
yielding a brick-red solid. The solid was redissolved in THF (20 ml), subjected to an N<sub>2</sub>O atmosphere (3x N<sub>2</sub>O/*vac* cycles) and heated at 50 °C for 2 h in a pre-heated oil bath. The solvent was removed under vacuum and water was added to quench the reaction. The product was extracted with ethyl acetate (100 ml). For the reaction screening, an aliquot of the organic phase was evaporated and the ratio of product and side-products was determined by <sup>1</sup>H NMR (CD<sub>2</sub>Cl<sub>2</sub>).

#### ES.2.1.4 General procedure



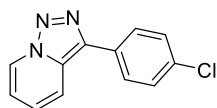
In a 250 ml oven-dried Schlenk flask: 2-Benzylpyridine (1 mmol) was dissolved in diethyl ether (10 ml). The reaction mixture was cooled to 0 °C and *n*-BuLi (1.1 equiv) was added, forming a red suspension. It was stirred for 30 min at 0 °C, followed by allowing to warm up to rt and stirring for additional 1.5 h. The solvent was removed under vacuum, yielding a brick-red solid. The solid was redissolved in THF (20 ml) and the solution was subjected to an N<sub>2</sub>O atmosphere (3x N<sub>2</sub>O/*vac* cycles) and heated at 50 °C for 2 h in a pre-heated oil bath. The solvent was removed under vacuum, water (50 ml) was added, and the product was extracted with ethyl acetate (100 ml). The organic phase was washed with brine and dried over MgSO<sub>4</sub>, filtered, and the solvent was evaporated. The resulting product was washed with diethyl ether/hexane and dried under vacuum.

#### ES.2.1.5 Scope

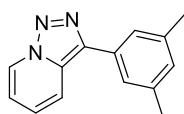


3-Phenyl-[1,2,3]triazolo[1,5-*a*]pyridine (**2.1**)

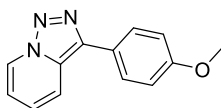
Triazolopyridine **2.1** was prepared from 2-benzylpyridine (1 mmol), following the general procedure. Yield (yellow solid): 160 mg (82%). <sup>1</sup>H NMR (600 MHz, CD<sub>2</sub>Cl<sub>2</sub>) δ 8.76 (dt, *J* = 7.1, 1.1 Hz, 1H), 8.02 (dt, *J* = 9.0, 1.2 Hz, 1H), 7.99 – 7.92 (m, 2H), 7.52 (dd, *J* = 8.5, 7.1 Hz, 2H), 7.43 – 7.37 (m, 1H), 7.34 (ddd, *J* = 9.0, 6.6, 1.0 Hz, 1H), 7.03 (td, *J* = 6.8, 1.2 Hz, 1H). <sup>13</sup>C NMR (151 MHz, CD<sub>2</sub>Cl<sub>2</sub>) δ 137.48, 131.63, 130.42, 128.91, 127.67, 126.39, 125.71, 125.57, 118.25, 115.26, 53.76, 53.58, 53.40, 53.22, 53.04. HRMS (ESI/QTOF) *m/z*: [M + H]<sup>+</sup> Calcd for C<sub>12</sub>H<sub>10</sub>N<sub>3</sub><sup>+</sup> 196.0869; Found 196.0872. The spectra are in agreement with what has been reported in the literature.<sup>274</sup>

3-(4-Chlorophenyl)-[1,2,3]triazolo[1,5-a]pyridine (**2.2**)

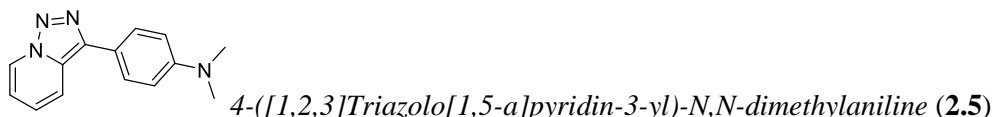
Triazolopyridine **2.2** was prepared from 2-(4-chlorobenzyl)pyridine (1 mmol), following the general procedure. Yield (orange solid): 206 mg (90%). **<sup>1</sup>H NMR** (400 MHz, CD<sub>2</sub>Cl<sub>2</sub>) δ 8.77 (dt, *J* = 7.0, 1.1 Hz, 1H), 7.99 (dt, *J* = 9.0, 1.2 Hz, 1H), 7.96 – 7.90 (m, 2H), 7.53 – 7.49 (m, 2H), 7.37 (ddd, *J* = 9.0, 6.6, 1.0 Hz, 1H), 7.05 (td, *J* = 6.9, 1.2 Hz, 1H). **<sup>13</sup>C NMR** (151 MHz, CD<sub>2</sub>Cl<sub>2</sub>) δ 136.38, 133.29, 130.41, 130.24, 129.07, 127.61, 126.09, 125.69, 118.01, 115.41, 53.76, 53.58, 53.40, 53.22, 53.04. **HRMS** (ESI/QTOF) *m/z*: [M + H]<sup>+</sup> Calcd for C<sub>12</sub>H<sub>9</sub>ClN<sub>3</sub><sup>+</sup> 230.0480; Found 230.0481. The spectra are in agreement with what has been reported in the literature.<sup>274</sup>

3-(3,5-Dimethylphenyl)-[1,2,3]triazolo[1,5-a]pyridine (**2.3**)

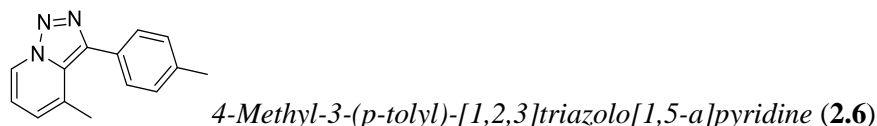
Triazolopyridine **2.3** was prepared from 2-(3,5-dimethylbenzyl)pyridine (0.41 mmol), following the general procedure. Yield (yellow solid): 62 mg (67%). **<sup>1</sup>H NMR** (400 MHz, CDCl<sub>3</sub>) δ 8.75 (dt, *J* = 7.0, 1.1 Hz, 1H), 8.02 (dt, *J* = 9.0, 1.2 Hz, 1H), 7.59 (dt, *J* = 1.5, 0.7 Hz, 2H), 7.30 (ddd, *J* = 9.0, 6.6, 1.0 Hz, 1H), 7.07 – 7.03 (m, 1H), 7.00 (td, *J* = 6.8, 1.2 Hz, 1H), 2.42 (d, *J* = 0.8 Hz, 6H). **<sup>13</sup>C NMR** (151 MHz, CD<sub>2</sub>Cl<sub>2</sub>) δ 138.58, 137.76, 131.32, 130.38, 129.39, 125.52, 125.44, 124.19, 118.46, 115.21, 53.76, 53.58, 53.40, 53.22, 53.04, 21.10. **HRMS** (ESI/QTOF) *m/z*: [M + H]<sup>+</sup> Calcd for C<sub>14</sub>H<sub>14</sub>N<sub>3</sub><sup>+</sup> 224.1182; Found 224.1187. The spectra are in agreement with what has been reported in the literature.<sup>274</sup>

3-(4-Methoxyphenyl)-[1,2,3]triazolo[1,5-a]pyridine (**2.4**)

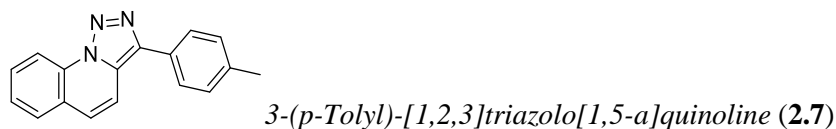
Triazolopyridine **2.4** was prepared from 2-(4-methoxybenzyl)pyridine (0.62 mmol), following the general procedure. Additional purification was performed by flash column chromatography, hexane/ethyl acetate (2:1 to 3:2). Yield (off-white solid): 78 mg (55%). **<sup>1</sup>H NMR** (400 MHz, CD<sub>2</sub>Cl<sub>2</sub>) δ 8.73 (dt, *J* = 7.1, 1.1 Hz, 1H), 7.97 (dt, *J* = 9.0, 1.2 Hz, 1H), 7.93 – 7.81 (m, 2H), 7.30 (ddd, *J* = 9.0, 6.6, 1.0 Hz, 1H), 7.11 – 7.03 (m, 2H), 7.00 (td, *J* = 6.9, 1.3 Hz, 1H), 3.87 (s, 3H). **<sup>13</sup>C NMR** (101 MHz, CD<sub>2</sub>Cl<sub>2</sub>) δ 159.57, 137.65, 130.15, 127.85, 125.60, 125.32, 124.34, 118.42, 115.26, 114.49, 55.41, 54.04, 53.77, 53.50, 53.23, 52.96. **HRMS** (ESI/QTOF) *m/z*: [M + H]<sup>+</sup> Calcd for C<sub>13</sub>H<sub>12</sub>N<sub>3</sub>O<sup>+</sup> 226.0975; Found 226.0978. The spectra are in agreement with what has been reported in the literature.<sup>274</sup>



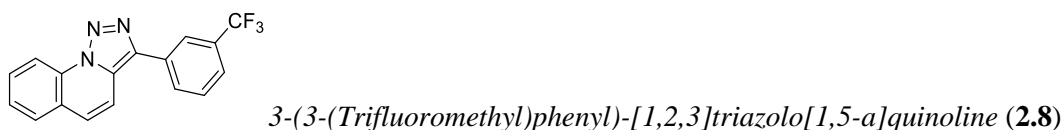
Triazolopyridine **2.5** was prepared from *N,N*-dimethyl-4-(pyridin-2-ylmethyl)aniline (0.53 mmol), following the general procedure. Additional purification was performed by flash column chromatography, hexane/ethyl acetate (2:1 to 3:2). Yield (yellow solid): 126 mg (49%). <sup>1</sup>H NMR (400 MHz, CD<sub>2</sub>Cl<sub>2</sub>) δ 8.78 – 8.62 (m, 1H), 7.97 (dd, *J* = 9.1, 1.3 Hz, 1H), 7.88 – 7.73 (m, 2H), 7.32 – 7.18 (m, 1H), 6.97 (t, *J* = 7.0 Hz, 1H), 6.90 – 6.80 (m, 2H), 3.02 (s, 6H). <sup>13</sup>C NMR (151 MHz, CD<sub>2</sub>Cl<sub>2</sub>) δ 150.23, 138.23, 129.66, 127.27, 125.33, 124.58, 119.42, 118.57, 115.02, 112.48, 53.76, 53.58, 53.40, 53.22, 53.04, 40.18. HRMS (ESI/QTOF) *m/z*: [M + H]<sup>+</sup> Calcd for C<sub>14</sub>H<sub>15</sub>N<sub>4</sub><sup>+</sup> 239.1291; Found 239.1292. New compound.



Triazolopyridine **2.6** was prepared from 3-methyl-2-(4-methylbenzyl)pyridine (1.15 mmol), following the general procedure. Yield (red/brown solid): 212 mg (91%). <sup>1</sup>H NMR (600 MHz, CD<sub>2</sub>Cl<sub>2</sub>) δ 8.60 (d, *J* = 7.0 Hz, 1H), 7.54 – 7.39 (m, 2H), 7.30 (d, *J* = 7.7 Hz, 2H), 6.98 (dt, *J* = 6.8, 1.2 Hz, 1H), 6.90 (t, *J* = 6.8 Hz, 1H), 2.44 (s, 3H), 2.33 (s, 3H). <sup>13</sup>C NMR (151 MHz, CD<sub>2</sub>Cl<sub>2</sub>) δ 139.30, 138.04, 131.22, 130.25, 129.49, 129.32, 128.65, 124.68, 123.04, 115.18, 53.76, 53.58, 53.40, 53.22, 53.04, 20.96, 19.29. HRMS (ESI/QTOF) *m/z*: [M + H]<sup>+</sup> Calcd for C<sub>14</sub>H<sub>14</sub>N<sub>3</sub><sup>+</sup> 224.1182; Found 224.1187. New compound.

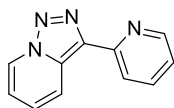


Triazoloquinoline **2.7** was prepared from 2-(4-methylbenzyl)quinoline (0.79 mmol), following the general procedure. Yield (yellow solid): 178 mg (86%). <sup>1</sup>H NMR (600 MHz, CD<sub>2</sub>Cl<sub>2</sub>) δ 8.79 (dd, *J* = 8.3, 1.1 Hz, 1H), 7.95 – 7.85 (m, 3H), 7.84 – 7.76 (m, 2H), 7.68 – 7.57 (m, 2H), 7.40 – 7.32 (m, 2H), 2.44 (s, 3H). <sup>13</sup>C NMR (151 MHz, CD<sub>2</sub>Cl<sub>2</sub>) δ 139.52, 137.78, 131.85, 129.87, 129.41, 128.36, 128.27, 127.94, 126.88, 126.51, 126.39, 123.79, 115.80, 115.10, 53.56, 53.38, 53.20, 53.02, 52.84, 20.78. HRMS (ESI/QTOF) *m/z*: [M + H]<sup>+</sup> Calcd for C<sub>17</sub>H<sub>14</sub>N<sub>3</sub><sup>+</sup> 260.1182; Found 260.1184. New compound.



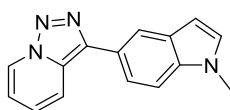
Triazoloquinoline **2.8** was prepared from 2-(3-(trifluoromethyl)benzyl)quinoline (0.76 mmol), following the general procedure. Yield (yellow solid): 219 mg (93%). <sup>1</sup>H NMR (400 MHz, CD<sub>2</sub>Cl<sub>2</sub>) δ

8.82 (d,  $J = 8.3$  Hz, 1H), 8.29 (s, 1H), 8.21 (ddd,  $J = 5.9, 3.7, 1.8$  Hz, 1H), 7.93 (dd,  $J = 8.0, 1.4$  Hz, 1H), 7.89 – 7.79 (m, 2H), 7.75 – 7.64 (m, 4H).  $^{13}\text{C}$  NMR (101 MHz,  $\text{CD}_2\text{Cl}_2$ )  $\delta$  137.99, 132.31, 131.85, 131.15, 130.26, 129.71, 129.40, 128.48, 128.42, 127.62, 127.19, 125.39, 124.23, 124.19, 123.78, 123.15, 123.11, 115.94, 114.47, 53.74, 53.47, 53.20, 52.93, 52.66. HRMS (ESI/QTOF)  $m/z$ :  $[\text{M} + \text{H}]^+$  Calcd for  $\text{C}_{17}\text{H}_{11}\text{F}_3\text{N}_3^+$  314.0900; Found 314.0887. New compound.



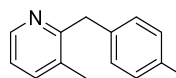
3-(Pyridin-2-yl)-[1,2,3]triazolo[1,5-a]pyridine (**2.9**)

Triazoloquinoline **2.9** was prepared from di(pyridin-2-yl)methane (0.53 mmol), following the general procedure. Heated under  $\text{N}_2\text{O}$  atmosphere for 19 hours. It was purified by flash column chromatography, petroleum ether/ ethyl acetate (10:1 to 1:1). Yield (white solid): 39 mg (37%).  $^1\text{H}$  NMR (400 MHz,  $\text{CDCl}_3$ )  $\delta$  8.84 – 8.72 (m, 2H), 8.69 (ddd,  $J = 4.9, 1.8, 0.9$  Hz, 1H), 8.38 (dt,  $J = 8.0, 1.1$  Hz, 1H), 7.83 (td,  $J = 7.8, 1.8$  Hz, 1H), 7.49 – 7.34 (m, 1H), 7.31 – 7.18 (m, 1H), 7.06 (td,  $J = 6.7, 1.3$  Hz, 1H).  $^{13}\text{C}$  NMR (151 MHz,  $\text{CDCl}_3$ )  $\delta$  151.83, 149.11, 137.17, 132.18, 126.70, 125.41, 122.23, 121.40, 120.81, 116.12. HRMS (nanochip-ESI/LTQ-Orbitrap)  $m/z$ :  $[\text{M} + \text{H}]^+$  Calcd for  $\text{C}_{11}\text{H}_9\text{N}_4^+$  197.0822; Found 197.0818. The spectra are in agreement with what has been reported in the literature.<sup>274</sup>



3-(1-Methyl-1H-indol-5-yl)-[1,2,3]triazolo[1,5-a]pyridine (**2.10**)

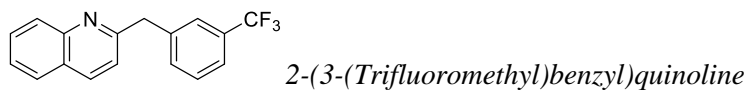
Triazolopyridine **2.10** was prepared from 1-methyl-5-(pyridin-2-ylmethyl)-1H-indole (0.51 mmol), following the general procedure. The reaction mixture was stirred for 4 h at 50 °C under  $\text{N}_2\text{O}$  atmosphere. Yield (yellow solid): 54 mg (44%).  $^1\text{H}$  NMR (600 MHz,  $\text{CD}_2\text{Cl}_2$ )  $\delta$  8.74 (dt,  $J = 7.1, 1.1$  Hz, 1H), 8.13 (dd,  $J = 1.7, 0.7$  Hz, 1H), 8.08 (dt,  $J = 9.0, 1.2$  Hz, 1H), 7.84 (dd,  $J = 8.5, 1.7$  Hz, 1H), 7.49 (d,  $J = 8.5$  Hz, 1H), 7.30 (ddd,  $J = 9.0, 6.6, 1.0$  Hz, 1H), 7.19 – 7.11 (m, 1H), 7.01 (td,  $J = 6.8, 1.2$  Hz, 1H), 6.57 (dd,  $J = 3.1, 0.9$  Hz, 1H), 3.85 (s, 3H).  $^{13}\text{C}$  NMR (151 MHz,  $\text{CD}_2\text{Cl}_2$ )  $\delta$  138.87, 136.23, 129.91, 129.55, 128.61, 125.18, 124.68, 122.58, 120.45, 118.58, 118.42, 114.89, 109.59, 100.90, 53.56, 53.38, 53.20, 53.02, 52.84, 32.63. HRMS (ESI/QTOF)  $m/z$ :  $[\text{M} + \text{H}]^+$  Calcd for  $\text{C}_{15}\text{H}_{13}\text{N}_4^+$  249.1135; Found 249.1140. New compound.



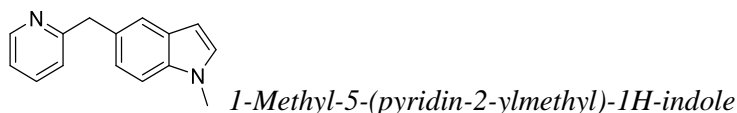
3-Methyl-2-(4-methylbenzyl)pyridine

3-Methyl-2-(4-methylbenzyl)pyridine was synthesized according to literature procedure.<sup>269</sup> With TMP, yield (yellow oil): 206 mg (65%).  $^1\text{H}$  NMR (600 MHz,  $\text{CD}_2\text{Cl}_2$ )  $\delta$  8.36 (dd,  $J = 4.9, 1.7$  Hz, 1H), 7.42 (ddd,  $J = 7.6, 1.9, 0.9$  Hz, 1H), 7.07 (s, 5H), 4.11 (s, 2H), 2.29 (s, 3H), 2.25 (s, 3H).  $^{13}\text{C}$  NMR (101 MHz,  $\text{CD}_2\text{Cl}_2$ )  $\delta$  158.93, 146.42, 137.49, 136.03, 135.34, 131.32, 128.71, 128.35, 121.26, 53.74,

53.67, 53.47, 53.20, 52.93, 52.66, 41.25, 20.43, 18.45. **HRMS** (ESI/QTOF)  $m/z$ :  $[M + H]^+$  Calcd for  $C_{14}H_{16}N^+$  198.1277; Found 198.1279. New compound.



*2-(3-(Trifluoromethyl)benzyl)quinoline* was synthesized according to literature procedure.<sup>269</sup> With TMP, yield (yellow oil): 217 mg (47%). **<sup>1</sup>H NMR** (400 MHz,  $CD_2Cl_2$ )  $\delta$  8.10 (dd,  $J = 8.4, 0.8$  Hz, 1H), 8.03 (dt,  $J = 8.4, 1.0$  Hz, 1H), 7.81 (dd,  $J = 8.1, 1.5$  Hz, 1H), 7.71 (ddd,  $J = 8.4, 6.9, 1.5$  Hz, 1H), 7.62 (t,  $J = 1.7$  Hz, 1H), 7.52 (tdd,  $J = 7.8, 5.2, 3.9$  Hz, 3H), 7.44 (t,  $J = 7.7$  Hz, 1H), 7.28 (d,  $J = 8.5$  Hz, 1H), 4.38 (s, 2H). **<sup>13</sup>C NMR** (101 MHz,  $CD_2Cl_2$ )  $\delta$  160.08, 147.97, 140.51, 136.60, 132.72, 130.65, 130.33, 129.47, 129.00, 128.93, 127.53, 126.80, 126.06, 125.81, 125.77, 125.73, 125.69, 125.61, 123.27, 123.23, 123.19, 123.15, 122.91, 121.37, 53.94, 53.87, 53.67, 53.40, 53.13, 52.86, 45.00. **HRMS** (ESI/QTOF)  $m/z$ :  $[M + H]^+$  Calcd for  $C_{17}H_{13}F_3N^+$  288.0995; Found 288.0998. New compound.



*1-Methyl-5-(pyridin-2-ylmethyl)-1H-indole* was synthesized by *N*-methylation of 5-bromoindole,<sup>270</sup> and then cross-coupling according to literature procedure.<sup>271</sup> Yield (pale orange solid): 113 mg (31%). **<sup>1</sup>H NMR** (400 MHz,  $CDCl_3$ )  $\delta$  8.57 (dt,  $J = 5.1, 1.5$  Hz, 1H), 7.70 (td,  $J = 7.7, 1.7$  Hz, 1H), 7.58 – 7.51 (m, 1H), 7.30 – 7.19 (m, 3H), 7.16 (dd,  $J = 8.3, 1.7$  Hz, 1H), 7.04 (d,  $J = 3.1$  Hz, 1H), 6.43 (dd,  $J = 3.1, 0.9$  Hz, 1H), 4.39 (s, 2H), 3.77 (s, 3H). **<sup>13</sup>C NMR** (151 MHz,  $CDCl_3$ )  $\delta$  161.22, 146.66, 138.96, 135.86, 129.43, 128.98, 128.95, 124.33, 123.10, 121.88, 121.38, 109.70, 100.87, 77.37, 77.16, 76.95, 43.35, 33.02. **HRMS** (ESI/QTOF)  $m/z$ :  $[M + H]^+$  Calcd for  $C_{15}H_{15}N_2^+$  223.1230; Found 223.1234. New compound.

## ES.2.2 Synthesis of the triazoles **2.11–2.15**

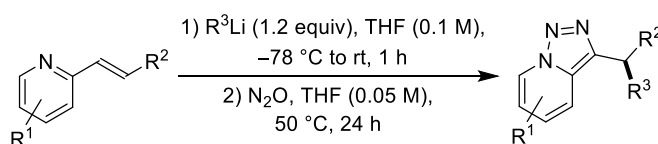
### ES.2.2.1 Examining lithiation efficiency

The substrate (0.05 mmol) was dissolved in THF (0.5 ml) and the respective additive (TMEDA or HMPA) was added (for entry 3 and 4). The mixture was cooled to  $-78$  °C and *n*-BuLi (1.5 equiv) was added. The red mixture was stirred for 1 h at  $-78$  °C, after which it was taken out of the cold bath, and allowed to warm up to room temperature over 1 h. Then, the solvent was evaporated and protonation was achieved with a few drops of water. The internal standard, trimethoxybenzene, was added and the yields were calculated by integration of selected <sup>1</sup>H NMR signals.

## ES.2.2.2 Reaction in two steps, one pot

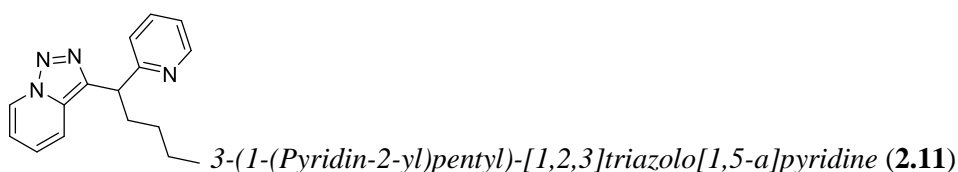
The reaction was optimized over 2 steps in one pot on a 0.3 mmol scale. After performing the lithiation, the solvent was evaporated *in situ* and fresh THF (0.05 M) was added. Subsequently, the reaction was subjected to N<sub>2</sub>O. The solvent was evaporated, yielding a yellow oil. It was redissolved in ethyl acetate (10 ml). An aliquot of 0.5 ml was taken and the solvent was evaporated to which the internal standard trimethoxybenzene was added. The yield was calculated by integration of selected <sup>1</sup>H NMR signals.

## ES.2.2.3 General procedure

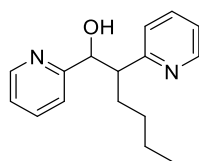


In a 250 ml oven-dried Schlenk flask: The olefinic pyridine or quinoline (0.3 mmol) was dissolved in THF (0.1 M). The reaction mixture was cooled to  $-78\text{ }^{\circ}\text{C}$  and RLi (1.2 equiv) was added. The reaction was allowed to warm up over 1 h. While the mixture was still cold, the solvent was removed under vacuum. The residue was redissolved in THF (0.05 M), subjected to an N<sub>2</sub>O atmosphere (3x N<sub>2</sub>O/*vac* cycles) and heated at  $50\text{ }^{\circ}\text{C}$  for 24 h in a pre-heated oil bath. The solvent was removed under vacuum. In the case of olefinic dipyrindines, the crude product was purified by reversed phase C18 column chromatography (gradient of 3–30% ACN/H<sub>2</sub>O with 0.1v% formic acid). For the 2-styryl quinolines, the crude product was purified by column chromatography with 10% ethyl acetate/hexane.

## ES.2.2.4 Scope

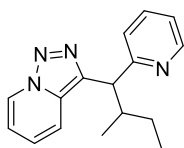


Triazolopyridine **2.11** was prepared from (*E*)-1,2-di(pyridin-2-yl)ethene (0.3 mmol) and *n*-BuLi, following the general procedure. Yield (yellow oil): 43 mg (54%). <sup>1</sup>H NMR (400 MHz, CD<sub>2</sub>Cl<sub>2</sub>)  $\delta$  8.61 (dt,  $J = 7.1, 1.1$  Hz, 1H), 8.50 (ddd,  $J = 4.9, 1.9, 1.0$  Hz, 1H), 7.76 (dt,  $J = 9.0, 1.2$  Hz, 1H), 7.58 (td,  $J = 7.7, 1.9$  Hz, 1H), 7.35 (dt,  $J = 7.8, 1.1$  Hz, 1H), 7.16 – 7.03 (m, 2H), 6.88 (td,  $J = 6.8, 1.3$  Hz, 1H), 4.56 (t,  $J = 7.9$  Hz, 1H), 2.46 – 2.24 (m, 2H), 1.44 – 1.16 (m, 4H), 0.84 (t,  $J = 7.2$  Hz, 3H). <sup>13</sup>C NMR (151 MHz, CD<sub>2</sub>Cl<sub>2</sub>)  $\delta$  162.55, 148.75, 139.74, 136.19, 131.27, 124.77, 123.62, 122.29, 121.23, 118.37, 114.78, 53.56, 53.38, 53.20, 53.02, 52.84, 45.75, 33.78, 29.77, 22.32, 13.51. HRMS (ESI/QTOF)  $m/z$ :  $[M + H]^+$  Calcd for C<sub>16</sub>H<sub>19</sub>N<sub>4</sub><sup>+</sup> 267.1604; Found 267.1605. New compound.

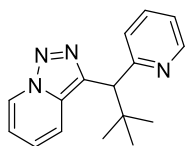


1,2-di(Pyridin-2-yl)hexan-1-ol

Side-product from the reaction of triazolopyridine **2.11**, isolated by RP-HPLC. Based on the  $^1\text{H}$  NMR spectra, diastereomers were found in a ratio of 1.8:1 (**A**:**B**). Yield (yellow oil): 5 mg.  $^1\text{H}$  NMR (400 MHz,  $\text{CDCl}_3$ )  $\delta$  8.59 (ddt,  $J = 4.9, 1.7, 0.9$  Hz, 2H, **A**), 8.53 – 8.42 (m, 2H, **B**), 7.70 (dtd,  $J = 11.0, 7.7, 1.8$  Hz, 2H, **A**), 7.56 (d,  $J = 7.9$  Hz, 1H, **A**), 7.48 (dtd,  $J = 9.8, 7.7, 1.8$  Hz, 2H, **B**), 7.32 – 7.16 (m, 4H, 3H, **A**, 1H, **B**), 7.09 (ddd,  $J = 7.6, 4.9, 1.2$  Hz, 1H, **B**), 7.03 (ddd,  $J = 7.5, 4.8, 1.3$  Hz, 1H, **B**), 6.89 (d,  $J = 7.8$  Hz, 1H, **B**), 5.16 (d,  $J = 3.0$  Hz, 1H, **A**), 5.12 (d,  $J = 3.4$  Hz, 1H, **B**), 3.48 – 3.41 (m, 1H, **B**), 3.36 (d,  $J = 10.9$  Hz, 1H, **B**), 2.03 (ddt,  $J = 8.9, 6.0, 3.4$  Hz, 1H, **A**), 1.85 (dddd,  $J = 13.5, 11.0, 9.9, 5.2$  Hz, 1H, **A**), 1.49 – 1.26 (m, 2H, **A**, 2H, **B**), 1.26 – 1.05 (m, 2H, **A**), 1.03 – 0.91 (m, 2H, **B**), 0.88 (t,  $J = 7.2$  Hz, 3H, **B**), 0.72 (t,  $J = 7.3$  Hz, 3H, **A**).  $^{13}\text{C}$  NMR (101 MHz,  $\text{CDCl}_3$ )  $\delta$  163.79, 163.60, 162.58, 161.66, 148.52, 148.42, 148.33, 148.10, 137.07, 136.73, 136.65, 136.34, 124.77, 124.45, 122.11, 122.01, 121.72, 121.65, 121.44, 120.59, 77.48, 77.36, 77.32, 77.16, 76.84, 76.32, 51.47, 51.27, 33.29, 29.97, 29.72, 27.73, 22.88, 22.72, 14.13, 13.95. HRMS (ESI/QTOF)  $m/z$ :  $[\text{M} + \text{H}]^+$  Calcd for  $\text{C}_{16}\text{H}_{21}\text{N}_2\text{O}^+$  257.1648; Found 257.1649. New compound.

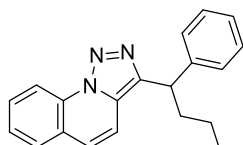
3-(2-Methyl-1-(pyridin-2-yl)butyl)-[1,2,3]triazolo[1,5-a]pyridine (**2.12**)

Triazolopyridine **2.12** was prepared from (*E*)-1,2-di(pyridin-2-yl)ethene (0.3 mmol) and *s*-BuLi, following the general procedure. Yield (yellow oil): 19 mg (29%).  $^1\text{H}$  NMR (400 MHz,  $\text{CDCl}_3$ )  $\delta$  8.62 (dq,  $J = 7.1, 1.1$  Hz, 1H), 8.51 (dq,  $J = 4.7, 1.6$  Hz, 1H), 8.04 (ddt,  $J = 8.9, 3.8, 1.2$  Hz, 1H), 7.61 (dq,  $J = 6.3, 2.2$  Hz, 2H), 7.13 (dddt,  $J = 10.9, 8.3, 5.0, 1.3$  Hz, 2H), 6.89 (td,  $J = 6.8, 1.2$  Hz, 1H), 4.42 (t,  $J = 10.3$  Hz, 1H), 2.75 (dddd,  $J = 10.3, 8.7, 6.8, 3.8$  Hz, 1H), 1.47 – 1.26 (m, 1H), 1.23 – 1.03 (m, 1H), 0.96 – 0.73 (m, 6H).  $^{13}\text{C}$  NMR (151 MHz,  $\text{CD}_2\text{Cl}_2$ )  $\delta$  161.56, 161.49, 147.27, 138.71, 137.28, 131.70, 131.66, 124.70, 123.82, 123.80, 123.71, 121.55, 121.52, 118.75, 114.91, 53.56, 53.38, 53.20, 53.02, 52.84, 50.97, 38.19, 38.07, 27.07, 26.77, 16.75, 16.48, 10.47, 10.31. HRMS (ESI/QTOF)  $m/z$ :  $[\text{M} + \text{H}]^+$  Calcd for  $\text{C}_{16}\text{H}_{19}\text{N}_4^+$  267.1604; Found 267.1608. New compound.

3-(2,2-Dimethyl-1-(pyridin-2-yl)propyl)-[1,2,3]triazolo[1,5-a]pyridine (**2.13**)

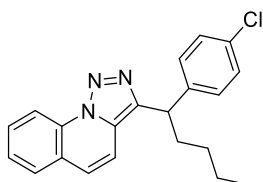
Triazolopyridine **2.13** was prepared from (*E*)-1,2-di(pyridin-2-yl)ethene (0.25 mmol) and *t*-BuLi, following the general procedure. Yield (pale yellow solid): 25 mg (38%).  $^1\text{H}$  NMR (400 MHz,

$\text{CDCl}_3$ )  $\delta$  8.70 – 8.59 (m, 1H), 8.56 – 8.49 (m, 1H), 8.01 (dt,  $J$  = 9.0, 1.2 Hz, 1H), 7.97 – 7.90 (m, 1H), 7.62 (td,  $J$  = 7.7, 1.9 Hz, 1H), 7.21 – 7.08 (m, 2H), 6.90 (td,  $J$  = 6.8, 1.3 Hz, 1H), 4.53 (s, 1H), 1.07 (s, 9H).  $^{13}\text{C}$  NMR (101 MHz,  $\text{CDCl}_3$ )  $\delta$  160.63, 148.03, 138.52, 136.17, 132.95, 125.46, 125.07, 124.15, 121.74, 119.34, 115.13, 56.11, 36.41, 28.67. **HRMS** (nanochip-ESI/LTQ-Orbitrap)  $m/z$ :  $[\text{M} + \text{H}]^+$  Calcd for  $\text{C}_{16}\text{H}_{19}\text{N}_4^+$  267.1604; Found 267.1605. New compound.



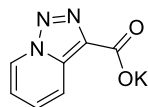
3-(1-Phenylpentyl)-[1,2,3]triazolo[1,5-a]quinoline (**2.14**)

Triazoloquinoline **2.14** was prepared from (*E*)-2-styrylquinoline (0.3 mmol) and *n*-BuLi, following the general procedure. The resulting yellow solid was washed with pentane and dried by vacuum. Yield (yellow solid): 43.6 mg (46%).  $^1\text{H}$  NMR (600 MHz,  $\text{CDCl}_3$ )  $\delta$  8.77 (d,  $J$  = 8.4 Hz, 1H), 7.77 (dd,  $J$  = 7.9, 1.4 Hz, 1H), 7.72 (ddd,  $J$  = 8.5, 7.2, 1.4 Hz, 1H), 7.55 (ddd,  $J$  = 8.1, 7.2, 1.2 Hz, 1H), 7.44 – 7.37 (m, 2H), 7.34 (d,  $J$  = 9.3 Hz, 1H), 7.30 (t,  $J$  = 7.7 Hz, 2H), 7.22 – 7.15 (m, 2H), 4.34 (t,  $J$  = 7.8 Hz, 1H), 2.52 (dddd,  $J$  = 13.3, 9.5, 7.8, 5.7 Hz, 1H), 2.24 (dddd,  $J$  = 13.5, 9.0, 7.7, 6.0 Hz, 1H), 1.48 – 1.18 (m, 4H), 0.87 (t,  $J$  = 7.2 Hz, 3H).  $^{13}\text{C}$  NMR (151 MHz,  $\text{CDCl}_3$ )  $\delta$  143.90, 143.22, 132.16, 129.95, 129.18, 128.68, 128.49, 128.10, 127.06, 126.63, 125.52, 124.11, 116.40, 114.88, 43.24, 35.39, 30.29, 22.78, 14.18. **HRMS** (ESI/QTOF)  $m/z$ :  $[\text{M} + \text{H}]^+$  Calcd for  $\text{C}_{21}\text{H}_{22}\text{N}_3^+$  316.1808; Found 316.1811. New compound.

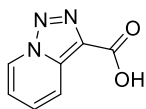


3-(1-(4-Chlorophenyl)pentyl)-[1,2,3]triazolo[1,5-a]quinoline (**2.15**)

Triazoloquinoline **2.15** was prepared from (*E*)-2-(4-chlorostyryl)quinoline (0.3 mmol) and *n*-BuLi, following the general procedure. The resulting yellow solid was washed with pentane and dried by vacuum. Yield (pale yellow solid): 40.0 mg (38%).  $^1\text{H}$  NMR (400 MHz,  $\text{CDCl}_3$ )  $\delta$  8.68 (dd,  $J$  = 8.3, 1.1 Hz, 1H), 7.75 – 7.59 (m, 2H), 7.48 (ddd,  $J$  = 8.2, 7.2, 1.1 Hz, 1H), 7.31 – 7.27 (m, 3H), 7.19 (dt,  $J$  = 6.4, 2.2 Hz, 2H), 7.12 (d,  $J$  = 9.4 Hz, 1H), 4.24 (t,  $J$  = 7.8 Hz, 1H), 2.51 – 2.29 (m, 1H), 2.23 – 2.03 (m, 1H), 1.40 – 1.08 (m, 4H), 0.79 (t,  $J$  = 7.1 Hz, 3H).  $^{13}\text{C}$  NMR (101 MHz,  $\text{CDCl}_3$ )  $\delta$  142.64, 142.42, 132.36, 132.16, 130.08, 129.46, 129.14, 128.80, 128.55, 127.16, 125.81, 124.10, 116.42, 114.57, 77.48, 77.36, 77.16, 76.84, 42.60, 35.48, 30.22, 22.73, 14.14. **HRMS** (ESI/QTOF)  $m/z$ :  $[\text{M} + \text{H}]^+$  Calcd for  $\text{C}_{21}\text{H}_{21}\text{ClN}_3^+$  350.1419; Found 350.1417. New compound.

ES.2.3 Synthesis of the triazole **2.17***Potassium [1,2,3]triazolo[1,5-a]pyridine-3-carboxylate (2.16)*

In a 100 ml oven-dried Schlenk flask: Methyl 2-(pyridin-2-yl)acetate (0.5 mmol) was dissolved in DMSO (5 ml) and KO<sup>t</sup>Bu (1.05 equiv) and 18-crown-6 (1.0 equiv) were added. The reaction mixture was subjected to N<sub>2</sub>O (3x N<sub>2</sub>O/*vac* cycles) and heated at 50 °C for 4 h in a pre-heated oil bath. After cooling down, the reaction mixture was poured slowly into a round bottom flask with toluene (50 ml). The resulting precipitate was isolated by filtration and washed with several portions of toluene and pentane. The brown residue was triturated with pentane and then dried under vacuum. Traces of 18-crown-6 and DMSO remained despite repeated washings. Yield (red/brown solid): 92 mg (91%). <sup>1</sup>H NMR (400 MHz, CD<sub>3</sub>OD) δ 8.88 (dt, *J* = 7.1, 1.1 Hz, 1H), 8.33 (dt, *J* = 8.9, 1.3 Hz, 1H), 7.49 (ddd, *J* = 9.0, 6.7, 1.0 Hz, 1H), 7.17 (td, *J* = 6.8, 1.3 Hz, 1H). <sup>13</sup>C NMR (101 MHz, CD<sub>3</sub>OD) δ 168.86, 137.11, 135.36, 128.35, 126.56, 121.21, 117.26, 71.33 (18-crown-6), 49.64, 49.43, 49.21, 49.00, 48.79, 48.57, 48.36.

*[1,2,3]Triazolo[1,5-a]pyridine-3-carboxylic acid (2.17)*

Further work-up was performed by dissolving **2.16** in a minimal amount of water while heating. The pH of the solution was lowered to pH 2 with HCl. The reaction mixture was concentrated and the liquid was removed. The remaining solid was washed with water, pentane, and freeze-dried in pentane. Yield (light brown solid): 73 mg (89%). <sup>1</sup>H NMR (400 MHz, CD<sub>3</sub>OD) δ 9.05 (dt, *J* = 7.0, 1.1 Hz, 1H), 8.27 (dt, *J* = 8.9, 1.2 Hz, 1H), 7.69 (ddd, *J* = 8.9, 6.7, 1.0 Hz, 1H), 7.32 (td, *J* = 6.9, 1.3 Hz, 1H). <sup>13</sup>C NMR (151 MHz, CD<sub>3</sub>OD) δ 164.08, 136.32, 131.03, 130.67, 127.52, 120.11, 118.20, 49.42, 49.28, 49.27, 49.14, 49.13, 49.00, 48.99, 48.86, 48.85, 48.72, 48.70, 48.57, 48.56. HRMS (APPI/LTQ-Orbitrap) *m/z*: [M]<sup>+</sup> Calcd for C<sub>7</sub>H<sub>5</sub>N<sub>3</sub>O<sub>2</sub><sup>+</sup> 163.0376; Found 163.0384.

## ES.2.4 X-ray crystallographic data

**Table ES 2.1** Crystallographic data of **2.16**.

Compound	<b>2.16</b>
Formula	C <sub>42</sub> H <sub>26</sub> K <sub>2</sub> N <sub>18</sub> Na <sub>4</sub> O <sub>13</sub>
$D_{calc.}/\text{g cm}^{-3}$	1.661
$\mu/\text{mm}^{-1}$	2.948
Formula Weight	1160.97
Colour	colourless
Shape	prism-shaped
Size/mm <sup>3</sup>	0.09×0.06×0.02
$T/\text{K}$	140.00(10)
Crystal System	monoclinic
Space Group	$P2_1/n$
$a/\text{\AA}$	14.2718(7)
$b/\text{\AA}$	6.5810(3)
$c/\text{\AA}$	24.714(3)
$\alpha^\circ$	90
$\beta^\circ$	90.107(7)
$\gamma^\circ$	90
$V/\text{\AA}^3$	2321.2(3)
$Z$	2
$Z'$	0.5
Wavelength/ $\text{\AA}$	1.54184
Radiation type	CuK $\alpha$
$\theta_{min}/^\circ$	3.573
$\theta_{max}/^\circ$	77.339
Measured Refl's.	22718
Indep't Refl's	4567
Refl's $I \geq 2\sigma(I)$	3099
$R_{int}$	0.0655
Parameters	360
Restraints	655
Largest Peak/e $\text{\AA}^{-3}$	0.715
Deepest Hole/e $\text{\AA}^{-3}$	-0.579
GooF	1.042
$wR_2$ (all data)	0.1704
$wR_2$	0.1545
$R_1$ (all data)	0.1061
$R_1$	0.0634
CCDC number	2094800

Colorless prism-shaped crystals of **2.16** were grown within 2 weeks by layering a solution of **2.16** in DMSO with ethyl acetate. A suitable crystal with dimensions  $0.09 \times 0.06 \times 0.02 \text{ mm}^3$  was selected and mounted on a XtaLAB Synergy R, DW system, HyPix-Arc 150 diffractometer. The crystal was kept at a steady  $T = 140.00(10) \text{ K}$  during data collection. The structure was solved with the ShelXT 2018/2<sup>275</sup> solution program using dual methods and by using Olex2 1.3<sup>276</sup> as the graphical interface. The model was refined with ShelXL 2018/3<sup>277</sup> using full matrix least squares minimization on  $|F|^2$ .

#### Structure Quality Indicators

<b>Reflections:</b>	d min (Cu $\lambda$ ) 2 $\theta$ =154.7° 0.79	I/ $\sigma$ (I) CIF 13.2	Rint CIF 6.55%	Full 135.4° 93% to 154.7° 99.8
<b>Refinement:</b>	Shift CIF 0.000	Max Peak CIF 0.7	Min Peak CIF -0.6	GooF CIF 1.042

Data were measured using  $\omega$  scans using CuK $\alpha$  radiation. The diffraction pattern was indexed and the total number of runs and images was based on the strategy calculation from the program CrysAlis<sup>Pro</sup> 1.171.41.110a.<sup>278</sup> The maximum resolution achieved was  $\theta = 77.339^\circ$  (0.79 Å). The unit cell was refined using CrysAlis<sup>Pro</sup> 1.171.41.110a on 6064 reflections, 27% of the observed reflections.

Data reduction, scaling and absorption corrections were performed using CrysAlis<sup>Pro</sup> 1.171.41.110a.<sup>278</sup> The final completeness is 99.80 % out to  $77.339^\circ$  in  $\theta$ . A Gaussian absorption correction was performed using CrysAlis<sup>Pro</sup> 1.171.41.110a. Numerical absorption correction based on Gaussian integration over a multifaceted crystal model. Empirical absorption correction using spherical harmonics as implemented in SCALE3 ABSPACK scaling algorithm. The absorption coefficient  $\mu$  of this material is  $2.948 \text{ mm}^{-1}$  at this wavelength ( $\lambda = 1.54184 \text{ Å}$ ) and the minimum and maximum transmissions are 0.802 and 1.000.

The structure was solved and the space group  $P2/n$  (# 13) determined by the ShelXT 2018/2<sup>275</sup> structure solution program using dual methods and refined by full matrix least squares minimization on  $|F|^2$  using version 2018/3 of ShelXL<sup>277</sup>. All non-hydrogen atoms were refined anisotropically. Hydrogen atom positions were calculated geometrically and refined using the riding model. Most hydrogen atom positions were calculated geometrically and refined using the riding model, but the hydrogen atom bound to O7 was found in a difference map and refined freely.

The value of Z' is 0.5. This means that only half of the formula unit is present in the asymmetric unit, with the other half consisting of symmetry equivalent atoms.

Crystallographic and refinement data are summarized in Table ES 2.1. Crystallographic data have been deposited with the Cambridge Crystallographic Data Centre and correspond to the CCDC number of 2094800. These data can be obtained free of charge via [www.ccdc.cam.ac.uk/data\\_request/cif](http://www.ccdc.cam.ac.uk/data_request/cif), or by emailing [data\\_request@ccdc.cam.ac.uk](mailto:data_request@ccdc.cam.ac.uk), or by contacting The Cambridge Crystallographic Data Centre, 12 Union Road, Cambridge CB2 1EZ, UK; fax: +44 1223 336033.

## ES.2.5 Biological assays

A selection of 4 compounds was submitted for a cytotoxicity assay (Figure ES 2.1). The screening was performed by the Biomolecular Screening Facility at the EPFL. The cytotoxicity values were determined with the Alamar Blue (resazurin) fluorescent dye measurement (for details, see Experimental section).<sup>279</sup> Dose-response curves were recorded for 6 cell lines: Hela (Human cervix adenocarcinoma), A2780 (human ovarian carcinoma), MDA-MB-231 (human breast adenocarcinoma), MCF7 (human breast adenocarcinoma (metastases from pleural effusion)), MCF-10A (human epithelial breast), HEK293T (human embryonic kidney).

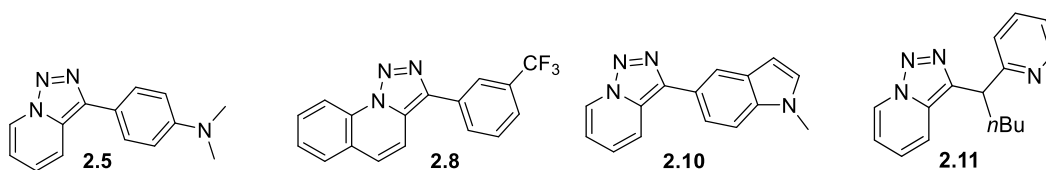


**Figure ES 2.1** List of compounds selected for biological assays.

For **2.10** it was poorly active against Hela (13% cytotoxicity at 10  $\mu$ M) with high  $IC_{50}$  values ( $> 100 \mu$ M). The other compounds did not show significant cytotoxicity ( $>10\%$ ) at 10  $\mu$ M.

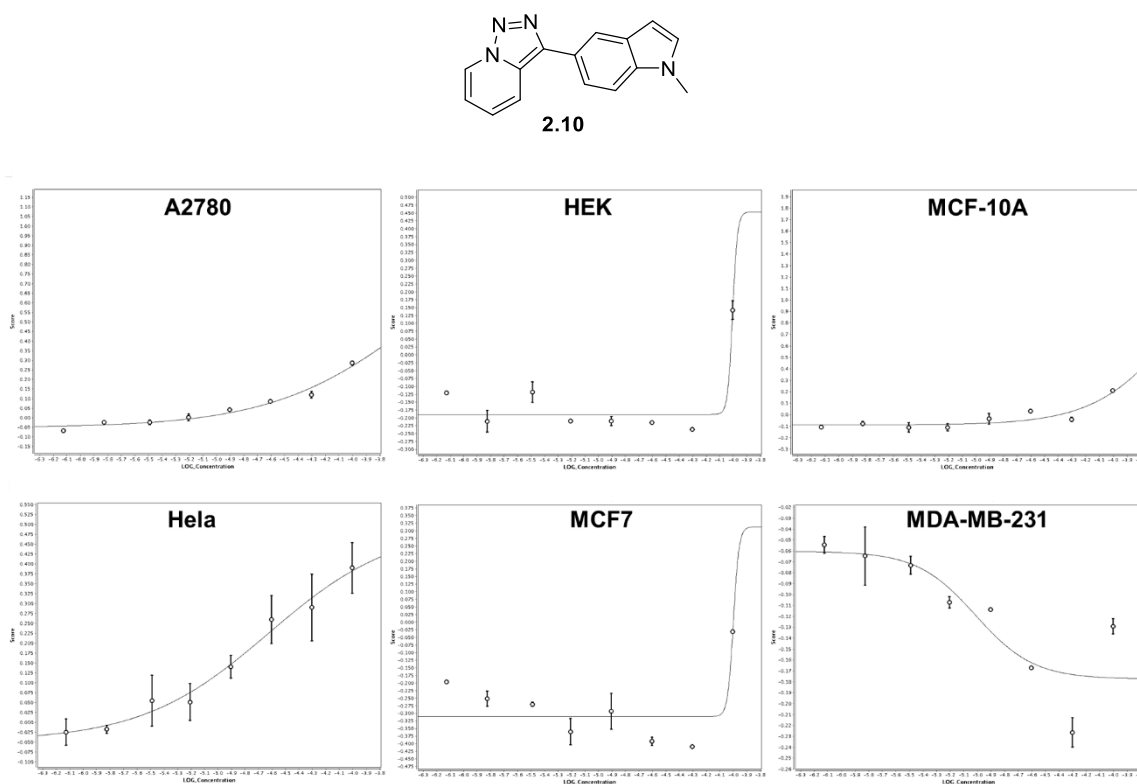


**Figure ES 2.2** Dose-response curves for 6 cell lines for **2.10**. Score vs. Log Concentration.

## ES.2.6 Selected NMR Spectra

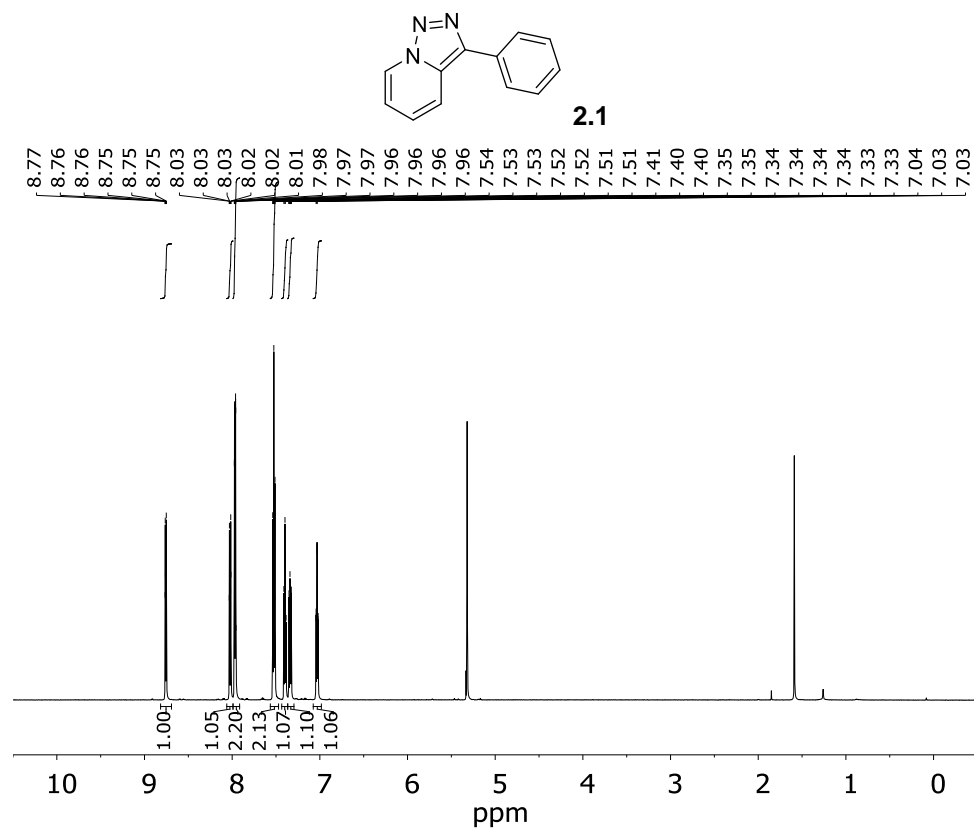


**Figure ES 2.3**  $^1\text{H}$  NMR spectrum of **2.1** (400 MHz,  $\text{CD}_2\text{Cl}_2$ ).

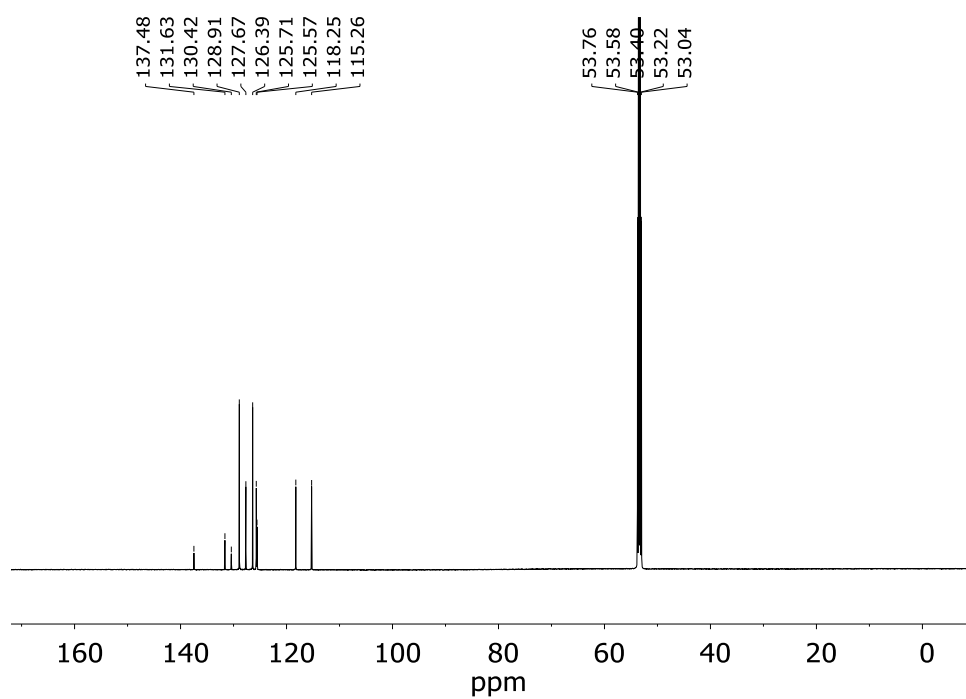


**Figure ES 2.4**  $^{13}\text{C}$  NMR spectrum of **2.1** (151 MHz,  $\text{CD}_2\text{Cl}_2$ ).

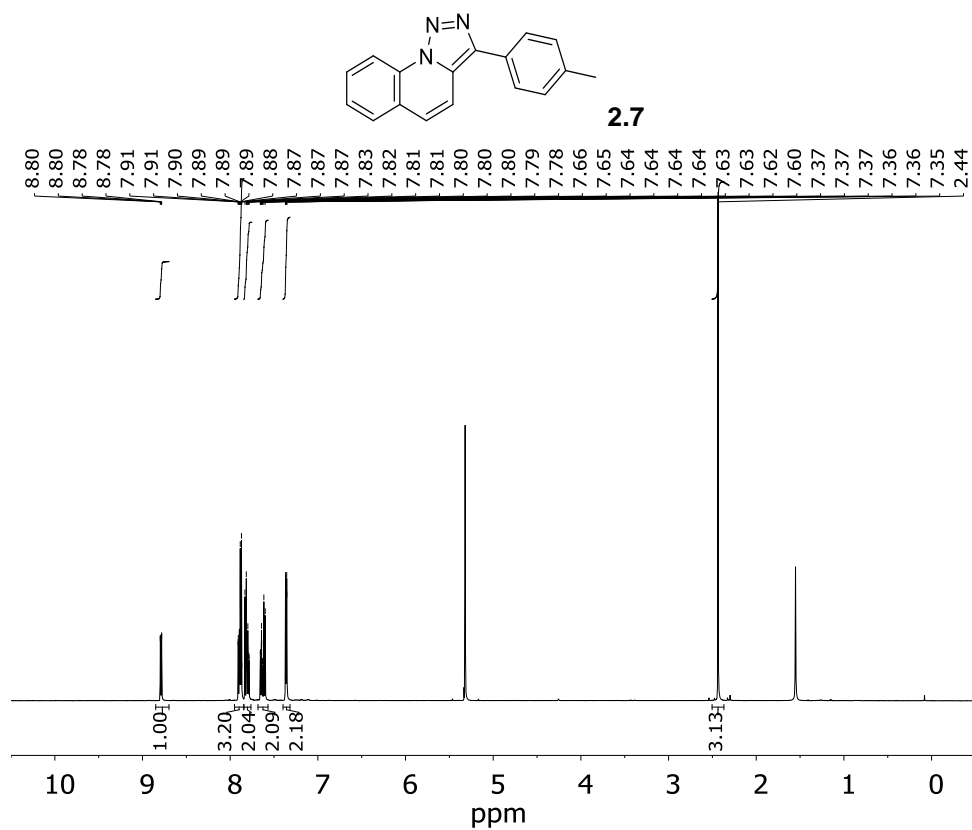


**Figure ES 2.5** <sup>1</sup>H NMR spectrum of **2.7** (600 MHz, CD<sub>2</sub>Cl<sub>2</sub>).

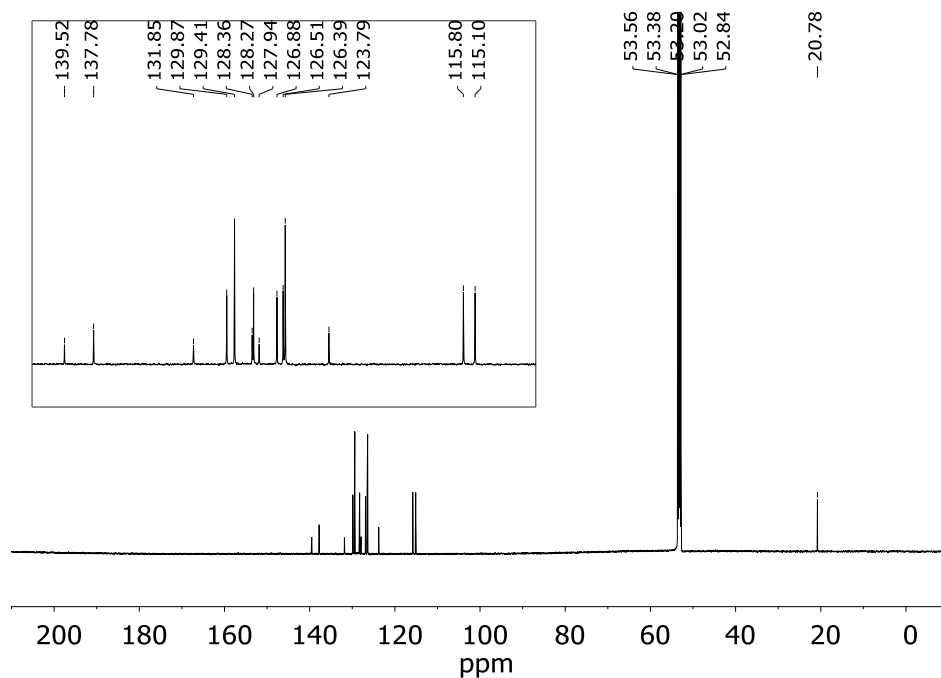


**Figure ES 2.6** <sup>13</sup>C NMR spectrum of **2.7** (151 MHz, CD<sub>2</sub>Cl<sub>2</sub>).

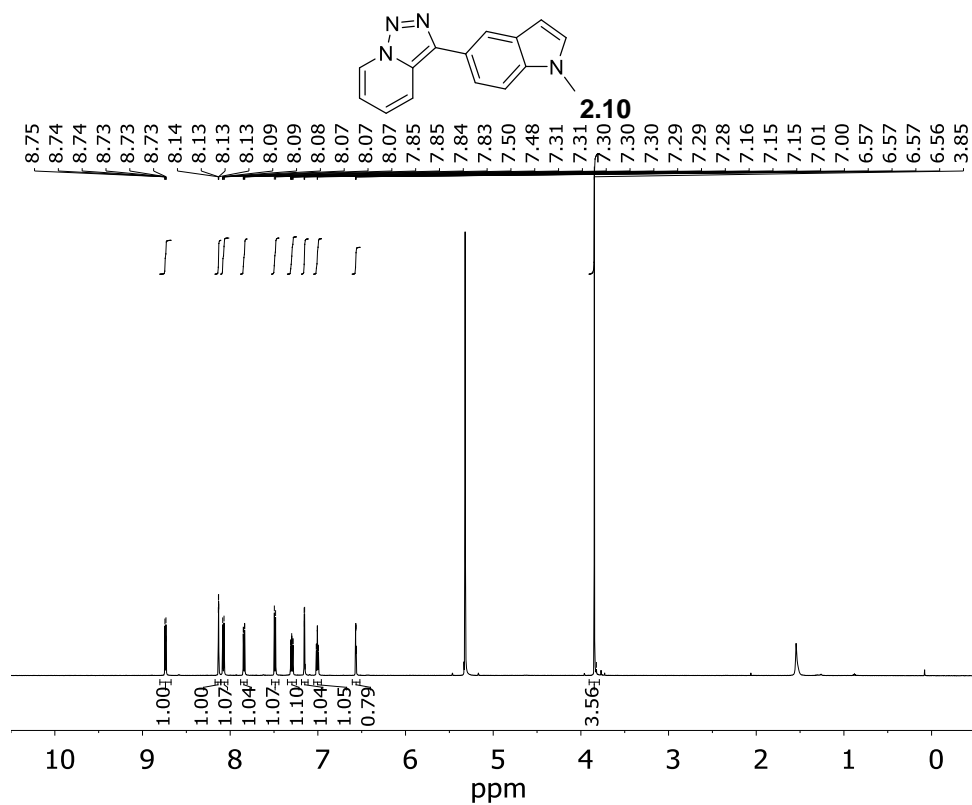


Figure ES 2.7  $^1\text{H}$  NMR spectrum of **2.10** (600 MHz,  $\text{CD}_2\text{Cl}_2$ ).

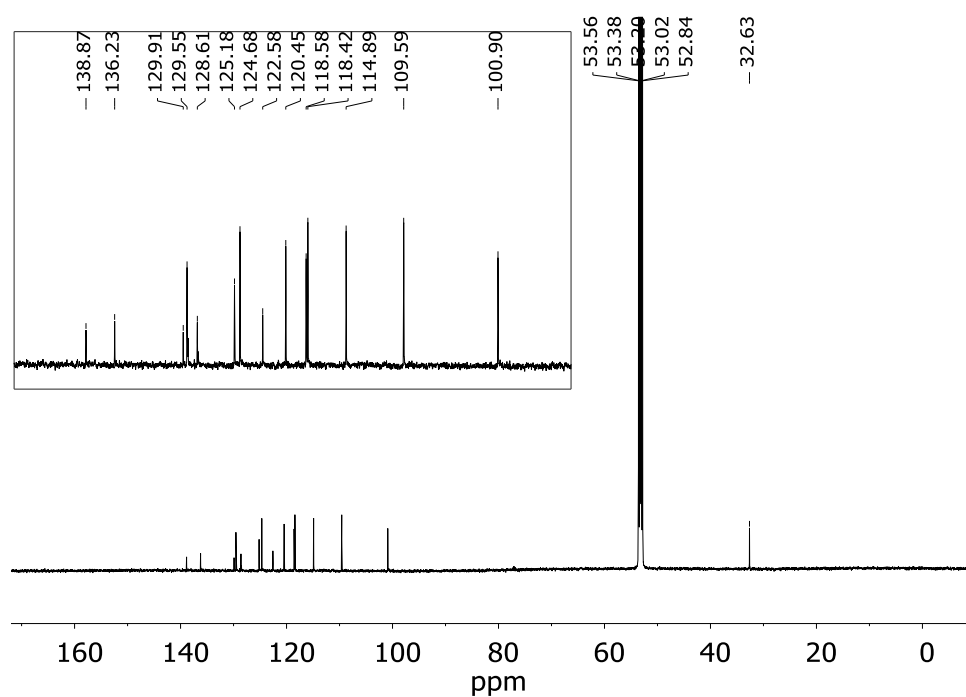
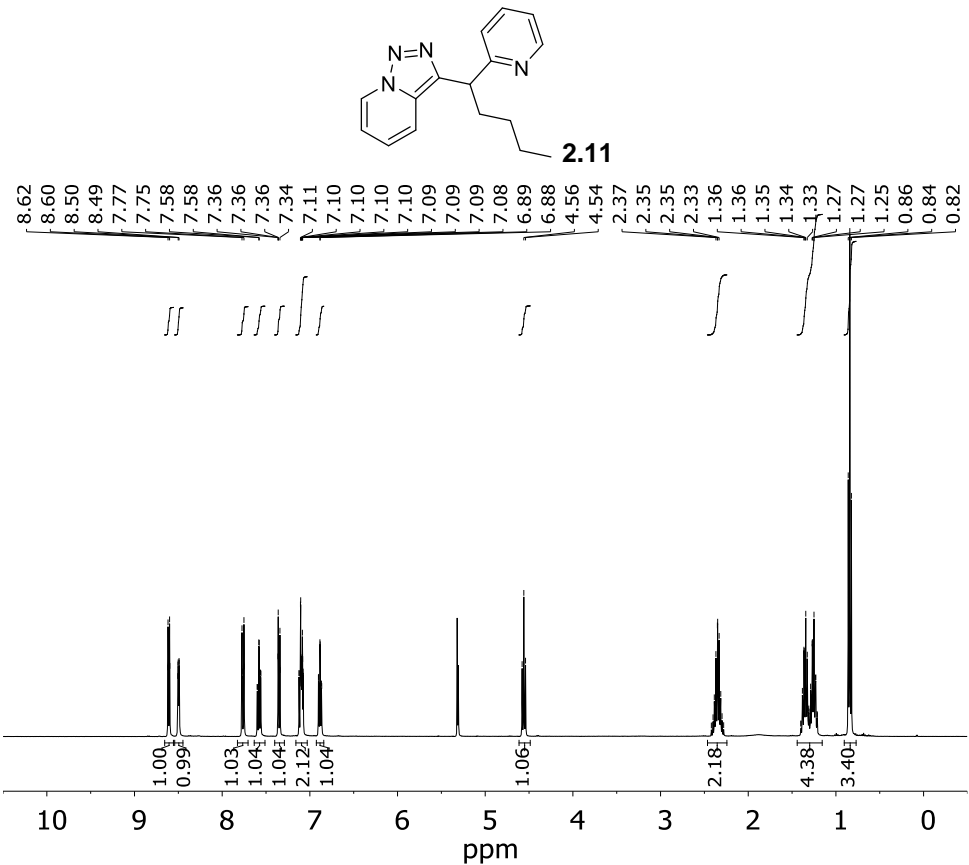
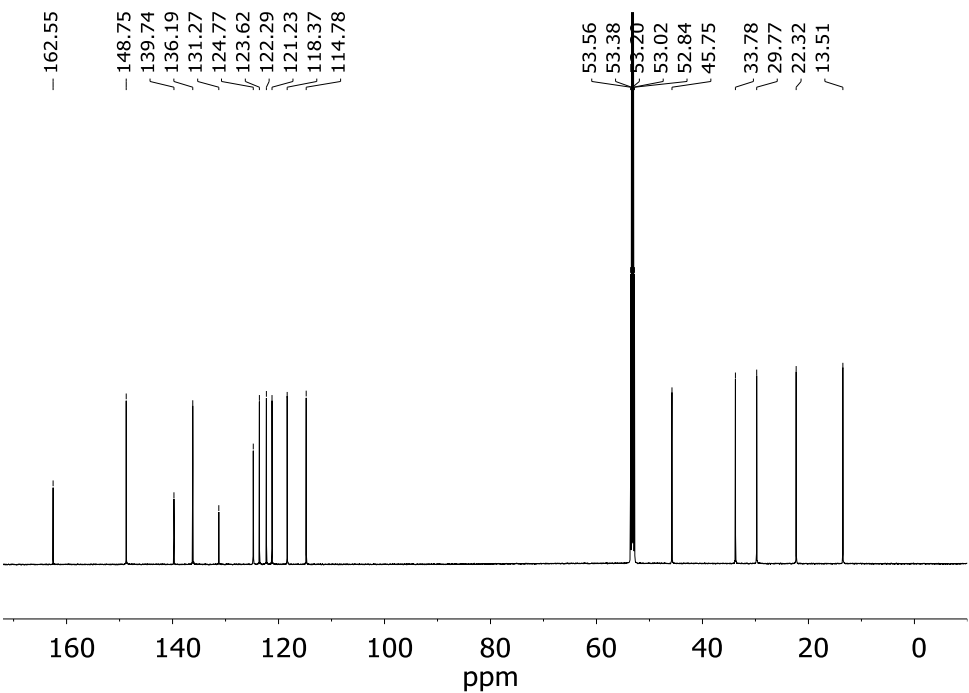


Figure ES 2.8  $^{13}\text{C}$  NMR spectrum of **2.10** (101 MHz,  $\text{CD}_2\text{Cl}_2$ ).



**Figure ES 2.9**  $^1\text{H}$  NMR spectrum of **2.11** (600 MHz,  $\text{CD}_2\text{Cl}_2$ ).



**Figure ES 2.10**  $^{13}\text{C}$  NMR spectrum of **2.11** (101 MHz,  $\text{CD}_2\text{Cl}_2$ ).

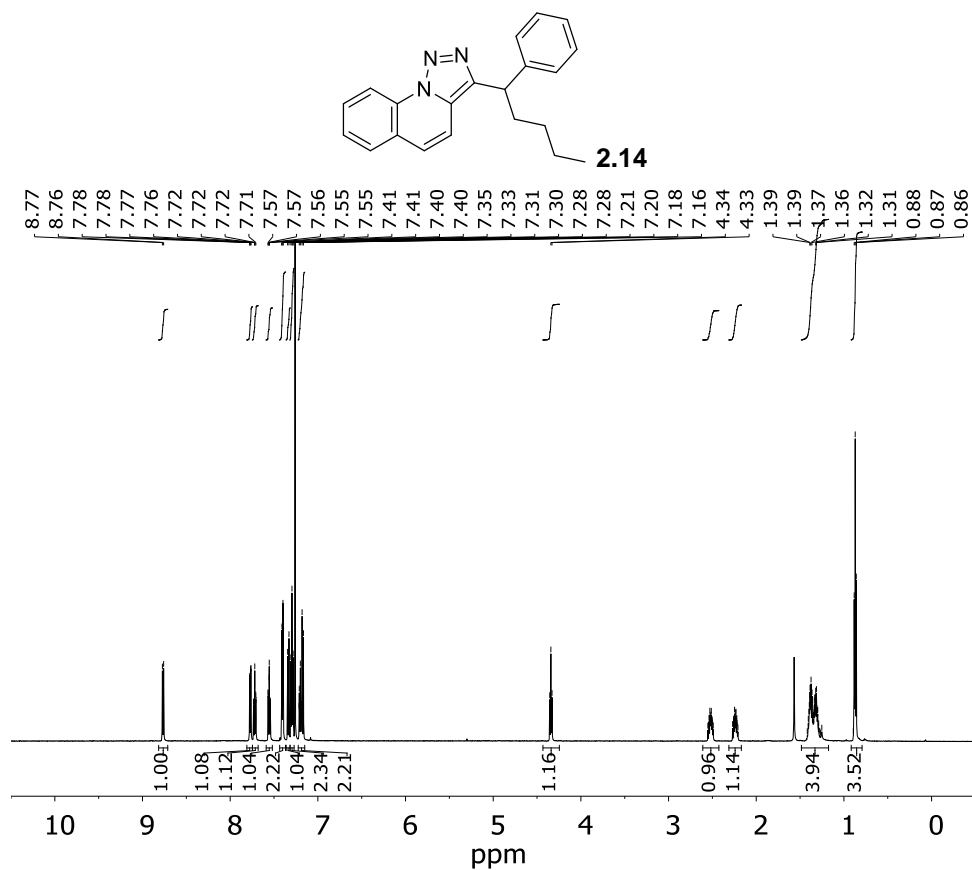


Figure ES 2.11  $^1\text{H}$  NMR spectrum of **2.14** (600 MHz,  $\text{CDCl}_3$ ).

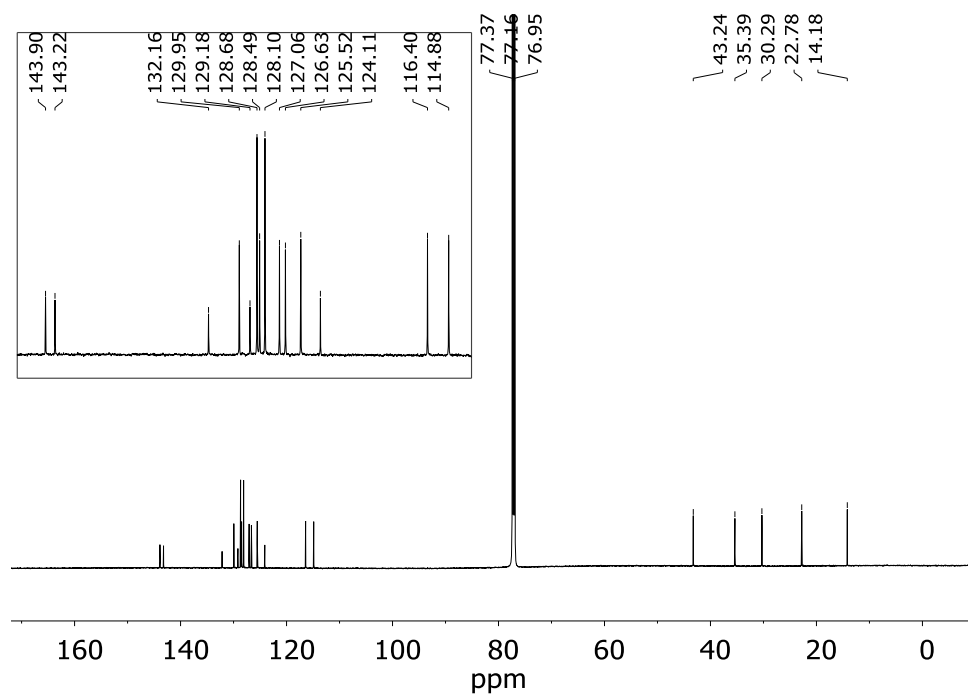
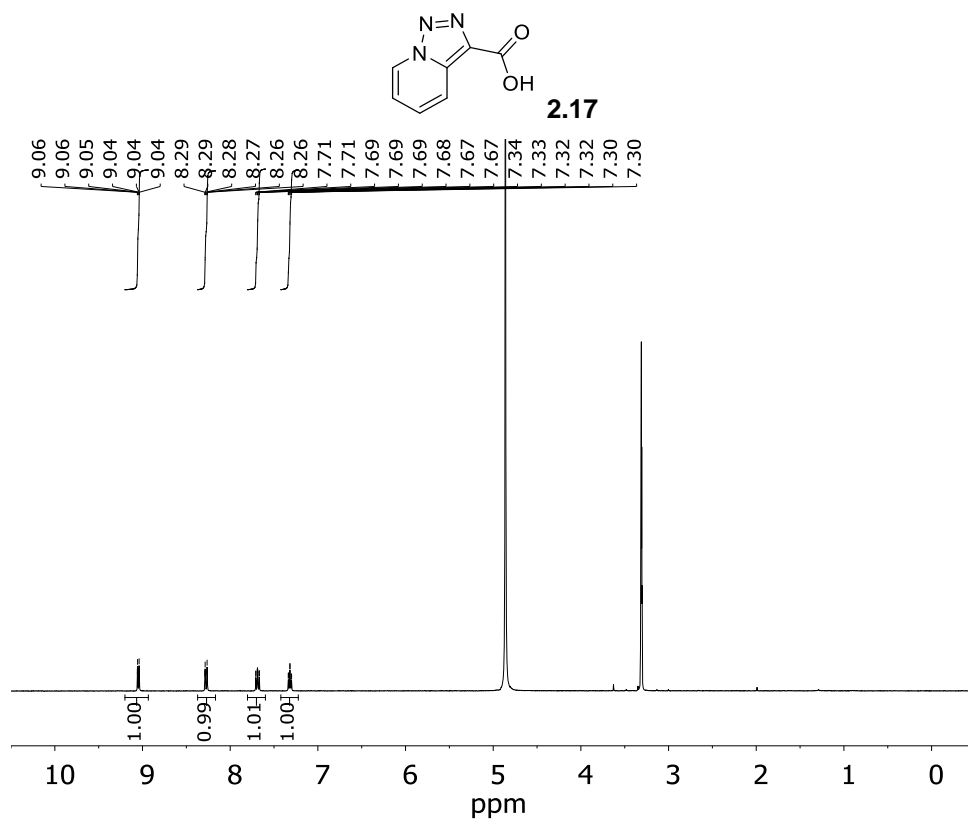
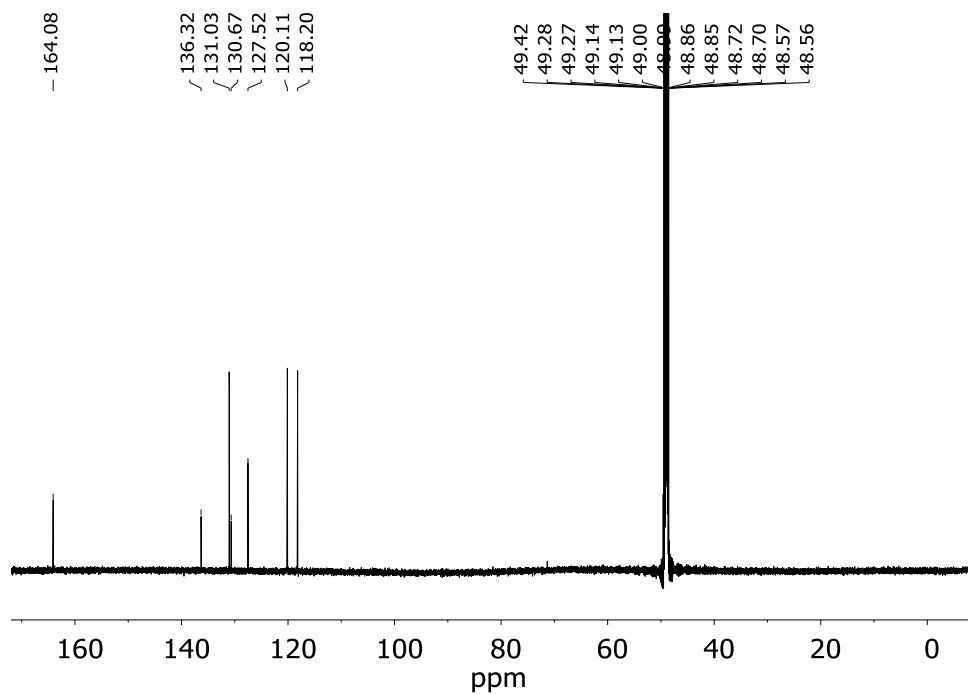


Figure ES 2.12  $^{13}\text{C}$  NMR spectrum of **2.14** (101 MHz,  $\text{CDCl}_3$ ).



**Figure ES 2.13** <sup>1</sup>H NMR spectrum of **2.17** (400 MHz, CD<sub>3</sub>OD).

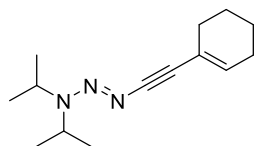


**Figure ES 2.14** <sup>13</sup>C NMR spectrum of **2.17** (151 MHz, CD<sub>3</sub>OD).

## ES.3 Experimental section: 1-acyl triazenes

### ES.3.1 Synthesis of the triazenes **3.a–3.b**

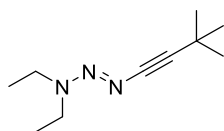
The triazenes were synthesized using an adapted method from Kiefer *et al.*<sup>139</sup> A typical procedure is as follows: under an inert atmosphere, the secondary amine (10 mmol) in THF (10 ml) was cooled down to  $-78\text{ }^{\circ}\text{C}$  in a dry ice bath and *n*-BuLi (4 ml, 2.5 M in hexanes) was added slowly. After stirring the reaction mixture for 5 min, the ice bath was removed. Once the reaction mixture was at room temperature, the *in situ* formed lithium amide was subjected to an  $\text{N}_2\text{O}$  atmosphere (99.999%) overnight. Meanwhile the Grignard reagent was also prepared overnight by taking the desired terminal alkyne (12 mmol) in THF (10 ml) and adding EtMgBr (12 ml, 1.0 M in THF). Subsequently, the *in situ* formed  $\text{N}_2\text{O}$ -adduct (a white precipitate) was subjected to  $\text{N}_2$  atmosphere and the Grignard reagent was added slowly and carefully by not scratching the sides of the flask. The resulting clear mixture was heated for 5 h at  $50\text{ }^{\circ}\text{C}$ . After quenching the reaction mixture with saturated  $\text{MgSO}_4$  (aq), the product was extracted with diethyl ether, followed by drying of the organic phase over  $\text{MgSO}_4$  and evaporation of the solvent. The crude product was purified by column chromatography using deactivated silica and a gradient of pentane to pentane-diethyl ether (5%). The product was freeze-dried in pentane.



(*E*)-1-(Cyclohex-1-en-1-ylethynyl)-3,3-diisopropyltriaz-1-ene (**3.a**)

10 mmol scale synthesis

Triazene **3.a** was prepared following the general procedure. Yield (yellow solid): 0.92 g (40%). <sup>1</sup>H NMR (400 MHz,  $\text{CDCl}_3$ )  $\delta$  6.04 (tt,  $J = 3.9, 1.8$  Hz, 1H, CH), 5.05 (p,  $J = 6.8$  Hz, 1H, CH(CH<sub>3</sub>)<sub>2</sub>), 3.99 (p,  $J = 6.7$  Hz, 1H, CH(CH<sub>3</sub>)<sub>2</sub>), 2.26 – 2.16 (m, 2H, CH<sub>2</sub>), 2.16 – 2.06 (m, 2H, CH<sub>2</sub>), 1.72 – 1.49 (m, 4H, CH<sub>2</sub>, CH<sub>2</sub>), 1.33 (d,  $J = 6.7$  Hz, 6H, CH(CH<sub>3</sub>)<sub>2</sub>), 1.20 (d,  $J = 6.8$  Hz, 6H, CH(CH<sub>3</sub>)<sub>2</sub>). <sup>13</sup>C NMR (101 MHz,  $\text{CDCl}_3$ )  $\delta$  132.38, 121.50, 91.59, 82.12, 77.48, 77.36, 77.16, 76.84, 50.18, 47.16, 29.98, 25.97, 23.51, 22.74, 21.87, 19.25. HRMS (ESI/QTOF)  $m/z$ :  $[\text{M} + \text{H}]^+$  Calcd for  $\text{C}_{14}\text{H}_{24}\text{N}_3^+$  234.1965; Found 234.1967.



(*E*)-1-(3,3-Dimethylbut-1-yn-1-yl)-3,3-diethyltriazen-1-ene (**3.b**)

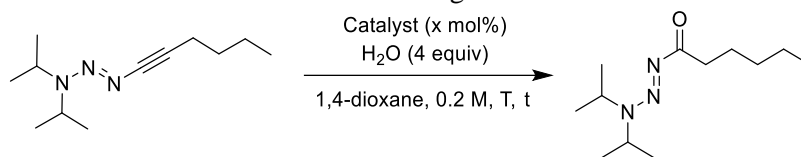
*20 mmol scale synthesis*

Triazene **3.b** was prepared following the general procedure. Yield (pale yellow solid/yellow oil): 0.76 g (21%). **<sup>1</sup>H NMR** (400 MHz, CDCl<sub>3</sub>) δ 4.02 – 3.30 (m, 4H, CH<sub>2</sub>CH<sub>3</sub>), 1.29 (m, 15H, CH<sub>3</sub>, CH<sub>2</sub>CH<sub>3</sub>). **<sup>13</sup>C NMR** (101 MHz, CDCl<sub>3</sub>) δ 88.33, 83.81, 77.48, 77.16, 76.84, 49.51, 41.46, 31.61, 28.15, 14.38, 11.07, 1.14. **HRMS** (ESI/QTOF) *m/z*: [M + H]<sup>+</sup> Calcd for C<sub>10</sub>H<sub>20</sub>N<sub>3</sub><sup>+</sup> 182.1652; Found 182.1655.

### ES.3.2 Synthesis of the alkyl 1-acyl triazenes **3.1–3.9**

#### ES.3.2.1 Lewis acid catalysis

Different Lewis acids were explored, because they are known to catalyse the hydration of alkynes.<sup>280</sup> The reactions were followed by <sup>1</sup>H NMR spectroscopy. First, a solution of the triazene (0.1 mmol), H<sub>2</sub>O (4 equiv), and the internal standard 1,2,3,4-tetramethylbenzene (0.5 equiv) in dioxane (0.2 M) was prepared. The reaction was initiated by adding the respective catalyst. After the given time, a 100 μl sample was removed from the reaction mixture and the solvent was evaporated. The yield was determined by NMR spectroscopy in CDCl<sub>3</sub>. The results are summarized in Table ES 3.1. The reactions described in entries 8–12 were carried out using a laboratory microwave (MW).

**Table ES 3.1** Screening of reaction conditions.

Entry	Catalyst	Catalyst loading (x mol%)	T (°C)	Time (h)	Yield (%) <sup>b</sup>
1	AgNTf <sub>2</sub>	40	80	1	64
2				2	75
3				4.25	>95
4	AgOTf	40	80	4.25	58
5	AgSbF <sub>4</sub>	40	80	4.25	46
6	AgBF <sub>4</sub>	40	80	4.25	62
7	[I(pyridine) <sub>2</sub> ]BF <sub>4</sub>	40	80	4.25	Mixture of compounds
8	AgNTf <sub>2</sub>	40	150 (MW)	0.25	>95
9	AgNTf <sub>2</sub>	20	120 (MW)	0.5	73
10	AgNTf <sub>2</sub>	10	150 (MW)	0.5	>95
11	AgNTf <sub>2</sub>	10	100 (MW)	2	65
12 <sup>a</sup>	x	x	150 (MW)	0.5	0

<sup>a</sup> No significant decomposition of the 1-alkynyl triazene was observed. <sup>b</sup> Yields were determined by <sup>1</sup>H NMR spectroscopy.

The conditions described under entry 8 gave the product in high yield, but the work-up of reactions on a preparative scale was found to be problematic. Therefore, a different approach was developed using acetic acid as catalyst.

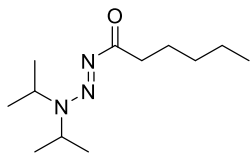
### ES.3.2.2 Acetic acid catalysis

All reactions were performed under air on a 0.2 mmol scale, and the products were isolated. For the work-up, the reaction mixture was diluted in 4 ml DCM, followed by washing with saturated NaHCO<sub>3</sub> (aq) three times (4 ml). After drying over MgSO<sub>4</sub>, the solvent was evaporated and the yield was determined.

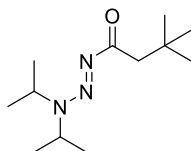
### ES.3.2.3 General procedure

Our brief screening indicated that 0.5 equivalents of acetic acid and a reaction temperature of 50 °C was suited for hydrolysis reactions of alkynyl triazenes (with the exception of the phenylethynyl triazene, for which 100 °C was better). Reactions with additional substrates were monitored by TLC. The work-up was performed by diluting the reaction mixture with ~15 ml DCM, followed by washing the organic layer with saturated NaHCO<sub>3</sub> (3 x ~10 ml). The organic phase was dried over MgSO<sub>4</sub>, filtered, and the solvent was evaporated. The resulting crude product was purified by filtration over a short plug of silica (~5 cm) using a solvent gradient of pentane to diethyl ether.

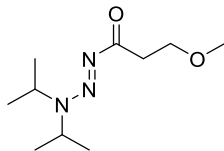
## ES.3.2.4 Scope

*(E)*-1-(3,3-Diisopropyltriaz-1-en-1-yl)hexan-1-one (**3.1**)

Triazene **3.1** was prepared following the general procedure using (*E*)-1-(hex-1-yn-1-yl)-3,3-diisopropyltriaz-1-ene (0.5 mmol) and acetic acid (0.5 equiv) in acetone/water (1:1, 2.5 ml). The reaction mixture was heated at 50 °C for 5 h. Yield (yellow oil): 77.5 mg (68%). **<sup>1</sup>H NMR** (400 MHz, CDCl<sub>3</sub>) δ 5.45 (hept, *J* = 6.8 Hz, 1H, CH(CH<sub>3</sub>)<sub>2</sub>), 4.12 (hept, *J* = 6.6 Hz, 1H, CH(CH<sub>3</sub>)<sub>2</sub>), 2.65 (t, 2H, CH<sub>2</sub>), 1.64 (p, *J* = 7.4 Hz, 2H, CH<sub>2</sub>), 1.36 (d, *J* = 6.7 Hz, 6H, CH(CH<sub>3</sub>)<sub>2</sub>), 1.33 – 1.26 (m, 4H, CH<sub>2</sub>, CH<sub>2</sub>), 1.21 (d, *J* = 6.8 Hz, 6H, CH(CH<sub>3</sub>)<sub>2</sub>), 0.87 (t, 3H, CH<sub>3</sub>). **<sup>13</sup>C NMR** (101 MHz, CDCl<sub>3</sub>) δ 188.15, 77.48, 77.16, 76.84, 50.66, 48.26, 34.50, 31.91, 25.14, 23.65, 22.58, 19.08, 14.08. **HRMS** (ESI/QTOF) *m/z*: [M + H]<sup>+</sup> Calcd for C<sub>12</sub>H<sub>26</sub>N<sub>3</sub>O<sup>+</sup> 228.2070; Found 228.2069.

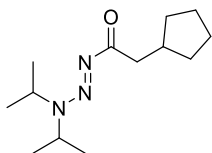
*(E)*-1-(3,3-Diisopropyltriaz-1-en-1-yl)-3,3-dimethylbutan-1-one (**3.2**)

Triazene **3.2** was prepared following the general procedure using (*E*)-1-(3,3-dimethylbut-1-yn-1-yl)-3,3-diisopropyltriaz-1-ene (0.2 mmol) and acetic acid (0.5 equiv) in acetone/water (1:1, 1 ml). The reaction mixture was heated at 50 °C for 4.5 h. Yield (yellow oil, white crystals): 37.9 mg (82%). **<sup>1</sup>H NMR** (400 MHz, CDCl<sub>3</sub>) δ 5.46 (hept, *J* = 6.8 Hz, 1H, CH(CH<sub>3</sub>)<sub>2</sub>), 4.14 (hept, *J* = 6.6 Hz, 1H, CH(CH<sub>3</sub>)<sub>2</sub>), 2.64 (s, 2H, CH<sub>2</sub>), 1.39 (d, *J* = 6.6 Hz, 6H, CH(CH<sub>3</sub>)<sub>2</sub>), 1.23 (d, *J* = 6.9 Hz, 6H, CH(CH<sub>3</sub>)<sub>2</sub>), 1.01 (s, 9H, CH<sub>3</sub>). **<sup>13</sup>C NMR** (101 MHz, CDCl<sub>3</sub>) δ 186.78, 77.48, 77.36, 77.16, 76.84, 50.79, 48.41, 46.84, 31.47, 30.41, 23.67, 19.15. **HRMS** (ESI/QTOF) *m/z*: [M + Na]<sup>+</sup> Calcd for C<sub>12</sub>H<sub>25</sub>N<sub>3</sub>NaO<sup>+</sup> 250.1890; Found 250.1892. Crystals were grown by keeping the yellow oil under vacuum at rt. White crystals. The *R* factor is 2.71% (< 3%).

*(E)*-1-(3,3-Diisopropyltriaz-1-en-1-yl)-3-methoxypropan-1-one (**3.3**)

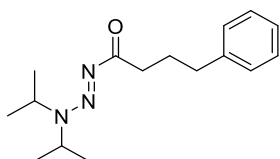
Triazene **3.3** was prepared following the general procedure using (*E*)-3,3-diisopropyl-1-(3-methoxyprop-1-yn-1-yl)triaz-1-ene (0.2 mmol) and acetic acid (0.5 equiv) in acetone/water (1:1, 1 ml). The reaction mixture was heated at 50 °C for 4.5 h. Yield (yellow/orange oil): 32.1 mg (75%). **<sup>1</sup>H NMR** (400 MHz, CDCl<sub>3</sub>) δ 5.47 (hept, *J* = 6.8 Hz, 1H, CH(CH<sub>3</sub>)<sub>2</sub>), 4.13 (hept, *J* = 6.6 Hz, 1H, CH(CH<sub>3</sub>)<sub>2</sub>), 3.75 (t, *J* = 7.0 Hz, 2H, CH<sub>2</sub>), 3.36 (s, 3H, CH<sub>3</sub>), 2.99 (t, *J* = 7.0 Hz, 2H, CH<sub>2</sub>), 1.37 (d, *J* = 6.5 Hz, 6H,

$\text{CH}(\text{CH}_3)_2$ ), 1.22 (d,  $J = 6.9$  Hz, 6H,  $\text{CH}(\text{CH}_3)_2$ ).  $^{13}\text{C}$  NMR (101 MHz,  $\text{CDCl}_3$ )  $\delta$  185.42, 77.48, 77.16, 76.84, 68.83, 58.89, 50.91, 48.64, 34.71, 23.64, 19.07. HRMS (ESI/QTOF)  $m/z$ :  $[\text{M} + \text{H}]^+$  Calcd for  $\text{C}_{10}\text{H}_{22}\text{N}_3\text{O}_2^+$  216.1707; Found 216.1709.



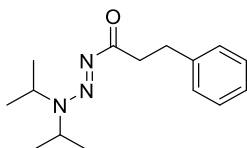
(*E*)-2-Cyclopentyl-1-(3,3-diisopropyltriaz-1-en-1-yl)ethan-1-one (**3.4**)

Triazene **3.4** was prepared following the general procedure using (*E*)-1-(cyclopentylethynyl)-3,3-diisopropyltriaz-1-ene (0.2 mmol) and acetic acid (0.5 equiv) in acetone/water (1:1, 1 ml). The reaction mixture was heated at 50 °C for 19 h. Yield (yellow oil): 28.7 mg (60%).  $^1\text{H}$  NMR (400 MHz,  $\text{CDCl}_3$ )  $\delta$  5.47 (hept,  $J = 6.8$  Hz, 1H,  $\text{CH}(\text{CH}_3)_2$ ), 4.14 (hept,  $J = 6.6$  Hz, 1H,  $\text{CH}(\text{CH}_3)_2$ ), 2.70 (d,  $J = 7.3$  Hz, 2H,  $\text{CH}_2$ ), 2.42 – 2.16 (m, 1H, CH), 1.93 – 1.73 (m, 2H,  $\text{CH}_2$ ), 1.70 – 1.46 (m, 4H,  $\text{CH}_2$ ,  $\text{CH}_2$ ), 1.39 (d,  $J = 6.6$  Hz, 6H,  $\text{CH}(\text{CH}_3)_2$ ), 1.24 (d,  $J = 6.8$  Hz, 6H,  $\text{CH}(\text{CH}_3)_2$ ), 1.21 – 1.04 (m, 2H,  $\text{CH}_2$ ).  $^{13}\text{C}$  NMR (101 MHz,  $\text{CDCl}_3$ )  $\delta$  187.75, 77.48, 77.36, 77.16, 76.84, 50.74, 48.33, 40.54, 37.05, 32.97, 25.15, 23.71, 19.16. Trace of pentane. HRMS (ESI/QTOF)  $m/z$ :  $[\text{M} + \text{Na}]^+$  Calcd for  $\text{C}_{13}\text{H}_{25}\text{N}_3\text{NaO}^+$  262.1890; Found 262.1893.



(*E*)-1-(3,3-Diisopropyltriaz-1-en-1-yl)-4-phenylbutan-1-one (**3.5**)

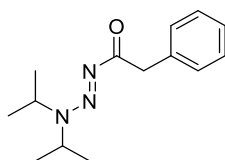
Triazene **3.5** was prepared following the general procedure using (*E*)-3,3-diisopropyl-1-(5-phenylpent-1-yn-1-yl)triaz-1-ene (1.5 mmol) and acetic acid (0.5 equiv) in acetone/water (1:1, 7.5 ml). The reaction mixture was heated at 50 °C until no significant further conversion was observed. Yield (yellow/orange oil): 237 mg (57%).  $^1\text{H}$  NMR (400 MHz,  $\text{CDCl}_3$ )  $\delta$  7.36 – 7.08 (m, 5H, Ph), 5.47 (hept,  $J = 6.8$  Hz, 1H,  $\text{CH}(\text{CH}_3)_2$ ), 4.12 (hept,  $J = 6.6$  Hz, 1H,  $\text{CH}(\text{CH}_3)_2$ ), 2.70 (dt,  $J = 11.9$ , 7.6 Hz, 4H,  $\text{CH}_2\text{CH}_2$ ), 2.01 (p,  $J = 7.6$  Hz, 2H,  $\text{CH}_2$ ), 1.34 (d,  $J = 6.5$  Hz, 6H,  $\text{CH}(\text{CH}_3)_2$ ), 1.23 (d,  $J = 6.8$  Hz, 6H,  $\text{CH}(\text{CH}_3)_2$ ).  $^{13}\text{C}$  NMR (101 MHz,  $\text{CDCl}_3$ )  $\delta$  187.69, 142.24, 128.69, 128.39, 125.88, 77.48, 77.36, 77.16, 76.84, 50.76, 48.40, 35.75, 33.93, 27.04, 23.67, 19.14. HRMS (ESI/QTOF)  $m/z$ :  $[\text{M} + \text{Na}]^+$  Calcd for  $\text{C}_{16}\text{H}_{25}\text{N}_3\text{NaO}^+$  298.1890; Found 298.1895.



(*E*)-1-(3,3-Diisopropyltriaz-1-en-1-yl)-3-phenylpropan-1-one (**3.6**)

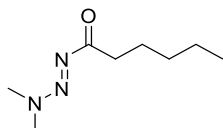
Triazene **3.6** was prepared following the general procedure using (*E*)-3,3-diisopropyl-1-(3-phenylprop-1-yn-1-yl)triaz-1-ene (0.2 mmol) and acetic acid (0.5 equiv) in acetone/water (1:1, 1 ml).

The reaction mixture was heated at 50 °C for 4.5 h. Yield (yellow oil, white crystals forming): 29.0 mg (56%). **<sup>1</sup>H NMR** (400 MHz, CDCl<sub>3</sub>) δ 7.33 – 7.14 (m, 5H, *Ph*), 5.47 (hept, *J* = 6.8 Hz, 1H, CH(CH<sub>3</sub>)<sub>2</sub>), 4.13 (hept, *J* = 6.6 Hz, 1H, CH(CH<sub>3</sub>)<sub>2</sub>), 3.01 (s, 4H, CH<sub>2</sub>, CH<sub>2</sub>), 1.36 (d, *J* = 6.6 Hz, 6H, CH(CH<sub>3</sub>)<sub>2</sub>), 1.23 (d, *J* = 6.8 Hz, 6H, CH(CH<sub>3</sub>)<sub>2</sub>). **<sup>13</sup>C NMR** (101 MHz, CDCl<sub>3</sub>) δ 186.98, 142.00, 128.60, 128.54, 126.05, 77.48, 77.36, 77.16, 76.84, 50.88, 48.54, 36.38, 31.56, 23.71, 19.13. **HRMS** (ESI/QTOF) *m/z*: [M + H]<sup>+</sup> Calcd for C<sub>15</sub>H<sub>24</sub>N<sub>3</sub>O<sup>+</sup> 262.1914; Found 262.1919.



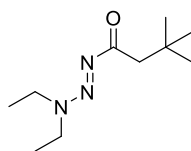
(*E*)-1-(3,3-Diisopropyltriaz-1-en-1-yl)-2-phenylethan-1-one (**3.7**)

Triazene **3.7** was prepared following the general procedure using (*E*)-3,3-diisopropyl-1-(phenylethynyl)triaz-1-ene (0.2 mmol) and acetic acid (2 equiv) in acetone/water (1:1, 1 ml). The reaction mixture was heated in a closed vial at 100 °C for 2 h. Yield (white solid): 18.3 mg (36%). **<sup>1</sup>H NMR** (400 MHz, CDCl<sub>3</sub>) δ 7.39 – 7.12 (m, 6H, *Ph*), 5.48 (hept, *J* = 13.5, 6.8 Hz, 1H, CH(CH<sub>3</sub>)<sub>2</sub>), 4.14 (hept, *J* = 6.5 Hz, 1H, CH(CH<sub>3</sub>)<sub>2</sub>), 4.04 (s, 2H, CH<sub>2</sub>), 1.36 (d, *J* = 6.7 Hz, 6H, CH(CH<sub>3</sub>)<sub>2</sub>), 1.23 (d, *J* = 6.8 Hz, 6H, CH(CH<sub>3</sub>)<sub>2</sub>). **<sup>13</sup>C NMR** (101 MHz, CDCl<sub>3</sub>) δ 185.11, 136.15, 129.33, 128.35, 126.32, 77.34, 77.02, 76.70, 50.88, 48.68, 41.59, 23.49, 18.98. **HRMS** (ESI/QTOF) *m/z*: [M + H]<sup>+</sup> Calcd for C<sub>14</sub>H<sub>22</sub>N<sub>3</sub>O<sup>+</sup> 248.1757; Found 248.1759.



(*E*)-1-(3,3-Dimethyltriaz-1-en-1-yl)hexan-1-one (**3.8**)

Triazene **3.8** was prepared following the general procedure using (*E*)-1-(hex-1-yn-1-yl)-3,3-dimethyltriaz-1-ene (0.5 mmol) and acetic acid (0.5 equiv) in acetone/water (1:1, 2.5 ml). The reaction mixture was heated at 50 °C for 5 h. Yield (yellow oil, pale white solid): 31 mg (36%). **<sup>1</sup>H NMR** (400 MHz, CDCl<sub>3</sub>) δ 3.63 (s, 3H, NCH<sub>3</sub>), 3.28 (s, 3H, NCH<sub>3</sub>), 2.67 (t, *J* = 7.6 Hz, 2H, CH<sub>2</sub>), 1.68 (p, *J* = 7.3 Hz, 2H, CH<sub>2</sub>), 1.43 – 1.20 (m, 4H, CH<sub>2</sub>, CH<sub>2</sub>), 1.01 – 0.77 (m, 3H, CH<sub>3</sub>). **<sup>13</sup>C NMR** (101 MHz, CDCl<sub>3</sub>) δ 187.22, 77.48, 77.36, 77.16, 76.84, 44.65, 37.37, 35.13, 31.78, 24.90, 22.61, 14.12. **HRMS** (nanochip-ESI/LTQ-Orbitrap) *m/z*: [M + Na]<sup>+</sup> Calcd for C<sub>8</sub>H<sub>17</sub>N<sub>3</sub>NaO<sup>+</sup> 194.1264; Found 194.1264.



(*E*)-1-(3,3-Diethyltriaz-1-en-1-yl)-3,3-dimethylbutan-1-one (**3.9**)

Triazene **3.9** was prepared following the general procedure using (*E*)-1-(3,3-dimethylbut-1-yn-1-yl)-3,3-diethyltriaz-1-ene (1.2 mmol) and acetic acid (0.5 equiv) in acetone/water (1:1, 6 ml). The reaction mixture was heated at 50 °C for 5 h. Yield (yellow oil, pale white solid): 158 mg (66%). **<sup>1</sup>H**

**NMR** (400 MHz, CDCl<sub>3</sub>)  $\delta$  3.84 (dq,  $J$  = 11.8, 7.2 Hz, 4H, CH<sub>2</sub>CH<sub>3</sub>), 2.61 (s, 2H, CH<sub>2</sub>), 1.37 (t,  $J$  = 7.2 Hz, 3H, CH<sub>3</sub>), 1.20 (t,  $J$  = 7.2 Hz, 3H, CH<sub>3</sub>), 1.01 (m, 9H, CH<sub>3</sub>, CH<sub>2</sub>CH<sub>3</sub>). **<sup>13</sup>C NMR** (101 MHz, CDCl<sub>3</sub>)  $\delta$  186.18, 77.48, 77.16, 76.84, 50.67, 48.03, 42.98, 31.48, 30.32, 14.06, 10.90. **HRMS** (ESI/QTOF)  $m/z$ : [M + Na]<sup>+</sup> Calcd for C<sub>10</sub>H<sub>21</sub>N<sub>3</sub>NaO<sup>+</sup> 222.1577; Found 222.1581.

### ES.3.3 Synthesis of the olefinic 1-acyl triazenes **3.10–3.16**

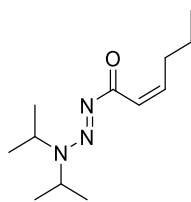
#### ES.3.3.1 Reaction optimization

Stock solutions were prepared in a glove box using 1,2-dichloroethane as solvent. The concentrations of the stock solutions were chosen in a way that 100  $\mu$ l of the 1-alkynyl triazene (0.1 mmol), 100  $\mu$ l of the internal standard 1,3,5-trimethoxybenzene (1/3 equiv), 200  $\mu$ l of pyridine *N*-oxide (1.1 equiv), and 100  $\mu$ l of the pre-mixed catalyst solution of LAuX (5 mol%) and AgY (5 mol%) were employed. The aliquots of the stock solutions were added to a J-Young NMR tube containing a closed capillary with D<sub>2</sub>O. A blank <sup>1</sup>H spectrum was recorded using a 500 MHz NMR spectrometer with a pre-set temperature and with suppression of the 1,2-dichloroethane solvent peak. Subsequently, the catalyst was added to the reaction mixture ( $t_0$ ) and the shimming, gain and atma were optimized again. The reaction was then followed by NMR. After 15 min, the first <sup>1</sup>H NMR spectrum was recorded, followed by further spectra every 5 min. Yields were calculated based on the ratio of H( $\alpha$ ) and the CH<sub>2</sub> of the starting material and the peaks of the internal standard at ~6 ppm. The *E/Z* ratio was determined by comparing the H( $\alpha$ ) signal *J*-values: *E* ~10 Hz, *Z* ~15 Hz.

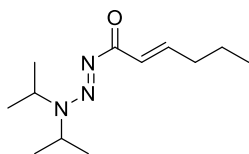
#### ES.3.3.2 General procedure

A solution of the respective triazene (0.5 mmol), pyridine *N*-oxide, (JohnPhos)AuCl (5 mol%), and AgNTF<sub>2</sub> (5 mol%) in dichloroethane (2.5 ml) was stirred at 70 °C in a glove box. After the indicated time, the reaction mixture was removed from the glove box, exposed to air, and the solvent was evaporated. The crude product was purified and the *E/Z*-isomers were separated by flash column chromatography over deactivated silica with a gradient of pentane to pentane/diethyl ether 25-30%. The product was freeze-dried in pentane.

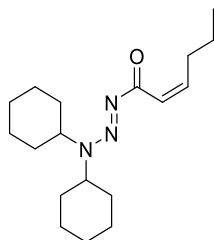
## ES.3.3.3 Scope

*(Z)*-1-((*E*)-3,3-Diisopropyltriaz-1-en-1-yl)hex-2-en-1-one (**3.10-Z**)

Triazene **3.10-Z** was prepared following the general procedure using (*E*)-1-(hex-1-yn-1-yl)-3,3-diisopropyltriaz-1-ene (0.5 mmol), JohnPhos AuCl (5 mol%), AgNTf<sub>2</sub> (5 mol%) and pyridine *N*-oxide (1.1 eq) in DCE (0.2 M). The reaction mixture was heated at 70 °C for 45 min. Yield (yellow oil): 4.3 mg (4%). <sup>1</sup>H NMR (400 MHz, CDCl<sub>3</sub>) δ 6.50 (d, *J* = 11.6, 1.7 Hz, 1H, CH), 6.20 (dt, *J* = 13.0, 6.0 Hz, 1H, CH), 5.46 (hept, 1H, CH(CH<sub>3</sub>)<sub>2</sub>), 4.13 (hept, 1H, CH(CH<sub>3</sub>)<sub>2</sub>), 2.77 – 2.61 (m, 2H, CH<sub>2</sub>), 1.55 – 1.43 (m, 2H, CH<sub>2</sub>), 1.39 (d, *J* = 6.6 Hz, 6H, CH(CH<sub>3</sub>)<sub>2</sub>), 1.25 (d, *J* = 6.8 Hz, 6H, CH(CH<sub>3</sub>)<sub>2</sub>), 0.95 (t, *J* = 7.3 Hz, 3H, CH<sub>3</sub>). <sup>13</sup>C NMR (101 MHz, CDCl<sub>3</sub>) δ 178.88, 148.41, 122.34, 50.94, 48.34, 31.67, 23.62, 22.70, 19.17, 13.99. HRMS (ESI/QTOF) *m/z* [M + H]<sup>+</sup> Calcd for C<sub>12</sub>H<sub>24</sub>N<sub>3</sub>O<sup>+</sup> 226.1914; Found 226.1916.

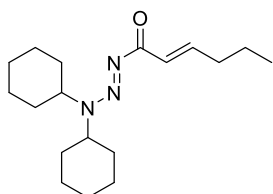
*(E)*-1-((*E*)-3,3-Diisopropyltriaz-1-en-1-yl)hex-2-en-1-one (**3.10-E**)

Triazene **3.10-E** was prepared following the general procedure using (*E*)-1-(hex-1-yn-1-yl)-3,3-diisopropyltriaz-1-ene (0.5 mmol), JohnPhos AuCl (5 mol%), AgNTf<sub>2</sub> (5 mol%) and pyridine *N*-oxide (1.1 eq) in DCE (0.2 M). The reaction mixture was heated at 70 °C for 45 min. Yield (yellow oil): 84.6 mg (75%). <sup>1</sup>H NMR (400 MHz, CDCl<sub>3</sub>) δ 7.07 (dt, *J* = 14.6, 7.0 Hz, 1H, CH), 6.58 (d, *J* = 15.5, 1.6 Hz, 1H, CH), 5.42 (hept, 1H, CH(CH<sub>3</sub>)<sub>2</sub>), 4.14 (hept, 1H, CH(CH<sub>3</sub>)<sub>2</sub>), 2.21 (q, *J* = 7.2 Hz, 2H, CH<sub>2</sub>), 1.49 (q, *J* = 7.4 Hz, 2H, CH<sub>2</sub>), 1.38 (d, 6H, CH(CH<sub>3</sub>)<sub>2</sub>), 1.23 (d, *J* = 6.8, 1.1 Hz, 6H, CH(CH<sub>3</sub>)<sub>2</sub>), 0.92 (t, 3H, CH<sub>3</sub>). <sup>13</sup>C NMR (101 MHz, CDCl<sub>3</sub>) δ 177.92, 148.32, 123.03, 77.39, 77.07, 76.76, 51.08, 48.42, 34.82, 23.41, 21.51, 18.98, 13.73. HRMS (ESI/QTOF) *m/z* [M + H]<sup>+</sup> Calcd for C<sub>12</sub>H<sub>24</sub>N<sub>3</sub>O<sup>+</sup> 226.1914; Found 226.1916.

*(Z)*-1-((*E*)-3,3-Dicyclohexyltriaz-1-en-1-yl)hex-2-en-1-one (**3.11-Z**)

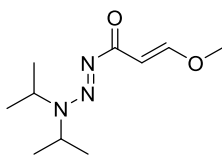
Triazene **3.11-Z** was prepared following the general procedure using (*E*)-3,3-dicyclohexyl-1-(hex-1-yn-1-yl)triaz-1-ene (0.5 mmol), JohnPhos AuCl (5 mol%), AgNTf<sub>2</sub> (5 mol%) and pyridine

*N*-oxide (1.1 eq) in DCE (0.2 M). The reaction mixture was heated at 70 °C for 45 min. Yield (off-white solid): 9.5 mg (6%). **<sup>1</sup>H NMR** (400 MHz, CDCl<sub>3</sub>) δ 6.50 (d, *J* = 11.7 Hz, 1H, *CH*), 6.18 (dt, *J* = 11.7, 7.3 Hz, 1H, *CH*), 5.39 – 5.08 (m, 1H, *Cy-CH*), 3.87 – 3.54 (m, 1H, *Cy-CH*), 2.67 (q, *J* = 7.4 Hz, 2H, *CH*<sub>2</sub>), 1.97 – 1.04 (m, 22H, *Cy-CH*<sub>2</sub>, *CH*<sub>2</sub>), 0.94 (t, *J* = 7.3 Hz, 3H, *CH*<sub>3</sub>). **<sup>13</sup>C NMR** (101 MHz, CDCl<sub>3</sub>) δ 179.15, 148.06, 122.46, 77.48, 77.16, 76.84, 59.44, 56.21, 34.16, 31.67, 29.47, 25.96, 25.39, 22.71, 13.99. **HRMS** (ESI/QTOF) *m/z* [*M* + *H*]<sup>+</sup> Calcd for C<sub>18</sub>H<sub>32</sub>N<sub>3</sub>O<sup>+</sup> 306.2540; Found 306.2544.



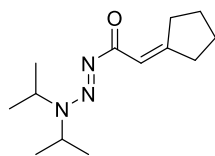
(*E*)-1-((*E*)-3,3-Dicyclohexyltriaz-1-en-1-yl)hex-2-en-1-one (**3.11-E**)

Triazene **3.11-E** was prepared following the general procedure using (*E*)-3,3-dicyclohexyl-1-(hex-1-yn-1-yl)triaz-1-ene (0.5 mmol), JohnPhos AuCl (5 mol%), AgNTf<sub>2</sub> (5 mol%) and pyridine *N*-oxide (1.1 eq) in DCE (0.2 M). The reaction mixture was heated at 70 °C for 45 min. Yield (off-white solid): 106 mg (70%). **<sup>1</sup>H NMR** (400 MHz, CDCl<sub>3</sub>) δ 7.08 (dt, *J* = 14.2, 7.0 Hz, 1H, *CH*), 6.61 (d, *J* = 15.6 Hz, 1H, *CH*), 5.50 – 4.97 (m, 1H, *Cy-CH*), 3.91 – 3.52 (m, 1H, *Cy-CH*), 2.24 (q, *J* = 7.3 Hz, 2H, *CH*<sub>2</sub>), 2.02 – 1.07 (m, 22H, *Cy-CH*<sub>2</sub>, *CH*<sub>2</sub>), 0.95 (t, *J* = 7.4 Hz, 3H, *CH*<sub>3</sub>). **<sup>13</sup>C NMR** (101 MHz, CDCl<sub>3</sub>) δ 178.41, 148.30, 123.13, 77.48, 77.16, 76.84, 59.63, 56.38, 35.01, 34.15, 29.45, 29.45, 25.97, 25.97, 25.39, 25.39, 21.71, 13.92. **HRMS** (ESI/QTOF) *m/z* [*M* + *H*]<sup>+</sup> Calcd for C<sub>18</sub>H<sub>32</sub>N<sub>3</sub>O<sup>+</sup> 306.2540; Found 306.2544. Crystals were grown by dissolving in small amount of pentane and leaving in the fridge overnight.



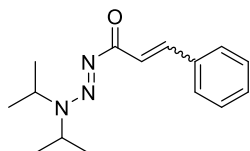
(*E*)-1-((*E*)-3,3-Diisopropyltriaz-1-en-1-yl)-3-methoxyprop-2-en-1-one (**3.12**)

Triazene **3.12** was prepared following the general procedure using (*E*)-3,3-diisopropyl-1-(3-methoxyprop-1-yn-1-yl)triaz-1-ene (0.5 mmol), JohnPhos AuCl (5 mol%), AgNTf<sub>2</sub> (5 mol%) and pyridine *N*-oxide (1.1 eq) in DCE (0.2 M). The reaction mixture was heated at 70 °C for 60 min. Purification, gradient up to 80% diethyl ether. Yield (white solid): 63.0 mg (58%). **<sup>1</sup>H NMR** (400 MHz, CDCl<sub>3</sub>) δ 7.79 (d, *J* = 12.5 Hz, 1H, *CH*), 5.98 (d, *J* = 12.4 Hz, 1H, *CH*), 5.39 (hept, 1H, *CH*(CH<sub>3</sub>)<sub>2</sub>), 4.15 (hept, 1H, *CH*(CH<sub>3</sub>)<sub>2</sub>), 3.73 (s, 3H, *CH*<sub>3</sub>), 1.39 (d, *J* = 6.5 Hz, 6H, *CH*(CH<sub>3</sub>)<sub>2</sub>), 1.25 (d, *J* = 6.8 Hz, 6H, *CH*(CH<sub>3</sub>)<sub>2</sub>). **<sup>13</sup>C NMR** (101 MHz, CDCl<sub>3</sub>) δ 178.81, 163.62, 98.39, 77.48, 77.16, 76.84, 57.64, 51.14, 48.48, 23.56, 19.14. **HRMS** (nanochip-ESI/LTQ-Orbitrap) *m/z* [*M* + *H*]<sup>+</sup> Calcd for C<sub>10</sub>H<sub>20</sub>N<sub>3</sub>O<sub>2</sub><sup>+</sup> 214.1550; Found 214.1550.



(*E*)-2-Cyclopentylidene-1-(3,3-diisopropyltriaz-1-en-1-yl)ethan-1-one (**3.13**)

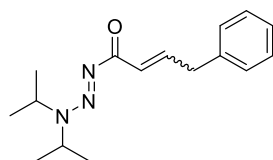
Triazene **3.13** was prepared following the general procedure using (*E*)-1-(cyclopentylethynyl)-3,3-diisopropyltriaz-1-ene (0.5 mmol), JohnPhos AuCl (5 mol%), AgNTf<sub>2</sub> (5 mol%) and pyridine *N*-oxide (1.1 eq) in DCE (0.2 M). The reaction mixture was heated at 70 °C for 90 min. Yield (yellow oil): 67.1 mg (56%). <sup>1</sup>H NMR (400 MHz, CDCl<sub>3</sub>) δ 6.55 (s, 1H, CH), 5.41 (hept, *J* = 6.8 Hz, 1H, CH(CH<sub>3</sub>)<sub>2</sub>), 4.12 (hept, *J* = 13.2, 6.6 Hz, 1H, CH(CH<sub>3</sub>)<sub>2</sub>), 2.98 – 2.81 (m, 2H, CH<sub>2</sub>), 2.57 – 2.41 (m, 2H, CH<sub>2</sub>), 1.73 (p, *J* = 6.9 Hz, 2H, CH<sub>2</sub>), 1.64 (p, *J* = 6.8 Hz, 2H, CH<sub>2</sub>), 1.38 (d, 6H, CH(CH<sub>3</sub>)<sub>2</sub>), 1.21 (d, *J* = 6.8 Hz, 6H, CH(CH<sub>3</sub>)<sub>2</sub>). <sup>13</sup>C NMR (101 MHz, CDCl<sub>3</sub>) δ 178.31, 168.82, 113.62, 77.48, 77.16, 76.84, 50.67, 47.96, 36.63, 33.35, 26.70, 25.60, 23.56, 19.10. Trace of starting material. HRMS (nanochip-ESI/LTQ-Orbitrap) *m/z*: [M + H]<sup>+</sup> Calcd for C<sub>13</sub>H<sub>24</sub>N<sub>3</sub>O<sup>+</sup> 238.1914; Found 238.1910.



(*E*)/(*Z*)-1-((*E*)-3,3-Diisopropyltriaz-1-en-1-yl)-3-phenylprop-2-en-1-one

(**3.14-E/Z** ~ 10:1)

Triazene **3.14** was prepared following the general procedure using (*E*)-3,3-diisopropyl-1-(3-phenylprop-1-yn-1-yl)triaz-1-ene (0.5 mmol), JohnPhos AuCl (5 mol%), AgNTf<sub>2</sub> (5 mol%) and pyridine *N*-oxide (1.1 eq) in DCE (0.2 M). The reaction mixture was heated at 70 °C for 60 min. Mixed fraction **3.14-E/Z** (yellow oil): 8.5 mg (4%), *E/Z* = 1:1. Yield **3.14-E** (yellow solid): 82.7 mg (46%). <sup>1</sup>H NMR (400 MHz, CDCl<sub>3</sub>) δ 7.82 (d, *J* = 16.0 Hz, 1H, CH), 7.55 (dd, *J* = 7.6, 2.0 Hz, 2H, Ph), 7.39 – 7.29 (m, 3H, Ph), 7.22 (d, *J* = 2.8 Hz, 1H, CH), 5.46 (hept, 1H, CH(CH<sub>3</sub>)<sub>2</sub>), 4.18 (hept, 1H, CH(CH<sub>3</sub>)<sub>2</sub>), 1.42 (d, *J* = 6.6 Hz, 6H, CH(CH<sub>3</sub>)<sub>2</sub>), 1.27 (d, *J* = 6.8 Hz, 6H, CH(CH<sub>3</sub>)<sub>2</sub>). <sup>13</sup>C NMR (101 MHz, CDCl<sub>3</sub>) δ 178.00, 143.80, 135.81, 129.93, 128.93, 128.24, 120.38, 77.48, 77.36, 77.16, 76.84, 51.50, 48.91, 23.62, 19.18. HRMS (ESI/QTOF) *m/z*: [M + H]<sup>+</sup> Calcd for C<sub>15</sub>H<sub>22</sub>N<sub>3</sub>O<sup>+</sup> 260.1757; Found 260.1759.

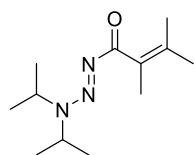


(*E*)/(*Z*)-1-((*E*)-3,3-Diisopropyltriaz-1-en-1-yl)-4-phenylbut-2-en-1-one

(**3.15-E/Z** ~ 2:1)

Triazene **3.15** was prepared following the general procedure using (*E*)-3,3-diisopropyl-1-(3-phenylprop-1-yn-1-yl)triaz-1-ene (0.5 mmol), JohnPhos AuCl (5 mol%), AgNTf<sub>2</sub> (5 mol%) and

pyridine *N*-oxide (1.1 eq) in DCE (0.2 M). The reaction mixture was heated at 70 °C for 90 min. For the purification, a gradient up to 50% diethyl ether was used. Yield (orange oil): 77.6 mg (59%). Mixture of *E/Z* ~ 2:1. **<sup>1</sup>H NMR** (400 MHz, CDCl<sub>3</sub>) δ 7.34 – 7.10 (m, 5H, *E/Z*-Ph), 6.59 – 6.32 (m, 1H, *E/Z*-CH), 5.52 – 5.31 (m, 1H, *E/Z*-CH(CH<sub>3</sub>)<sub>2</sub>), 4.19 – 4.01 (m, 1H, *E/Z*-CH(CH<sub>3</sub>)<sub>2</sub>), 3.59 (d, *J* = 5.8 Hz, 1H, *E*-CH), 3.52 (d, *J* = 6.7, 1.6 Hz, 1H, *Z*-CH), 1.37 (d, *J* = 6.5 Hz, 6H, *E*-CH(CH<sub>3</sub>)<sub>2</sub>), 1.30 (d, *J* = 6.6 Hz, 6H, *Z*-CH(CH<sub>3</sub>)<sub>2</sub>), 1.20 (d, *J* = 6.9, 5.2 Hz, 6H, *E/Z*-CH(CH<sub>3</sub>)<sub>2</sub>). **<sup>13</sup>C NMR** (101 MHz, CDCl<sub>3</sub>) δ 185.23, 177.70, 146.13, 138.42, 137.38, 132.49, 128.91, 128.54, 128.45, 127.15, 126.42, 126.19, 124.30, 124.13, 77.36, 77.24, 77.04, 76.72, 51.13, 50.89, 48.68, 48.54, 39.00, 38.89, 23.63, 23.45, 23.37, 19.00. **HRMS** (ESI/QTOF) *m/z* [M + H]<sup>+</sup> Calcd for C<sub>16</sub>H<sub>24</sub>N<sub>3</sub>O<sup>+</sup> 274.1914; Found 274.1918.



(*E*)-1-(3,3-Diisopropyltriaz-1-en-1-yl)-2,3-dimethylbut-2-en-1-one (**3.16**)

Triazene **3.16** was prepared following the general procedure using (*E*)-1-(3,3-dimethylbut-1-yn-1-yl)-3,3-diisopropyltriaz-1-ene (0.5 mmol), JohnPhos AuCl (5 mol%), AgNTf<sub>2</sub> (5 mol%) and pyridine *N*-oxide (1.1 eq) in DCE (0.2 M). The reaction mixture was heated at 70 °C for 45 min. Yield (off-white solid): 101.5 mg (90%). **<sup>1</sup>H NMR** (400 MHz, CDCl<sub>3</sub>) δ 5.43 (hept, *J* = 6.9 Hz, 1H, CH(CH<sub>3</sub>)<sub>2</sub>), 4.13 (hept, *J* = 6.7 Hz, 1H, CH(CH<sub>3</sub>)<sub>2</sub>), 1.84 (s, 3H, CH<sub>3</sub>), 1.74 (s, 3H, CH<sub>3</sub>), 1.68 (s, 3H, CH<sub>3</sub>), 1.34 (d, *J* = 6.6 Hz, 6H, CH(CH<sub>3</sub>)<sub>2</sub>), 1.25 (d, *J* = 6.8 Hz, 6H, CH(CH<sub>3</sub>)<sub>2</sub>). **<sup>13</sup>C NMR** (101 MHz, CDCl<sub>3</sub>) δ 186.50, 132.36, 128.68, 77.48, 77.36, 77.16, 76.84, 51.06, 48.66, 23.49, 22.77, 20.16, 19.19, 16.84. **HRMS** (LTQ-Orbitrap) *m/z* [M + H]<sup>+</sup> Calcd for C<sub>12</sub>H<sub>24</sub>N<sub>3</sub>O<sup>+</sup> 226.1914; Found 226.1914. Crystals were grown by dissolving the compound in a minimal amount of pentane and keeping it the fridge (5 °C) overnight.

## ES.3.4 Synthesis of the 1,2-diketo triazenes **3.17–3.22**

### ES.3.4.1 Reaction optimization

The reaction mixtures were prepared under N<sub>2</sub> in a J-Young NMR tube using 1,2,4,5-tetramethylbenzene as internal standard. The reactions were followed by recording <sup>1</sup>H spectra using a 400 MHz NMR spectrometer.

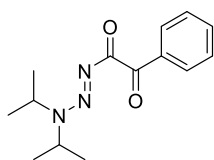
### ES.3.4.2 General procedure

Conditions A: A solution of the respective 1-alkynyl triazene (1 equiv), 2-chloropyridine *N*-oxide<sup>281</sup> (3 equiv), and I<sub>2</sub> (50 mol%) in acetonitrile (0.1 M) under N<sub>2</sub> was stirred for 50 min. Subsequently, the mixture was exposed to air and the solvent was evaporated. The crude product was

purified by flash column chromatography over deactivated silica with a gradient of pentane to pentane/diethyl ether 50%. The resulting product was freeze-dried in pentane.

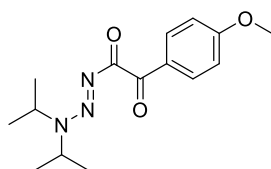
Conditions **B**: The general procedure was adapted by using the following conditions: (JohnPhos)AuCl (10 mol%), AgNTf<sub>2</sub> (10 mol%), pyridine *N*-oxide (2.2 equiv).

### ES.3.4.3 Scope



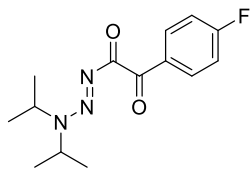
(*E*)-1-(3,3-Diisopropyltriaz-1-en-1-yl)-2-phenylethane-1,2-dione (**3.17**)

Triazene **3.17** was synthesized following procedure **A** or **B**, using (*E*)-3,3-diisopropyl-1-(phenylethynyl)triaz-1-ene (1 or 0.5 mmol, respectively). **A**: For purification, gradient up to 70% diethyl ether. **B**: 1.5 h reaction time. Yield **A** (pale yellow solid): 223 mg (85%). Yield **B** (white crystalline solid): 80.3 mg (61%). <sup>1</sup>H NMR (400 MHz, CDCl<sub>3</sub>) δ 7.94 – 7.77 (m, 2H, Ph), 7.64 – 7.52 (m, 1H, Ph), 7.52 – 7.40 (m, 2H, Ph), 5.52 (hept, *J* = 6.8 Hz, 1H, CH(CH<sub>3</sub>)<sub>2</sub>), 4.08 (hept, *J* = 6.6 Hz, 1H, CH(CH<sub>3</sub>)<sub>2</sub>), 1.28 (d, *J* = 6.8 Hz, 6H, CH(CH<sub>3</sub>)<sub>2</sub>), 1.04 (d, *J* = 6.6 Hz, 6H, CH(CH<sub>3</sub>)<sub>2</sub>). <sup>13</sup>C NMR (101 MHz, CDCl<sub>3</sub>) δ 196.51, 181.63, 134.07, 133.96, 129.21, 128.88, 77.48, 77.36, 77.16, 76.84, 52.31, 50.21, 23.08, 18.99. HRMS (nanochip-ESI/LTQ-Orbitrap) *m/z*: [M + H]<sup>+</sup> Calcd for C<sub>14</sub>H<sub>20</sub>N<sub>3</sub>O<sub>2</sub><sup>+</sup> 262.1550; Found 262.1547.

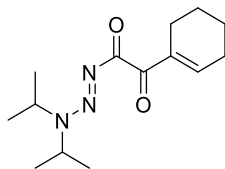


(*E*)-1-(3,3-Diisopropyltriaz-1-en-1-yl)-2-(4-methoxyphenyl)ethane-1,2-dione (**3.18**)

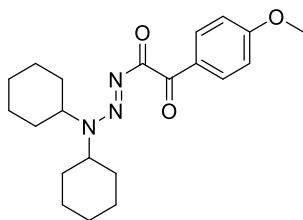
Triazene **3.18** was synthesized following procedure **A** using (*E*)-3,3-diisopropyl-1-((4-methoxyphenyl)ethynyl)triaz-1-ene (0.75 mmol). Purification with a gradient of 5% to 75% diethyl ether. Product was freeze-dried in diethyl ether/pentane and some dichloromethane. Yield **A** (yellow solid): 188.2 mg (86%). <sup>1</sup>H NMR (400 MHz, CDCl<sub>3</sub>) δ 7.91 – 7.72 (m, 2H, Ph), 7.01 – 6.84 (m, 2H, Ph), 5.51 (hept, *J* = 6.8 Hz, 1H, CH(CH<sub>3</sub>)<sub>2</sub>), 4.09 (hept, *J* = 6.6 Hz, 1H, CH(CH<sub>3</sub>)<sub>2</sub>), 3.86 (s, 3H, CH<sub>3</sub>), 1.28 (d, *J* = 6.9 Hz, 6H, CH(CH<sub>3</sub>)<sub>2</sub>), 1.07 (d, *J* = 6.5 Hz, 6H, CH(CH<sub>3</sub>)<sub>2</sub>). <sup>13</sup>C NMR (101 MHz, CDCl<sub>3</sub>) δ 194.94, 181.92, 164.20, 131.61, 127.25, 114.15, 77.48, 77.16, 76.84, 55.66, 52.26, 50.08, 23.15, 18.99. HRMS (ESI/QTOF) *m/z*: [M + H]<sup>+</sup> Calcd for C<sub>15</sub>H<sub>22</sub>N<sub>3</sub>O<sub>3</sub><sup>+</sup> 292.1656; Found 292.1661. Crystals were grown by dissolving in warm diethyl ether (40 °C), letting cool to room temperature, followed by slow evaporation of solvent.

*(E)-1-(3,3-Diisopropyltriaz-1-en-1-yl)-2-(4-fluorophenyl)ethane-1,2-dione***(3.19)**

Triazene **3.19** was synthesized following procedure **A** using (*E*)-1-((4-fluorophenyl)ethynyl)-3,3-diisopropyltriaz-1-ene (0.75 mmol). Yield (yellow solid): 171.9 mg (82%). **<sup>1</sup>H NMR** (400 MHz, CDCl<sub>3</sub>) δ 7.88 (dd, *J* = 8.8, 5.4 Hz, 2H, Ph), 7.15 (dd, *J* = 8.6 Hz, 2H, Ph), 5.51 (hept, *J* = 6.8 Hz, 1H, CH(CH<sub>3</sub>)<sub>2</sub>), 4.11 (hept, *J* = 6.5 Hz, 1H, CH(CH<sub>3</sub>)<sub>2</sub>), 1.29 (d, *J* = 6.8 Hz, 6H, CH(CH<sub>3</sub>)<sub>2</sub>), 1.07 (d, *J* = 6.5 Hz, 6H, CH(CH<sub>3</sub>)<sub>2</sub>). **<sup>13</sup>C NMR** (101 MHz, CDCl<sub>3</sub>) δ 194.74, 181.27, 167.52, 164.97, 131.93, 131.84, 130.59, 130.56, 116.33, 116.11, 77.48, 77.16, 76.84, 23.14, 18.99. **HRMS** (nanochip-ESI/LTQ-Orbitrap) *m/z*: [M + H]<sup>+</sup> Calcd for C<sub>14</sub>H<sub>19</sub>FN<sub>3</sub>O<sub>2</sub><sup>+</sup> 280.1456; Found 280.1458.

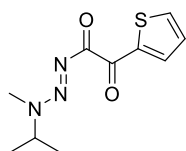
*(E)-1-(Cyclohex-1-en-1-yl)-2-(3,3-diisopropyltriaz-1-en-1-yl)ethane-1,2-dione***(3.20)**

Triazene **3.20** was synthesized following procedure **B** using (*E*)-1-(cyclohex-1-en-1-ylethynyl)-3,3-diisopropyltriaz-1-ene (0.5 mmol). Reaction time of 1.5 h. Only conditions **B** gave the desired product. Yield (pastel pink crystalline solid): 56.1 mg (42%). **<sup>1</sup>H NMR** (400 MHz, CDCl<sub>3</sub>) δ 6.68 (tt, *J* = 3.7, 1.6 Hz, 1H, CH), 5.48 (hept, *J* = 6.9 Hz, 1H, CH(CH<sub>3</sub>)<sub>2</sub>), 4.16 (hept, *J* = 6.5 Hz, 1H, CH(CH<sub>3</sub>)<sub>2</sub>), 2.37 – 2.16 (m, 4H, CH<sub>2</sub>, CH<sub>2</sub>), 1.76 – 1.58 (m, 4H, CH<sub>2</sub>, CH<sub>2</sub>), 1.27 (d, *J* = 7.8, 6.7 Hz, 12H, CH(CH<sub>3</sub>)<sub>2</sub>, CH(CH<sub>3</sub>)<sub>2</sub>). **<sup>13</sup>C NMR** (101 MHz, CDCl<sub>3</sub>) δ 197.79, 182.39, 147.13, 137.23, 77.48, 77.36, 77.16, 76.84, 52.06, 49.91, 26.50, 23.37, 22.02, 21.84, 21.77, 19.02. **HRMS** (ESI/QTOF) *m/z*: [M + H]<sup>+</sup> Calcd for C<sub>14</sub>H<sub>24</sub>N<sub>3</sub>O<sub>2</sub><sup>+</sup> 266.1863; Found 266.1864. Crystals were grown by dissolving in warm diethyl ether (40 °C) and left at rt >48 h.

*(E)-1-(3,3-Dicyclohexyltriaz-1-en-1-yl)-2-(4-methoxyphenyl)ethane-1,2-dione (3.21)*

Triazene **3.21** was synthesized following procedure **A** using (*E*)-3,3-dicyclohexyl-1-((4-methoxyphenyl)ethynyl)triaz-1-ene (0.5 mmol). Reaction time of 140 min. Yield (pale yellow solid):

150 mg (81%). **<sup>1</sup>H NMR** (400 MHz, CDCl<sub>3</sub>) δ 7.96 – 7.65 (m, 2H, CH<sub>2</sub>), 7.08 – 6.77 (m, 2H, CH<sub>2</sub>), 5.41 – 5.13 (m, 1H, Cy-CH), 3.87 (s, 3H, CH<sub>3</sub>), 3.62 (dd, *J* = 10.9, 3.4 Hz, 1H, Cy-CH), 1.95 – 0.77 (m, 20H, Cy-CH<sub>2</sub>). **<sup>13</sup>C NMR** (101 MHz, CDCl<sub>3</sub>) δ 195.10, 182.15, 164.16, 131.61, 127.38, 114.14, 77.48, 77.36, 77.16, 76.84, 60.58, 57.82, 55.69, 33.59, 29.28, 25.59, 25.36, 25.22, 24.96. **HRMS** (ESI/QTOF) *m/z*: [M + H]<sup>+</sup> Calcd for C<sub>21</sub>H<sub>30</sub>N<sub>3</sub>O<sub>3</sub><sup>+</sup> 372.2282; Found 372.2277. Crystals were grown by dissolving in warm diethyl ether (40 °C), letting cool to room temperature, followed by slow evaporation of solvent.



(*E*)-1-(3-Isopropyl-3-methyltriaz-1-en-1-yl)-2-(thiophen-2-yl)ethane-1,2-dione (**3.22**)

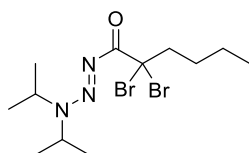
Triazene **3.22** was synthesized following procedure **A** using (*E*)-3-isopropyl-3-methyl-1-(thiophen-2-ylethynyl)triaz-1-ene (0.32 mmol). Reaction time of 60 min. Yield (brown solid): 64 mg (82%). **<sup>1</sup>H NMR** (400 MHz, CDCl<sub>3</sub>) δ 8.09 (dd, *J* = 2.9, 1.1 Hz, 1H, thiophene), 7.55 (dd, *J* = 5.1, 1.2 Hz, 1H, thiophene), 7.34 (dd, *J* = 5.1, 2.9 Hz, 1H, thiophene), 4.29 – 4.01 (m, 1H, CH(CH<sub>3</sub>)<sub>2</sub>), 3.34 (s, 3H, CH<sub>3</sub>), 1.28 (d, *J* = 6.7 Hz, 6H, CH(CH<sub>3</sub>)<sub>2</sub>). **<sup>13</sup>C NMR** (101 MHz, CDCl<sub>3</sub>) δ 188.36, 180.04, 139.30, 135.48, 126.92, 126.90, 77.48, 77.36, 77.16, 76.84, 60.43, 34.72, 20.60. **HRMS** (ESI/QTOF) *m/z*: [M + Na]<sup>+</sup> Calcd for C<sub>10</sub>H<sub>13</sub>N<sub>3</sub>NaO<sub>2</sub>S<sup>+</sup> 262.0621; Found 262.0623.

## ES.3.5 Synthesis of the α-halogenated 1-acyl triazenes **3.23–3.28**

### ES.3.5.1 General procedure

A solution of the respective triazene (1 equiv) in a mixture of acetonitrile/water (20:1, 0.35 M) was cooled to 0 °C in an ice bath. NXS (X = Br or Cl; 2 equiv) was added, and the mixture was left stirring for the indicated time and temperature. Subsequently, it was diluted with DCM and purified by flash column chromatography on deactivated silica. The final product was freeze-dried in pentane or DCM.

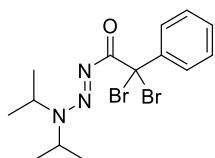
### ES.3.5.2 Scope



(*E*)-2,2-Dibromo-1-(3,3-diisopropyltriaz-1-en-1-yl)hexan-1-one (**3.23**)

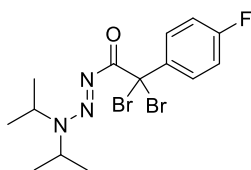
Triazene **3.23** was synthesized using (*E*)-1-(hex-1-yn-1-yl)-3,3-diisopropyltriaz-1-ene (0.72 mmol) following the general procedure. Reaction time 10 min, pentane/diethyl ether (3:1) as

eluent. Yield (yellow oil): 222 mg (80%). **<sup>1</sup>H NMR** (400 MHz, CDCl<sub>3</sub>) δ 4.97 (hept, *J* = 6.9 Hz, 1H, CH(CH<sub>3</sub>)<sub>2</sub>), 4.29 (hept, *J* = 6.7 Hz, 1H, CH(CH<sub>3</sub>)<sub>2</sub>), 2.74 – 2.59 (m, 2H, CH<sub>2</sub>), 1.75 – 1.59 (m, 2H, CH<sub>2</sub>), 1.52 – 1.34 (m, 14H, CH<sub>2</sub>, CH(CH<sub>3</sub>)<sub>2</sub>), 0.94 (t, *J* = 7.3 Hz, 3H, CH<sub>3</sub>). **<sup>13</sup>C NMR** (101 MHz, CDCl<sub>3</sub>) δ 176.11, 68.51, 54.93, 51.67, 46.91, 30.05, 22.74, 22.34, 19.02, 14.08. **HRMS** (ESI/QTOF) *m/z*: [M + H]<sup>+</sup> Calcd for C<sub>12</sub>H<sub>24</sub>Br<sub>2</sub>N<sub>3</sub>O<sup>+</sup> 384.0281; Found 384.0281.



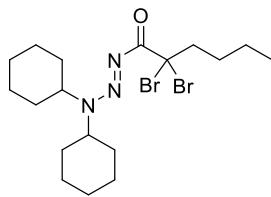
(*E*)-2,2-Dibromo-1-(3,3-diisopropyltriaz-1-en-1-yl)-2-phenylethan-1-one (**3.24**)

Triazene **3.24** was synthesized using (*E*)-3,3-diisopropyl-1-(phenylethynyl)triaz-1-ene (0.157 mmol) following the general procedure. Reaction time 20 min, gradient of pentane/diethyl ether (9:1 to 3:1). Yield (yellow oil): 46 mg (72%). **<sup>1</sup>H NMR** (400 MHz, CDCl<sub>3</sub>) δ 7.83 – 7.62 (m, 2H, CH), 7.33 (td, *J* = 7.1, 6.2, 1.3 Hz, 2H, CH), 7.29 – 7.22 (m, 1H, CH), 4.77 (hept, *J* = 6.8 Hz, 1H, CH(CH<sub>3</sub>)<sub>2</sub>), 4.20 (hept, *J* = 6.7 Hz, 1H, CH(CH<sub>3</sub>)<sub>2</sub>), 1.29 (d, *J* = 6.7 Hz, 6H, CH(CH<sub>3</sub>)<sub>2</sub>), 1.17 (d, *J* = 6.8 Hz, 6H, CH(CH<sub>3</sub>)<sub>2</sub>). **<sup>13</sup>C NMR** (101 MHz, CDCl<sub>3</sub>) δ 175.47, 142.13, 128.75, 128.14, 127.61, 77.48, 77.36, 77.16, 76.84, 67.37, 54.90, 51.49, 22.55, 18.76. **HRMS** (ESI/QTOF) *m/z*: [M + Na]<sup>+</sup> Calcd for C<sub>14</sub>H<sub>19</sub>Br<sub>2</sub>N<sub>3</sub>NaO<sup>+</sup> 425.9787; Found 425.9785.



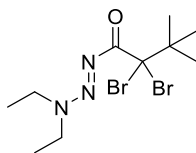
(*E*)-2,2-Dibromo-1-(3,3-diisopropyltriaz-1-en-1-yl)-2-(4-fluorophenyl)ethan-1-one (**3.25**)

Triazene **3.25** was synthesized using (*E*)-1-((4-fluorophenyl)ethynyl)-3,3-diisopropyltriaz-1-ene (0.21 mmol) following the general procedure. Reaction time of 20 min at 0 °C and then 20 min at rt, gradient of pentane/diethyl ether (7:3 to 6:4). Yield (yellow solid): 65 mg (75%). **<sup>1</sup>H NMR** (400 MHz, CDCl<sub>3</sub>) δ 7.86 – 7.64 (m, 2H, CH), 7.12 – 6.91 (m, 2H, CH), 4.77 (hept, *J* = 6.8 Hz, 1H, CH(CH<sub>3</sub>)<sub>2</sub>), 4.23 (hept, *J* = 6.7 Hz, 1H, CH(CH<sub>3</sub>)<sub>2</sub>), 1.34 (d, *J* = 6.6 Hz, 6H, CH(CH<sub>3</sub>)<sub>2</sub>), 1.21 (d, *J* = 6.8 Hz, 6H, CH(CH<sub>3</sub>)<sub>2</sub>). **<sup>13</sup>C NMR** (101 MHz, CDCl<sub>3</sub>) δ 175.34, 163.84, 161.36, 138.11, 138.08, 129.92, 129.83, 115.04, 114.82, 77.48, 77.36, 77.16, 76.84, 66.04, 55.11, 51.74, 22.60, 18.79, 1.17. **HRMS** (ESI/QTOF) *m/z*: [M + H]<sup>+</sup> Calcd for C<sub>14</sub>H<sub>19</sub>Br<sub>2</sub>FN<sub>3</sub>O<sup>+</sup> 421.9873; Found 421.9869.



(*E*)-2,2-Dibromo-1-(3,3-dicyclohexyltriaz-1-en-1-yl)hexan-1-one (**3.26**)

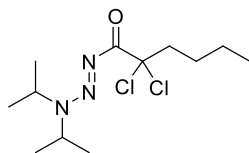
Triazene **3.26** was synthesized using (*E*)-3,3-dicyclohexyl-1-(hex-1-yn-1-yl)triaz-1-ene (0.198 mmol) following the general procedure. Reaction time of 15 min. Purification with a gradient of pentane/diethyl ether (1:0 to 19:1). There remained an impurity which was the triethylammonium salt. The product was further purified by dissolving in DCM and washing with water and brine, after which it was concentrated and freeze-dried for 5h in pentane over  $\text{CaCl}_2$ . Yield (yellow solid): 48.6 mg (53%).  **$^1\text{H}$  NMR** (400 MHz,  $\text{CDCl}_3$ )  $\delta$  4.76 (m, 1H, Cy-CH), 3.83 (m, 1H, Cy-CH), 2.80 – 2.58 (m, 2H,  $\text{CH}_2$ ), 2.15 – 1.03 (m, 24H, Cy- $\text{CH}_2$ ,  $\text{CH}_2$ ), 0.95 (t,  $J = 7.3$  Hz, 3H,  $\text{CH}_3$ ).  **$^{13}\text{C}$  NMR** (101 MHz,  $\text{CDCl}_3$ )  $\delta$  176.03, 77.48, 77.16, 76.84, 68.82, 62.64, 60.33, 47.15, 33.31, 30.08, 29.00, 25.75, 25.55, 25.07, 22.37, 14.09. **HRMS** (ESI/QTOF)  $m/z$ :  $[\text{M} + \text{H}]^+$  Calcd for  $\text{C}_{18}\text{H}_{32}\text{Br}_2\text{N}_3\text{O}^+$  464.0907; Found 464.0907.



(*E*)-2,2-Dibromo-1-(3,3-diethyltriaz-1-en-1-yl)-3,3-dimethylbutan-1-one

(**3.27**)

Triazene **3.27** was synthesized using (*E*)-1-(3,3-dimethylbut-1-yn-1-yl)-3,3-diethyltriaz-1-ene (0.33 mmol) following the general procedure. Reaction time 10 min at 0 °C and then 10 min at rt, gradient of pentane/diethyl ether (9:1 to 3:1). Yield (pale yellow solid): 41 mg (35%).  **$^1\text{H}$  NMR** (400 MHz,  $\text{CDCl}_3$ )  $\delta$  3.98 (q,  $J = 7.3$  Hz, 2H,  $\text{CH}_2\text{CH}_3$ ), 3.87 (q,  $J = 7.2$  Hz, 2H,  $\text{CH}_2\text{CH}_3$ ), 1.42 – 1.38 (m, 12H,  $\text{CH}_2\text{CH}_3$ ,  $\text{CH}_3$ ), 1.30 (t,  $J = 7.2$  Hz, 3H,  $\text{CH}_2\text{CH}_3$ ).  **$^{13}\text{C}$  NMR** (101 MHz,  $\text{CDCl}_3$ )  $\delta$  176.38, 83.43, 77.48, 77.16, 76.84, 51.71, 44.62, 43.84, 27.87, 13.98, 11.23. **HRMS** (ESI/QTOF)  $m/z$ :  $[\text{M} + \text{H}]^+$  Calcd for  $\text{C}_{10}\text{H}_{20}\text{Br}_2\text{N}_3\text{O}^+$  355.9968; Found 355.9964.

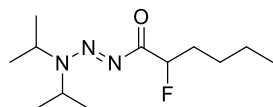


(*E*)-2,2-Dichloro-1-(3,3-diisopropyltriaz-1-en-1-yl)hexan-1-one (**3.28**)

Triazene **3.28** was synthesized using (*E*)-1-(hex-1-yn-1-yl)-3,3-diisopropyltriaz-1-ene (0.29 mmol) following the general procedure. Reaction time of 1 min, then 2 h at rt, gradient of pentane/diethyl ether (9:1 to 3:1). Yield (yellow oil): 61 mg (71%).  **$^1\text{H}$  NMR** (400 MHz,  $\text{CDCl}_3$ )  $\delta$  5.02 (hept,  $J = 6.6$  Hz, 1H,  $\text{CH}(\text{CH}_3)_2$ ), 4.29 (hept,  $J = 6.6$  Hz, 1H,  $\text{CH}(\text{CH}_3)_2$ ), 2.58 – 2.47 (m, 2H,  $\text{CH}_2$ ), 1.66 – 1.57 (m, 2H,  $\text{CH}_2$ ), 1.44 (d,  $J = 6.7$  Hz, 6H,  $\text{CH}(\text{CH}_3)_2$ ), 1.38 (d,  $J = 6.9$  Hz, 6H,  $\text{CH}(\text{CH}_3)_2$ ), 0.93

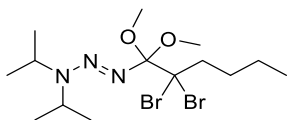
(t,  $J = 7.3$  Hz, 3H,  $\text{CH}_3$ ).  $^{13}\text{C}$  NMR (101 MHz,  $\text{CDCl}_3$ )  $\delta$  175.63, 89.29, 77.48, 77.37, 77.16, 76.84, 54.72, 51.52, 45.12, 27.55, 22.78, 22.45, 18.85, 14.03. HRMS (ESI/QTOF)  $m/z$ :  $[\text{M} + \text{H}]^+$  Calcd for  $\text{C}_{12}\text{H}_{24}\text{Cl}_2\text{N}_3\text{O}^+$  296.1291; Found 296.1294.

### ES.3.6 Synthesis of the unpublished triazenes **3.31**–**3.33**



(*E*)-1-(3,3-diisopropyltriaz-1-en-1-yl)-2-fluorohexan-1-one (**3.31**)

Triazene **3.31** was synthesized using (*E*)-1-(hex-1-yn-1-yl)-3,3-diisopropyltriaz-1-ene (0.382 mmol). In a vial, the starting material was dissolved in acetonitrile (0.26 ml) and water was added (0.034 ml, 5 equiv). The reaction mixture was cooled at  $0^\circ\text{C}$  in an ice bath and 1-chloromethyl-4-fluoro-1,4-diazoniabicyclo[2.2.2]octane bis(tetrafluoroborate) (207 mg, 0.764 mmol, 2 equiv) in acetonitrile (2.32 ml) and water (0.013 ml) was added dropwise to the reaction mixture. After 35 min, it was allowed to warm up to rt and the reaction mixture was stirred at rt for additional 4 h. It was quenched with saturated aq.  $\text{NH}_4\text{Cl}$ , and extracted with diethyl ether. Then the combined organic phases were washed with water, brine, and then dried over  $\text{MgSO}_4$ , filtered, and concentrated. The product was purified by flash column chromatography on deactivated silica starting with a gradient of pentane / diethyl ether (4:1 to 1:1). The product was freeze-dried in pentane. Yield (white solid): 22.42 mg (24%).  $^1\text{H}$  NMR (400 MHz,  $\text{CDCl}_3$ )  $\delta$  5.59 – 5.32 (m (hept + ddd), 2H), 4.21 (hept,  $J = 6.6$  Hz, 1H), 1.97 – 1.74 (m, 2H), 1.54 – 1.44 (m, 2H), 1.40 (d,  $J = 3.0$  Hz, 3H), 1.39 (d,  $J = 3.0$  Hz, 3H), 1.38 – 1.30 (m, 1H), 1.28 (d,  $J = 6.8$  Hz, 6H), 0.91 (t,  $J = 7.2$  Hz, 3H).  $^{13}\text{C}$  NMR (101 MHz,  $\text{CDCl}_3$ )  $\delta$  182.51 (d,  $^2\text{JC-F} = 18.5$  Hz), 90.63 (d,  $^1\text{JC-F} = 179.5$  Hz), 51.86, 49.29, 32.81 (d,  $^2\text{JC-F} = 21.6$  Hz), 27.22 (d,  $^3\text{JC-F} = 2.8$  Hz), 23.57, 23.43, 22.50, 19.02, 19.00, 14.03. HRMS (ESI/QTOF)  $m/z$ :  $[\text{M} + \text{Na}]^+$  Calcd for  $\text{C}_{12}\text{H}_{24}\text{FN}_3\text{NaO}^+$  268.1796; Found 268.1795.

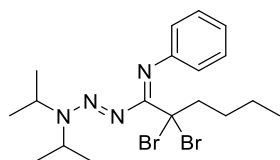


(*E*)-1-(2,2-dibromo-1,1-dimethoxyhexyl)-3,3-diisopropyltriaz-1-ene

**(3.32)**

Triazene **3.32** was synthesized using (*E*)-1-(hex-1-yn-1-yl)-3,3-diisopropyltriaz-1-ene (0.48 mmol). In a vial, the starting material was dissolved in acetonitrile (1.28 ml) and methanol (0.097 ml, 2.39 mmol, 5 equiv) was added. The reaction mixture was cooled at  $0^\circ\text{C}$  in an ice bath and freshly recrystallized *N*-bromosuccinimide (170 mg, 0.96 mmol, 2 equiv) was added and the mixture was left stirring for 20 min. The product was purified by flash column chromatography on deactivated silica with a gradient of pentane to pentane diethyl ether (98:2) as eluent. The product was freeze-dried in

pentane. Yield (yellow liquid): 144.5 mg (70%). **<sup>1</sup>H NMR** (400 MHz, CDCl<sub>3</sub>) δ 4.90 (hept, *J* = 5.7 Hz, 1H), 3.98 (hept, *J* = 13.3, 6.7 Hz, 1H), 3.52 (s, 6H), 2.37 – 2.22 (m, 2H), 1.78 (ddd, *J* = 11.4, 9.9, 6.4 Hz, 2H), 1.42 – 1.34 (m, 2H), 1.34 (d, *J* = 6.4 Hz, 6H), 1.23 (d, *J* = 6.8 Hz, 6H), 0.94 (t, *J* = 7.4 Hz, 3H). **<sup>13</sup>C NMR** (101 MHz, CDCl<sub>3</sub>) δ 108.63, 83.41, 53.63, 49.80, 46.98, 43.59, 30.03, 23.79, 22.53, 19.31, 14.21. **HRMS** (ESI/QTOF) *m/z*: [M + Na]<sup>+</sup> Calcd for C<sub>14</sub>H<sub>29</sub>Br<sub>2</sub>N<sub>3</sub>NaO<sub>2</sub><sup>+</sup> 452.0519; Found 452.0526.



(*E*)-2,2-dibromo-1-((*E*)-3,3-diisopropyltriaz-1-en-1-yl)-*N*-phenylhexan-1-imine (**3.33**)

Triazene **3.33** was synthesized using (*E*)-1-(hex-1-yn-1-yl)-3,3-diisopropyltriaz-1-ene (0.38 mmol). In a vial, the starting material was dissolved in acetonitrile (1 ml) and aniline (0.57 mmol, 1.5 equiv) was added. The reaction mixture was cooled at 0 °C in an ice bath and *N*-bromosuccinimide (136 mg, 0.76 mmol, 2 equiv) was added. After the addition, the reaction mixture was heated at 40 °C for 2.5 h. The reaction mixture was diluted in DCM and loaded on silica. It was purified by column chromatography on deactivated silica with pentane/diethyl ether (98:2) as eluent. It was freeze-dried in diethyl ether. Yield: 100 mg (57%). From NMR spectra, two isomers are present in a 12.7:1 ratio. Full characterization major isomer (presumably *E* isomer): **<sup>1</sup>H NMR** (400 MHz, CDCl<sub>3</sub>) δ 7.23 – 7.14 (m, 2H), 6.89 (tt, *J* = 7.3, 1.2 Hz, 1H), 6.80 – 6.69 (m, 2H), 4.79 (hept, *J* = 6.8 Hz, 1H), 3.80 (hept, *J* = 6.6 Hz, 1H), 2.85 – 2.78 (m, 2H), 1.87 – 1.75 (m, 2H), 1.51 – 1.41 (m, 2H), 1.31 – 1.24 (m, 2H), 1.15 (d, *J* = 6.8 Hz, 6H), 1.02 – 0.93 (m, 9H). **<sup>13</sup>C NMR** (101 MHz, CDCl<sub>3</sub>) δ 161.91, 149.77, 128.40, 122.35, 120.83, 69.83, 50.94, 48.25, 48.07, 30.17, 22.95, 22.39, 19.00, 14.22. **HRMS** (ESI/QTOF) *m/z*: [M + H]<sup>+</sup> Calcd for C<sub>18</sub>H<sub>29</sub>Br<sub>2</sub>N<sub>4</sub><sup>+</sup> 459.0753; Found 459.0751.

### ES.3.7 NMR Coalescence studies

A solution of the respective triazene in DMSO-*d*<sub>6</sub> (0.5 ml) was added to a J-Young NMR tube. NMR spectra were recorded on a 400 MHz NMR spectrometer and the sample was heated *in situ*. After increasing the temperature, the sample was allowed to stabilize for 2–3 min.

Calculations<sup>282</sup>: Equation (1) is valid if i) the dynamic process is kinetically 1<sup>st</sup> order, ii) the two singlets have equal intensity, iii) the exchanging nuclei are not coupled to each other.

$$(1) \quad k_c = \frac{\pi \Delta \nu}{\sqrt{2}} = 2.22 \Delta \nu \quad (2) \quad \Delta G_c^\ddagger = 4.58 T_c (10.32 + \log \left( \frac{T_c}{k_c} \right)) \text{ cal mol}^{-1} = 19.14 T_c (10.32 + \log \left( \frac{T_c}{k_c} \right)) J \text{ mol}^{-1}$$

### ES.3.8 Temperature stability

#### ES.3.8.1 Liquid state (NMR)

The triazenes were dissolved in a deuterated solvent in a J-Young NMR tube and the samples were heated in an oil bath unless stated otherwise. At a given time, a  $^1\text{H}$  NMR spectrum was recorded on a 400 MHz spectrometer.

#### ES.3.8.2 Thermogravimetric analysis (TGA)

The TGA measurements were performed on a TGA 4000 from Perkin Elmer. The weight of the given triazenes (2–15 mg) was followed while increasing the temperature (10 °C/min). Starting T = 30 °C.

### ES.3.9 Hydrolytic stability

The hydrolytic stability of compound **3.3** was evaluated by NMR using a 400 MHz NMR spectrometer. In a J-Young NMR tube, compound **3.3** (0.04 mmol) was dissolved in a mixture of  $d_6$ -acetone (0.1 ml) and  $\text{D}_2\text{O}$  (0.4 ml) and a drop of THF was added as internal standard. First, the reaction mixture was heated at 50 °C in a sand bath for 12 days and a conversion of 28% was observed. Subsequently, the reaction mixture was heated at 100 °C for 22 hours and a conversion of 61% was observed.

### ES.3.10 Acid sensitivity

#### ES.3.10.1 Acetic acid

The triazene (0.025 mmol) was dissolved in  $d_6$ -acetone/ $\text{D}_2\text{O}$  (0.05 M) in a J-Young NMR tube (under air), and a small amount of DCM was added as internal standard. First, a blank spectrum was recorded. Subsequently, various equivalents of acetic acid were added, and the NMR tube was heated in a sand bath at 50 °C. Spectra were recorded periodically.

#### ES.3.10.2 Trifluoroacetic acid (TFA)

The triazene (0.025 mmol) was dissolved in  $d_6$ -acetone/ $\text{D}_2\text{O}$  (0.05 M) in a J-Young NMR tube (under air), and a small amount of DCM was added as internal standard. First, a blank spectrum was recorded. Subsequently, various equivalents of TFA were added, and the NMR tube was heated at 50 °C.

### ES.3.10.3 Triflic acid (HOTf)

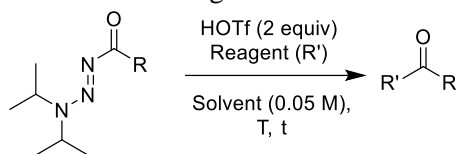
In a glove box, a stock solution of triflic acid was prepared by dissolving 87.8  $\mu\text{l}$  of HOTf in 200  $\mu\text{l}$  of  $d_3$ -acetonitrile. The triazene (0.025 mmol) was dissolved in  $d_3$ -acetonitrile/ $\text{D}_2\text{O}$  (0.05 M) in an NMR tube (under air), and a small amount of DCM was added as internal standard. First, a blank spectrum was recorded. Subsequently, 2 equiv of HOTf were added, and the time course of the reaction was followed by NMR spectroscopy.

## ES.3.11 Reactivity studies

### ES.3.11.1 Acid cleavage

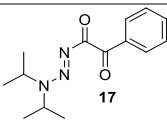
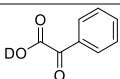
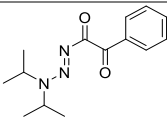
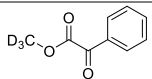
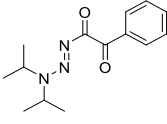
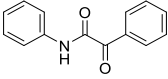
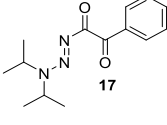
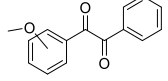
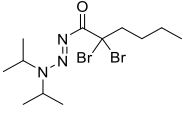
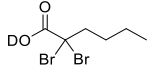
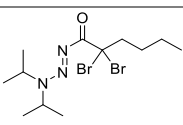
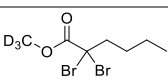
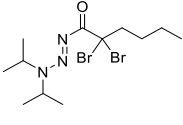
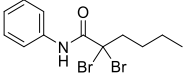
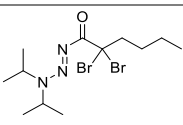
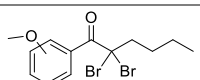
The reaction mixture was prepared in a glovebox by dissolving the corresponding triazene (0.025 mmol), hexamethylbenzene as internal standard (0.2 equiv), and the nucleophilic reagent (anisole or aniline, 2 equiv) in the corresponding deuterated solvent (0.5 ml). After recording a blank spectrum, HOTf (2 equiv) was added and the reaction mixture was kept at room temperature or heated at 70  $^{\circ}\text{C}$  and the conversion was followed by  $^1\text{H}$  NMR spectroscopy. In the case of the experiments with  $\text{D}_2\text{O}$ , the reaction mixture was set-up outside the glovebox under air atmosphere.

**Table ES 3.2** Triflic acid-induced cleavage of the triazene in the presence of nucleophiles.



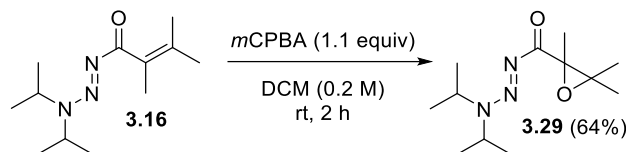
Entry	Triazene	Reagent	Solvent	T (°C)	Time	Yield (%) <sup>a</sup>	Product
1	 <b>3.1</b>	-	<i>d</i> <sub>3</sub> -acetonitrile/D <sub>2</sub> O	rt	11 min	>95 <sup>b</sup>	 <b>3.1.1</b>
2	 <b>3.1</b>	-	<i>d</i> <sub>4</sub> -methanol	rt	44 min	>95	 <b>3.1.2</b>
3	 <b>3.1</b>	Aniline (2 equiv)	<i>d</i> <sub>3</sub> -acetonitrile	70	70 min	>95	 <b>3.1.3</b>
4	 <b>3.1</b>	Anisole (2 equiv)	<i>d</i> <sub>3</sub> -acetonitrile	70	21 hours	>95	 <b>3.1.4</b> <i>para/ortho</i> = 8:1
5	 <b>3.16</b>	-	<i>d</i> <sub>3</sub> -acetonitrile/D <sub>2</sub> O	rt	21 min	>95 <sup>b</sup>	 <b>3.16.1</b>
6	 <b>3.16</b>	-	<i>d</i> <sub>4</sub> -methanol	rt	48 min	85	 <b>3.16.2</b>
7	 <b>3.16</b>	Aniline (2 equiv)	<i>d</i> <sub>3</sub> -acetonitrile	70	70 min	91	 <b>3.16.3</b>
8	 <b>3.16</b>	Anisole (2 equiv)	<i>d</i> <sub>3</sub> -acetonitrile	70	21 hours	78	 <b>3.16.4</b> <i>para/ortho</i> = 3:1

# Experimental section

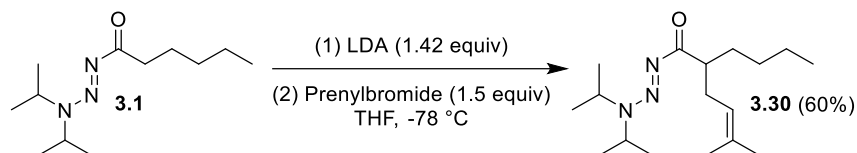
<b>9</b>	 <b>3.17</b>	-	<i>d</i> <sub>3</sub> -acetonitrile/D <sub>2</sub> O	70	60 min	>95 <sup>b</sup>	 <b>3.17.1</b>
<b>10</b>	 <b>3.17</b>	-	<i>d</i> <sub>4</sub> -methanol	rt	59 min	63	 <b>3.17.2</b>
<b>11</b>	 <b>3.17</b>	Aniline (2 equiv)	<i>d</i> <sub>3</sub> -acetonitrile	70	18 hours	85	 <b>3.17.3</b>
<b>12</b>	 <b>3.17</b>	Anisole (2 equiv)	<i>d</i> <sub>3</sub> -acetonitrile	70	20 hours	58	 <b>3.17.4</b> <i>para/ortho</i> = 17:1
<b>13</b>	 <b>3.23</b>	-	<i>d</i> <sub>3</sub> -acetonitrile/D <sub>2</sub> O	70	90 min	76 <sup>b</sup>	 <b>3.23.1</b>
<b>14</b>	 <b>3.23</b>	-	<i>d</i> <sub>4</sub> -methanol	rt	52 min	94	 <b>3.23.2</b>
<b>15</b>	 <b>3.23</b>	Aniline (2 equiv)	<i>d</i> <sub>3</sub> -acetonitrile	70	3 days	~ 64	 <b>3.23.3</b> <i>Mixture of signals and no complete cleavage of the triazene</i>
<b>16</b>	 <b>3.23</b>	Anisole (2 equiv)	<i>d</i> <sub>3</sub> -acetonitrile	70	19 hours	~ 22	 <b>3.23.4</b> <i>Complete cleavage of the triazene, but a mixture of signals</i>

<sup>a</sup> Yields and product ratios are based on the <sup>1</sup>H NMR spectra using hexamethylbenzene as internal standard. <sup>b</sup>

DCM was used as internal standard.

ES.3.11.2 Epoxidation (**3.29**)*(E)*-(3,3-Diisopropyltriaz-1-en-1-yl)(2,3,3-trimethyloxiran-2-yl)methanone (**3.29**)

(*E*)-1-(3,3-Diisopropyltriaz-1-en-1-yl)-2,3-dimethylbut-2-en-1-one **3.16** (0.670 mmol) was dissolved in DCM (3.4 ml) and 3-chloroperoxybenzoic acid (77%, 1.1 equiv) was added. The reaction mixture was stirred at rt for 2 h. It was quenched with saturated NaHCO<sub>3</sub> (aq), extracted with diethyl ether, and the combined organic phases were filtered through a Pasteur pipet packed with MgSO<sub>4</sub>. After evaporation of the solvent, the product was freeze-dried with pentane, yielding **3.29**. Yield (grey solid): 102 mg (64%). <sup>1</sup>H NMR (400 MHz, CDCl<sub>3</sub>) δ 5.50 (hept, *J* = 6.8 Hz, 1H, CH(CH<sub>3</sub>)<sub>2</sub>), 4.21 (hept, *J* = 6.6 Hz, 1H, CH(CH<sub>3</sub>)<sub>2</sub>), 1.52 (s, 3H, CH<sub>3</sub>), 1.43 (d, *J* = 6.5 Hz, 3H, CH(CH<sub>3</sub>)<sub>2</sub>), 1.40 (d, *J* = 6.6 Hz, 3H, CH(CH<sub>3</sub>)<sub>2</sub>), 1.38 (s, 3H, CH<sub>3</sub>), 1.27 (d, *J* = 5.5 Hz, 3H, CH(CH<sub>3</sub>)<sub>2</sub>), 1.26 (d, *J* = 5.5 Hz, 3H, CH(CH<sub>3</sub>)<sub>2</sub>), 1.19 (s, 3H, CH<sub>3</sub>). <sup>13</sup>C NMR (101 MHz, CDCl<sub>3</sub>) δ 184.33, 67.27, 62.04, 51.23, 49.09, 23.80, 23.55, 22.39, 19.92, 19.08, 19.06, 17.96. HRMS (APCI/QTOF) *m/z*: [M + Na]<sup>+</sup> Calcd for C<sub>12</sub>H<sub>23</sub>N<sub>3</sub>NaO<sub>2</sub><sup>+</sup> 264.1682; Found 264.1683.

ES.3.11.3 Alkylation (**3.30**)*(E)*-2-Butyl-1-(3,3-diisopropyltriaz-1-en-1-yl)-5-methylhex-4-en-1-one (**3.30**)

Water was removed from (*E*)-1-(3,3-diisopropyltriaz-1-en-1-yl)hexan-1-one **3.1** by filtering with pentane through a pipet containing MgSO<sub>4</sub>, followed by freeze-drying in pentane. LDA was prepared at −78 °C by dissolving diisopropylamine (1.42 equiv) in dry THF (3.0 ml) and adding *n*-butyllithium (2.5 M in hexanes, 1.47 equiv) dropwise. After 5 min the reaction mixture was allowed to warm up to rt for 15 min, after which it was cooled down again to −78 °C. Subsequently, (*E*)-1-(3,3-diisopropyltriaz-1-en-1-yl)hexan-1-one **3.1** (0.34 mmol) in dry THF (1.0 ml) was added dropwise and it was stirred for 20 min, followed by allowing to warm up to rt for 90 min. After cooling the reaction mixture down again to −78 °C, 1-bromo-3-methyl-2-butene (1.5 equiv) in dry THF (0.5 ml) was added dropwise and the reaction mixture was left stirring overnight while slowly warming to rt. It was quenched with 3 ml of aqueous AcOH (20%), extracted with diethyl ether (3x), and the combined organic phases were washed with sat. NaHCO<sub>3</sub> (aq), brine, and dried over MgSO<sub>4</sub>. The product was

purified by flash column chromatography on deactivated silica with pentane ether (13:7) as eluent. It was freeze-dried with pentane, yielding **3.30**. Yield (yellow oil): 62.3 mg (60%). **<sup>1</sup>H NMR** (400 MHz, CDCl<sub>3</sub>) δ 5.46 (hept, *J* = 6.8 Hz, 1H, CH(CH<sub>3</sub>)<sub>2</sub>), 5.05 (t, *J* = 7.3 Hz, 1H, CH=C), 4.14 (hept, *J* = 6.6 Hz, 1H, CH(CH<sub>3</sub>)<sub>2</sub>), 3.35 – 3.18 (m, 1H, CH), 2.38 – 2.27 + 2.24 – 2.12 (m, 2H, CH<sub>2</sub>), 1.77 – 1.66 (m, 1H, CH<sub>2</sub>), 1.63 (s, 3H, CHCH<sub>3</sub>), 1.58 (s, 3H, CHCH<sub>3</sub>), 1.53 – 1.44 (m, 1H, CH<sub>2</sub>), 1.39 (d, *J* = 6.6 Hz, 6H, CH(CH<sub>3</sub>)<sub>2</sub>), 1.30 – 1.13 (m, 10H, CH(CH<sub>3</sub>)<sub>2</sub>, CH<sub>2</sub>, CH<sub>2</sub>), 0.84 (t, *J* = 6.9 Hz, 3H, CH<sub>2</sub>CH<sub>3</sub>). **<sup>13</sup>C NMR** (101 MHz, CDCl<sub>3</sub>) δ 190.52, 132.69, 122.55, 77.48, 77.16, 76.84, 50.86, 48.37, 43.90, 32.26, 31.88, 30.04, 25.93, 23.57, 23.55, 22.93, 19.13, 17.90, 14.14. **HRMS** (ESI/QTOF) *m/z*: [M + Na]<sup>+</sup> Calcd for C<sub>17</sub>H<sub>33</sub>N<sub>3</sub>NaO<sup>+</sup> 318.2516; Found 318.2517.

### ES.3.12 X-ray crystallographic data

Crystallographic and refinement data of **3.2**, **3.11-E**, **3.16**, **3.18**, **3.20** and **3.21** are summarized in Table ES 3.3. Bragg-intensities of **3.2**, **3.11-E**, **3.16**, **3.18**, **3.20** and **3.21** were collected at 140.00(10) K using CuKα radiation. A Rigaku SuperNova dual system diffractometer with an Atlas S2 CCD detector was used for compounds **3.2**, **3.11-E**, **16**, **3.20** and **3.21**, and one equipped with an Atlas CCD detector for compound **3.18**. The datasets were reduced and corrected for absorption, with the help of a set of faces enclosing the crystals as snugly as possible, with *CrysAlis<sup>Pro</sup>*.<sup>283</sup>

The solutions and refinements of the structures were performed by the latest available version of *ShelXT*<sup>275</sup> and *ShelXL*.<sup>277</sup> All non-hydrogen atoms were refined anisotropically using full-matrix least-squares based on  $|F|^2$ . The hydrogen atoms were placed at calculated positions by means of the “riding” model where each H-atom was assigned a fixed isotropic displacement parameter with a value equal to 1.2 *U*<sub>eq</sub> of its parent C-atom (1.5 *U*<sub>eq</sub> for the methyl groups), but in the structures of **3.11-E** and **3.21**, hydrogen atom positions were found in a difference map and refined freely. Crystallographic and refinement data are summarized in Table ES 3.3. Crystallographic data have been deposited to the CCDC and correspond to the following codes: **3.2** (1921567), **3.11-E** (1921565), **3.16** (1921563), **3.18** (1921564), **3.20** (1921566) and **3.21** (1921568). Copies of the data can be obtained free of charge from the Cambridge Crystallographic Data Centre, 12 Union Road, Cambridge, CB2 1EZ, U.K. (fax, (internat.) +44-1223-336033; E-mail, deposit@ccdc.cam.ac.uk).

In the structure **3.16**, the acryloyl group is disordered over two positions found in a difference map and which were refined anisotropically imposing distance and similarity restraints (SADI and SIMU) for the least-squares refinement, yielding site occupancies of 0.631(4)/0.369(4). The structure **3.20**, is partially disordered over two positions; atoms of both orientations were located in difference Fourier map. The major and minor parts were refined anisotropically, but distance and similarity restraints (SADI and DFIX) were used for a convergent least-squares refinement, yielding site

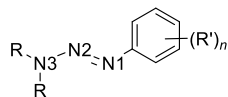
occupancies of 0.728(4)/0.272(4).

**Table ES 3.3** Crystallographic data of **3.2**, **3.11-E**, **3.16**, **3.18**, **3.20** and **3.21**.

Compound	3.2	3.11-E	3.16	3.18	3.20	3.21
Formula	C <sub>12</sub> H <sub>25</sub> N <sub>3</sub> O	C <sub>18</sub> H <sub>31</sub> N <sub>3</sub> O	C <sub>12</sub> H <sub>23</sub> N <sub>3</sub> O	C <sub>15</sub> H <sub>21</sub> N <sub>3</sub> O <sub>3</sub>	C <sub>14</sub> H <sub>23</sub> N <sub>3</sub> O <sub>2</sub>	C <sub>21</sub> H <sub>29</sub> N <sub>3</sub> O <sub>3</sub>
$D_{\text{calc.}}/\text{g cm}^{-3}$	1.038	1.101	1.049	1.202	1.174	1.230
$\mu/\text{mm}^{-1}$	0.528	0.534	0.537	0.694	0.640	0.666
Formula Weight	227.35	305.46	225.33	291.35	265.35	371.47
Colour	colourless	colourless	colourless	colourless	colourless	colourless
Shape		prism	prism	prism	prism	
Size/mm <sup>3</sup>	0.69 x 0.43 x 0.29	0.51 x 0.44 x 0.35	0.39 x 0.20 x 0.13	0.42 x 0.14 x 0.06	0.88 x 0.55 x 0.32	0.49 x 0.39 x 0.30
$T/\text{K}$	140.00(10)	139.99(10)	140.00(10)	140.00(10)	140.00(10)	140.00(10)
Crystal System	orthorhombic	monoclinic	triclinic	monoclinic	monoclinic	monoclinic
Space Group	$P2_12_12$	$P2_1/n$	$P\bar{1}$	$Cc$	$P2_1/n$	$P2_1/c$
$a/\text{\AA}$	15.30245(10)	9.37856(9)	6.5155(3)	11.0428(2)	8.56795(8)	11.05262(8)
$b/\text{\AA}$	13.74527(9)	15.21346(13)	8.3737(3)	18.4477(3)	16.30488(14)	15.28143(10)
$c/\text{\AA}$	6.91413(5)	13.21869(12)	13.7303(6)	8.36510(17)	11.35076(12)	11.88997(9)
$\alpha^\circ$	90	90	88.278(3)	90	90	90
$\beta^\circ$	90	102.3750(9)	85.778(4)	109.114(2)	108.7740(11)	93.1298(7)
$\gamma^\circ$	90	90	72.753(4)	90	90	90
$V/\text{\AA}^3$	1454.293(17)	1842.23(3)	713.46(5)	1610.14(6)	1501.33(3)	2005.22(2)
$Z$	4	4	2	4	4	4
$Z'$		1	1	1	1	
Wavelength/ $\text{\AA}$	1.54184 $\text{\AA}$	1.54184	1.54184	1.54184	1.54184	1.54184
Radiation type	CuK $\alpha$	CuK $\alpha$	CuK $\alpha$	CuK $\alpha$	CuK $\alpha$	CuK $\alpha$
$\theta_{\text{min}}^\circ$	4.324	4.492	3.228	4.794	4.929	4.006
$\theta_{\text{max}}^\circ$	76.017	76.038	75.920	76.652	76.103	75.968
Measured Refl.	13777	17450	4747	15104	13290	18963
Independent Refl.	3034	3834	2882	3332	3122	4163
Reflections with $I > 2(I)$	3011	3666	2548	3258	3019	4163
$R_{\text{int}}$	0.0150	0.0197	0.0083	0.0247	0.0262	0.0226
Parameters	154	324	219	196	196	361
Restraints	0	0	197	2	11	0
Largest Peak/e $\text{\AA}^{-3}$	0.179	0.242	0.211	0.151	0.345	0.328
Deepest Hole/e $\text{\AA}^{-3}$	-0.105	-0.158	-0.157	-0.121	-0.200	-0.184
GooF	1.084	1.049	1.054	1.033	1.073	1.076
$wR_2$ (all data)	0.0748	0.1000	0.1215	0.0718	0.0999	0.1084
$wR_2$	0.0747	0.0987	0.1173	0.0711	0.0988	0.1078
$R_I$ (all data)	0.0272	0.0377	0.0470	0.0271	0.0392	0.0429
$R_I$	0.0271	0.0362	0.0424	0.0265	0.0381	0.0420
CCDC code	1921567	1921565	1921563	1921564	1921566	1921568

## ES.3.12.1 CCDC database analysis

To compare the bond lengths of the 1-acyl triazenes (Table ES 3.4) with aryl triazenes, a CCDC database search was performed. For the search, the program ConQuest (v2.0.1, CCDC 2019) was used with a CCDC database (CSD version 5.40 (November 2018) + 1 update).



The query that was searched:

With the following additional requirements: R = any atom except H, R' = one or multiple substituents (*n*), Filter = only organics and must not contain:

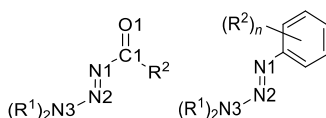


The resulting **122 hits** were analysed and taken out of the data set if:

- (1) The triazene is cyclic.
- (2) It contains any other atom than H, C, N, O, F, Cl, Br, S.
- (3) The amount of connected N atoms > 3.
- (4) R is another atom than C, or if R is C–O.
- (5) No coordinates are available in the database.

The resulting **67 hits** were analysed with Mercury (v3.10, CCDC 2001-2017) and the bond lengths were measured.

**Table ES 3.4** Selected bond lengths of **3.2**, **3.11-E**, **3.16**, **3.18**, **3.20** and **3.21**.



Compound	N3–N2 (Å)	N2–N1 (Å)	N1–C1 (Å)	C1–O1 (Å)
<b>3.2</b>	1.2955(14)	1.2927(13)	1.4049(14)	1.2228(15)
<b>3.11-E</b>	1.2963(11)	1.2896(11)	1.4178(12)	1.2172(12)
<b>3.16</b>	1.2911(13)	1.2987(13)	1.386(7)	1.220(5)
<b>3.18</b>	1.2859(18)	1.3058(18)	1.390(2)	1.2187(19)
<b>3.20</b>	1.2892(11)	1.3040(11)	1.3918(12)	1.2154(12)
<b>3.21</b>	1.2901(13)	1.3075(13)	1.3812(14)	1.2151(15)
<b>Aryl triazene</b>	1.328 <sup>b</sup>	1.274 <sup>b</sup>	-	-

<sup>b</sup> Average bond lengths calculated from 67 structures from the CCDC database.

## ES.3.13 Biological assays

A selection of 15 compounds was submitted for a cytotoxicity assay. The screening was performed by the Biomolecular Screening Facility at the EPFL. The cytotoxicity values were determined with the Alamar Blue (resazurin) fluorescent dye measurement (for details, see Experimental section).<sup>279</sup> Dose-response curves were recorded for 6 cell lines: Hela (Human cervix adenocarcinoma), A2780 (human ovarian carcinoma), MDA-MB-231 (human breast adenocarcinoma), MCF7 (human breast adenocarcinoma (metastases from pleural effusion)), MCF-10A (human epithelial breast), HEK293T (human embryonic kidney).

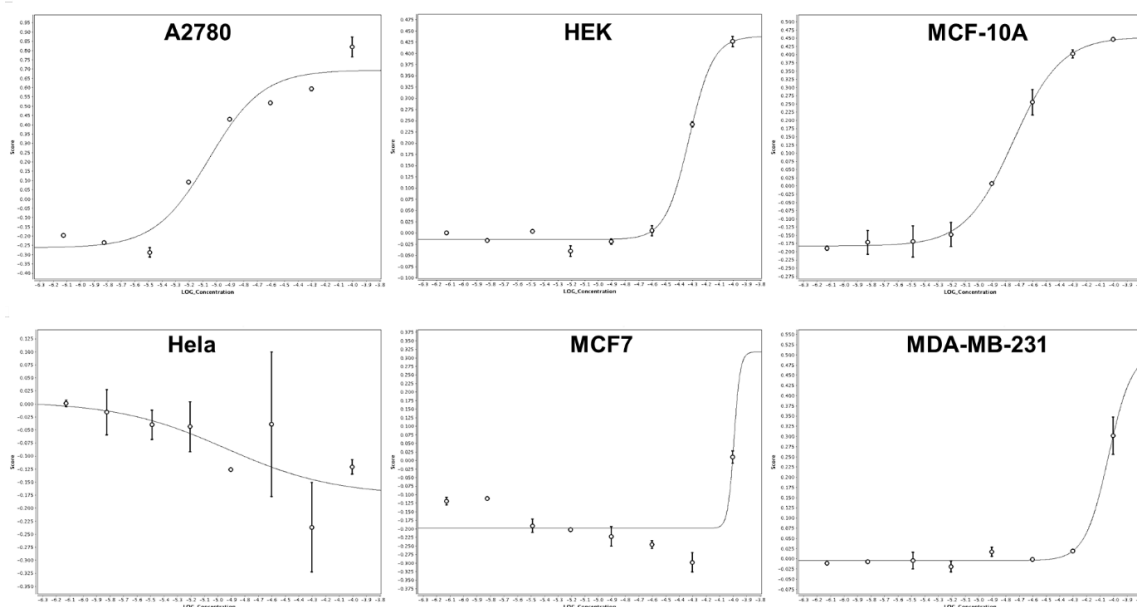
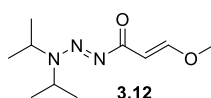


**Figure ES 3.1** Dose-response curves for 6 cell lines for **3.12**. Score vs. Log Concentration.

## Experimental section

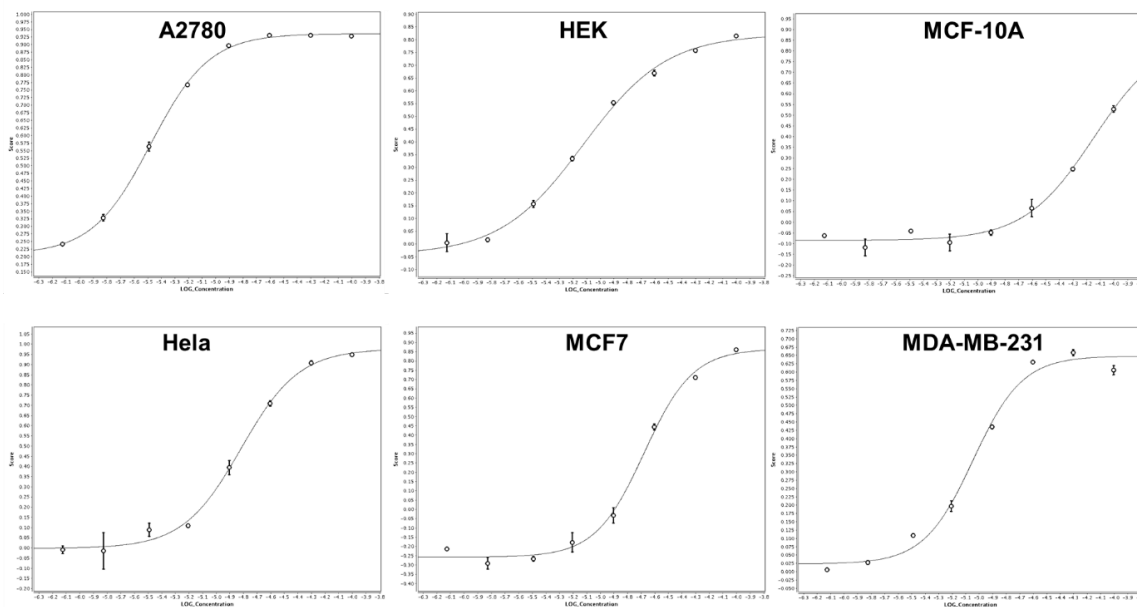
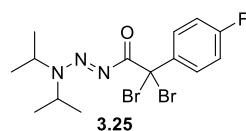


**Figure ES 3.2** Dose-response curves for 6 cell lines for **3.25**. Score vs. Log Concentration.

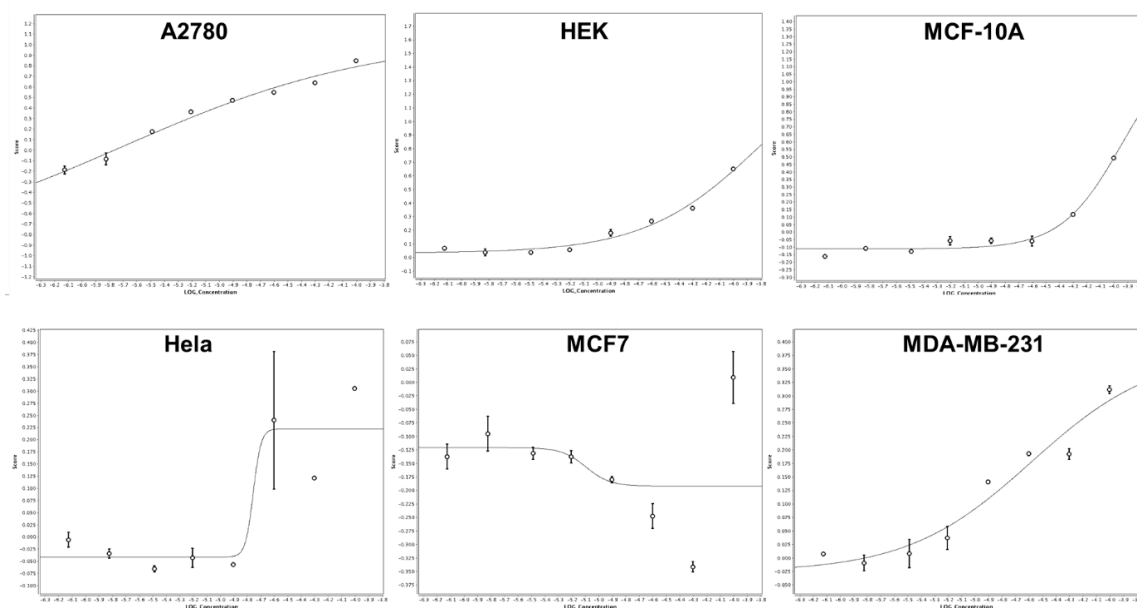
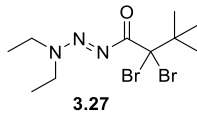


**Figure ES 3.3** Dose-response curves for 6 cell lines for **3.27**. Score vs. Log Concentration.

## Experimental section

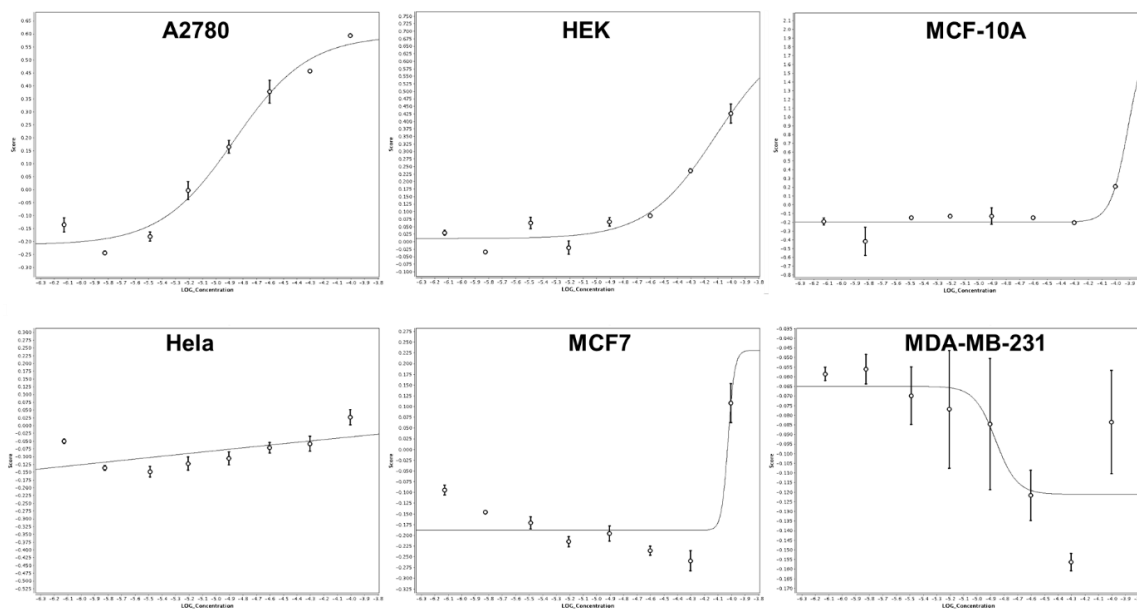
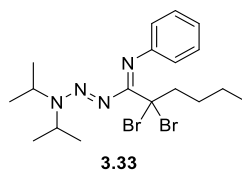


**Figure ES 3.4** Dose-response curves for 6 cell lines for **3.33**. Score vs. Log Concentration.

## ES.3.14 Selected NMR Spectra

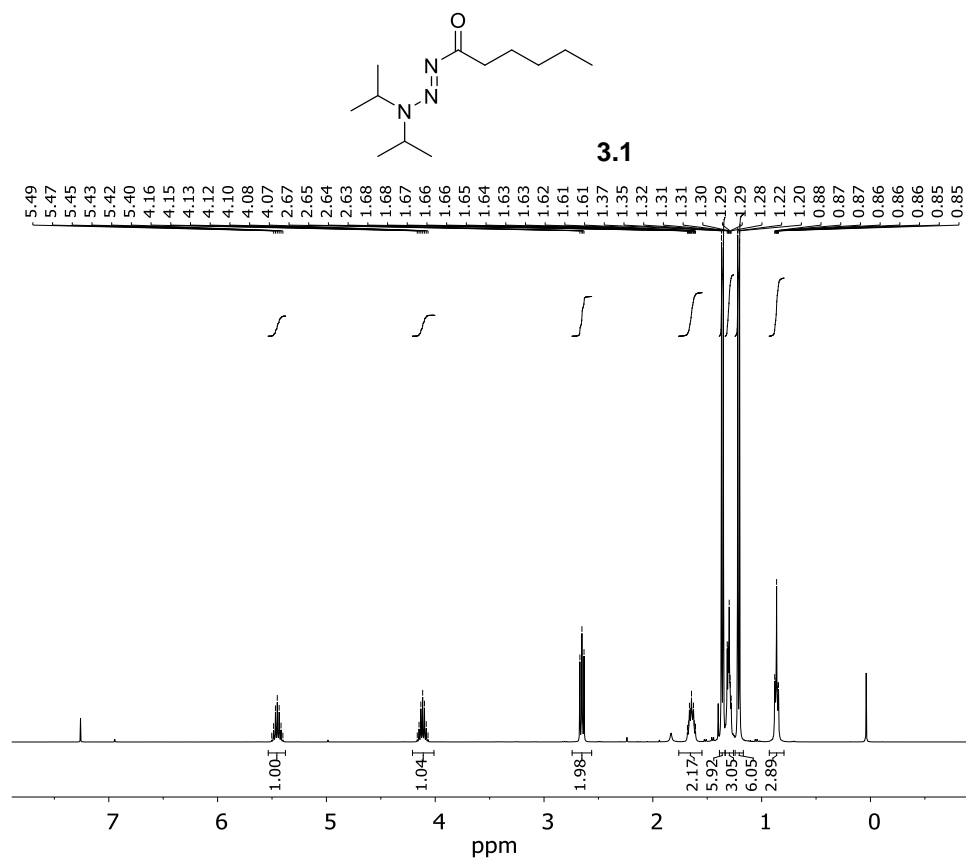


**Figure ES 3.5**  $^1\text{H}$  NMR spectrum of **3.1** (400 MHz,  $\text{CDCl}_3$ ).

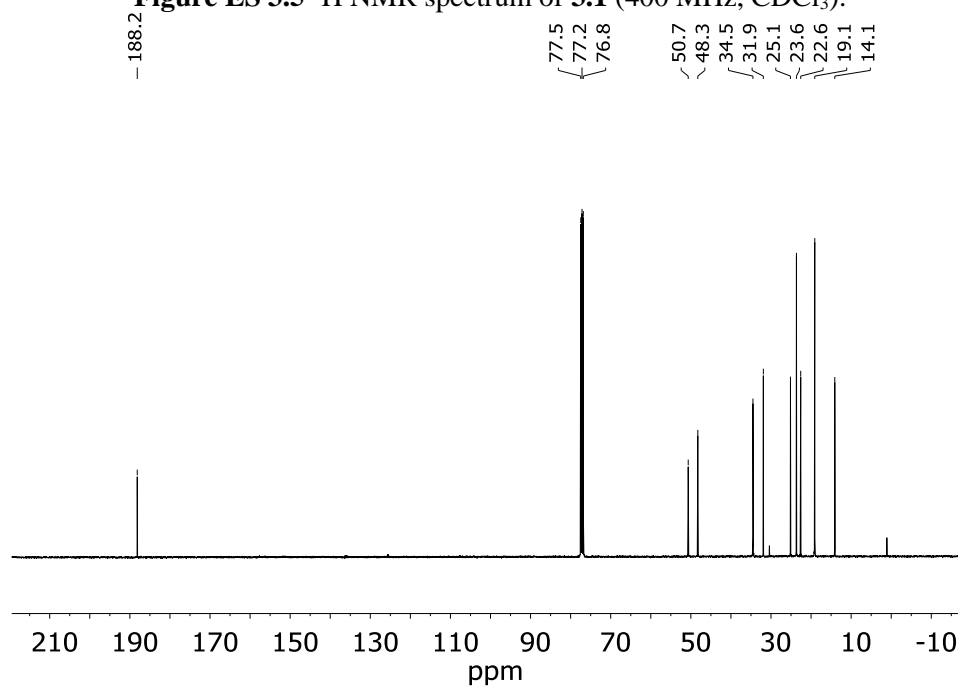


**Figure ES 3.6**  $^{13}\text{C}$  NMR spectrum of **3.1** (101 MHz,  $\text{CDCl}_3$ ).

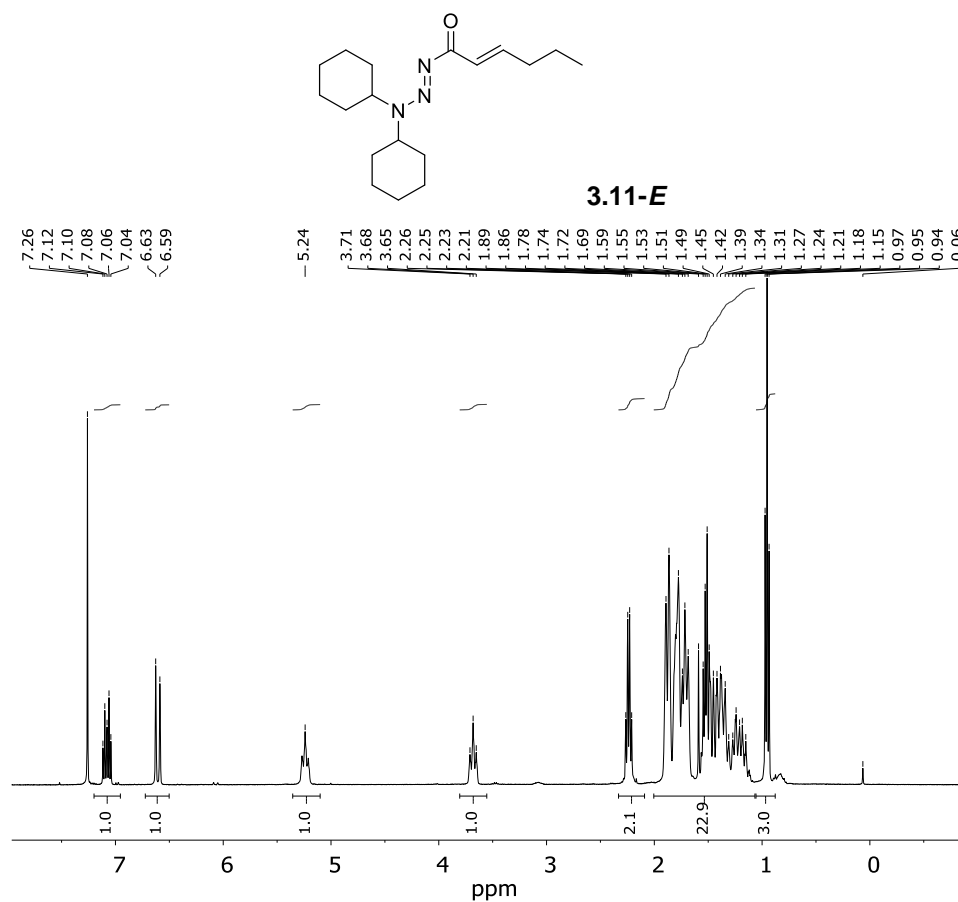


**Figure ES 3.7** <sup>1</sup>H NMR spectrum of **3.11-E** (400 MHz, CDCl<sub>3</sub>).

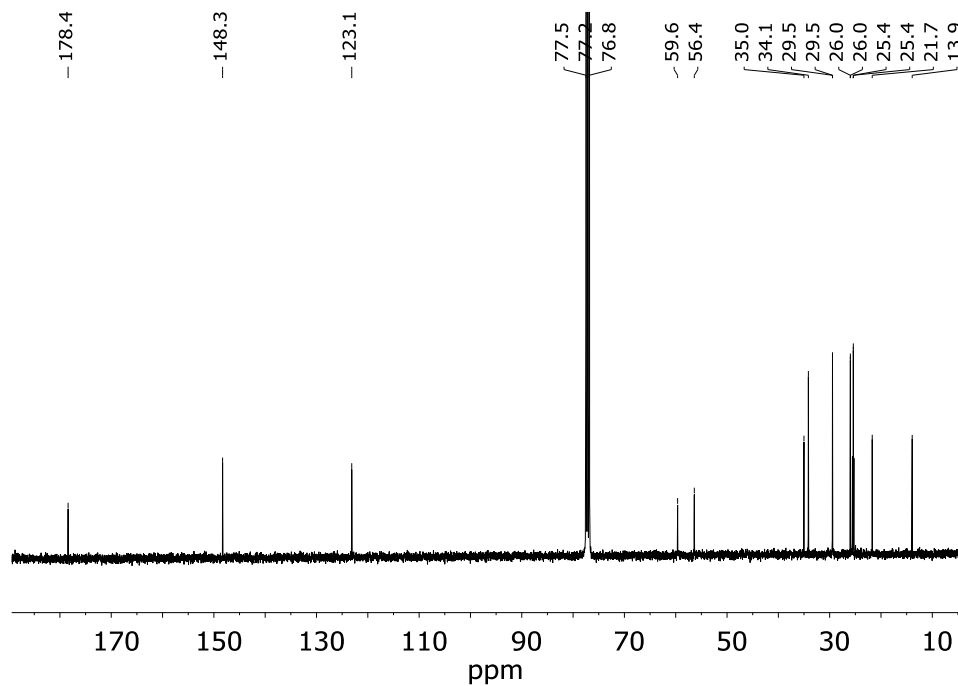


**Figure ES 3.8** <sup>13</sup>C NMR spectrum of **3.11-E** (101 MHz, CDCl<sub>3</sub>).

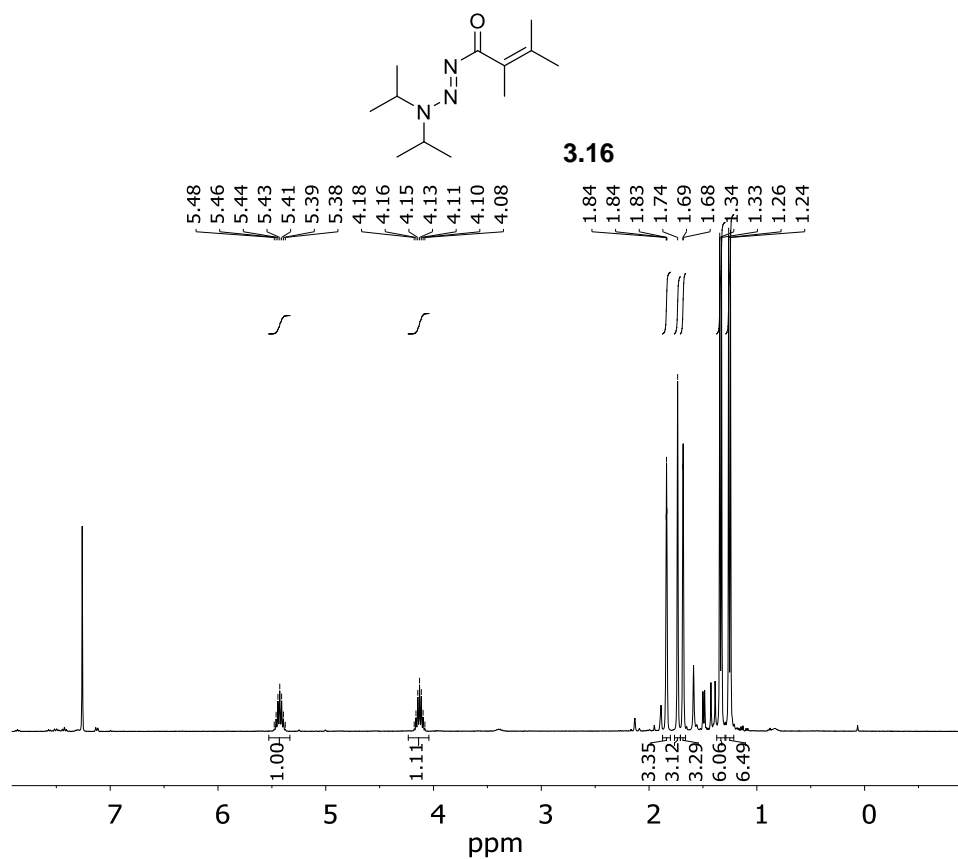


**Figure ES 3.9** <sup>1</sup>H NMR spectrum of **3.16** (400 MHz, CDCl<sub>3</sub>).

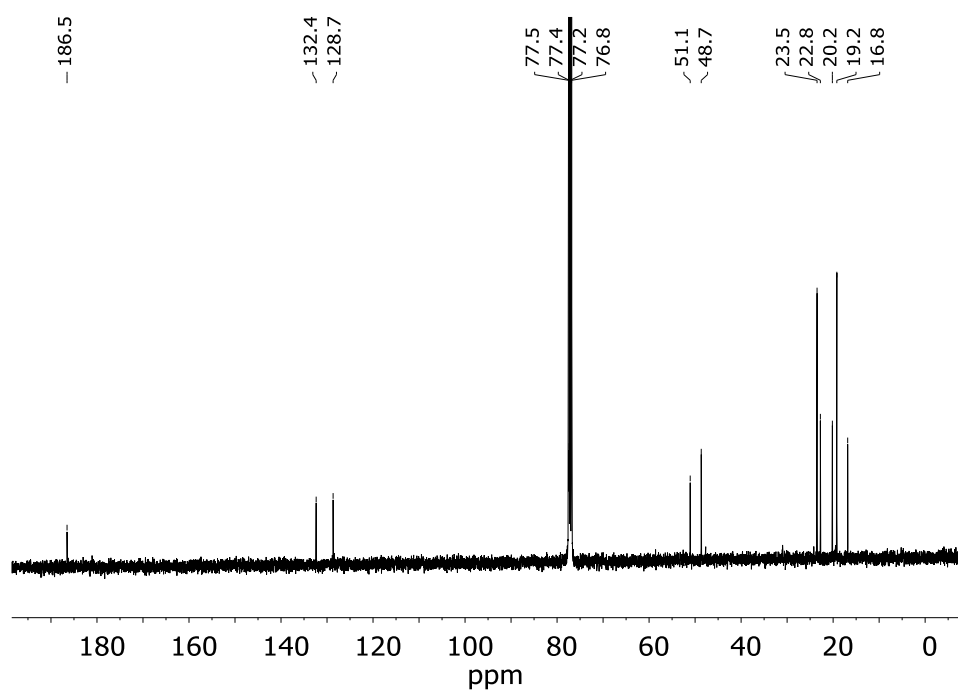


**Figure ES 3.10** <sup>13</sup>C NMR spectrum of **3.16** (101 MHz, CDCl<sub>3</sub>).

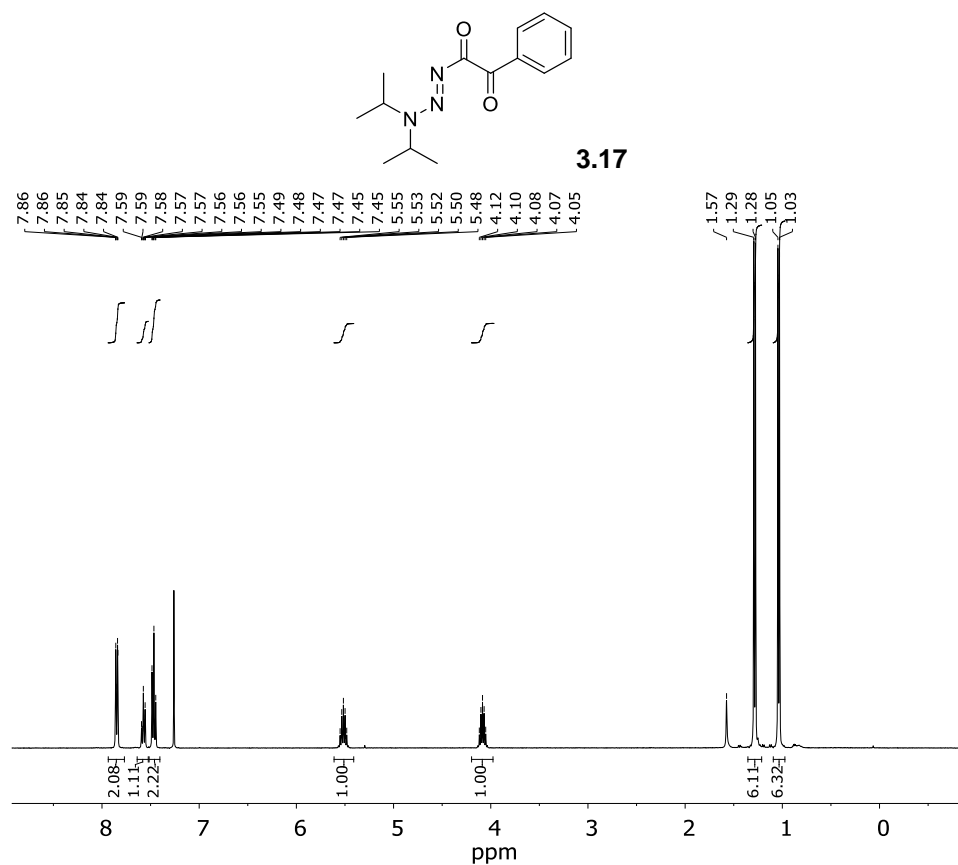


**Figure ES 3.11**  $^1\text{H}$  NMR spectrum of **3.17** (400 MHz,  $\text{CDCl}_3$ ).

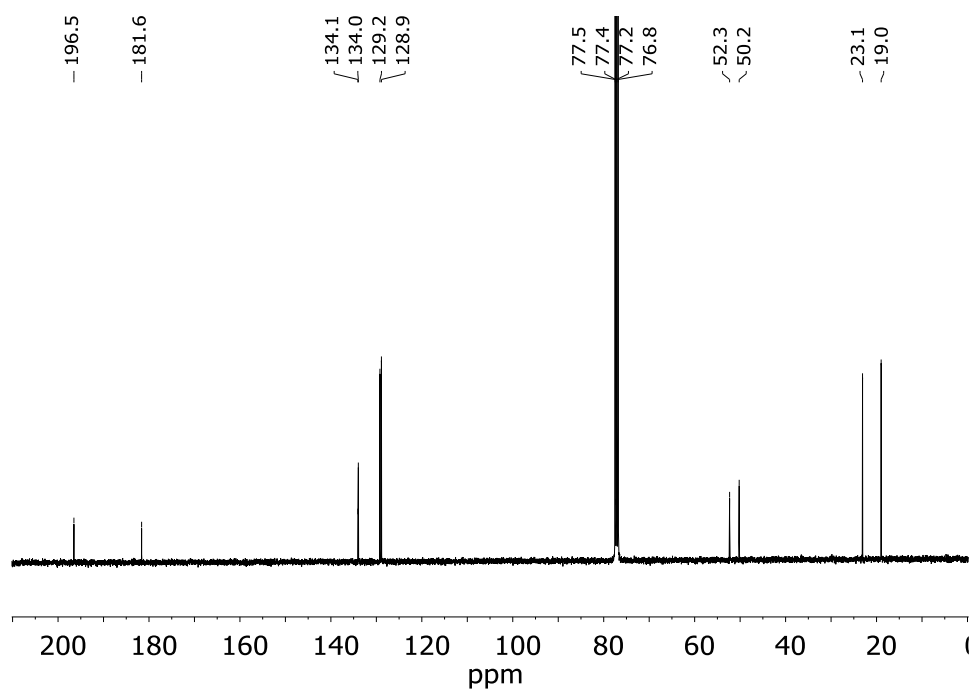


**Figure ES 3.12**  $^{13}\text{C}$  NMR spectrum of **3.17** (101 MHz,  $\text{CDCl}_3$ ).

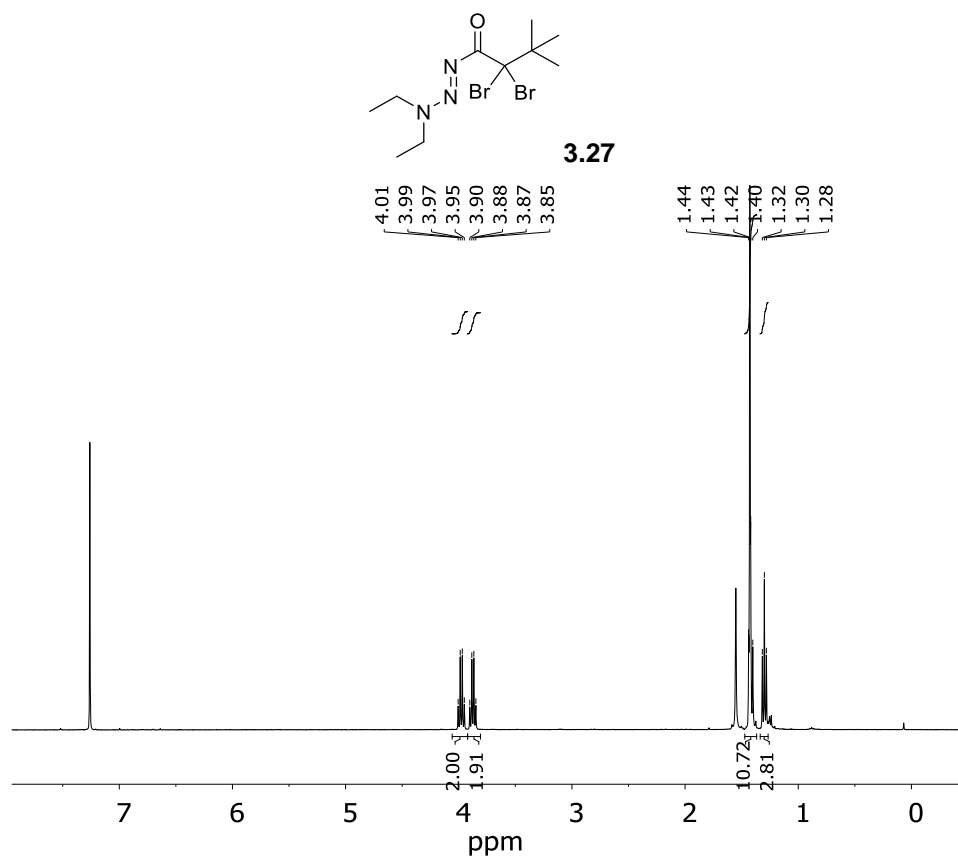


**Figure ES 3.13** <sup>1</sup>H NMR spectrum of **3.27** (400 MHz, CDCl<sub>3</sub>).

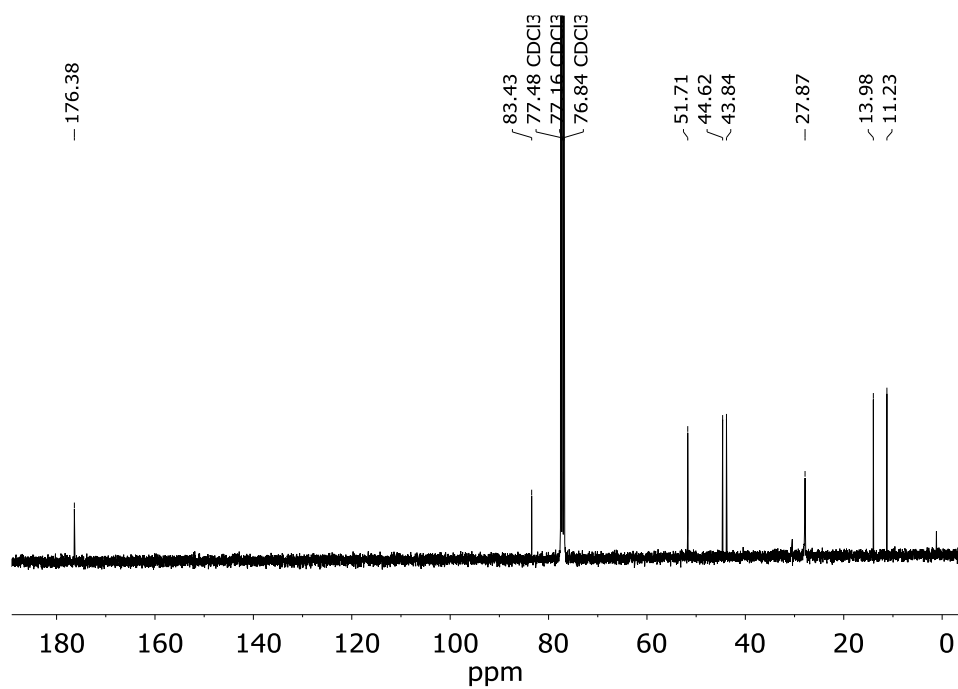
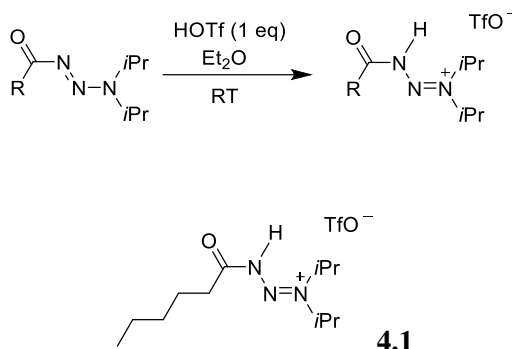


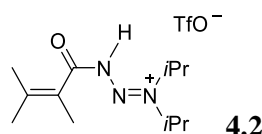
**Figure ES 3.14** <sup>13</sup>C NMR spectrum of **3.27** (101 MHz, CDCl<sub>3</sub>).

## ES.4 Experimental section: triazene adducts

### ES.4.1 Synthesis of the protonated 1-acyl triazenes **4.1–4.3**

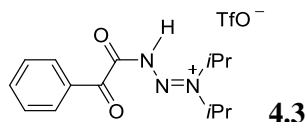


In the glovebox, triazene **3.1** (68.4 mg, 0.30 mmol) was dissolved in diethyl ether (0.6 ml) and it was cooled to  $-40\text{ }^{\circ}\text{C}$ . HOTf (26.7  $\mu\text{l}$ , 1 equiv) was added and the reaction mixture was cooled to  $-40\text{ }^{\circ}\text{C}$ . The precipitate was isolated by vacuum filtration, rinsed with a small amount of diethyl ether, and dried under vacuum. Yield (white solid): 79.0 mg (70%). The product was stored in the glovebox at  $-40\text{ }^{\circ}\text{C}$ .  **$^1\text{H}$  NMR** (600 MHz,  $\text{CD}_3\text{CN}$ )  $\delta$  11.82 (s, 1H, NH), 4.76 (hept,  $J = 6.5\text{ Hz}$ , 1H,  $\text{CH}(\text{CH}_3)_2$ ), 4.64 (hept,  $J = 6.5\text{ Hz}$ , 1H,  $\text{CH}(\text{CH}_3)_2$ ), 2.80 (t,  $J = 7.4\text{ Hz}$ , 2H,  $\text{CH}_2$ ), 1.77–1.63 (m, 2H,  $\text{CH}_2$ ), 1.46 (dd,  $J = 7.4, 6.5\text{ Hz}$ , 12H,  $\text{CH}(\text{CH}_3)_2$ ), 1.37 (ddd,  $J = 7.3, 4.4, 3.1\text{ Hz}$ , 4H,  $\text{CH}_2$ ), 0.99–0.84 (m, 3H,  $\text{CH}_3$ ).  **$^{13}\text{C}$  NMR** (151 MHz,  $\text{CD}_3\text{CN}$ )  $\delta$  173.96, 59.93, 59.70, 34.42, 31.69, 24.03, 23.25, 23.03, 18.44, 14.17. **IR** ( $\nu_{\text{max}}$ ,  $\text{cm}^{-1}$ ): 1765 (m, C=O stretch), 1545 (m, N-H bend). **HRMS** (ESI/QTOF)  $m/z$ :  $[\text{M} + \text{H}]^+$  Calcd for  $\text{C}_{12}\text{H}_{26}\text{N}_3\text{O}^+$  228.2070; Found 228.2066.  $[\text{M} + \text{K}]^+$  Calcd for  $\text{C}_{12}\text{H}_{25}\text{KN}_3\text{O}^+$  266.1629; Found 266.1624.



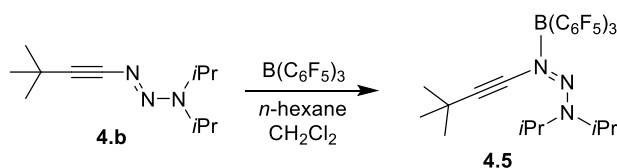
In the glovebox, triazene **3.16** (36.7 mg, 0.16 mmol) was dissolved in diethyl ether (1.6 ml). HOTf (14.0  $\mu\text{l}$ , 1 equiv) was added and a white precipitate formed immediately. The precipitate was isolated by vacuum filtration, rinsed with a small amount of diethyl ether, and dried under vacuum. Yield (white solid): 49.5 mg (81%). The product was stored in the glovebox at  $-40\text{ }^{\circ}\text{C}$ .  **$^1\text{H}$  NMR** (600 MHz,  $\text{CD}_3\text{CN}$ )  $\delta$  11.68 (s, 1H, NH), 4.75 (hept,  $J = 6.5\text{ Hz}$ , 1H,  $\text{CH}(\text{CH}_3)_2$ ), 4.68 (hept,  $J = 6.6\text{ Hz}$ , 1H,  $\text{CH}(\text{CH}_3)_2$ ), 1.88 (s, 3H,  $\text{CH}_3$ ), 1.85–1.81 (s, 3H,  $\text{CH}_3$ ), 1.78 (s, 3H,  $\text{CH}_3$ ), 1.48 (d,  $J = 6.5\text{ Hz}$ , 6H,  $\text{CH}(\text{CH}_3)_2$ ), 1.40 (d,  $J = 6.5\text{ Hz}$ , 6H,  $\text{CH}(\text{CH}_3)_2$ ).  **$^{13}\text{C}$  NMR** (151 MHz,  $\text{CD}_3\text{CN}$ )  $\delta$  171.13, 142.27, 122.89, 59.92, 59.82, 23.18, 22.64, 19.05, 18.47, 15.93. **IR** ( $\nu_{\text{max}}$ ,  $\text{cm}^{-1}$ ): 1743 (m, C=O stretch), 1553

(m, N-H bend). **HRMS** (ESI/QTOF)  $m/z$ :  $[M + H]^+$  Calcd for  $C_{12}H_{24}N_3O^+$  226.1914; Found 226.1911.  $[M + K]^+$  Calcd for  $C_{12}H_{23}KN_3O^+$  264.1473; Found 264.1470. *Single crystals were obtained by layering a solution of 3.16 in THF with THF and then a solution of HOTf in THF (~1 equiv). The mixture was kept at  $-40\text{ }^\circ\text{C}$  in the glovebox.*



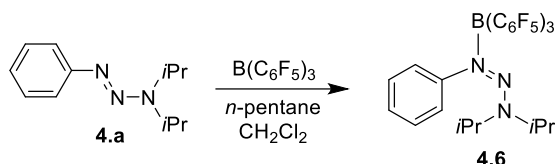
In the glovebox, triazene **3.17** (19.1 mg, 0.073 mmol) was dispersed in diethyl ether (1.5 ml), it did not dissolve completely. HOTf (6.4  $\mu\text{l}$ , 1 equiv) was added and a white precipitate formed immediately. The precipitate was isolated by vacuum filtration, rinsed with small amount of diethyl ether and dried under vacuum. Yield (white solid): 27.3 mg (91%). The product was stored in the glovebox at  $-40\text{ }^\circ\text{C}$ .  **$^1\text{H}$  NMR** (600 MHz,  $\text{CD}_3\text{CN}$ )  $\delta$  8.17–7.88 (m, 2H, Ph), 7.88–7.72 (m, 1H, Ph), 7.63 (t,  $J = 7.9\text{ Hz}$ , 2H, Ph), 6.98 (s, 1H, NH), 4.86 (hept,  $J = 6.6\text{ Hz}$ , 1H,  $\text{CH}(\text{CH}_3)_2$ ), 4.65 (hept,  $J = 6.5\text{ Hz}$ , 1H,  $\text{CH}(\text{CH}_3)_2$ ), 1.46 (d,  $J = 6.6\text{ Hz}$ , 6H,  $\text{CH}(\text{CH}_3)_2$ ), 1.13 (d,  $J = 6.5\text{ Hz}$ , 6H,  $\text{CH}(\text{CH}_3)_2$ ).  **$^{13}\text{C}$  NMR** (151 MHz,  $\text{CD}_3\text{CN}$ )  $\delta$  136.81, 132.98, 130.58, 130.44, 59.66, 23.03, 18.56 (C=O signals were not detected). **IR** ( $\nu_{\text{max}}$ ,  $\text{cm}^{-1}$ ) 1763 (m, C=O stretch), 1679 (m, C=O stretch), 1579 (m, N-H bend). **HRMS** (ESI/QTOF)  $m/z$ :  $[M + H]^+$  Calcd for  $C_{14}H_{20}N_3O_2^+$  262.1550; Found 262.1546.  $[M + K]^+$  Calcd for  $C_{14}H_{19}KN_3O_2^+$  300.1109; Found 300.1104. *Single crystals were obtained by layering a solution of 3.17 in diethyl ether with diethyl ether and then a solution of HOTf in diethyl ether (~1 equiv). The mixture was kept at  $-40\text{ }^\circ\text{C}$  in the glovebox.*

#### ES.4.2 Synthesis of the $\text{B}(\text{C}_6\text{F}_5)_3$ adducts **4.5** and **4.6**

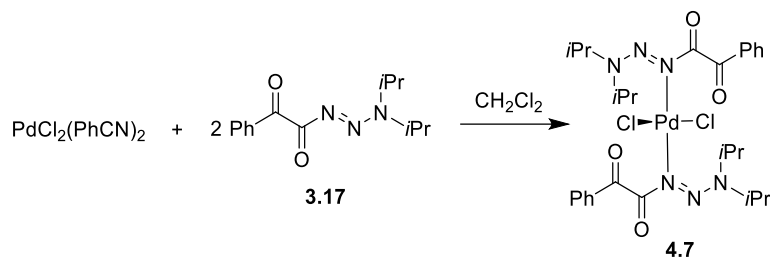


In the glovebox, triazene **4.b** (98.4 mg, 0.47 mmol) was dissolved in hexane (5 ml) and  $\text{B}(\text{C}_6\text{F}_5)_3$  (241.0 mg, 0.47 mmol) was dissolved in DCM (1 ml) and hexane (1 ml). The solutions were combined and the mixture was immediately placed in a freezer ( $-40\text{ }^\circ\text{C}$ ). After 12 h, the resulting precipitate was collected by decanting the liquid, washed with hexane (3 x 3 ml), and dried under vacuum. Yield (pale yellow solid): 295.0 mg (87 %). The product was stored in the glovebox at  $-40\text{ }^\circ\text{C}$ .  **$^1\text{H}$  NMR** (400 MHz,  $\text{CD}_2\text{Cl}_2$ )  $\delta$  6.62 (hept,  $J = 6.6\text{ Hz}$ , 1H,  $\text{CH}(\text{CH}_3)_2$ ), 4.16 (hept,  $J = 6.6\text{ Hz}$ , 1H,  $\text{CH}(\text{CH}_3)_2$ ), 1.42 (d,  $J = 6.6\text{ Hz}$ , 6H,  $\text{CH}(\text{CH}_3)_2$ ), 1.16 (d,  $J = 6.5\text{ Hz}$ , 6H,  $\text{CH}(\text{CH}_3)_2$ ), 1.05 (s, 9H,  $\text{CH}_3$ ).  **$^{13}\text{C}$  NMR** (151 MHz,

CD<sub>2</sub>Cl<sub>2</sub>)  $\delta$  148.55 (dm, *o*-CF,  $^1J(^{13}\text{C}-^{19}\text{F}) = 242$  Hz), 139.96 (dm, *p*-CF,  $^1J(^{13}\text{C}-^{19}\text{F}) = 248$  Hz), 137.28 (dm, *m*-CF,  $^1J(^{13}\text{C}-^{19}\text{F}) = 257$  Hz), 118.99 (ipso, C), 95.47 (alkyne), 74.95 (alkyne), 56.04 (CH(CH<sub>3</sub>)<sub>2</sub>), 54.86 (CH(CH<sub>3</sub>)<sub>2</sub>), 29.78 (*t*Bu), 28.33 (*t*Bu), 23.23 (CH(CH<sub>3</sub>)<sub>2</sub>), 21.12 (CH(CH<sub>3</sub>)<sub>2</sub>). **<sup>11</sup>B NMR** (128 MHz, CD<sub>2</sub>Cl<sub>2</sub>)  $\delta$  -3.46. **<sup>19</sup>F NMR** (376 MHz, CD<sub>2</sub>Cl<sub>2</sub>)  $\delta$  -132.61, -159.46, -165.85. **HRMS** (APPI/QTOF) *m/z*: [M]<sup>-</sup> Calcd for C<sub>30</sub>H<sub>23</sub>BF<sub>15</sub>N<sub>3</sub><sup>-</sup> 721.1751; Found 721.1725.



In the glovebox, triazene **4.a** (30.8 mg, 0.15 mmol) was dissolved in pentane (0.5 ml) and B(C<sub>6</sub>F<sub>5</sub>)<sub>3</sub> (72.0 mg, 0.14 mmol) was dissolved in DCM (0.5 ml) and pentane (1 ml). The solutions were combined and the mixture was immediately placed in a freezer (-40 °C). After 12 h, the resulting precipitate was collected by filtration and washed with pentane. The filtrate was kept at -40 °C for another 12 h, resulting in the formation of more precipitate, which was isolated by filtration and combined with the first fraction. Yield (pale pink solid): 47.0 mg (47 %). The product was stored in the glovebox at -40 °C. **<sup>1</sup>H NMR** (400 MHz, CD<sub>2</sub>Cl<sub>2</sub>)  $\delta$  7.26 (dd, *J* = 5.4, 2.0 Hz, 3H, Ph), 7.15–7.02 (m, 2H, Ph), 4.36 (p, *J* = 6.6 Hz, 1H, CH(CH<sub>3</sub>)<sub>2</sub>), 4.09 (p, *J* = 6.5 Hz, 1H, CH(CH<sub>3</sub>)<sub>2</sub>), 1.23 (d, *J* = 6.5 Hz, 6H, CH(CH<sub>3</sub>)<sub>2</sub>), 1.03 (d, *J* = 6.6 Hz, 6H, CH(CH<sub>3</sub>)<sub>2</sub>). **<sup>13</sup>C NMR** (151 MHz, CD<sub>2</sub>Cl<sub>2</sub>)  $\delta$  148.35 (dm, *o*-CF,  $^1J(^{13}\text{C}-^{19}\text{F}) = 244$  Hz), 145.73 (Ph), 139.87 (dm, *p*-CF,  $^1J(^{13}\text{C}-^{19}\text{F}) = 245$  Hz), 137.13 (dm, *m*-CF,  $^1J(^{13}\text{C}-^{19}\text{F}) = 250$  Hz), 129.92 (Ph), 129.57 (Ph), 123.70 (Ph), 120.53 (ipso, C), 57.44 (CH(CH<sub>3</sub>)<sub>2</sub>), 54.55 (CH(CH<sub>3</sub>)<sub>2</sub>), 23.13 (CH(CH<sub>3</sub>)<sub>2</sub>), 19.10 (CH(CH<sub>3</sub>)<sub>2</sub>). **<sup>11</sup>B NMR** (128 MHz, CD<sub>2</sub>Cl<sub>2</sub>)  $\delta$  -3.95. **<sup>19</sup>F NMR** (376 MHz, CD<sub>2</sub>Cl<sub>2</sub>)  $\delta$  -131.85, -159.39, -165.78. **HRMS** (APPI/QTOF) *m/z*: [M]<sup>-</sup> Calcd for C<sub>30</sub>H<sub>19</sub>BF<sub>15</sub>N<sub>3</sub><sup>-</sup> 717.1438; Found 717.1415. *Single crystals were obtained by mixing triazene 4.7 and B(C<sub>6</sub>F<sub>5</sub>)<sub>3</sub> in pentane and a small amount of DCM to dissolve. The mixture was kept at -40 °C in the glovebox.*

ES.4.3 Synthesis of the Pd complex **4.7**

$\text{PdCl}_2(\text{PhCN})_2$  (76.3 mg, 0.2 mmol) was dissolved in DCM, to which a solution of triazene **3.17** (104.0 mg, 0.4 mmol) in DCM was added (5 ml total volume). It was stirred overnight, forming a yellow precipitate, which was filtered and washed with a small amount of dichloromethane and pentane. The yellow solid was dried under vacuum, after which it was taken out of the glovebox for analysis. Yield (yellow solid): 103 mg (74%).  **$^1\text{H}$  NMR** (600 MHz,  $\text{CD}_2\text{Cl}_2$ )  $\delta$  10.16 (hept,  $J = 6.6$  Hz, 1H,  $\text{CH}(\text{CH}_3)_2$ ), 8.00 – 7.91 (m, 2H, Ph), 7.63 (ddt,  $J = 8.7, 7.2, 1.3$  Hz, 1H, Ph), 7.55 – 7.47 (m, 2H, Ph), 4.35 (hept,  $J = 6.4$  Hz, 1H,  $\text{CH}(\text{CH}_3)_2$ ), 1.73 (d,  $J = 6.6$  Hz, 6H,  $\text{CH}(\text{CH}_3)_2$ ), 0.88 (d,  $J = 6.5$  Hz, 6H,  $\text{CH}(\text{CH}_3)_2$ ).  **$^{13}\text{C}$  NMR** (151 MHz,  $\text{CD}_2\text{Cl}_2$ )  $\delta$  192.46, 177.70, 135.15, 133.17, 129.71, 129.52, 55.98, 55.76, 54.20, 54.02, 53.84, 53.66, 53.48, 22.86, 19.97. **HRMS** (ESI/QTOF)  $m/z$ :  $[\text{M} + \text{Na}]^+$  Calcd for  $\text{C}_{28}\text{H}_{38}\text{Cl}_2\text{N}_6\text{NaO}_4\text{Pd}^+$  721.1259; Found 721.1257. **Anal.** Calcd for  $\text{Pd} \cdot \text{Cl} \cdot \text{Cl} \cdot \text{C}_{14}\text{H}_{19}\text{N}_3\text{O}_2 \cdot \text{C}_{14}\text{H}_{19}\text{N}_3\text{O}_2$ : C, 48.05; H, 5.47; N, 12.01. Found: C, 48.18; H, 5.33; N, 11.48.

## ES.4.4 IR Spectroscopic data

The IR spectra for compounds **3.16**, **4.2**, **3.17**, **4.3** and **4.7** were recorded. The C=O stretching (\*) shifts from below 1700 to above 1700  $\text{cm}^{-1}$ . In addition, for the protonated triazenes the N—H bend (x) is visible around 1540 – 1580  $\text{cm}^{-1}$ .

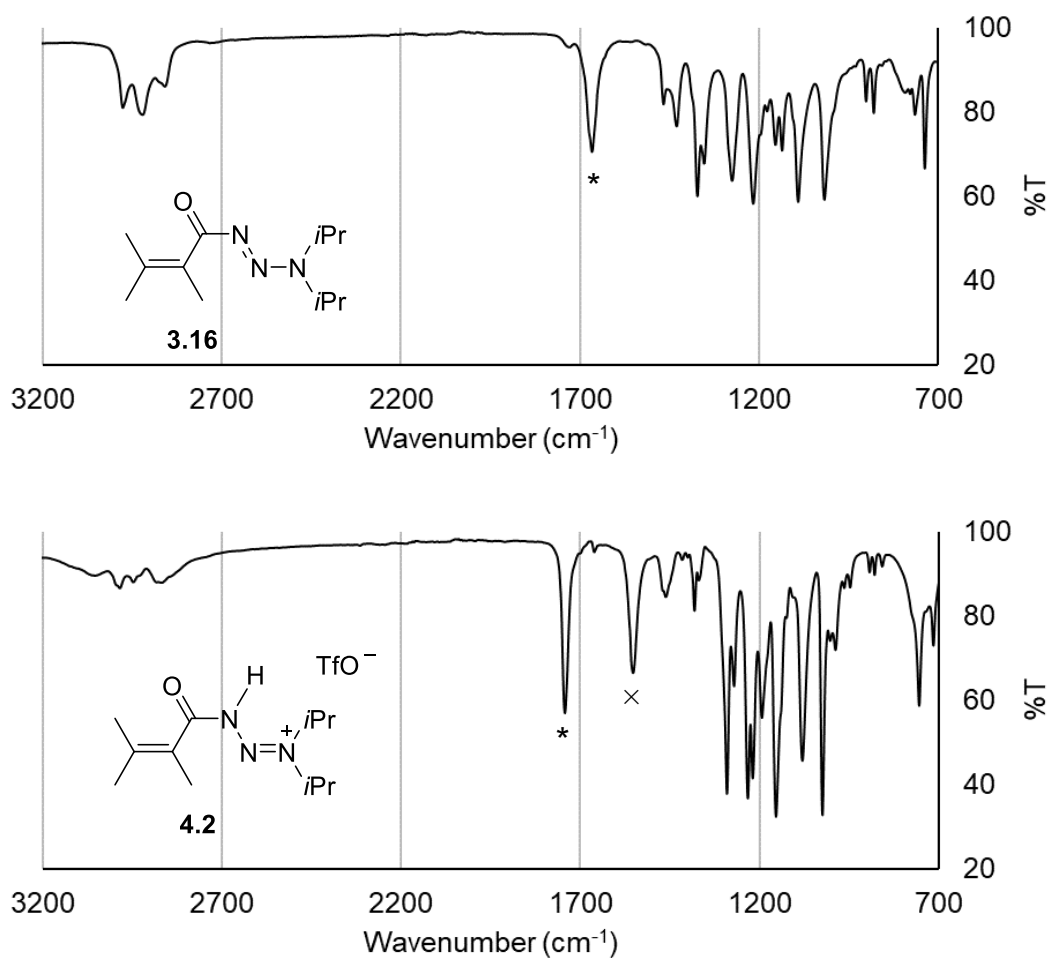


**Figure ES 4.1** IR spectra of **3.16** and **4.2**.

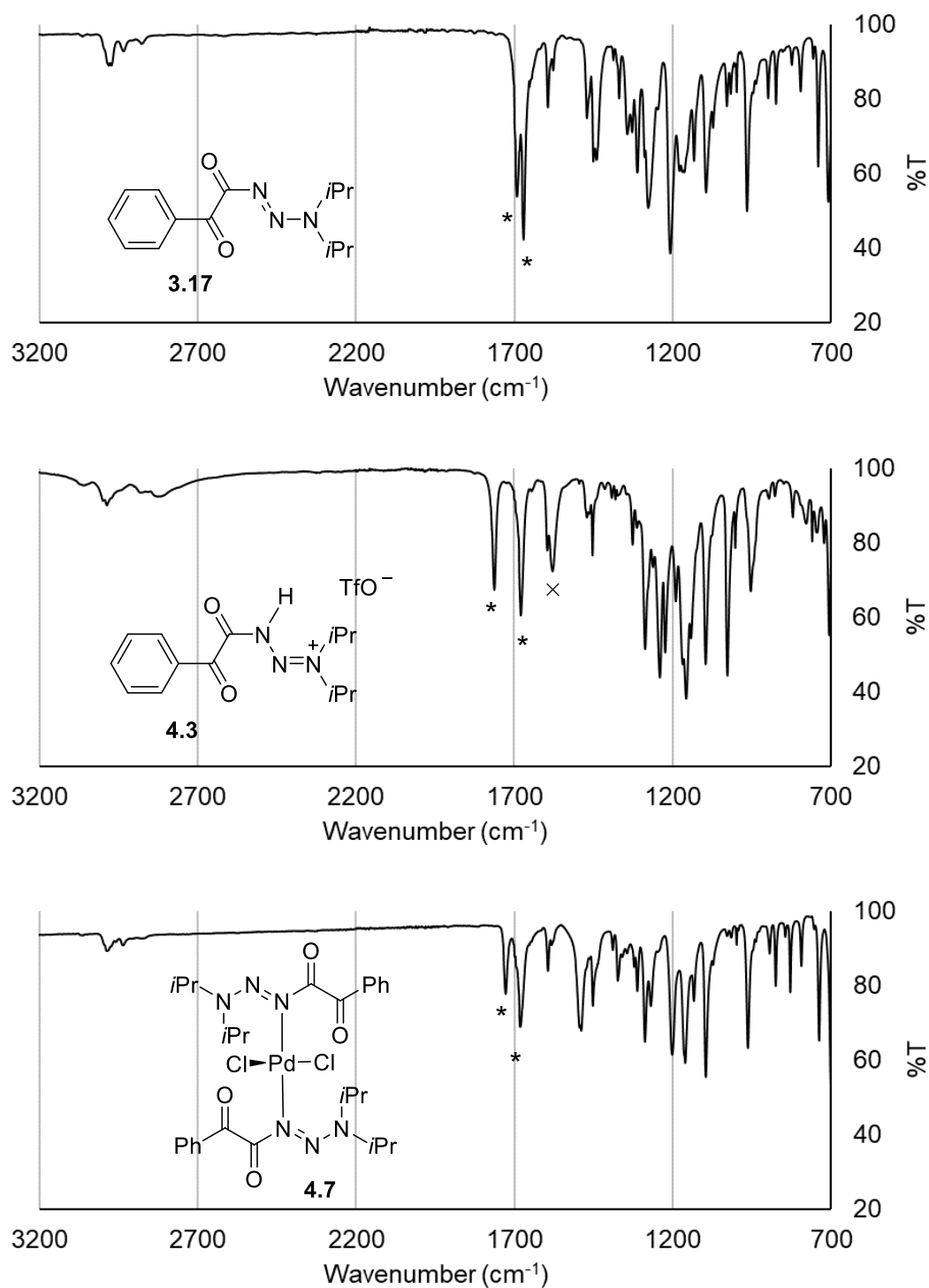


Figure ES 4.2 IR spectra of **3.17**, **4.3**, and **4.7**.

## ES.4.5 X-ray crystallographic data

Crystallographic and refinement data are summarized in Table ES 4.1.

Bragg-intensities of **4.2**, **4.3**, **4.4**, **4.6** and **4.7** were collected at low temperature using CuK $\alpha$  radiation. A Rigaku SuperNova dual system diffractometer with an Atlas CCD detector was used for compounds **4.3**, **4.4**, **4.6** and **4.7**, and one equipped with an Atlas S2 CCD detector for compound **4.2**. The datasets were reduced and corrected for absorption, with the help of a set of faces enclosing the crystals as snugly as possible, with *CrysAlis<sup>Pro</sup>*.<sup>284</sup>

The solutions and refinements of the structures were performed by the latest available version of *ShelXT*<sup>275</sup> and *ShelXL*.<sup>277</sup> All non-hydrogen atoms were refined anisotropically using full-matrix leastsquares based on  $|F|^2$ . The hydrogen atoms were placed at calculated positions by means of the “riding” model where each H-atom was assigned a fixed isotropic displacement parameter with a value equal to 1.2  $U_{eq}$  of its parent C-atom (1.5  $U_{eq}$  for the methyl groups), but in the structures **4.2**, **4.3** and **4.4** the hydrogen atom bound to nitrogen (N1) was found in a difference map and refined freely.

Crystallographic data have been deposited with the Cambridge Crystallographic Data Centre and correspond to the following codes: **4.2** (1966936), **4.3** (1966937), **4.4** (1966935), **4.6** (1966938), and **4.7** (1966939). These data can be obtained free of charge via [www.ccdc.cam.ac.uk/data\\_request/cif](http://www.ccdc.cam.ac.uk/data_request/cif), or by emailing [data\\_request@ccdc.cam.ac.uk](mailto:data_request@ccdc.cam.ac.uk), or by contacting The Cambridge Crystallographic Data Centre, 12 Union Road, Cambridge CB2 1EZ, UK; fax: +44 1223 336033.

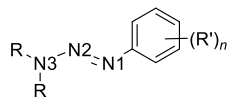
In the structure **4.6**, one of the isopropyl groups is disordered over two orientations each, found in a difference map. These were anisotropically refined imposing distance and similarity restraints (SADI and SIMU) for the least-squares refinement which yielded site occupancies of 0.706(17)/0.294(17).

**Table ES 4.1** Crystallographic and refinement data.

Compound	4.2	4.3	4.4	4.6	4.7
Formula	C <sub>13</sub> H <sub>24</sub> F <sub>3</sub> N <sub>3</sub> O <sub>4</sub> S	C <sub>15</sub> H <sub>20</sub> F <sub>3</sub> N <sub>3</sub> O <sub>5</sub> S	C <sub>13</sub> H <sub>20</sub> F <sub>3</sub> N <sub>3</sub> O <sub>3</sub> S	C <sub>30</sub> H <sub>19</sub> BF <sub>15</sub> N <sub>3</sub>	C <sub>28</sub> H <sub>38</sub> Cl <sub>2</sub> N <sub>6</sub> O <sub>4</sub> Pd
$D_{\text{calc.}}/\text{g cm}^{-3}$	1.338	1.408	1.362	1.595	1.459
$\mu/\text{mm}^{-1}$	2.013	2.033	2.095	1.439	6.588
Formula Weight	375.41	411.40	355.38	717.29	699.94
Colour	clear colourless	clear colourless	clear colourless	clear colourless	clear intense orange
Shape	prism	needle	prism	irregular	prism
Size/mm <sup>3</sup>	0.66×0.44×0.37	0.27×0.08×0.04	0.21×0.11×0.07	0.31×0.14×0.13	0.55×0.12×0.08
$T/\text{K}$	139.98(11)	140.00(10)	150.01(10)	140.00(10)	150.01(10)
Crystal System	monoclinic	triclinic	monoclinic	orthorhombic	triclinic
Space Group	$P2_1/n$	$P\bar{1}$	$P2_1/n$	$Pbca$	$P\bar{1}$
$a/\text{\AA}$	11.05100(19)	8.8991(5)	8.0352(3)	18.9040(6)	8.1628(4)
$b/\text{\AA}$	10.81512(18)	10.8721(10)	25.0842(6)	16.3612(6)	8.4628(4)
$c/\text{\AA}$	15.9625(3)	11.4526(9)	8.6190(3)	19.3108(5)	12.1951(6)
$\alpha/^\circ$	90	117.321(9)	90	90	98.576(4)
$\beta/^\circ$	102.2766(16)	91.458(6)	94.100(3)	90	106.738(4)
$\gamma/^\circ$	90	97.837(6)	90	90	90.520(4)
$V/\text{\AA}^3$	1864.18(5)	970.37(15)	1732.76(10)	5972.7(3)	796.52(7)
$Z$	4	2	4	8	1
$Z'$	1	1	1	1	0.5
Wavelength/ $\text{\AA}$	1.54184	1.54184	1.54184	1.54184	1.54184
Radiation type	CuK $\alpha$	CuK $\alpha$	CuK $\alpha$	CuK $\alpha$	CuK $\alpha$
$\theta_{\text{min}}/^\circ$	4.457	4.367	5.439	4.244	3.833
$\theta_{\text{max}}/^\circ$	76.004	73.411	76.837	72.428	76.558
Measured Refl.	16719	6582	16441	15890	6988
Independent Refl.	3844	3768	3623	5770	3299
Reflections with $I > 2(I)$	3730	2904	2746	4910	3206
$R_{\text{int}}$	0.0312	0.0340	0.0526	0.0355	0.0285
Parameters	231	252	216	468	191
Restraints	0	0	0	43	0
Largest Peak/e $\text{\AA}^{-3}$	0.416	0.351	0.331	0.646	1.208
Deepest Hole/e $\text{\AA}^{-3}$	-0.358	-0.405	-0.397	-0.291	-0.518
GooF	1.068	1.033	1.046	1.056	1.061
$wR_2$ (all data)	0.1265	0.1230	0.1240	0.1510	0.0937
$wR_2$	0.1256	0.1093	0.1104	0.1445	0.0926
$R_1$ (all data)	0.0490	0.0627	0.0637	0.0643	0.0365
$R_1$	0.0478	0.0449	0.0440	0.0554	0.0354
CCDC code	1966936	1966937	1966935	1966938	1966939

### ES.4.5.1 CCDC database analysis

To compare the bond lengths of the protonated triazenes with aryl triazenes, a CCDC database search was performed. For the search, the program ConQuest (v2.0.1, CCDC 2019) was used with a CCDC database (CSD version 5.40 (November 2018) + 2 updates).



The query that was searched:

With the following additional requirements: R = any atom except H, R' = one or multiple substituents

(n), Filter = only organics and must not contain:

The resulting **122 hits** were analysed and taken out of the data set if:

- (1) The triazene is cyclic.
- (2) It contains any other atom than H, C, N, O, F, Cl, Br, S.
- (3) The amount of connected N atoms > 3.
- (4) R is another atom than C, or if R is C–O.
- (5) No coordinates are available in the database.
- (6) R > 9 atoms (excl. H).
- (7) (R')<sub>n</sub> > 21 atoms (excl. H).

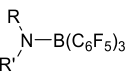
The resulting **30 hits** were analysed with Mercury (v3.10, CCDC 2001-2017) and the bond lengths were measured.

*30 Structures from the CCDC database:*

BOCYUO, BOCZAV, BOCZEZ, BOCZID, CMPDZB, DEHFUT, EMUDEX, FUZLUI, HAHQOZ, HOBXAY, IPUDEE, IPUDII, JANXAA, JANXEE, JANXII, JOLNED, JOWTOE, KUJXOC, LOXWOM, MIJDEP, MTZPCX, OFUBUO, OPAVUX, PIGRUT, PIGSAA, RUJQIX, UDINEC, VUYGEB, YUMWIO, ZIKQOZ.

*Average bond lengths:* N1-N2 = 1.276 Å; N2-N3 = 1.325 Å

To compare the bond lengths of the B–N dative bonds with B(C<sub>6</sub>F<sub>5</sub>)<sub>3</sub>, a CCDC database search was performed. For the search, the program ConQuest (v2.0.1, CCDC 2019) was used with a CCDC database (CSD version 5.40 (November 2018) + 2 updates).

The query that was searched: 

The resulting 184 hits were analysed and taken out of the data set if:

- (1) R, R' contains any other atom than C, H, N, (O).
- (2) The B–N adduct is charged.
- (3) No coordinates available.

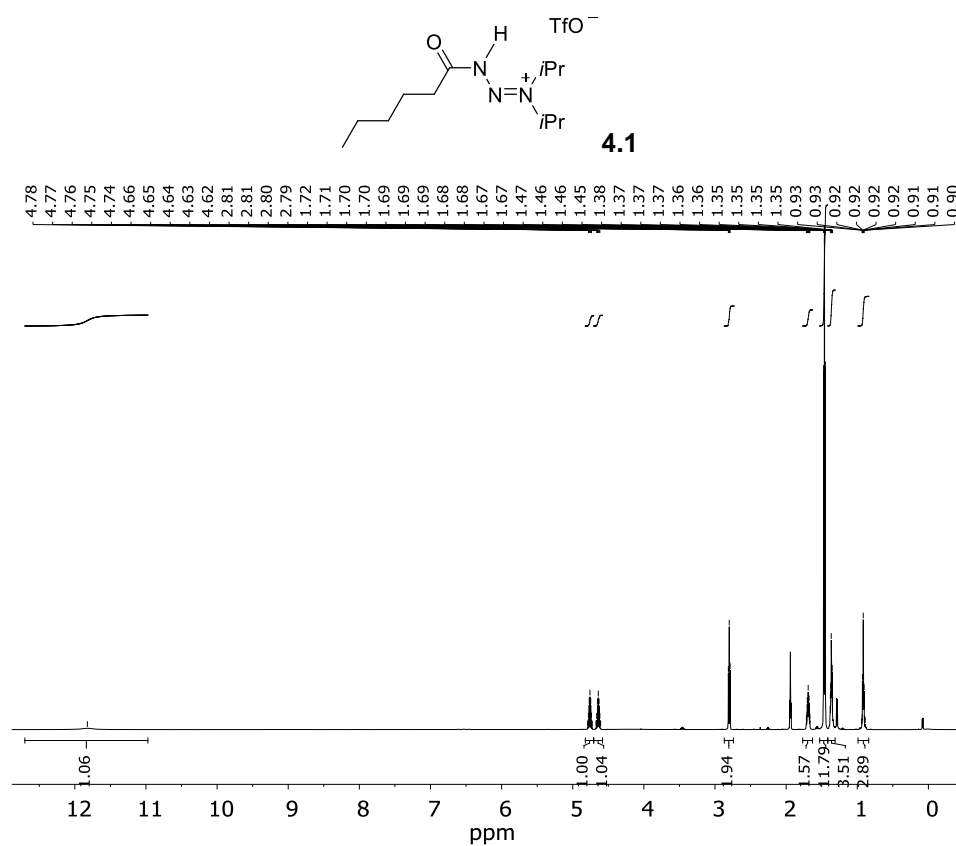
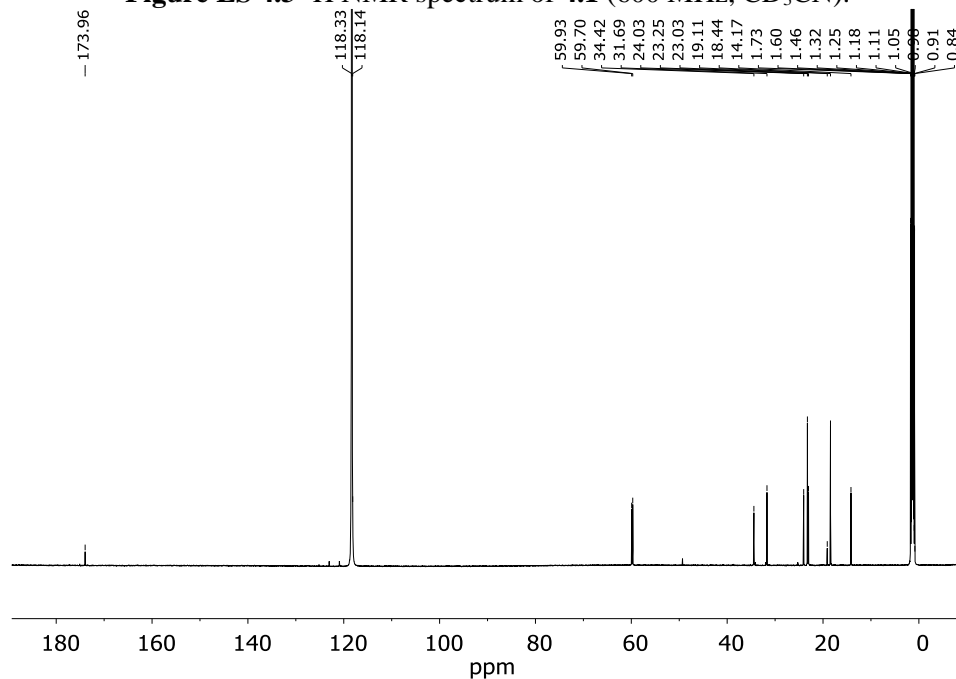
The resulting **46** hits were analysed with Mercury (v3.10, CCDC 2001-2017) and the bond lengths were measured.

*46 Structures from the CCDC database:*

AGASAF, BAZRIE, BUNXEO, DERGOZ, DERGUF, EKUBOB, EKUBUH, FEYHIB, GABQUW, GABRAD, HAFFAX, IFUFIA, IJOHAQ, IJOHEU, IJOHIY, IPAPIA, IPAPOG, JEGKUC, KECRUG, MIVLOS, MIVLUY, MIVMAF, MIVMEJ, MIVMIN, MOJVOX, NOWJEQ, OGACUX, PIKDAQ, PIKFAS, QEYSAO, RASQEI, RASQIM, RASQOS, RASQUY, RASRAF, SELTIO, TURPOM, UKITUF, WAWCEE, WAWCII, XERWIC, XERWOI, XUCCIH, YALTAJ, YALTOX, ZILXEA.

*Average bond length:* B–N = 1.626 Å

## ES.4.6 NMR Spectra

Figure ES 4.3  $^1\text{H}$  NMR spectrum of **4.1** (600 MHz,  $\text{CD}_3\text{CN}$ ).Figure ES 4.4  $^{13}\text{C}$  NMR spectrum of **4.1** (101 MHz,  $\text{CD}_3\text{CN}$ ).

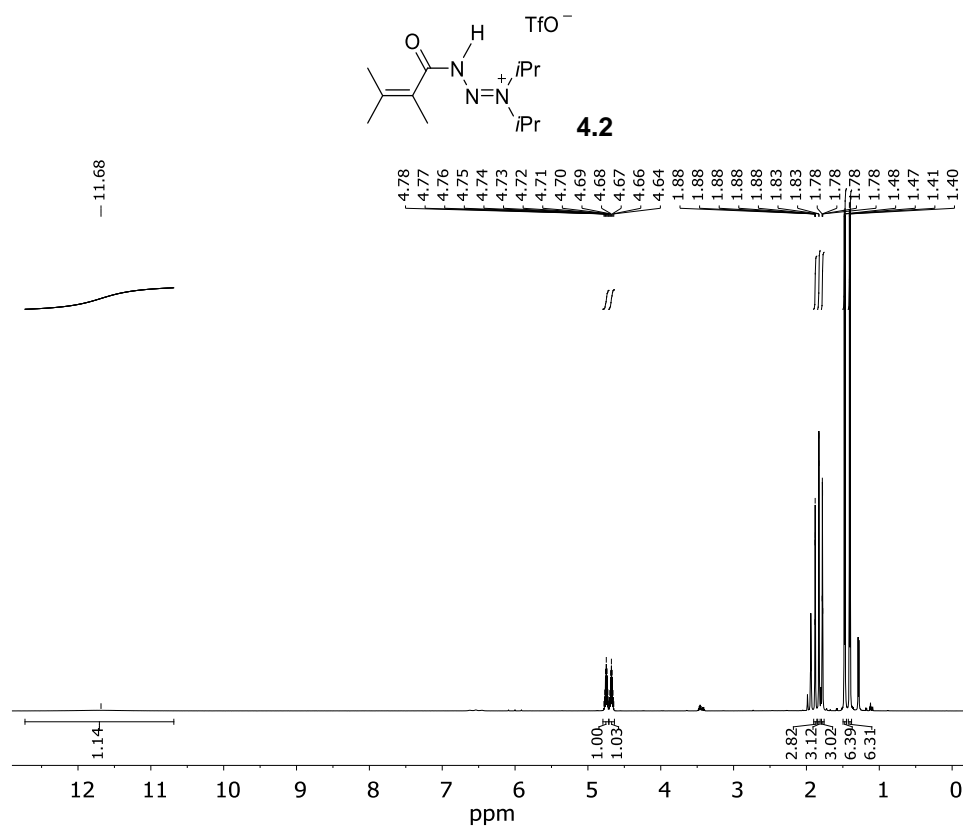


Figure ES 4.5 <sup>1</sup>H NMR spectrum of **4.2** (600 MHz, CD<sub>3</sub>CN).

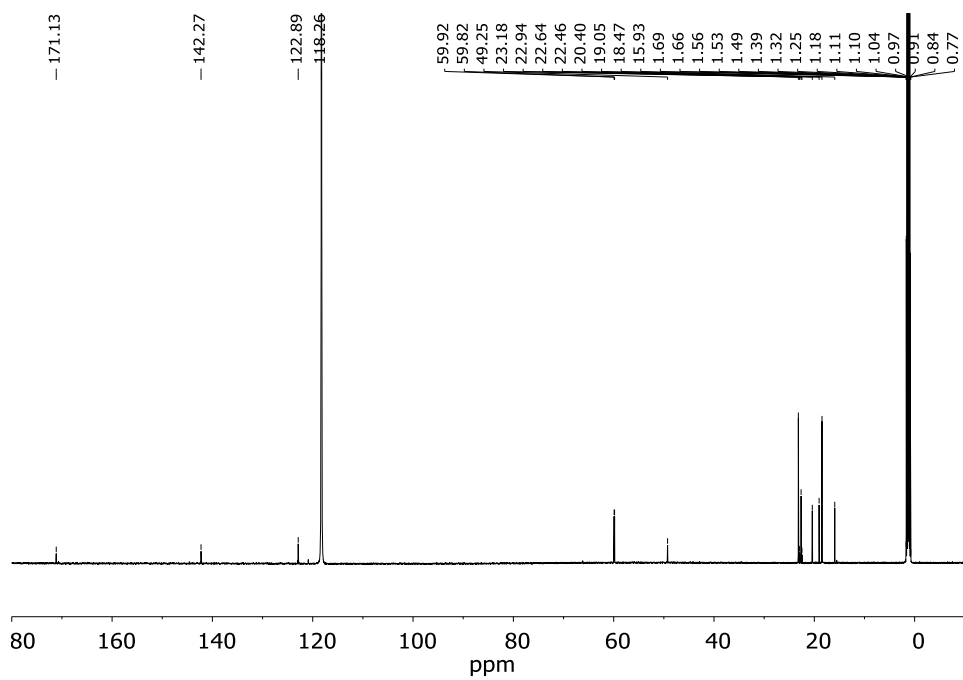
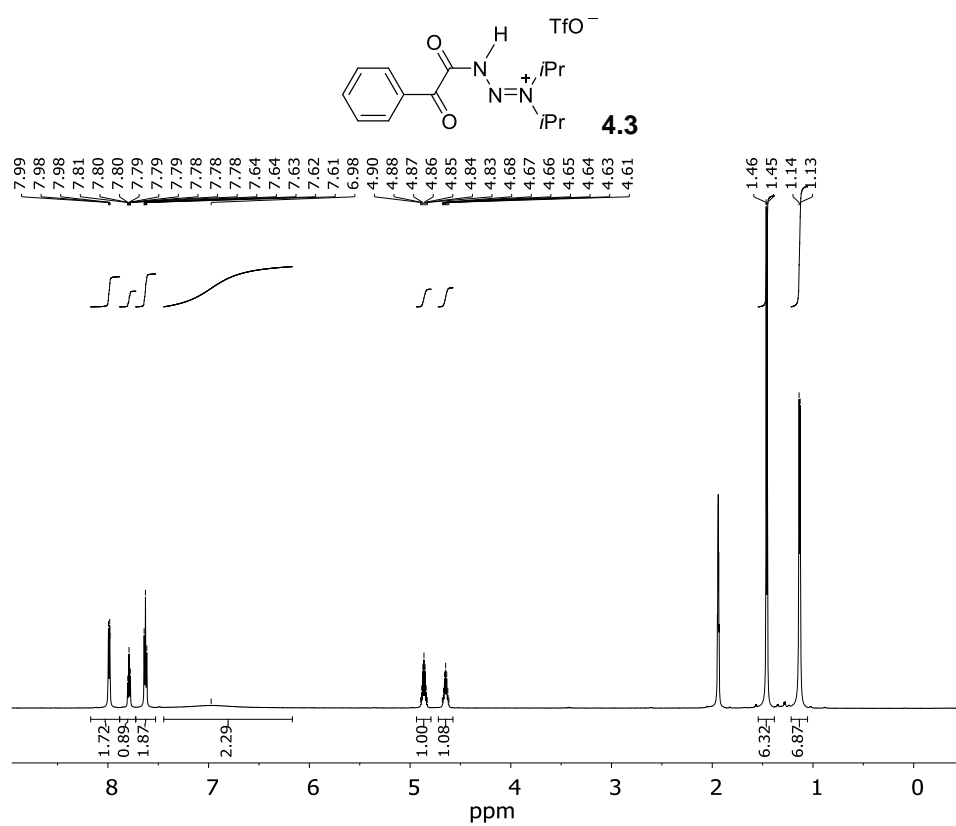
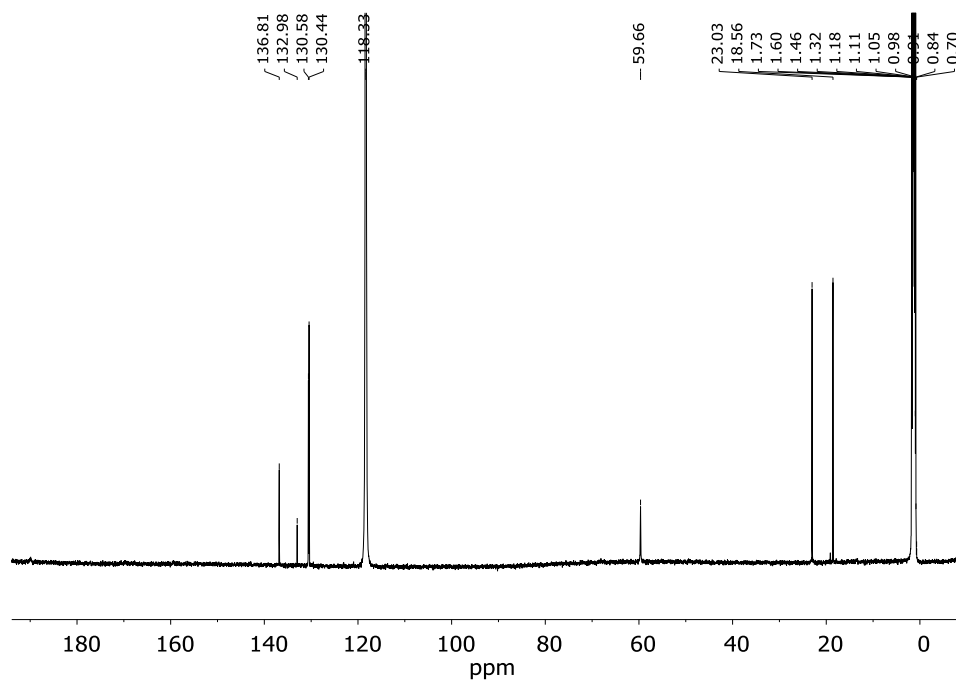


Figure ES 4.6 <sup>13</sup>C NMR spectrum of **4.2** (101 MHz, CD<sub>3</sub>CN).



**Figure ES 4.7** <sup>1</sup>H NMR spectrum of **4.3** (600 MHz, CD<sub>3</sub>CN).



**Figure ES 4.8** <sup>13</sup>C NMR spectrum of **4.3** (101 MHz, CD<sub>3</sub>CN). C=O signals were not detected.

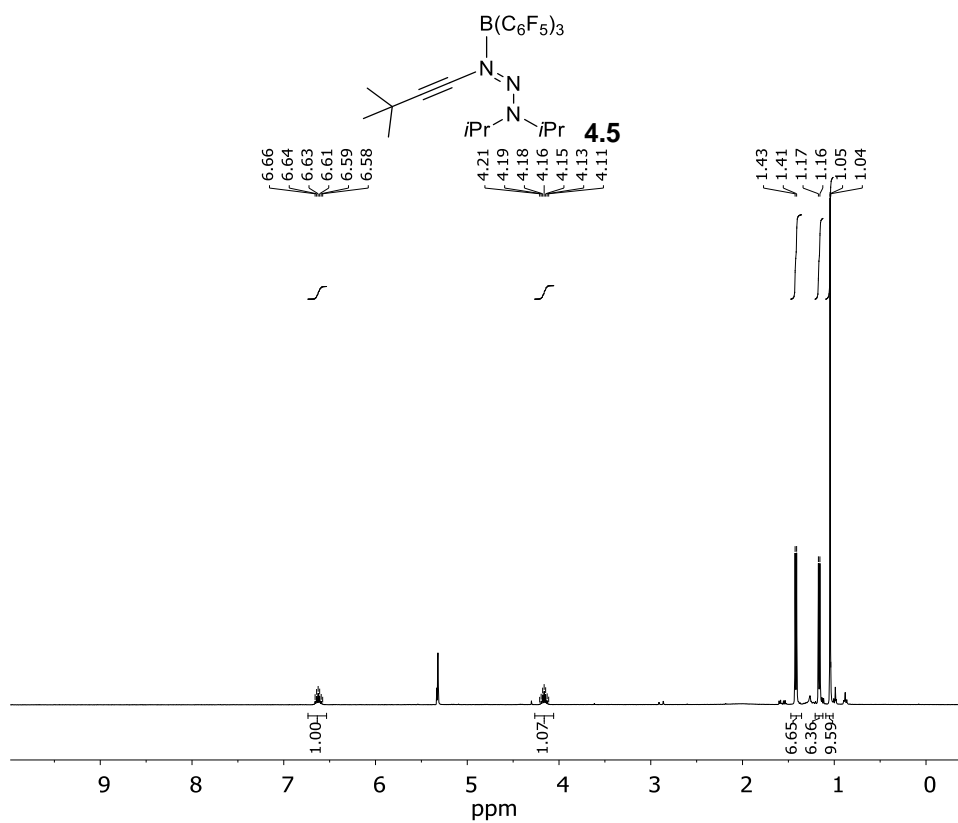


Figure ES 4.9 <sup>1</sup>H NMR spectrum of **4.5** (400 MHz, CD<sub>2</sub>Cl<sub>2</sub>).

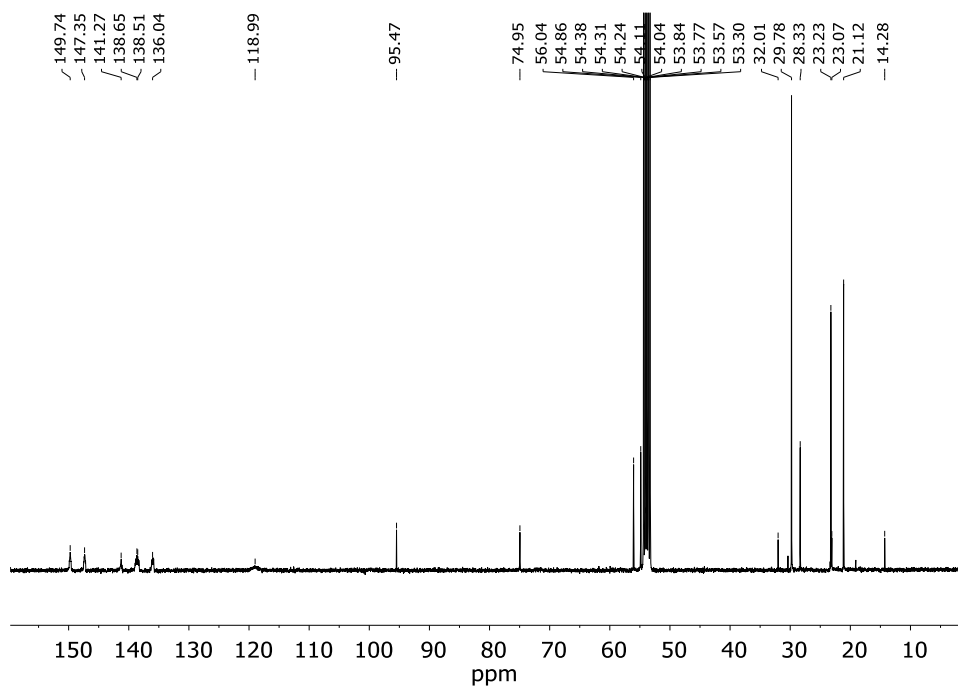
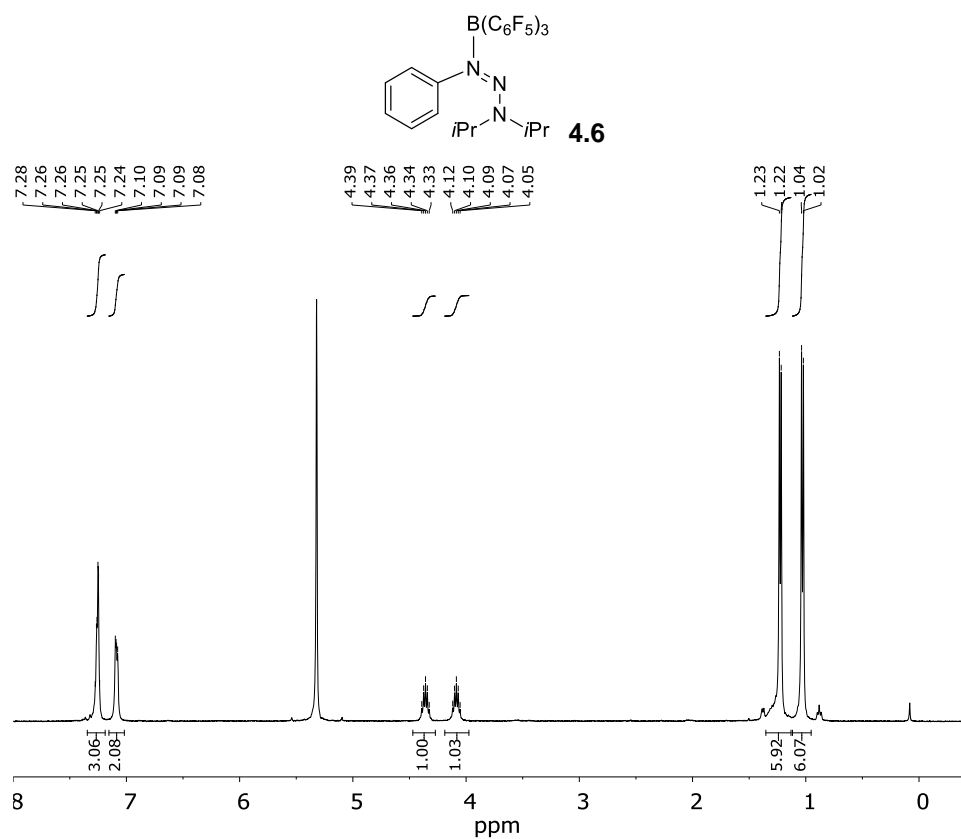
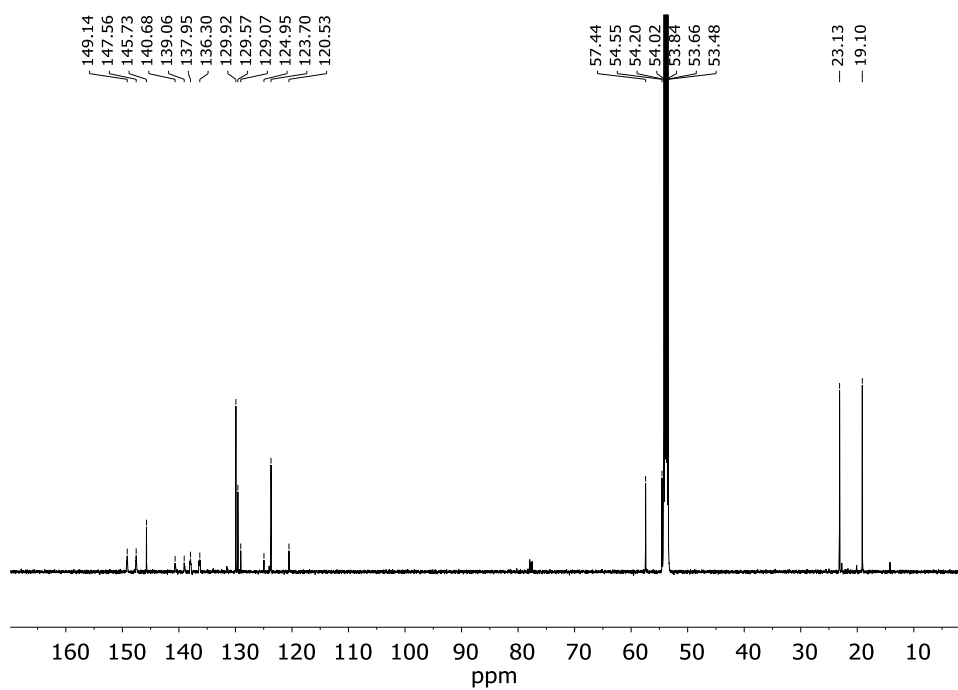


Figure ES 4.10 <sup>13</sup>C NMR spectrum of **4.5** (101 MHz, CD<sub>2</sub>Cl<sub>2</sub>).



**Figure ES 4.11**  $^1\text{H}$  NMR spectrum of **4.6** (400 MHz,  $\text{CD}_2\text{Cl}_2$ ).



**Figure ES 4.12**  $^{13}\text{C}$  NMR spectrum of **4.6** (101 MHz,  $\text{CD}_2\text{Cl}_2$ ).

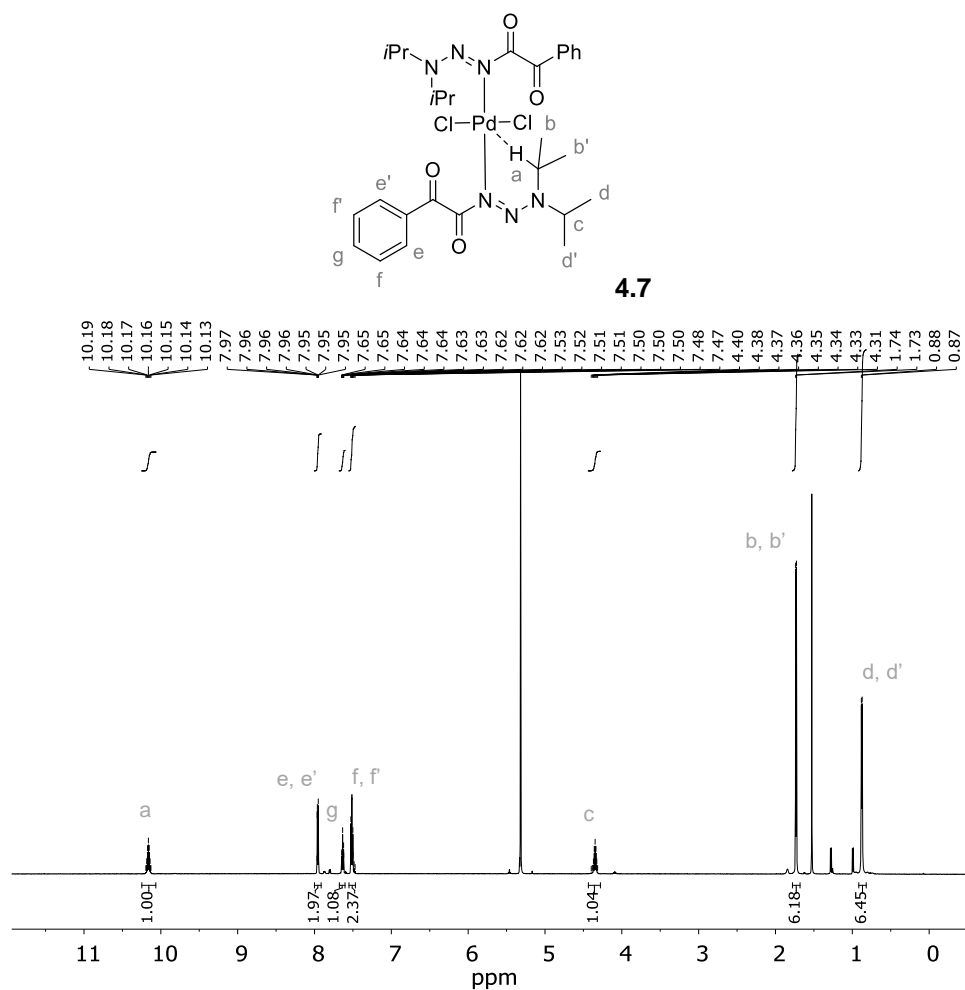


**Figure ES 4.13**  $^1\text{H}$  NMR spectrum of **4.7**, small amount of free ligand (600 MHz,  $\text{CD}_2\text{Cl}_2$ ).

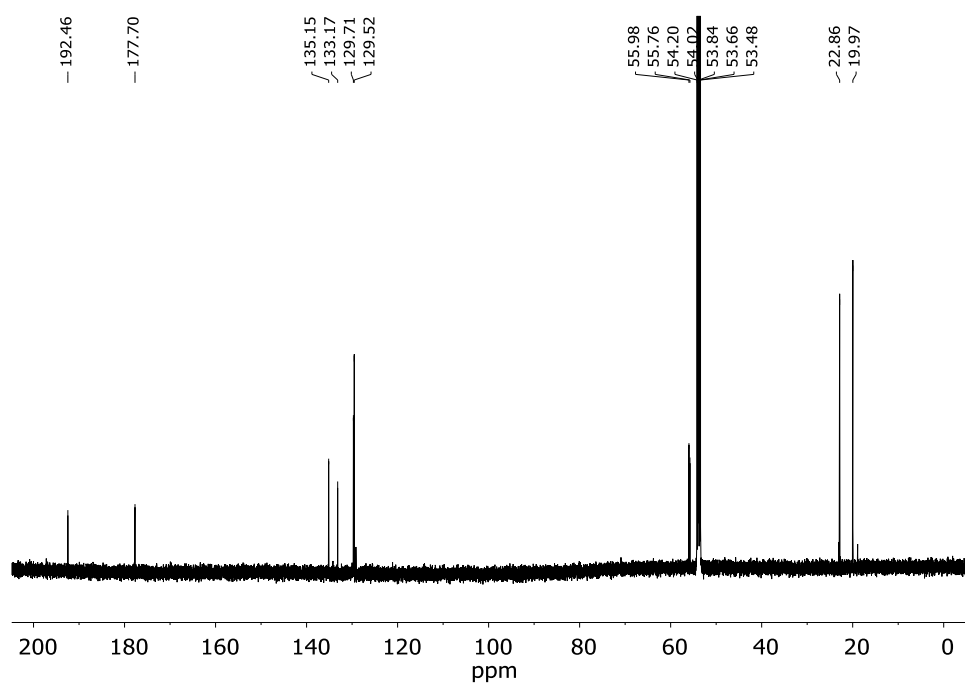


**Figure ES 4.14**  $^{13}\text{C}$  NMR spectrum of **4.7** (101 MHz,  $\text{CD}_2\text{Cl}_2$ ).

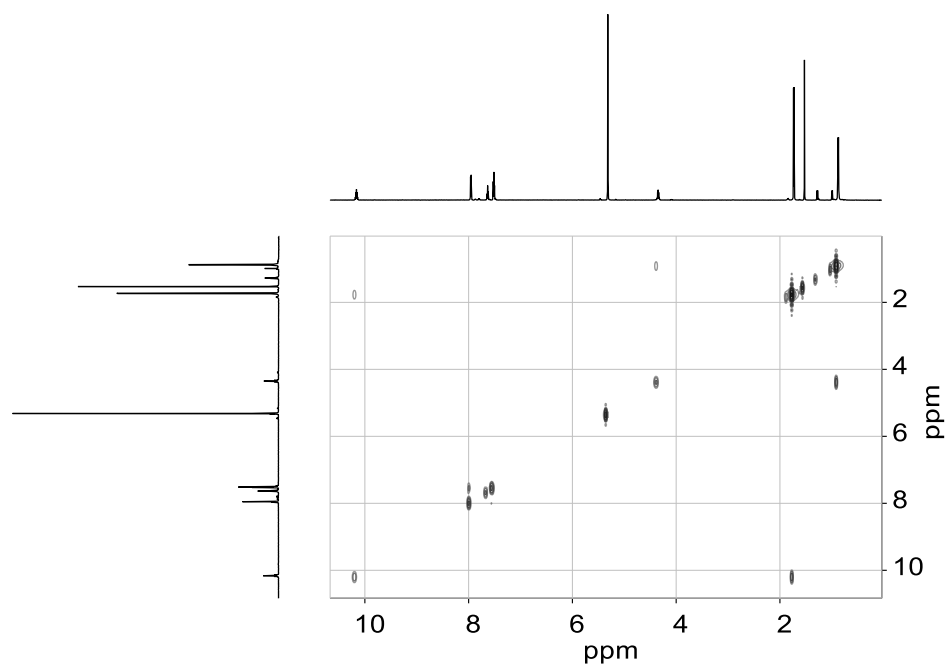


**Figure ES 4.15**  $^1\text{H}$ - $^1\text{H}$  COSY NMR spectrum of **4.7** ( $\text{CD}_2\text{Cl}_2$ ).

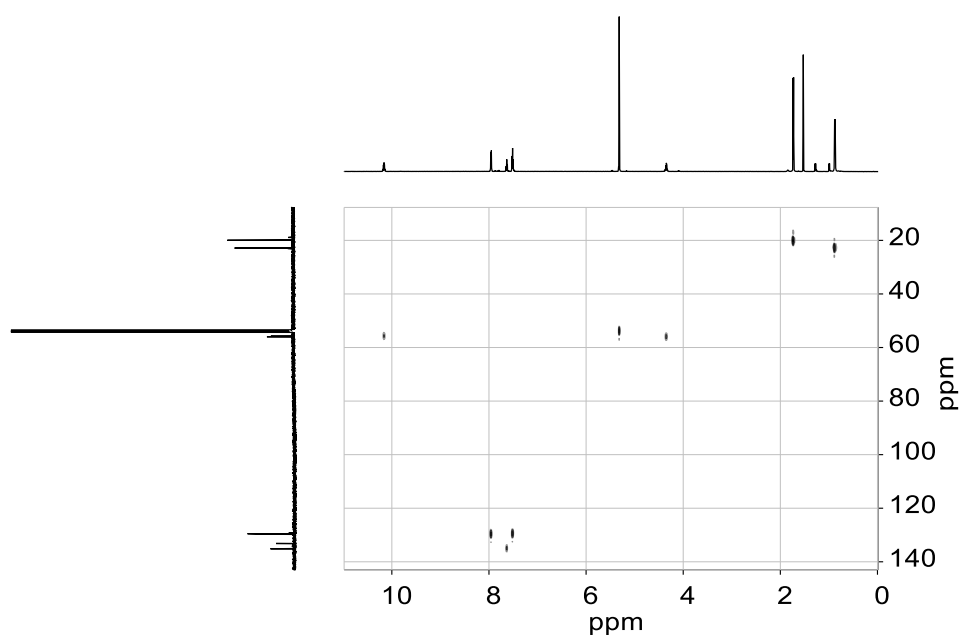


**Figure ES 4.16**  $^1\text{H}$ - $^{13}\text{C}$  HSQC NMR spectrum of **4.7** ( $\text{CD}_2\text{Cl}_2$ ).

## References

- (1) Lew, V.; McKay, E.; Maze, M. Past, Present, and Future of Nitrous Oxide. *Br. Med. Bull.* **2018**, *125* (1), 103–119.
- (2) World Health Organization [WHO]. World Health Organization Model List of Essential Medicines. *Ment. Holist. Heal. Some Int. Perspect.* **2019**, *21*, 23–24.
- (3) Tian, H.; Xu, R.; Canadell, J. G.; Thompson, R. L.; Winiwarter, W.; Suntharalingam, P.; Davidson, E. A.; Ciais, P.; Jackson, R. B.; Janssens-Maenhout, G.; et al. A Comprehensive Quantification of Global Nitrous Oxide Sources and Sinks. *Nature* **2020**, *586* (7828), 248–256.
- (4) Kanter, D. R.; Ogle, S. M.; Winiwarter, W. Building on Paris: Integrating Nitrous Oxide Mitigation into Future Climate Policy. *Curr. Opin. Environ. Sustain.* **2020**, *47*, 7–12.
- (5) Makowski, D. N<sub>2</sub>O Increasing Faster than Expected. *Nat. Clim. Chang.* **2019**, *9* (December), 907–910.
- (6) Ravishankara, A. R.; Daniel, J. S.; Portmann, R. W. Nitrous Oxide (N<sub>2</sub>O): The Dominant Ozone-Depleting Substance Emitted in the 21st Century. *Science* (80-. ). **2009**, *326*, 123–125.
- (7) Patel, P. Nitrous Oxide: The Unnoticed Greenhouse Gas. *C&EN*. 2021, pp 20–23.
- (8) Prather, M. J.; Hsu, J.; Deluca, N. M.; Jackman, C. H.; Oman, L. D.; Douglass, A. R.; Fleming, E. L.; Strahan, S. E.; Steenrod, S. D.; Søvde, O. A.; et al. Measuring and Modeling the Lifetime of Nitrous Oxide Including Its Variability. *J. Geophys. Res. Atmos.* **2015**, *120*, 5693–5705.
- (9) Rathnayaka, S. C.; Mankad, N. P. Coordination Chemistry of the CuZ Site in Nitrous Oxide Reductase and Its Synthetic Mimics. *Coord. Chem. Rev.* **2021**, *429*, 213718.
- (10) Lehnert, N.; Dong, H. T.; Harland, J. B.; Hunt, A. P.; White, C. J. Reversing Nitrogen Fixation. *Nat. Rev. Chem.* **2018**, *2* (10), 278–289.
- (11) Denisova, K. O.; Ilyin, A. A.; Rummyantsev, R. N.; Ilyin, A. P.; Volkova, A. V. Nitrous Oxide: Production, Application, and Protection of the Environment. *Russ. J. Gen. Chem.* **2019**, *89* (6), 1338–1346.
- (12) Griffis, T. J.; Chen, Z.; Baker, J. M.; Wood, J. D.; Millet, D. B.; Lee, X.; Venterea, R. T.; Turner, P. A. Nitrous Oxide Emissions Are Enhanced in a Warmer and Wetter World. *Proc. Natl. Acad. Sci. U. S. A.* **2017**, *114* (45), 12081–12085.
- (13) Reay, D. S.; Davidson, E. A.; Smith, K. A.; Smith, P.; Melillo, J. M.; Dentener, F.; Crutzen, P. J. Global Agriculture and Nitrous Oxide Emissions. *Nat. Clim. Chang.* **2012**, *2* (6), 410–416.
- (14) Severin, K. Synthetic Chemistry with Nitrous Oxide. *Chem. Soc. Rev.* **2015**, *44* (17), 6375–6386.
- (15) Conway, J. H. Nitrous Oxide. *Encycl. Reagents Org. Synth.* **2018**.
- (16) Otten, E.; Neu, R. C.; Stephan, D. W. Complexation of Nitrous Oxide by Frustrated Lewis Pairs. *J. Am. Chem. Soc.* **2009**, *131*, 9918–9919.
- (17) Parmon, V. N.; Panov, G. I.; Uriarte, A.; Noskov, A. S. Nitrous Oxide in Oxidation Chemistry and Catalysis: Application and Production. *Catal. Today* **2005**, *100*, 115–131.
- (18) Severin, K. Synthetic Chemistry with Nitrous Oxide. *Chem. Soc. Rev.* **2015**, *44* (17), 6375–6386.
- (19) Landaeta, V. R.; Rodríguez-Lugo, R. E. Catalytic Oxygenation of Organic Substrates: Toward Greener Ways for Incorporating Oxygen. *Inorganica Chim. Acta* **2015**, *431*, 21–47.
- (20) Ferousi, C.; Majer, S. H.; Dimucci, I. M.; Lancaster, K. M. Biological and Bioinspired Inorganic N–N Bond-Forming Reactions. *Chem. Rev.* **2020**, *120* (12), 5252–5307.
- (21) Chang, A. H. H.; Yarkony, D. R. On the Electronic Structure Aspects of Spin-Forbidden Processes in N<sub>2</sub>O. *J. Chem. Phys.* **1993**, *99* (9), 6824–6831.
- (22) Dubkov, K. A.; Panov, G. I.; Parmon, V. N. Nitrous Oxide as a Selective Oxidant for Ketonization of C=C Double Bonds in Organic Compounds. *Russ. Chem. Rev.* **2017**, *86* (6), 510–529.
- (23) Semikolenov, S.; Ivanov, D.; Babushkin, D.; Malykhin, S.; Kharitonov, A.; Dubkov, K. Generation of Methylene by the Liquid Phase Oxidation of Isobutene with Nitrous Oxide. *Tetrahedron* **2018**, *74* (27), 3589–3595.
- (24) Bridson-Jones, F. S.; Buckley, G. D.; Cross, L. H.; Driver, A. P. Oxidation of Organic Compounds by Nitrous Oxide. *J. Chem. Soc.* **1951**, 2999–3008.
- (25) Davis, J. V.; Guio, O.; Captain, B.; Hoff, C. D. Production of Cis-Na<sub>2</sub>N<sub>2</sub>O<sub>2</sub> and NaNO<sub>3</sub> by Ball Milling Na<sub>2</sub>O and N<sub>2</sub>O in Alkali Metal Halide Salts. *ACS Omega* **2021**, *6* (28), 18248–18252.
- (26) Pirutko, L. V.; Chernyavsky, V. S.; Uriarte, A. K.; Panov, G. I. Oxidation of Benzene to Phenol by Nitrous Oxide. *Appl. Catal. A Gen.* **2002**, *227*, 143–157.
- (27) Starokon, E. V.; Parfenov, M. V.; Arzumanov, S. S.; Pirutko, L. V.; Stepanov, A. G.; Panov, G. I. Oxidation of Methane to Methanol on the Surface of FeZSM-5 Zeolite. *J. Catal.* **2013**, *300*, 47–54.
- (28) Tolman, W. B. Binding and Activation of N<sub>2</sub>O at Transition-Metal Centers: Recent Mechanistic Insights. *Angew. Chemie - Int. Ed.* **2010**, *49* (6), 1018–1024.
- (29) Armor, J. N.; Taube, H. Formation and Reactions of [(NH<sub>3</sub>)<sub>5</sub>RuN<sub>2</sub>O<sub>2</sub>]<sup>+</sup>. *J. Am. Chem. Soc.* **1969**, *91*, 6874–6876.
- (30) Pamplin, C. B.; Ma, E. S. F.; Safari, N.; Rettig, S. J.; James, B. R. The Nitrous Oxide Complex, RuCl<sub>2</sub>(H<sub>2</sub>O)(P-N)(PPh<sub>3</sub>) (P-N = [o-(N,N-Dimethylamino)Phenyl]Diphenylphosphine); Low Temperature Conversion of N<sub>2</sub>O to N<sub>2</sub> and O<sub>2</sub>. *J. Am. Chem. Soc.* **2001**, *123* (35), 8596–8597.
- (31) Piro, N. A.; Lichterman, M. F.; Harman, W. H.; Chang, C. J. A Structurally Characterized Nitrous Oxide Complex of Vanadium. *J. Am. Chem. Soc.* **2011**, *133* (7), 2108–2111.
- (32) Hartmann, N. J.; Wu, G.; Hayton, T. W. Synthesis of a “Masked” Terminal Nickel(II) Sulfide by Reductive

- Deprotection and Its Reaction with Nitrous Oxide. *Angew. Chemie - Int. Ed.* **2015**, *127* (49), 15169–15172.
- (33) Zhuravlev, V.; Malinowski, P. J. A Stable Crystalline Copper(I)-N<sub>2</sub>O Complex Stabilized as the Salt of a Weakly Coordinating Anion. *Angew. Chemie - Int. Ed.* **2018**, *130* (36), 11871–11874.
- (34) Gyton, M. R.; Leforestier, B.; Chaplin, A. B. Rhodium(I) Pincer Complexes of Nitrous Oxide. *Angew. Chemie - Int. Ed.* **2019**, *58* (43), 15295–15298.
- (35) Mokhtarzadeh, C. C.; Chan, C.; Moore, C. E.; Rheingold, A. L.; Figueroa, J. S. Side-On Coordination of Nitrous Oxide to a Mononuclear Cobalt Center. *J. Am. Chem. Soc.* **2019**, *141* (38), 15003–15007.
- (36) Puerta Lombardi, B. M.; Gendy, C.; Gelfand, B. S.; Bernard, G. M.; Wasylshen, R. E.; Tuononen, H. M.; Roesler, R. Side-on Coordination in Isostructural Nitrous Oxide and Carbon Dioxide Complexes of Nickel. *Angew. Chemie - Int. Ed.* **2021**, *60* (13), 7077–7081.
- (37) Doyle, L. E.; Piers, W. E.; Borau-Garcia, J. Ligand Cooperation in the Formal Hydrogenation of N<sub>2</sub>O Using a PCsp<sup>2</sup>P Iridium Pincer Complex. *J. Am. Chem. Soc.* **2015**, *137* (6), 2187–2190.
- (38) Smith, J. D.; Chih, E.; Piers, W. E.; Spasyuk, D. M. Tuning Iridium (I) PCcarbeneP Frameworks for Facile Cooperative N<sub>2</sub>O Reduction. *Polyhedron* **2018**, *155*, 281–290.
- (39) Cook, B. J.; Chen, C. H.; Caulton, K. G. A Multifunctional Pincer Ligand for Cobalt-Promoted Oxidation by N<sub>2</sub>O. *Chem. - A Eur. J.* **2018**, *24* (22), 5962–5966.
- (40) Hartmann, N. J.; Wu, G.; Hayton, T. W. Synthesis and Reactivity of a Nickel(II) Thioperoxide Complex: Demonstration of Sulfide-Mediated N<sub>2</sub>O Reduction. *Chem. Sci.* **2018**, *9* (31), 6580–6588.
- (41) Aguirre Quintana, L. M.; Yang, Y.; Ramanathan, A.; Jiang, N.; Bacs, J.; Maron, L.; La Pierre, H. S. Chalcogen-Atom Abstraction Reactions of a Di-Iron Imidophosphorane Complex. *Chem. Commun.* **2021**, *57* (54), 6664–6667.
- (42) Kaplan, A. W.; Bergman, R. G. Nitrous Oxide Mediated Synthesis of Monomeric Hydroxoruthenium Complexes. Reactivity of (DMPE)<sub>2</sub>Ru(H)(OH) and the Synthesis of a Silica-Bound Ruthenium Complex. *Organometallics* **1998**, *17* (23), 5072–5085.
- (43) Lee, J. H.; Pink, M.; Tomaszewski, J.; Fan, H.; Caulton, K. G. Facile Hydrogenation of N<sub>2</sub>O by an Operationally Unsaturated Osmium Polyhydride. *J. Am. Chem. Soc.* **2007**, *129* (28), 8706–8707.
- (44) Zeng, R.; Feller, M.; Ben-David, Y.; Milstein, D. Hydrogenation and Hydrosilylation of Nitrous Oxide Homogeneously Catalyzed by a Metal Complex. *J. Am. Chem. Soc.* **2017**, *139* (16), 5720–5723.
- (45) Nobukawa, T.; Yoshida, M.; Okumura, K.; Tomishige, K.; Kunimori, K. Effect of Reductants in N<sub>2</sub>O Reduction over Fe-MFI Catalysts. *J. Catal.* **2005**, *229* (2), 374–388.
- (46) Vance, J. E.; Dixon, J. K. The Reaction between Nitrous Oxide and Hydrogen on Alumina. *J. Am. Chem. Soc.* **1941**, *63*, 176–181.
- (47) Vance, J. E.; Dixon, J. K. The Reaction between Nitrous Oxide and Hydrogen on Platinum. *J. Am. Chem. Soc.* **1935**, *57*, 818–821.
- (48) Jurt, P.; Abels, A. S.; Gamboa-Carballo, J. J.; Fernández, I.; Le Corre, G.; Aebli, M.; Baker, M. G.; Eiler, F.; Müller, F.; Wörle, M.; et al. Reduction of Nitrogen Oxides by Hydrogen with Rh(I)-Pt(II) Olefin Complexes as Catalysts. *Angew. Chemie - Int. Ed.* **2021**, *60*, DOI: 10.1002/anie.202109642.
- (49) Chen, X.; Wang, H.; Du, S.; Driess, M.; Mo, Z. Deoxygenation of Nitrous Oxide and Nitro Compounds Using Bis(N-Heterocyclic Silylene)Amido Iron Complexes as Catalysts. *Angew. Chemie Int. Ed.* **2021**, No. 60, e2021145.
- (50) Kjellberg, M.; Ohleier, A.; Thuéry, P.; Nicolas, E.; Anthore-Dalion, L.; Cantat, T. Photocatalytic Deoxygenation of N–O Bonds with Rhenium Complexes: From the Reduction of Nitrous Oxide to Pyridine N-Oxides. *Chem. Sci.* **2021**, *12* (30), 10266–10272.
- (51) Deeba, R.; Molton, F.; Chardon-Noblat, S.; Costentin, C. Effective Homogeneous Catalysis of Electrochemical Reduction of Nitrous Oxide to Dinitrogen at Rhenium Carbonyl Catalysts. *ACS Catal.* **2021**, *11* (10), 6099–6103.
- (52) Zeng, R.; Feller, M.; Diskin-Posner, Y.; Shimon, L. J. W.; Ben-David, Y.; Milstein, D. CO Oxidation by N<sub>2</sub>O Homogeneously Catalyzed by Ruthenium Hydride Pincer Complexes Indicating a New Mechanism. *J. Am. Chem. Soc.* **2018**, *140* (23), 7061–7064.
- (53) Tanaka, H.; Hashimoto, K.; Suzuki, K.; Kitaichi, Y.; Sato, M.; Ikeno, T.; Yamada, T. Nitrous Oxide Oxidation Catalyzed by Ruthenium Porphyrin Complex. *Bull. Chem. Soc. Jpn.* **2004**, *77* (10), 1905–1914.
- (54) Hashimoto, K.; Kitaichi, Y.; Tanaka, H.; Ikeno, T.; Yamada, T. Nitrous Oxide Oxidation of Secondary and Benzylic Alcohols Using Ruthenium Complex Catalyst. *Chem. Lett.* **2001**, *30* (9), 922–923.
- (55) Goldberg, H.; Kumar, D.; Sastry, G. N.; Leitens, G.; Neumann, R. An Antimony(V) Substituted Keggin Heteropolyacid, H<sub>4</sub>PSbMo<sub>11</sub>O<sub>40</sub>: Why Is Its Catalytic Activity in Oxidation Reactions so Different from That of H<sub>4</sub>PVMo<sub>11</sub>O<sub>40</sub>? *J. Mol. Catal. A Chem.* **2012**, *356*, 152–157.
- (56) Ettedgui, J.; Neumann, R. Phenanthroline Decorated by a Crown Ether as a Module for Metallorganic Polyoxometalate Hybrid Catalysts: The Wacker Type Oxidation of Alkenes with Nitrous Oxide as Terminal Oxidant. *J. Am. Chem. Soc.* **2009**, *131* (1), 4–5.
- (57) Ben-Daniel, R.; Neumann, R. Activation of Nitrous Oxide and Selective Oxidation of Alcohols and Alkylarenes Catalyzed by the [PV<sub>2</sub>Mo<sub>10</sub>O<sub>40</sub>]<sup>5-</sup> Polyoxometalate Ion. *Angew. Chemie - Int. Ed.* **2003**, *42* (1), 92–95.
- (58) Yonke, B. L.; Reeds, J. P.; Zavalij, P. Y.; Sita, L. R. Catalytic Degenerate and Nondegenerate Oxygen Atom Transfers Employing N<sub>2</sub>O and CO<sub>2</sub> and a M(II)/M(IV) Cycle Mediated by Group 6 m(IV) Terminal Oxo Complexes. *Angew. Chemie - Int. Ed.* **2011**, *50* (51), 12342–12346.
- (59) Kiefer, G.; Jeanbourquin, L.; Severin, K. Oxidative Coupling Reactions of Grignard Reagents with Nitrous Oxide. *Angew. Chemie - Int. Ed.* **2013**, *52* (24), 6302–6305.
- (60) Gianetti, T. L.; Rodríguez-Lugo, R. E.; Harmer, J. R.; Trincado, M.; Vogt, M.; Santiso-Quinones, G.; Grützmacher,

- H. Zero-Valent Amino-Olefin Cobalt Complexes as Catalysts for Oxygen Atom Transfer Reactions from Nitrous Oxide. *Angew. Chemie - Int. Ed.* **2016**, 55 (49), 15323–15328.
- (61) Gianetti, T. L.; Annen, S. P.; Santiso-Quinones, G.; Reiher, M.; Driess, M.; Grützmacher, H. Nitrous Oxide as a Hydrogen Acceptor for the Dehydrogenative Coupling of Alcohols. *Angew. Chemie - Int. Ed.* **2016**, 55 (5), 1854–1858.
- (62) Ricker, J. D.; Mohammadrezaei, V.; Crippen, T. J.; Zell, A. M.; Geary, L. M. Nitrous Oxide Promoted Pauson-Khand Cycloadditions. *Organometallics* **2018**, 37 (24), 4556–4559.
- (63) Qu, Y.; Wang, Z.; Zhang, Z.; Zhang, W.; Huang, J.; Yang, Z. Asymmetric Total Synthesis of (+)-Waihoensene. *J. Am. Chem. Soc.* **2020**, 142 (14), 6511–6515.
- (64) Alvarado-Beltran, I.; Rosas-Sánchez, A.; Baceiredo, A.; Saffon-Merceron, N.; Branchadell, V.; Kato, T. A Fairly Stable Crystalline Silanone. *Angew. Chemie - Int. Ed.* **2017**, 56 (35), 10481–10485.
- (65) Rosas-Sánchez, A.; Alvarado-Beltran, I.; Baceiredo, A.; Saffon-Merceron, N.; Massou, S.; Hashizume, D.; Branchadell, V.; Kato, T. Cyclic (Amino)(Phosphonium Bora-Ylide)Silanone: A Remarkable Room-Temperature-Persistent Silanone. *Angew. Chemie - Int. Ed.* **2017**, 56 (50), 15916–15920.
- (66) Anker, M. D.; Coles, M. P. Aluminium-Mediated Carbon Dioxide Reduction by an Isolated Monoalumoxane Anion. *Angew. Chemie - Int. Ed.* **2019**, 131 (50), 18429–18433.
- (67) Szykiewicz, N.; Chojnacki, J.; Grubba, R. Activation of N<sub>2</sub>O and SO<sub>2</sub> by the P-B Bond System. Reversible Binding of SO<sub>2</sub> by the P-O-B Geminal Frustrated Lewis Pair. *Inorg. Chem.* **2020**, 59 (9), 6332–6337.
- (68) Weetman, C.; Porzelt, A.; Bag, P.; Hanusch, F.; Inoue, S. Dialumenes-Aryl: Vs. Silyl Stabilisation for Small Molecule Activation and Catalysis. *Chem. Sci.* **2020**, 11 (18), 4817–4827.
- (69) Reiter, D.; Frisch, P.; Wendel, D.; Hörmann, F. M.; Inoue, S. Oxidation Reactions of a Versatile, Two-Coordinate, Acyclic Iminosiloxysilylene. *Dalt. Trans.* **2020**, 49, 7060–7068.
- (70) Chen, C.; Daniliuc, C. G.; Kehr, G.; Erker, G. Formation and Cycloaddition Reactions of a Reactive Boraalkene Stabilized Internally by N-Heterocyclic Carbene. *Angew. Chemie - Int. Ed.* **2021**, 60 (36), 19905–19911.
- (71) Pang, Y.; Leutzsch, M.; Nöthling, N.; Cornella, J. Catalytic Activation of N<sub>2</sub>O at a Low-Valent Bismuth Redox Platform. *J. Am. Chem. Soc.* **2020**, 142 (46), 19473–19479.
- (72) Anthore-Dalio, L.; Nicolas, E.; Cantat, T. Catalytic Metal-Free Deoxygenation of Nitrous Oxide with Disilanes. *ACS Catal.* **2019**, 9 (12), 11563–11567.
- (73) Wislicenus, W. Synthese der Stickstoff-Wasserstoffsäure. *Berichte der Dtsch. Chem. Gesellschaft* **1891**, 2084–2087.
- (74) Bräse, S.; Banert, K. *Organic Azides Syntheses and Applications*; 2010.
- (75) Kurosawa, M.; Nankawa, T.; Matsuda, T.; Kubo, K.; Kurihara, M.; Nishihara, H. Synthesis of Azo-Bridged Ferrocene Oligomers and a Polymer and Electrochemical and Optical Analysis of Internuclear Electronic Interactions in Their Mixed-Valence States. *Inorg. Chem.* **1999**, 38 (22), 5113–5123.
- (76) Koga, G.; Anselme, J.-P. N-Nitrenes. IX. The Reaction of 1,1-Dibenzylhydrazine Anions with Tosyl Azide, Oxygen, and Nitrous Oxide. *J. Org. Chem.* **1970**, 35, 960–964.
- (77) Koga, G.; Anselme, J. H. The Formation of Azides by the Reaction of Amine Anions with Nitrous Oxide. *Chem. Commun.* **1968**, 446–447.
- (78) Nesmeyanov, A. N.; Perevalova, E. G.; Nikitina, T. V. Ferrocene Li + N<sub>2</sub>O, Nitrous Oxide. *Dokl. Akad. Nauk SSSR* **1961**, 138 (5), 1118–1121.
- (79) Müller, E.; Rundel, W. Zur Kenntnis der Umsetzung von Diazomethan mit Methylithium. *Chem. Ber.* **1957**, 90, 1299–1302.
- (80) Müller, E.; Rundel, W. Eine neue Synthese von Diazomethan und von Isodiazomethan. *Chem. Ber.* **1957**, 90, 1302–1306.
- (81) Meier, R.; Frank, W. Über die Reaktion von Phenyllithium mit Stickoxydul (II. Mitteil. Über Reaktionen metallorganischer Verbindungen mit Stickoxydul). *Chem. Ber.* **1956**, 89, 2747–2750.
- (82) Müller, E.; Ludsteck, D.; Rundel, W. Ein neuer Weg zur Diazomethan. *Angew. Chemie* **1955**, 67 (19), 617.
- (83) Meier, R. Reaktionen metallorganischer Verbindungen mit Stickoxydul. *Chem. Ber.* **1953**, 86, 1483–1492.
- (84) Beringer, F. M.; Farr, J. A.; Sands, S. The reactions of nitrous oxide with organolithium compounds. *J. Am. Chem. Soc.* **1953**, 75 (16), 3984–3987.
- (85) Schlenk, W.; Bergmann, E. Versuche mit triphenylmethyl- und diphenylmethyl-Natrium. *Liebigs Ann. Chem.* **1928**, 464, 1–21.
- (86) Tskhovrebov, A. G.; Solari, E.; Scopelliti, R.; Severin, K. Reactions of Grignard reagents with nitrous oxide. *Organometallics* **2014**, 33 (10), 2405–2408.
- (87) Wei, B.; Zhang, W. X.; Xi, Z. Well-defined styryl and biphenyl calcium complexes from dilithio compounds and calcium iodide: Synthesis, structure and reactivity toward nitrous oxide. *Dalt. Trans.* **2018**, 47 (36), 12540–12545.
- (88) Hays, M. L.; Hanusa, T. P. A reinvestigation of the reaction of arylcalcium iodides with nitrous oxide. *Tetrahedron Lett.* **1995**, 36 (14), 2435–2436.
- (89) Meier, R.; Rappold, K. Umsetzung von Phenyl-Calciumjodid mit Distickstoffoxyd. *Angew. Chemie* **1953**, 65 (22), 560–561.
- (90) Forstinger, K.; Metz, H. J.; Koch, P. Diazo compounds and diazo reactions. *Ullmann's Encycl. Ind. Chem.* **2015**, 1–22.
- (91) Zerner, E. Über einwirkung von organomagnesium-Verbindungen auf diazoessigester. *Monatsh. Chem.* **1913**, 34, 1609.
- (92) Lai, Z.; Wang, C.; Li, J.; Cui, S. Redox cyclization of amides and sulfonamides with nitrous oxide for direct

- Synthesis of Heterocycles. *Org. Lett.* **2020**, 22 (5), 2017–2021.
- (93) Tskhovrebov, A. G.; Solari, E.; Wodrich, M. D.; Scopelliti, R.; Severin, K. Covalent Capture of Nitrous Oxide by N-Heterocyclic Carbenes. *Angew. Chemie - Int. Ed.* **2012**, 51 (1), 232–234.
- (94) Eymann, L. Y. M.; Scopelliti, R.; Tirani, F. F.; Severin, K. Synthesis of Azo Dyes from Mesoionic Carbenes and Nitrous Oxide. *Chem. - A Eur. J.* **2018**, 24 (31), 7957–7963.
- (95) Tskhovrebov, A. G.; Naested, L. C. E.; Solari, E.; Scopelliti, R.; Severin, K. Synthesis of Azoimidazolium Dyes with Nitrous Oxide. *Angew. Chemie - Int. Ed.* **2015**, 54 (4), 1289–1292.
- (96) Liu, Y.; Varava, P.; Fabrizio, A.; Eymann, L. Y. M.; Tskhovrebov, A. G.; Planes, O. M.; Solari, E.; Fadaei-Tirani, F.; Scopelliti, R.; Sienkiewicz, A.; et al. Synthesis of Aminyl Biradicals by Base-Induced Csp<sup>3</sup>-Csp<sup>3</sup> Coupling of Cationic Azo Dyes. *Chem. Sci.* **2019**, 10 (22), 5719–5724.
- (97) Eymann, L. Y. M.; Tskhovrebov, A. G.; Sienkiewicz, A.; Bila, J. L.; Živković, I.; Rønnow, H. M.; Wodrich, M. D.; Vannay, L.; Corminboeuf, C.; Pattison, P.; et al. Neutral Aminyl Radicals Derived from Azoimidazolium Dyes. *J. Am. Chem. Soc.* **2016**, 138 (46), 15126–15129.
- (98) Chadwick, F. M.; Curchod, B. F. E.; Scopelliti, R.; Fadaei Tirani, F.; Solari, E.; Severin, K. Azo-MICs: Redox-Active Mesoionic Carbene Ligands Derived from Azoimidazolium Dyes. *Angew. Chemie - Int. Ed.* **2019**, 58 (6), 1764–1767.
- (99) Eymann, L. Y. M.; Varava, P.; Shved, A. M.; Curchod, B. F. E.; Liu, Y.; Planes, O. M.; Sienkiewicz, A.; Scopelliti, R.; Fadaei Tirani, F.; Severin, K. Synthesis of Organic Super-Electron-Donors by Reaction of Nitrous Oxide with N-Heterocyclic Olefins. *J. Am. Chem. Soc.* **2019**, 141 (43), 17112–17116.
- (100) Varava, P.; Dong, Z.; Scopelliti, R.; Fadaei-Tirani, F.; Severin, K. Isolation and Characterization of Diazoolefins. *Nat. Chem.* **2021**, DOI: 10.1038/s41557-021-00790-3.
- (101) Antoni, P. W.; Golz, C.; Holstein, J. J.; Pantazis, D. A.; Hansmann, M. M. Isolation and Reactivity of an Elusive Diazoalkene. *Nat. Chem.* **2021**, 13 (6), 587–593.
- (102) Banert, K.; Plefka, O. Synthesis with Perfect Atom Economy: Generation of Diazo Ketones by 1,3-Dipolar Cycloaddition of Nitrous Oxide at Cyclic Alkynes under Mild Conditions. *Angew. Chemie - Int. Ed.* **2011**, 50 (27), 6171–6174.
- (103) Kimball, D. B.; Haley, M. M. Triazenes: A Versatile Tool in Organic Synthesis. *Angew. Chemie - Int. Ed.* **2002**, 41 (18), 3338–3351.
- (104) Zhang, Y.; Cao, D.; Liu, W.; Hu, H.; Zhang, X.; Liu, C. Recent Applications of Aryltriazenes in Organic Synthesis via C–N/N–N Bond Cleavage. *Curr. Org. Chem.* **2015**, 19, 151–178.
- (105) Suleymanov, A. A.; Severin, K. Vinyl and Alkynyl Triazenes: Synthesis, Reactivity, and Applications. *Angew. Chemie - Int. Ed.* **2021**, 60 (13), 6879–6889.
- (106) Connors, T. A.; Goddard, P. M.; Merai, K.; Ross, W. C. J.; Wilman, D. E. V. *Triazenes: Chemical, Biological and Clinical Aspects*, 25th ed.; Biochem. Pharmacol., 1976.
- (107) Smith, R. H.; Scudiero, D. A.; Michejda, C. J. 1,3-Dialkyl-3-Acyltriazenes, a Novel Class of Antineoplastic Alkylating Agents. *J. Med. Chem.* **1990**, 33, 2579–2583.
- (108) Nicolaou, K. C.; Natarajan, S.; Li, H.; Jain, N. F.; Hughes, R.; Solomon, M. E.; Ramanjulu, J. M.; Boddy, C. N. C.; Takayanagi, M. Total Synthesis of Vancomycin Aglycon Part 1 : Synthesis of Amino Acids 4-7 and Construction of the AB-COD Ring Skeleton. *Angew. Chemie - Int. Ed.* **1998**, 37 (19), 2708–2714.
- (109) Bräse, S. The Virtue of the Multifunctional Triazene Linkers in the Efficient Solid-Phase Synthesis of Heterocycle Libraries. *Acc. Chem. Res.* **2004**, 37 (10), 805–816.
- (110) Bräse, S.; Dahmen, S.; Lormann, M. E. P. Multifunctional Linkers as an Efficient Tool for the Synthesis of Diverse Small Molecule Libraries: The Triazene Anchors. *Methods Enzymol.* **2003**, 369, 127–150.
- (111) Jones, L. R.; Schumm, J. S.; Tour, J. M. Rapid Solution and Solid Phase Syntheses of Oligo(1,4-Phenylene Ethynylene)s with Thioester Termini: Molecular Scale Wires with Alligator Clips. Derivation of Iterative Reaction Efficiencies on a Polymer Support. *J. Org. Chem.* **1997**, 62 (5), 1388–1410.
- (112) Jung, N.; Bräse, S. *Science of Synthesis*; Banert, K., Ed.; Georg Thieme Verlag: Stuttgart, 2010; Vol. 41.
- (113) Sieh, D. H.; Wilbur, D. J.; Michejda, C. J. Preparation of Trialkyltriazenes. A Comparison of the N–N Bond Rotation in Trialkyltriazenes and Aryldialkyltriazenes by Variable Temperature <sup>13</sup>C NMR. *J. Am. Chem. Soc.* **1980**, 102 (11), 3883–3887.
- (114) Sieh, D. H.; Michejda, C. J. Acid-Catalyzed Decomposition of Trialkyltriazenes: Protected Alkylidiazonium Ions. *J. Am. Chem. Soc.* **1981**, 103 (2), 442–445.
- (115) Laila, A.; Isaacs, N. S. Effect of Pressure on the Reaction between 3-Methyl-1-p-Tolyl-Triazene. *J. für Prakt. Chemie* **1996**, 338, 691–694.
- (116) Farnsworth, D. W.; Wink, D. A.; Roscher, N. M.; Michejda, C. J.; Smith, R. H. Decomposition of Pyridinyltriazenes in Aqueous Buffer: A Kinetic and Mechanistic Investigation. *J. Org. Chem.* **1994**, 59 (20), 5942–5950.
- (117) Pytela, O.; Bednář, R.; Kaválek, J. Mechanism of Acid-Catalysed Decomposition of 3-Alkyl-1,3-Diphenyltriazenes by Trichloroacetic Acid in Hexane. *J. Phys. Org. Chem.* **2004**, 17 (4), 343–349.
- (118) Smith, R. H.; Denlinger, C. L.; Kupper, R.; Mehl, A. F.; Michejda, C. J. Decomposition of 1, 3-Dialkyltriazenes in Aqueous Buffers: Kinetic and Mechanistic Studies. *J. Am. Chem. Soc.* **1986**, 108 (13), 3726–3730.
- (119) Jones, C. C.; Kelly, M. A.; Sinnott, M. L.; Smith, P. J.; Tzotzos, G. T. Pathways for the Decomposition of Alkylaryltriazenes in Aqueous Solution. *J. Chem. Soc., Perkin Trans. 2* **1982**, 1655–1664.
- (120) Jones, C. C.; Kelly, M. A.; Sinnott, M. L.; Smith, P. J. Unimolecular Heterolysis of a Nitrogen-Nitrogen Bond. *J.C.S. Chem. Comm.* **1980**, 322–323.
- (121) Isaacs, N. S.; Rannala, E. Kinetics and Mechanism of the Decomposition of 3-Alkyl-1-Aryltriazenes by Carboxylic

- Acids. *J. Chem. Soc., Perkin Trans. 2* **1974**, 899–902.
- (122) Hanusek, J.; Bělohlová, H.; Příkryl, J.; Macháček, V. Acid-Catalyzed Decomposition of Stable 1-(2,1-Benzisothiazol-3-Yl)-3-Phenyltriazenes. *Dye. Pigment.* **2009**, *80* (1), 136–140.
- (123) Smith, R. H.; Denlinger, C. L.; Kupper, R.; Koepke, S. R.; Michejda, C. J. Specific Acid Catalysis in the Decomposition of Trialkyltriazenes. *J. Am. Chem. Soc.* **1984**, *106* (4), 1056–1059.
- (124) Sieh, D. H.; Michejda, C. J. Acid-Catalyzed Decomposition of Trialkyltriazenes: Protected Alkyldiazonium Ions. *J. Am. Chem. Soc.* **1981**, *103* (2), 442–445.
- (125) Rakotonradany, F.; Williams, C. I.; Whitehead, M. A.; Jean-Claude, B. J. Semi-Empirical PM3 Treatment of Diaryl and Dialkyl Triazene Decomposition in Acid Media. *J. Mol. Struct. THEOCHEM* **2001**, *535*, 217–234.
- (126) Schmiedekamp, A. M.; Topol, I. A.; Burt, S. K.; Razafinjanahary, H.; Chermette, H.; Pfaltzgraff, T.; Michejda, C. J. Triazene Proton Affinities: A Comparison between Density Functional, Hartree–Fock, and Post-Hartree–Fock Methods. *J. Comput. Chem.* **1994**, *15* (8), 875–892.
- (127) Ozment, J. L.; Schmiedekamp, A. M.; Schultz-Merkel, L. A.; Smith, R. H.; Michejda, C. J. Theoretical Analysis of Acetyltriene and the Mechanistic Implications of Its Reaction with Acid. *J. Am. Chem. Soc.* **1991**, *113* (2), 397–405.
- (128) Schmiedekamp, A.; Smith, R. H.; Michejda, C. J. Ab Initio Studies of Triazenes in Relation to Experimental Findings. *J. Org. Chem.* **1988**, *53* (15), 3433–3436.
- (129) Nguyen, M.-T.; Hoesch, L. Triazene: An Ab Initio Molecular-Orbital Study of Structure, Properties, and Hydrogen-Transfer Reaction Pathways. *Helv. Chim. Acta* **1986**, *69*, 1627–1637.
- (130) Francisco, A. P.; Mendes, E.; Santos, A. R.; Perry, M. J. Anticancer Triazenes: From Bioprecursors to Hybrid Molecules. *Curr. Pharm. Des.* **2019**, *25*, 1–21.
- (131) Marchesi, F.; Turriziani, M.; Tortorelli, G.; Avvisati, G.; Torino, F.; De Vecchis, L. Triazene Compounds: Mechanism of Action and Related DNA Repair Systems. *Pharmacol. Res.* **2007**, *56* (4), 275–287.
- (132) Gyton, M. R.; Leverett, A. R.; Cole, M. L.; McKay, A. I. Bulky Bis(Aryl)Triazenides: Just Aspiring Amidinates? A Structural and Spectroscopic Study. *Dalt. Trans.* **2020**, *49* (17), 5653–5661.
- (133) Camarena-Díaz, J. P.; Iglesias, A. L.; Chávez, D.; Aguirre, G.; Grotjahn, D. B.; Rheingold, A. L.; Parra-Hake, M.; Miranda-Soto, V. Rh (III) Cp\* and Ir (III) Cp\* Complexes of 1-[(4-Methyl)Phenyl]-3-[(2-Methyl-4'-R)Imidazol-1-Yl]Triazenide (R = t-Bu or H): Synthesis, Structure, and Catalytic Activity. *Organometallics* **2019**, *38* (4), 844–851.
- (134) Kalden, D.; Kriek, S.; Görls, H.; Westerhausen, M. Coordination Chemistry of N-(2-Pyridylethyl)-Substituted Bulky Amidinates and Triazenides of Magnesium. *Eur. J. Inorg. Chem.* **2018**, *2018* (39), 4361–4369.
- (135) Beweries, T.; Reiß, F.; Rothe, J.; Schulz, A.; Villinger, A. Triazenido Complexes of Titanocene(III). *Eur. J. Inorg. Chem.* **2019**, *2019* (14), 1993–1998.
- (136) McKay, A. I.; Cole, M. L. Structural Diversity in a Homologous Series of Donor Free Alkali Metal Complexes Bearing a Sterically Demanding Triazenide. *Dalt. Trans.* **2019**, *48* (9), 2948–2952.
- (137) Kalden, D.; Kriek, S.; Görls, H.; Westerhausen, M. 1,3-Bis(2,4,6-Trimethylphenyl)Triazenides of Potassium, Magnesium, Calcium, and Strontium. *Dalt. Trans.* **2015**, *44* (17), 8089–8099.
- (138) Barrett, A. G. M.; Crimmin, M. R.; Hill, M. S.; Hitchcock, P. B.; Kociok-Köhn, G.; Procopiou, P. A. Triazenide Complexes of the Heavier Alkaline Earths: Synthesis, Characterization, and Suitability for Hydroamination Catalysis. *Inorg. Chem.* **2008**, *47*, 7366–7376.
- (139) Kiefer, G.; Riedel, T.; Dyson, P. J.; Scopelliti, R.; Severin, K. Synthesis of Triazenes with Nitrous Oxide. *Angew. Chemie - Int. Ed.* **2015**, *54* (1), 302–305.
- (140) Perrin, F. G.; Kiefer, G.; Jeanbourquin, L.; Racine, S.; Perrotta, D.; Waser, J.; Scopelliti, R.; Severin, K. 1-Alkynyltriazenes as Functional Analogues of Ynamides. *Angew. Chemie - Int. Ed.* **2015**, *54* (45), 13393–13396.
- (141) Jeanbourquin, L. N.; Scopelliti, R.; Fadaei Tirani, F.; Severin, K. Synthesis and Reactivity of 1-Allenyltriazenes. *Org. Lett.* **2017**, *19* (8), 2070–2073.
- (142) Wang, C.; Lai, Z.; Xie, H.; Cui, S. Triazenyl Alkynes as Versatile Building Blocks in Multicomponent Reactions: Diastereoselective Synthesis of  $\beta$ -Amino Amides. *Angew. Chemie - Int. Ed.* **2021**, No. 60, 5147–5151.
- (143) Jeanbourquin, L. N.; Scopelliti, R.; Tirani, F. F.; Severin, K. Gold-Catalyzed Synthesis of 1,3-Diaminopyrazoles from 1-Alkenyltriazenes and Imines. *Helv. Chim. Acta* **2017**, *100* (10), e1700186.
- (144) Kossler, D.; Perrin, F. G.; Suleymanov, A. A.; Kiefer, G.; Scopelliti, R.; Severin, K.; Cramer, N. Divergent Asymmetric Synthesis of Polycyclic Compounds via Vinyl Triazenes. *Angew. Chemie - Int. Ed.* **2017**, *129*, 11648–11651.
- (145) Tan, J.-F.; Bormann, C. T.; Perrin, F. G.; Chadwick, F. M.; Severin, K.; Cramer, N. Divergent Synthesis of Densely Substituted Arenes and Pyridines via Cyclotrimerization Reactions of Alkynyl Triazenes. *J. Am. Chem. Soc.* **2019**, *141* (26), 10372–10383.
- (146) Wezeman, T.; Scopelliti, R.; Tirani, F. F.; Severin, K. Synthesis of Heteroaryl Triazenes via Rh(III)-Catalyzed Annulation Reactions with Alkynyl Triazenes. *Adv. Synth. Catal.* **2019**, *361*, 1383–1388.
- (147) Tan, J.; Bormann, C. T.; Severin, K.; Cramer, N. Alkynyl Triazenes as Fluoroalkyne Surrogates: Regioselective Access to 4-Fluoro-2-Pyridones by a Rh(III)-Catalyzed C–H Activation – Lossen Rearrangement – Wallach Reaction. *ACS Catal.* **2020**, *10* (6), 3790–3796.
- (148) Bormann, C. T.; Abela, F. G.; Scopelliti, R.; Fadaei-Tirani, F.; Severin, K. Synthesis of Indenyl Triazenes by Rhodium-Catalyzed Annulation Reactions. *European J. Org. Chem.* **2020**, *2020* (14), 2130–2139.
- (149) Zeng, L.; Lai, Z.; Zhang, C.; Xie, H.; Cui, S. Directing-Group-Enabled Cycloaddition of Azides and Alkynes toward Functionalized Triazoles. *Org. Lett.* **2020**, *22* (6), 2220–2224.

- (150) Abdusalom A. Suleymanov, Rosario Scopelliti, Farzaneh Fadaei Tirani, K. S. Synthesis of Vinyl Triazenes by Palladium-Catalyzed Addition Reactions to Alkynyl Triazenes. *Adv. Synth. Catal.* **2018**, 360, 4178–4183.
- (151) Bormann, C. T.; Fadaei-Tirani, F.; Scopelliti, R.; Severin, K. Synthesis of Bicyclic Vinyl Triazenes by Ficini-Type Reactions. *Org. Biomol. Chem.* **2021**, 19, 8113–8117.
- (152) Yadagiri, D.; Rivas, M.; Gevorgyan, V. Denitrogenative Transformations of Pyridotriazoles and Related Compounds: Synthesis of N-Containing Heterocyclic Compounds and Beyond. *J. Org. Chem.* **2020**, 85 (17), 11030–11046.
- (153) Filippov, I. P.; Titov, G. D.; Rostovskii, N. V. Recent Advances in Denitrogenative Reactions of Pyridotriazoles. *Synthesis (Stuttg.)* **2020**, 52 (23), 3564–3576.
- (154) Abarca, B.; Ballesteros-Garrido, R. 1,2,3-Triazoles Fused to Aromatic Rings. In *Topics in Heterocyclic Chemistry*; 2014; pp 325–378.
- (155) Chattopadhyay, B.; Gevorgyan, V. Transition-Metal-Catalyzed Denitrogenative Transannulation: Converting Triazoles into Other Heterocyclic Systems. *Angew. Chemie - Int. Ed.* **2012**, 51 (4), 862–872.
- (156) Jones, G.; Abarca, B. The Chemistry of the [1,2,3]Triazolo[1,5-a]Pyridines: An Update. *Adv. Heterocycl. Chem.* **2010**, 100 (10), 195–252.
- (157) Abarca-González, B. The Chemistry of [1,2,3]Triazolo[1,5-a]Pyridines. *J. Enzyme Inhib. Med. Chem.* **2002**, 17 (6), 359–367.
- (158) Landman, I. R.; Fadaei-Tirani, F.; Severin, K. Nitrous Oxide as a Diazo Transfer Reagent: The Synthesis of Triazolopyridines. *Chem. Commun.* **2021**, 57 (87), 11537–11540.
- (159) Das, S.; Pradhan, B. Photophysical and Photochemical Properties of a Family of Isoelectronic Tris Chelated Ruthenium(II) Aza-/Azo-Aromatic Complexes. *RSC Adv.* **2015**, 5 (90), 73726–73731.
- (160) Palepu, N. R.; Kollipara, M. R. Half-Sandwich Ruthenium, Rhodium and Iridium Complexes of Triazolopyridine Ligand: Synthesis and Structural Studies. *J. Chem. Sci.* **2017**, 129 (2), 177–184.
- (161) Roy, S.; Das, S. K.; Chattopadhyay, B. Cobalt(II)-Based Metalloradical Activation of 2-(Diazomethyl)Pyridines for Radical Transannulation and Cyclopropanation. *Angew. Chemie - Int. Ed.* **2018**, 57 (8), 2238–2243.
- (162) Shi, Y.; Gevorgyan, V. Cu-Catalyzed Transannulation Reaction of Pyridotriazoles: General Access to Fused Polycyclic Indolizines. *Chem. Commun.* **2015**, 51 (96), 17166–17169.
- (163) Helan, V.; Gulevich, A. V.; Gevorgyan, V. Cu-Catalyzed Transannulation Reaction of Pyridotriazoles with Terminal Alkynes under Aerobic Conditions: Efficient Synthesis of Indolizines. *Chem. Sci.* **2015**, 6 (3), 1928–1931.
- (164) Lamaa, D.; Lin, H. P.; Bzeih, T.; Retailleau, P.; Alami, M.; Hamze, A. TBAB-Catalyzed Csp<sup>3</sup>–N Bond Formation by Coupling Pyridotriazoles with Anilines: A New Route to (2-Pyridyl)Alkylamines. *European J. Org. Chem.* **2019**, 2019 (15), 2602–2611.
- (165) Dong, C.; Wang, X.; Pei, Z.; Shen, R. Metal-Free Denitrogenative C–C Couplings of Pyridotriazoles with Boronic Acids to Afford  $\alpha$ -Secondary and  $\alpha$ -Tertiary Pyridines. *Org. Lett.* **2019**, 21, 4148–4152.
- (166) Martín-Montes, Á.; Ballesteros-Garrido, R.; Martín-Escolano, R.; Marín, C.; Guitiérrez-Sánchez, R.; Abarca, B.; Ballesteros, R.; Sanchez-Moreno, M. Synthesis and in Vitro Leishmanicidal Activity of Novel [1,2,3]Triazolo[1,5-a]Pyridine Salts. *RSC Adv.* **2017**, 7 (26), 15715–15726.
- (167) Adam, R.; Bilbao-Ramos, P.; Abarca, B.; Ballesteros, R.; González-Rosende, M. E.; Dea-Ayuela, M. A.; Estevan, F.; Alzuet-Piña, G. Triazolopyridopyrimidines: An Emerging Family of Effective DNA Photocleavers. DNA Binding. Antileishmanial Activity. *Org. Biomol. Chem.* **2015**, 13 (17), 4903–4917.
- (168) Gornitzka, H.; Stalke, D. Coordination of the Bis(Pyridyl)Methyl Substituent to Group 1 and 13 Metals. *Organometallics* **1994**, 13 (11), 4398–4405.
- (169) Stentzel, M. R.; Klumpp, D. A. Michael Addition with an Olefinic Pyridine: Organometallic Nucleophiles and Carbon Electrophiles. *J. Org. Chem.* **2020**, 85 (19), 12740–12746.
- (170) Hněvšová, V.; Ernest, I. Anlagerung von Metallorganischen Verbindungen an Ungesättigte Pyridinbasen. *Collect. Czechoslov. Chem. Commun.* **1960**, 25 (5), 1468–1474.
- (171) Tie, L.; Shan, X. H.; Qu, J. P.; Kang, Y. B.  $\alpha$ -Trideuteration of Methylarenes. *Org. Chem. Front.* **2021**, 8 (12), 2981–2984.
- (172) Patel, M.; Saunthwal, R. K.; Verma, A. K. Base-Mediated Deuteration of Organic Molecules: A Mechanistic Insight. *ACS Omega* **2018**, 3 (9), 10612–10623.
- (173) Bank, S.; Dorr, R. NMR Studies of Arylmethyl Anions with Nitrogen Heterocyclic Rings. *J. Org. Chem.* **1987**, 52 (4), 501–510.
- (174) Corset, J.; Froment, F.; Lautié, M. F.; Ratovelomanana, N.; Seyden-Penne, J.; Strzalko, T.; Roux-Schmitt, M. C. Structural Study of Methyl and Tert-Butyl Phenylacetate Enolates in Solution: Spectroscopic Determination of Their E or Z Configuration. *J. Am. Chem. Soc.* **1993**, 115 (5), 1684–1694.
- (175) Lu, P.; Sanchez, C.; Cornella, J.; Larrosa, I. Silver-Catalyzed Protodecarboxylation of Heteroaromatic Carboxylic Acids. *Org. Lett.* **2009**, 11 (24), 5710–5713.
- (176) Green, S. P.; Wheelhouse, K. M.; Payne, A. D.; Hallett, J. P.; Miller, P. W.; Bull, J. A. Thermal Stability and Explosive Hazard Assessment of Diazo Compounds and Diazo Transfer Reagents. *Org. Process Res. Dev.* **2020**, 24 (1), 67–84.
- (177) Hirayama, T.; Ueda, S.; Okada, T.; Tsurue, N.; Okuda, K.; Nagasawa, H. Facile One-Pot Synthesis of [1,2,3]Triazolo[1,5-a]Pyridines from 2-Acylpyridines by Copper(II)-Catalyzed Oxidative N–N Bond Formation. *Chem. - A Eur. J.* **2014**, 20 (14), 4156–4162.
- (178) Cai, Y. M.; Zhang, X.; An, C.; Yang, Y. F.; Liu, W.; Gao, W. X.; Huang, X. B.; Zhou, Y. B.; Liu, M. C.; Wu, H. Y. Catalyst-Free Oxidative N–N Coupling for the Synthesis of 1,2,3-Triazole Compounds with: TBuONO. *Org. Chem. Front.* **2019**, 6 (9), 1481–1488.

- (179) Chuprakov, S.; Hwang, F. W.; Gevorgyan, V. Rh-Catalyzed Transannulation of Pyridotriazoles with Alkynes and Nitriles. *Angew. Chemie - Int. Ed.* **2007**, *46* (25), 4757–4759.
- (180) Kölmel, D. K.; Jung, N.; Bräse, S. Azides – Diazonium Ions – Triazenes: Versatile Nitrogen-Rich Functional Groups. *Aust. J. Chem.* **2014**, *67*, 328–336.
- (181) Nifontov, V. I.; Bel'skaya, N. P.; Shtokareva, E. A. Manufacture Methods of Synthesizing Triazenes (Review). *Pharm. Chem. J.* **1993**, *27* (9), 652–665.
- (182) Vaughan, B. K.; Stevens, M. F. G. Monoalkyltriazenes. *Chem. Soc. Rev.* **1978**, 377–397.
- (183) Smith, R. H.; Mehl, A. F.; Shantz, D. L.; Michejda, C. J.; Chmurny, G. N. Novel Cross-Linking Alkylating Agents, 1-(2-Chloroethyl)-3-Methyl-3-Acyltriazenes. *J. Org. Chem.* **1988**, *53* (7), 1467–1471.
- (184) Smith, R. H. J.; Michejda, C. J. Synthesis of Triazenes: Efficient Preparation of the Simple Di- and Trialkyltriazenes and a Novel 3-Acyl-1,3-Dialkyltriene. *Synthesis (Stuttg.)* **1983**, 476–477.
- (185) Wanner, M. J.; Koch, M.; Koomen, G. J. Synthesis and Antitumor Activity of Methyltriene Prodrugs Simultaneously Releasing DNA-Methylating Agents and the Antiresistance Drug O 6-Benzylguanine. *J. Med. Chem.* **2004**, *47* (27), 6875–6883.
- (186) Beukers, M. W.; Wanner, M. J.; Von Frijtag Drabbe Künzel, J. K.; Klaasse, E. C.; IJzerman, A. P.; Koomen, G. J. N6-Cyclopentyl-2-(3-Phenylaminocarbonyltriene-1-Yl)Adenosine (TCPA), a Very Selective Agonist with High Affinity for the Human Adenosine A1 Receptor. *J. Med. Chem.* **2003**, *46* (8), 1492–1503.
- (187) Curtin, D. Y.; Druliner, J. D. 1,3-Acyl Migrations in the Thermal Decomposition of N-Acetyltriazenes. *J. Org. Chem.* **1967**, *32* (5), 1552–1557.
- (188) Ito, S.; Fukuyama, T. Studies of Hydrazine Derivatives. II. The Formation of 1-Phenyl-3-Benzoyltriene by the Base-Catalyzed Condensation of Nitrosobenzene with Benzhydrazide. *J. Org. Chem.* **1971**, *36* (14), 2008–2009.
- (189) Bertho, A. Über Die Einwirkung von Grignard-Reagens Auf Carbonazidokörper. *J. Prakt. Chem.* **1927**, *36*, 2008–2009.
- (190) Vajs, J.; Proud, C.; Brozovic, A.; Gazvoda, M.; Lloyd, A.; Roper, D. I.; Osmak, M.; Košmrlj, J.; Dowson, C. G. Diaryltriazenes as Antibacterial Agents against Methicillin Resistant Staphylococcus Aureus (MRSA) and Mycobacterium Smegmatis. *Eur. J. Med. Chem.* **2017**, *127*, 223–234.
- (191) Sousa, A.; Santos, F.; Gaspar, M. M.; Calado, S.; Pereira, J. D.; Mendes, E.; Francisco, A. P.; Perry, M. J. The Selective Cytotoxicity of New Triene Compounds to Human Melanoma Cells. *Bioorganic Med. Chem.* **2017**, *25* (15), 3900–3910.
- (192) Senhaji Mouhri, Z.; Goodfellow, E.; Kelley, S. P.; Stein, R. S.; Rogers, R. D.; J Jean-Claude, B. 15N-, 13C- and 1H-NMR Spectroscopy Characterization and Growth Inhibitory Potency of a Combi-Molecule Synthesized by Acetylation of an Unstable Monoalkyltriene. *Molecules* **2017**, *22* (7), 1–13.
- (193) Cappoen, D.; Vajs, J.; Uythethofken, C.; Virag, A.; Mathys, V.; Kočevár, M.; Verschaeve, L.; Gazvoda, M.; Polanc, S.; Huygen, K.; et al. Anti-Mycobacterial Activity of 1,3-Diaryltriazenes. *Eur. J. Med. Chem.* **2014**, *77*, 193–203.
- (194) Monteiro, A. S.; Almeida, J.; Cabral, G.; Severino, P.; Videira, P. A.; Sousa, A.; Nunes, R.; Pereira, J. D.; Francisco, A. P.; Perry, M. J.; et al. Synthesis and Evaluation of N-Acylamino Acids Derivatives of Triazenes. Activation by Tyrosinase in Human Melanoma Cell Lines. *Eur. J. Med. Chem.* **2013**, *70*, 1–9.
- (195) Perry, M. J.; Mendes, E.; Simplício, A. L.; Coelho, A.; Soares, R. V.; Iley, J.; Moreira, R.; Francisco, A. P. Dopamine- and Tyramine-Based Derivatives of Triazenes: Activation by Tyrosinase and Implications for Prodrug Design. *Eur. J. Med. Chem.* **2009**, *44* (8), 3228–3234.
- (196) Carvalho, E.; Iley, J.; Rosa, E. Triene Drug Metabolites .13. the Decomposition of 3-Acyl-3-Alkyl-1-Aryltriazenes in Aqueous Sulfuric-Acid. *J. Chem. Soc. Trans. 2* **1993**, 865–870.
- (197) Smith, R. H.; Wladkowski, B. D.; Herling, J. A.; Pfaltzgraff, T. D.; Taylor, J. E.; Thompson, E. J.; Pruski, B.; Klose, J. R.; Michejda, C. J. Novel Triazenes and Triazolines from the Base-Catalyzed Hydrolysis of 1,3-Dialkyl-3-Acyltriazenes. *J. Org. Chem.* **1992**, *57* (24), 6448–6454.
- (198) Smith, R. H.; Wladkowski, B. D.; Herling, J. A.; Pfaltzgraff, T. D.; Klose, J.; Pruski, B.; Michejda, C. J. 1,3-Dialkyl-3-Acyltriazenes: Products and Rates of Decomposition in Acidic and Neutral Aqueous Solutions. *J. Org. Chem.* **1992**, *57* (2), 654–661.
- (199) Smith, R. H.; Mehl, A. F.; Hicks, A.; Denlinger, C. L.; Kratz, L.; Andrews, A. W.; Michejda, C. J. 1,3-Dimethyl-3-Acyltriazenes: Synthesis and Chemistry of a Novel Class of Biological Methylating Agents. *J. Org. Chem.* **1986**, *51* (20), 3751–3757.
- (200) Ludwig, M.; Pytela, O.; Večeřa, M. Salt Effect in Hydrolysis of 3-Acyl-1,3-Diphenyltriazenes. *Collect. Czechoslov. Chem. Commun.* **1981**, *46* (12), 3104–3109.
- (201) Pytela, O.; Večeřa, M.; Vetešník, P. Calculation of Isokinetic Temperature of Non-Catalyzed Hydrolysis of Substituted 3-(N-Methylcarbamoyl)-1,3-Diphenyltriazenes. *Collect. Czechoslov. Chem. Commun.* **1981**, *46* (4), 898–905.
- (202) Pytela, O.; Vecera, M.; Vetešník, P. Hydrolysis Kinetics and Mechanism of Acyl-1,3-Diphenyltriazenes. *Collect. Czechoslov. Chem. Commun.* **1980**, *45* (4), 1269–1278.
- (203) Lu, H.; Li, C. Facile Cyclization of Amidyl Radicals Generated from N-Acyltriazenes. *Tetrahedron Lett.* **2005**, *46* (36), 5983–5985.
- (204) Štefane, B.; Ernigoj, U.; Kočevár, M.; Polanc, S. 3-Acyl-1,3-Diaryltriazenes as Neutral and Selective Acylating Agents. *Tetrahedron Lett.* **2001**, *42* (38), 6659–6662.
- (205) Chung, Y.; Lee, H.; Kyo, H. A. N-Acyl Triazenes as Tunable and Selective Chemodosimeters toward Cyanide Ion. *J. Org. Chem.* **2006**, *71* (25), 9470–9474.

- (206) Glowacki, A.; Jeux, V.; Gasnier, G.; Joucla, L.; Jacob, G.; Lacôte, E. C- vs N-Oxidations of Benzyltriazanes: Selective Access to Triazones, Azimines, and Triazenes. *Synlett*. **2018**, 29 (5), 566–570.
- (207) Egger, N.; Hoesch, L.; Dreiding, A. S. 3,3-Dialkyltriazencarbonsaure-Derivate Durch Oxydative Hydro-Acyl-Elimination von 3,3-Dialkyltriazan-1, 2-Dicarbonsaure-Derivaten. *Helv. Chim. Acta* **1983**, 66 (134), 1416–1426.
- (208) Shi, W. M.; Ma, X. P.; Pan, C. X.; Su, G. F.; Mo, D. L. Tandem C-O and C-N Bonds Formation Through O-Arylation and [3,3]-Rearrangement by Diaryliodonium Salts: Synthesis of N-Aryl Benzo[1,2,3]Triazin-4(1H)-One Derivatives. *J. Org. Chem.* **2015**, 80 (21), 11175–11183.
- (209) Dunkin, I. R.; Lynch, M. A.; Withnall, R.; Boulton, A. J.; Henderson, N. The Thermal Decomposition of 1-Methyl-1,2,3-Benzotriazin-4-(1H)-One: Matrix Isolation of the Reactive Intermediates. *J. Chem. Soc. Chem. Commun.* **1989**, 1777–1778.
- (210) Boulton, A. J.; Devi, P. 1-Methyl-1,2,3-Benzotriazin-4(1H)-One. *J. Chem. Soc., Chem. Commun.* **1988**, 631–632.
- (211) Patil, S.; White, K.; Bugarin, A. Novel Triazene Dyes from N-Heterocyclic Carbenes and Azides: Syntheses, Stability, and Spectroscopic Properties. *Tetrahedron Lett.* **2014**, 55 (34), 4826–4829.
- (212) Landman, I. R.; Acuña-Bolomey, E.; Scopelliti, R.; Fadaei-Tirani, F.; Severin, K. Synthesis and Properties of 1-Acyl Triazenes. *Org. Lett.* **2019**, 21, 6408–6412.
- (213) Huang, H.; Tang, L.; Xi, Y.; He, G.; Zhu, H. Metal-Free Hydration of Ynamides: Convenient Approach to Amides. *Tetrahedron Lett.* **2016**, 57 (17), 1873–1876.
- (214) Xu, S.; Liu, J.; Hu, D.; Bi, X. Metal-Free Hydroacyloxylation and Hydration Reactions of Ynamides: Synthesis of  $\alpha$ -Acyloxyenamides and N-Acylsulfonamides. *Green Chem.* **2015**, 17 (1), 184–187.
- (215) Ghosh, N.; Nayak, S.; Sahoo, A. K. Gold(I)-Catalyzed 6- *Endo* -Dig Hydrative Cyclization of an Alkyne-Tethered Ynamide: Access to 1,6-Dihydropyridin-2(3H)Ones. *Chem. - A Eur. J.* **2013**, 19 (29), 9428–9433.
- (216) Compain, G.; Jouvin, K.; Martin-Mingot, A.; Evano, G.; Marrot, J.; Thibaudeau, S. Stereoselective Hydrofluorination of Ynamides: A Straightforward Synthesis of Novel  $\alpha$ -Fluoroenamides. *Chem. Commun.* **2012**, 48 (42), 5196–5198.
- (217) Jin, X.; Yamaguchi, K.; Mizuno, N. A Green Synthetic Route to Imides from Terminal Alkynes and Amides by Simple Solid Catalysts. *Chem. Lett.* **2012**, 41 (9), 866–867.
- (218) Davies, P. W.; Cremonesi, A.; Martin, N. Site-Specific Introduction of Gold-Carbenoids by Intermolecular Oxidation of Ynamides or Ynol Ethers. *Chem. Commun.* **2011**, 47, 379–381.
- (219) Dorel, R.; Echavarren, A. M. Gold(I)-Catalyzed Activation of Alkynes for the Construction of Molecular Complexity. *Chem. Rev.* **2015**, 115 (17), 9028–9072.
- (220) Lu, B.; Li, C.; Zhang, L. Gold-Catalyzed Highly Regioselective Oxidation of C-C Triple Bonds without Acid Additives: Propargyl Moieties as Masked  $\alpha,\beta$ -Unsaturated Carbonyls. *J. Am. Chem. Soc.* **2010**, 132 (40), 14070–14072.
- (221) Schulz, J.; Jašíková, L.; Škríba, A.; Roithová, J. Role of Gold(i)  $\alpha$ -Oxo Carbenes in the Oxidation Reactions of Alkynes Catalyzed by Gold(i) Complexes. *J. Am. Chem. Soc.* **2014**, 136 (32), 11513–11523.
- (222) Kim, S. W.; Um, T.-W.; Shin, S. Metal-Free Iodine-Catalyzed Oxidation of Ynamides and Diaryl Acetylenes into 1,2-Diketo Compounds. *J. Org. Chem.* **2018**, 83 (8), 4703–4711.
- (223) Finck, L.; Brals, J.; Pavuluri, B.; Gallou, F.; Handa, S. Micelle-Enabled Photoassisted Selective Oxyhalogenation of Alkynes in Water under Mild Conditions. *J. Org. Chem.* **2018**, 83 (14), 7366–7372.
- (224) Sadhukhan, S.; Baire, B. An Expeditious Approach to  $\alpha,\alpha$ -Dihalo- $\alpha'$ -Acetoxyketones from Propargylic Acetates. *ChemistrySelect* **2017**, 2 (27), 8500–8503.
- (225) Liu, J.; Lin, W.; Wang, C.; Li, Y.; Li, Z. Selective 1,2-Dihalogenation and Oxy-1,1-Dihalogenation of Alkynes by N-Halosuccinimides. *Tetrahedron Lett.* **2011**, 52 (33), 4320–4323.
- (226) Heasley, V. L.; Shellhamer, D. F.; Chappell, A. E.; Cox, J. M.; Hill, D. J.; McGovern, S. L.; Eden, C. C.; Kissel, C. L. Reactions of Carbonyl-Conjugated Alkynes with N-Bromosuccinimide and N-Iodosuccinimide in DMF/H<sub>2</sub>O and Methanol/Sulfuric Acid: Syntheses of Dihalo Diketones, Dihalo Ketoesters, and Dihalo Acetals. *J. Org. Chem.* **1998**, 63 (13), 4433–4437.
- (227) Sieh, D. H.; Wilbur, D. J.; Michejda, C. J. Preparation of Trialkyltriazenes. A Comparison of the Nitrogen-Nitrogen Bond Rotation in Trialkyltriazenes and Aryldialkyltriazenes by Variable Temperature Carbon-13 NMR. *J. Am. Chem. Soc.* **2005**, 127 (11), 3883–3887.
- (228) Marnilo, N. P.; Mayfield, C. B.; Wagener, E. H. Restricted Rotation about the N-N Single Bond. Linear Correlation of Rate with Substituent. *J. Am. Chem. Soc.* **1968**, 90 (2), 510–511.
- (229) Acta, H. C.; Egged, N.; Hoesch, L.; Zurich, U.; Derivatives, D.; Hydro-acyl-elimination, O. 3,3-Dialkyltriazencarbonsaure-Derivate Durch Oxydative Hydro-Acyl-Elimination von 3,3-Dialkyltriazan-1,2-Dicarbonsaure-Derivaten. *Helv. Chim. Acta* **1983**, 66 (134), 1416–1426.
- (230) Felpin, F. X.; Sengupta, S. Biaryl Synthesis with Arenediazonium Salts: Cross-Coupling, CH-Arylation and Annulation Reactions. *Chem. Soc. Rev.* **2019**, 48 (4), 1150–1193.
- (231) Habraken, E. R. M.; Jupp, A. R.; Slootweg, J. C. Diazonium Salts as Nitrogen-Based Lewis Acids. *Synlett*. **2019**, 30 (8), 875–884.
- (232) Mo, F.; Qiu, D.; Zhang, Y.; Wang, J. Renaissance of Sandmeyer-Type Reactions: Conversion of Aromatic C-N Bonds into C-X Bonds (X = B, Sn, P, or CF<sub>3</sub>). *Acc. Chem. Res.* **2018**, 51 (2), 496–506.
- (233) Koziakov, D.; Wu, G.; Jacobi Von Wangelin, A. Aromatic Substitutions of Arenediazonium Salts: Via Metal Catalysis, Single Electron Transfer, and Weak Base Mediation. *Org. Biomol. Chem.* **2018**, 16 (27), 4942–4953.
- (234) Taylor, J. G.; Moro, A. V.; Correia, C. R. D. Evolution and Synthetic Applications of the Heck-Matsuda Reaction: The Return of Arenediazonium Salts to Prominence. *European J. Org. Chem.* **2011**, No. 8, 1403–1428.


- (235) Ullrich, R.; Grewer, T. Decomposition of Aromatic Diazonium Compounds. *Thermochim. Acta* **1993**, 225 (2), 201–211.
- (236) Zollinger, H. Reactivity and Stability of Arenediazonium Ions. *Acc. Chem. Res.* **1973**, 6 (10), 335–341.
- (237) Dong, W.; Chen, Z.; Xu, J.; Miao, M.; Ren, H. Synthesis of Benzo-Fused Cyclic Compounds via Intramolecular Cyclization of Aryltriazines. *Synlett*. **2016**, 27 (9), 1318–1334.
- (238) Chand, S.; Kumar, S.; Singh, R.; Singh, K. N. A Practical Copper Catalyzed N-Arylation of Amines Using Aryl Triazines as Aryl Source. *ChemistrySelect* **2019**, 4 (2), 718–721.
- (239) Pandey, A. K.; Kumar, S.; Singh, R.; Singh, K. N. A Practical Synthesis of Aryl Sulfones via Cross-Coupling of Sulfonyl Hydrazides with Aryltriazines Using Copper/Ionic Liquid Combination. *Tetrahedron* **2018**, 10–15.
- (240) Cao, D.; Zhang, Y.; Liu, C.; Wang, B.; Sun, Y.; Abdulkadara, A.; Hu, H.; Liu, Q. Ionic Liquid Promoted Diazenylation of N-Heterocyclic Compounds with Aryltriazines under Mild Conditions. *Org. Lett.* **2016**, 18 (9), 2000–2003.
- (241) Zhang, Y.; Li, Y.; Zhang, X.; Jiang, X. Sulfide Synthesis through Copper-Catalyzed C-S Bond Formation under Biomolecule-Compatible Conditions. *Chem. Commun.* **2015**, 51 (5), 941–944.
- (242) Bräse, S.; Dahmen, S. Traceless Linkers - Only Disappearing Links in Solid-Phase Organic Synthesis? *Chem. - A Eur. J.* **2000**, 6 (11), 1899–1905.
- (243) Barragan, E.; Noonikara Poyil, A.; Yang, C. H.; Wang, H.; Bugarin, A. Metal-Free Cross-Coupling of  $\pi$ -Conjugated Triazines with Unactivated Arenes: Via Photoactivation. *Org. Chem. Front.* **2019**, 6 (2), 152–161.
- (244) Kimani, F. W.; Jewett, J. C. Water-Soluble Triazabutadienes That Release Diazonium Species upon Protonation under Physiologically Relevant Conditions. *Angew. Chemie - Int. Ed.* **2015**, 54 (13), 4051–4054.
- (245) He, J.; Kimani, F. W.; Jewett, J. C. A Photobasic Functional Group. *J. Am. Chem. Soc.* **2015**, 137 (31), 9764–9767.
- (246) Fanghanel, E.; Ortmann, W. Zur Bestimmung Des Oberflächenpotentials Und Des Relativen PH-Wertes In Der Sternregion Anionischer Mizellen Unter Verwendung von 1-(4'-Chlorphenyl)-3-(3-Methylbenzthia-Zolinylden-(2))-Triazen Als Sonde. *J. Prakt. Chem.* **1989**, 331, 721–725.
- (247) Fanghanel, E.; Poleschner, H.; Radeaglia, R.; Hänsel, R. Untersuchungen Zur Cis-Trans-Isomerie von 1-Aryl-1-Äthyl-3-[3-Methyl-Benzthiazolinylden-(2)]-Triazeniumtetrafluorboraten. *J. Prakt. Chem.* **1977**, 319, 813–826.
- (248) Ozment, J. L.; Schmiedekamp, A. M.; Schultz-Merkel, L. A.; Smith, R. H.; Michejda, C. J. Theoretical Analysis of Acetyltriazene and the Mechanistic Implications of Its Reaction with Acid. *J. Am. Chem. Soc.* **1991**, 113 (2), 397–405.
- (249) Landman, I. R.; Acuña-Bolomey, E.; Scopelliti, R.; Fadaei-Tirani, F.; Severin, K. Synthesis and Properties of 1-Acyl Triazines. *Org. Lett.* **2019**, 21 (16), 6408–6412.
- (250) Landman, I. R.; Suleymanov, A. A.; Scopelliti, R.; Fadaei-Tirani, F.; Chadwick, F. M.; Severin, K. Brønsted and Lewis Acid Adducts of Triazines. *Dalt. Trans.* **2020**, 49, 2317–2322.
- (251) Ji, Y.; Yang, X.; Ji, Z.; Zhu, L.; Ma, N.; Chen, D.; Jia, X.; Tang, J.; Cao, Y. DFT-Calculated IR Spectrum Amide I, II, and III Band Contributions of N-Methylacetamide Fine Components. *ACS Omega* **2020**, 5 (15), 8572–8578.
- (252) Liu, C.; Wang, Z.; Wang, L.; Li, P.; Zhang, Y. Palladium-Catalyzed Direct C2-Arylation of Azoles with Aromatic Triazines. *Org. Biomol. Chem.* **2019**, 17 (41), 9209–9216.
- (253) Dai, W. C.; Wang, Z. X. Palladium-Catalyzed Coupling of Azoles with 1-Aryltriazines: Via C-H/C-N Cleavage. *Org. Chem. Front.* **2017**, 4 (7), 1281–1288.
- (254) Yin, Z.; Wang, Z.; Wu, X. F. Palladium-Catalyzed Carbonylative Synthesis of Amides from Aryltriazines under Additive-Free Conditions. *European J. Org. Chem.* **2017**, 2017 (27), 3992–3995.
- (255) Chandrasekhar, A.; Sankararaman, S. Selective Synthesis of 3-Arylbenzo-1,2,3-Triazin-4(3H)-Ones and 1-Aryl-(1H)-Benzo-1,2,3-Triazoles from 1,3-Diaryltriazines through Pd(0) Catalyzed Annulation Reactions. *J. Org. Chem.* **2017**, 82 (21), 11487–11493.
- (256) Li, W.; Wu, X. F. Palladium-Catalyzed Carbonylative Sonogashira Coupling between Aryl Triazines and Alkynes. *Org. Biomol. Chem.* **2015**, 13 (18), 5090–5093.
- (257) Li, W.; Wu, X. F. N<sub>2</sub> Extrusion and Co Insertion: A Novel Palladium-Catalyzed Carbonylative Transformation of Aryltriazines. *Org. Lett.* **2015**, 17 (8), 1910–1913.
- (258) Saeki, T.; Matsunaga, T.; Son, E. C.; Tamao, K. Palladium-Catalyzed Cross-Coupling Reaction of 1-Aryltriazines with Aryl- and Alkenyltrifluorosilanes. *Adv. Synth. Catal.* **2004**, 346 (13–15), 1689–1692.
- (259) Wang, D.; Unold, J.; Bubrin, M.; Elser, I.; Frey, W.; Kaim, W.; Xu, G.; Buchmeiser, M. R. Ruthenium-Triazene Complexes as Latent Catalysts for UV-Induced ROMP. *Eur. J. Inorg. Chem.* **2013**, No. 31, 5462–5468.
- (260) Albertin, G.; Antonlutti, S.; Bedin, M.; Castro, J.; Garcia-Fontán, S. Synthesis and Characterization of Triazenide and Triazene Complexes of Ruthenium and Osmium. *Inorg. Chem.* **2006**, 45 (9), 3816–3825.
- (261) McKay, A. I.; Cole, M. L. Structural Diversity in a Homologous Series of Donor Free Alkali Metal Complexes Bearing a Sterically Demanding Triazenide. *Dalt. Trans.* **2019**, 2948–2952.
- (262) Scherer, W.; Dunbar, A. C.; Barquera-Lozada, J. E.; Schmitz, D.; Eickerling, G.; Kratzert, D.; Stalke, D.; Lanza, A.; Macchi, P.; Casati, N. P. M.; et al. Anagostic Interactions under Pressure: Attractive or Repulsive? *Angew. Chemie - Int. Ed.* **2015**, 54 (8), 2505–2509.
- (263) Mao, S.; Chen, Z.; Wang, L.; Khadka, D. B.; Xin, M.; Li, P.; Zhang, S. Q. Synthesis of Aryl Trimethylstannane via BF<sub>3</sub>·OEt<sub>2</sub>-Mediated Cross-Coupling of Hexaalkyl Distannane Reagent with Aryl Triazene at Room Temperature. *J. Org. Chem.* **2019**, 84 (1), 463–471.
- (264) Liu, C.; Lv, J.; Luo, S.; Cheng, J. P. Sc(OTf)<sub>3</sub>-Catalyzed Transfer Diazenylation of 1,3-Dicarbonyls with Triazines via N-N Bond Cleavage. *Org. Lett.* **2014**, 16 (20), 5458–5461.
- (265) Li, W.; Beller, M.; Wu, X. F. Catalytic Conversion of Aryl Triazines into Aryl Sulfonamides Using Sulfur Dioxide

- as the Sulfonyl Source. *Chem. Commun.* **2014**, 50 (67), 9513–9516.
- (266) Zhu, C.; Yamane, M. Transition-Metal-Free Borylation of Aryltriazene Mediated by BF<sub>3</sub>·OEt<sub>2</sub>. *Org. Lett.* **2012**, 14 (17), 4560–4563.
- (267) Saeki, T.; Son, E. C.; Tamao, K. Boron Trifluoride Induced Palladium-Catalyzed Cross-Coupling Reaction of 1-Aryltriazenes with Areneboronic Acids. *Org. Lett.* **2004**, 6 (4), 617–619.
- (268) Fulmer, G. R.; Miller, A. J. M.; Sherden, N. H.; Gottlieb, H. E.; Nudelman, A.; Stoltz, B. M.; Bercaw, J. E.; Goldberg, K. I. NMR Chemical Shifts of Trace Impurities: Common Laboratory Solvents, Organics, and Gases in Deuterated Solvents Relevant to the Organometallic Chemist. *Organometallics* **2010**, 29 (9), 2176–2179.
- (269) Duez, S.; Steib, A. K.; Manolikakes, S. M.; Knochel, P. Lewis Acid Promoted Benzylic Cross-Couplings of Pyridines with Aryl Bromides. *Angew. Chemie - Int. Ed.* **2011**, 50 (33), 7686–7690.
- (270) Jiang, X.; Tiwari, A.; Thompson, M.; Chen, Z.; Cleary, T. P.; Lee, T. B. K. A Practical Method for N-Methylation of Indoles Using Dimethyl Carbonate. *Org. Process Res. Dev.* **2001**, 5 (6), 604–608.
- (271) Jin, W.; Zheng, P.; Wong, W. T.; Law, G. L. Efficient Selenium-Catalyzed Selective C(Sp<sup>3</sup>)-H Oxidation of Benzylpyridines with Molecular Oxygen. *Adv. Synth. Catal.* **2017**, 359 (9), 1588–1593.
- (272) Nguyen, T. B.; Nguyen, T. M.; Retailleau, P. [2+2] Photodimerization of Stilbazoles Promoted by Oxalic Acid in Suspension. *Chem. - A Eur. J.* **2020**, 26 (21), 4682–4689.
- (273) Kiefer, G.; Riedel, T.; Dyson, P. J.; Scopelliti, R.; Severin, K. Synthesis of Triazenes with Nitrous Oxide. *Angew. Chemie - Int. Ed.* **2015**, 54 (1), 302–305.
- (274) Jiang, G.; Lin, Y.; Cai, M.; Zhao, H. Recyclable Heterogeneous Copper(II)-Catalyzed Oxidative Cyclization of 2-Pyridine Ketone Hydrazones towards [1,2,3]Triazolo[1,5-a]Pyridines. *Synth.* **2019**, 51 (23), 4487–4497.
- (275) Sheldrick, G. M. SHELXT - Integrated Space-Group and Crystal-Structure Determination. *Acta Cryst.* **2015**, A71, 3–8.
- (276) Dolomanov, O. V.; Bourhis, L. J.; Gildea, R. J.; Howard, A. K.; Puschmann, H. OLEX2: A Complete Structure Solution, Refinement and Analysis Program. *J. Appl. Cryst.* **2009**, 42, 339–341.
- (277) Sheldrick, G. M. Crystal Structure Refinement with SHELXL. *Acta Cryst.* **2015**, C71, 3–8.
- (278) CrysAlisPro Software System, Rigaku Oxford Diffraction, 2021.
- (279) O'Brien, J.; Wilson, I.; Orton, T.; Pognan, F. Investigation of the Alamar Blue (Resazurin) Fluorescent Dye for the Assessment of Mammalian Cell Cytotoxicity. *Eur. J. Biochem.* **2000**, 267 (17), 5421–5426.
- (280) Cabrero-Antonino, J. R.; Leyva-Pérez, A.; Corma, A. Regioselective Hydration of Alkynes by Iron(III) Lewis/Brønsted Catalysis. *Chem. - A Eur. J.* **2012**, 18 (35), 11107–11114.
- (281) Schießl, J.; Stein, P.; Stirn, J.; Emler, K.; Rudolph, M.; Rominger, F.; Hashmi, A. S. K. Strategic Approach on N-Oxides in Gold Catalysis - A Case Study. *Adv. Synth. Catal.* **2019**, 361, 725–738.
- (282) Gasparro, F. P.; Kolodny, N. H. NMR Determination of the Rotational Barrier in N,N-Dimethylacetamide. A Physical Chemistry Experiment. *J. Chem. Educ.* **1977**, 54 (4), 258–261.
- (283) CrysAlisPro Software System, Rigaku Oxford Diffraction, 2015.
- (284) CrysAlisPro Software System, Rigaku Oxford Diffraction, 2019.

# Iris R. Landman

## Curriculum Vitae


### Personal information

 Iris Roswitha Landman

The Netherlands

born June 18<sup>th</sup>, 1993

@ iris.r.landman@gmail.com

 (+31)6 313 433 76

 @irisrlandman

 Chemin de Fornache 11

1029 Villars-Ste-Croix VD

Switzerland

 [Linkedin.com/in/irisr/](https://www.linkedin.com/in/irisr/)

 [0000-0002-2389-3150](https://orcid.org/0000-0002-2389-3150)

Google Scholar ID: [ya-ypTEAAAJ&hl](https://scholar.google.com/citations?user=ya-ypTEAAAJ&hl)



### Education

**PhD Chemistry**, EPFL, Switzerland

Oct 2017 – Jan 2022

- **PhD thesis:** “*Synthetic chemistry with nitrous oxide and triazenes*”  
Thesis advisor: Prof. K. Severin, LCS laboratory, EPFL
- **Extracurricular:**
  - Drug/device development course by EPFL & SDSU (Oct – Nov 2019): grade A
  - Merck compound challenge (Mar – Apr 2021): proposal was rated top 25% after peer review

**MSc Chemistry**, University of Amsterdam, the Netherlands

Sep 2014 – Nov 2016

- **Excellence program:** top 10% of cohort, Holland Research School of Molecular Chemistry (HRSMC)
- **MSc thesis:** “*Developing bifunctional alkene isomerization catalysts by modelling structure-activity relationships*” (Sep 2015 – Oct 2016, 8 months in the Netherlands, 5 months in USA)  
Thesis advisors: Prof. G. Rothenberg, UvA, the Netherlands and Prof. D. Grotjahn, SDSU, USA
- **Other MSc research projects:**
  - “*Red light activation of Ru(II) polypyridyl prodrugs via triplet-triplet annihilation upconversion: feasibility in air and through meat*”, lab of Prof. S. Bonnet, Leiden University (NL, Jun 2015, 4 weeks)
  - “*Fine-tuning the balance between peptide thioester cyclization and racemization*”, lab of Prof. J. van Maarseveen, UvA (NL, Sep 2015, 4 weeks)

**BSc Chemistry**, University of Amsterdam, the Netherlands

Sep 2011 – Aug 2014

- **BSc thesis:** “*Novel functional materials based on graphene*”  
Thesis advisor: Prof. G. Rothenberg, UvA, the Netherlands
- **Extracurricular:** Summer research program at The Weizmann Institute of Science, in the research group of Prof. M. E. van der Boom (Jul – Aug 2012, 8 weeks, Israel)

### Prizes, awards and fellowships

Apr 2021	<b>Researcher Development Grant</b> (D20-921), Royal Society of Chemistry (4 days ISOS summer program).
Jun 2020	<b>Teaching excellence award</b> from the EPFL. <a href="#">Link to message for the students (Instagram)</a> .
Dec 2015 – Apr 2016	<b>Research grant</b> for MSc project, co-financed by the HRSMC, the research priority area sustainable chemistry, the Van 't Hoff Institute for Molecular Sciences. <a href="#">Link to travel report (5-month MSc project in USA)</a> .
Dec 2015 – Apr 2016	<b>Travel grant</b> from the Royal Netherlands Chemical Society (5 months MSc project in USA).
Aug 2014	<b>Scholarship</b> from the Utrecht University for the “Nanomaterials: Science and Applications for Advanced Bachelors course”, the Netherlands (2 weeks program).
Jul – Aug 2013	<b>Scholarship</b> from the Weizmann Institute of Science (8 weeks program).

### Publications in peer-reviewed scientific journals

(6) Synthetic chemistry with nitrous oxide: the synthesis of triazolopyridines

**Landman, I.R.;** Acuña-Bolomey, E.; Scopelliti, R.; Fadaei-Tirani, F.; Severin, K. *Chem. Commun.* 2021, 57, 11537-11540. DOI: [10.1039/d1cc04907k](https://doi.org/10.1039/d1cc04907k) (link).

(5) Synthesis and properties of 1-acyl triazenes

**Landman, I.R.;** Acuña-Bolomey, E.; Scopelliti, R.; Fadaei-Tirani, F.; Severin, K. *Org. Lett.* 2019, 21, 6408–6412. DOI: [10.1021/acs.orglett.9b02248](https://doi.org/10.1021/acs.orglett.9b02248) (link)

(4) Brønsted and Lewis acid adducts of triazenes

**Landman, I.R.\*;** Suleymanov, A. A.\*; Fadaei-Tirani, F.; Scopelliti, R.; Chadwick, F. M.; Severin, K. *Dalton Trans.* 2020, 49, 2317–2322. \*Authors contributed equally. DOI: [10.1039/D0DT00049C](https://doi.org/10.1039/D0DT00049C) (link)

(3) Designing bifunctional alkene isomerization catalysts using predictive modelling

**Landman, I.R.;** Paulson, E.R.; Rheingold, A. L.; Grotjahn, D.B.; Rothenberg, G. *Catal. Sci. Technol.* 2017, 7, 4842–4851. DOI: [10.1039/C7CY01106G](https://doi.org/10.1039/C7CY01106G) (link)

(2) Red light activation of Ru(II) polypyridyl prodrugs via triplet-triplet annihilation upconversion: feasibility in air and through meat.

Askes, S.H.C.; Meijer, M.S.; Bouwens, T.; **Landman, I.;** Bonnet, S. *Molecules* 2016, 21, 1460. DOI: [10.3390/molecules21111460](https://doi.org/10.3390/molecules21111460) (link)

(1) Fine-tuning the balance between peptide thioester cyclization and racemization.

Popovic, S.; Wijsman, L.; **Landman, I.R.;** Sangster, M.F.; Pastoors, D.; Veldhorst, B.B.; Hiemstra, H.; Van Maarseveen, J.H. *Eur. J. Org. Chem.* 2016, 3, 443–446. DOI: [10.1002/ejoc.201501366](https://doi.org/10.1002/ejoc.201501366)

### Contributions to conferences

- *Synthetic chemistry with nitrous oxide: 1-acyl triazenes and triazolopyridines*
- 2021 **Online live presentation**, A. Corbella International summer school on organic synthesis, June 14-17
- 2021 **Online live presentation**, ACS Spring meeting, April 15
- *Synthesis and properties of 1-acyl triazenes*
- 2019 **Oral presentation**, Swiss Summer School, “Trends in Organic Chemistry”, Villars-sur-Ollon (CH), August 18-22
- Poster presentations:**
- *Brønsted and Lewis acid adducts of triazenes*
- 2020 SCS, Swiss Chemical Society fall meeting, online (CH)
- 2020 RSC twitter conference
- 2019 CHAINS, Dutch Chemical Society conference (NL)
- *Synthesis and properties of 1-acyl triazenes*
- 2019 SCS, Swiss Chemical Society fall meeting, Zürich (CH)
- 2019 PhD retreat, Les Diablerets (CH)
- 2018 CHAINS, Dutch Chemical Society conference (NL)
- 2018 SCS, Swiss Chemical Society fall meeting, Lausanne (CH)
- *Designing bifunctional alkene isomerization catalysts using predictive modelling*
- 2016 Southern-California Organometallics meeting, UC Irvine (CA, USA)

### Employment history

- |                     |  |
|---------------------|--|
| May – Sep 2017      | <b>Science Teacher</b> at Bèta Instituut Amsterdam, the Netherlands.   |
| May 2013 – Jun 2016 | <b>Science Tutor</b> in Chemistry, Biology, Mathematics and Physics, at a homework institute (SMILE), the Netherlands.                             |
| Jun – Dec 2014      | <b>Personal assistant teacher</b> , guiding final projects in Chemistry of high school students at the Hermann Wesselink College, the Netherlands. |

### Personal skills

- **Languages:** Dutch (native), English (working proficiency), French (A2/B1), German (A1/A2).
- **Leadership:** mentoring, supervising, and organizing teaching activities.
- **International competences:** worked and lived in four different countries (CH, NL, IL, USA).
- **Critical thinking:** curious, creative, adaptable and problem-solving.
- **Communication to experts and non-experts:** peer-reviewed articles, oral presentations, (online) reports and articles for a general audience.
- **Social awareness:** *e.g.* volunteering work as Dutch language coach for refugees (Stichting Wereldbuur), Amstelveen, the Netherlands (Mar – Jul 2017).

### General interests

Spending time with family and friends. Driving motorcycle. Snowboarding.